CORRELATION OF AERODYNAMIC STABILITY AND CONTROL DERIVATIVES OBTAINED FROM FLIGHT TESTS AND WIND TUNNEL TESTS ON THE XC-142A AIRPLANE

ERNEST L. BLACK

GEORGE C. BOOTH

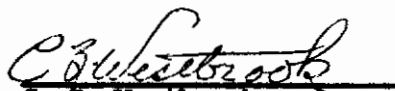*** Export controls have been removed ***

FOREWORD

This research and development program was performed by the Vought Aeronautics Division of the LTV Aerospace Corporation, Dallas, Texas, under Air Force Contract No. AF 33(615)-2897, BPSN 5(638219-62405364).

The work was supervised by Ernest L. Black, Principal Investigator. The report was prepared by Messrs. Black and George C. Booth. This project was initiated by the Air Force Flight Dynamics Laboratory under Project 8219, task 821907, and was administered under the technical coordination of Fred S. Thomas, FDCC.

This document was submitted by the authors in November 1968. The report covers work performed from June 1965 to November 1968, and is the final report under Contract AF 33(615)-2897.

This technical report has been reviewed and approved.

C. B. Westbrook
Chief, Control Criteria Branch
Air Force Flight Dynamics Laboratory

ABSTRACT

A wind tunnel-flight data correlation program using the XC-142A airplane was undertaken to assess the degree of correlation attainable and to establish the areas where present wind tunnel testing and correction techniques appear to be inadequate. Wind tunnel data obtained from tests of three models of the XC-142A airplane in four different size test sections could not be satis-factorily correlated because of differences in model configuration and test conditions. Three special tests were performed using the same model but in different size test sections of the same tunnel. The results of these tests indicated that with proper equipment and techniques, valid V/STOL wind tunnel data can be acquired. The flight data were obtained from the Contractor's Category I test program. The objective of this flight test program was pri-marily to perform a qualitative evaluation of the airplane rather than to obtain the quantitative data desired for aerodynamic analysis purposes. The flight data were not acquired in a manner that would provide suitable quality to allow a high degree of confidence in inverse solutions for aerodynamic derivatives. It is recommended that future programs include a critical review of the instrumentation system and flight maneuvers in order to obtain the best possible data for determining the low speed flight aerodynamic characteristics.

TABLE OF CONTENTS

LIST OF FIGURES

LIST OF FIGURES
(Continued)

LIST OF FIGURES
(Concluded)

LIST OF FIGURES
(Concluded)

LIST OF TABLES

LIST OF SYMBOLS FOR SECTIONS III AND IV

A — Propeller area, sq. ft.

$\bar{c}$ — Wing mean geometric chord, ft.

C_D — Drag coefficient based on free stream, $\dfrac{\text{Drag}}{qS}$

C_{D_S} — Drag coefficient based on slipstream, $\dfrac{\text{Drag}}{q_s S}$

C_L — Lift coefficient based on free stream, $\dfrac{\text{Lift}}{qS}$

C_{L_s} — Lift coefficient based on slipstream, $\dfrac{\text{Lift}}{q_s S}$

C_m — Pitching Moment based on free stream, $\dfrac{\text{Pitching moment}}{qS\,\bar{c}}$

C_{m_s} — Pitching Moment based on slipstream, $\dfrac{\text{Pitching Moment}}{q_s S\,\bar{c}}$

$C_{T,s}$ — Thrust coefficient based on slipstream, $\dfrac{\text{Thrust}}{q_s A}$

i_t — Horizontal tail incidence angle with respect to the fuselage reference line, degrees

i_w — Wing incidence angle with respect to fuselage reference line, degree

q — Free stream dynamic pressure, lbs/ft.^{2}

q_s — Slipstream dynamic pressure, $q + T/A$, lbs./ft.^{2}

S — Wing area, ft.^{2}

T — Thrust, lbs.

T'_c — Thrust coefficient based on free stream, $\dfrac{T}{qS}$

α — Angle of attack of fuselage reference line, degrees

β — Propeller blade angle, measured at 75% radius, degrees

δ_F — Trailing edge flap deflection, degrees

δ_K — Krüger flap defection, degrees

C_L — Lift coefficient, stability axis

C_P — Power coefficient, torque/$\rho n^2 D^5$

C_T — Thurst coefficient, thrust/$\rho n^2 D^4$

C_{T_s} — Slipstream thrust coefficient

D — Main prop diameter, ft.

H_P — Pressure altitude, ft.

i_T — Unit horizontal tail position, degrees

i_w — Wing position, degrees

I_x — Moment of inertia about x axis, slug-ft^2

I_y — Moment of inertia about y axis, slug-ft^2

I_z — Moment of inertia about z axis, slug-ft^2

I_{xz} — Product of inertia

J — Advance ratio, V/nD

J_x — $-I_{xz}/I_x$

J_z — $-I_{xz}/I_z$

L — Moment about the x-body axis, roll, ft-lbs

L_p — $1/I_x(\partial L/\partial p)$

L_v — $1/I_x(\partial L/\partial v)$

L_r — $1/I_x(\partial L/\partial r)$

$L\delta_A$ — $1/I_x(\partial L/\partial \delta_A)$

$L\delta_\beta$ — $1/I_x(\partial L/\partial \delta_\beta)$

$L\delta_R$ — $1/Ix(\partial L/\partial \delta_R)$

L^*_p — $(L_p - J_x N_p)/(1 - J_x J_z)$

L^*_v — $(L_v - J_x N_p)/(1 - J_x J_z)$

L^*_r — $(L_r - J_x N_r)/(1 - J_x J_z)$

$L^*\delta_A$ — $(L\delta_A - J_x N\delta_A)/(1 - J_x J_z)$

$L*_{\delta_\beta}$ — $(L\delta_\beta - J_x N\delta_\beta)/(1 - J_x J_z)$

$L*_{\delta_R}$ — $(L\delta_R - J_x N\delta_R)/(1 - J_x J_z)$

$L\beta$ — $1/I_x (\partial L/\partial \beta)$

M — Moment about the y body axis, pitch, ft-lbs

m — Mass

M_{i_t} — $1/I_y (\partial M/\partial i_T)$

M_q — $1/I_y (\partial M/\partial q)$

M_u — $1/I_y (\partial M/\partial u)$

M_w — $1/I_y (\partial M/\partial w)$

$M_{\dot{w}}$ — $1/I_y (\partial M/\partial w)$

M_α — $1/I_y (\partial M/\partial \alpha)$

$M_{\Delta\beta}$ — $1/I_y (\partial M/\partial \Delta\beta)$

$M_{\Delta N}$ — $1/I_y (\partial M/\partial \Delta N)$

$M*_{i_T}$ — $M_{i_t} + M_{\dot{w}} Z_{i_t}$

$M*_q$ — $M_q + M_{\dot{w}} (Z_q + U_o)$

$M*_u$ — $M_u + M_{\dot{w}} Z_u$

$M*_w$ — $M_w + M_{\dot{w}} Z_w$

$M*_\alpha$ — $M_\alpha + M_{\dot{w}} Z_\alpha$

$M*_{\Delta\beta}$ — $M_{\Delta\beta} + M_{\dot{w}} Z_{\Delta\beta}$

$M*_{\Delta N}$ — $M_{\Delta N} + M_{\dot{w}} Z_{\Delta N}$

N — Moment about Z body axis, yaw, ft-lbs

n — Prop RPM

N_p — $1/I_z (\partial N/\partial p)$

N_r — $1/I_z (\partial N/\partial r)$

N_v — $1/I_z (\partial N/\partial v)$

N_β — $1/I_z (\partial N/\partial \beta)$

N_{δ_A} — $1/I_z (\partial N/\partial \delta_A)$

$N_{\delta\beta}$ - $1/I_z \, (\partial N / \partial \delta_\beta)$

$N\delta_R$ - $1/I_z \, (\partial N / \partial \delta_R)$

N^*_p - $(N_p - J_z L_p)/(1 - J_x J_z)$

N^*_r - $(N_r - J_z L_r)/(1 - J_x J_z)$

N^*_v - $(N_v - J_z L_v)/(1 - J_x J_z)$

N^*_β - $(N_\beta - J_x L_\beta)/(1 - J_x J_z)$

$N^*\delta_A$ - $(N_{\delta_A} - J_z L_{\delta_A})/(1 - J_x J_z)$

$N^*\delta_\beta$ - $(N_{\delta_\beta} - J_z L_{\delta_\beta})/(1 - J_x J_z)$

$N^*\delta_R$ - $(N_{\delta_R} - J_z L_{\delta_R})/(1 - J_x J_z)$

n_x -   Axial load factor

n_y -   Lateral load factor

N_z -   Normal load factor

p -   Roll rate

$\dot{p}$ -   Roll acceleration

q -   Pitch rate

$\dot{q}$ -   Pitch acceleration

r -   Yaw rate

$\dot{r}$ -   Yaw acceleration

U_o -   Trim axial velocity

u -   Linear velocity along X axis

$\dot{u}$ -   Linear acceleration along X axis

V -   Airspeed

v -   Linear velocity along Y axis

$\dot{v}$ -   Linear acceleration along Y axis

w -   Linear velocity along Z axis

$\dot{w}$ -   Linear acceleration along Z axis

w_o -   Trim normal velocity

X	—	Force along X axis, lbs
X_{i_T}	—	$(\partial X/\partial i_T)/m$
X_u	—	$(\partial X/\partial u)/m$
X_w	—	$(\partial X/\partial w)/m$
$X_w{}^2$	—	$(\partial X/\partial w^2)/m$
$X_{\Delta\beta}$	—	$(\partial X/\partial \Delta\beta)/m$
X_{Δ_N}	—	$(\partial X/\partial \Delta N)/m$
Y	—	Force along Y axis, lbs
Y_p	—	$(\partial Y/\partial p)/m$
Y_r	—	$(\partial Y/\partial r)/m$
Y_v	—	$(\partial Y/\partial v)/m$
Y_{δ_A}	—	$(\partial Y/\partial \delta A)/m$
Y_{δ_β}	—	$(\partial Y/\partial \delta\beta)/m$
Y_{δ_R}	—	$(\partial Y/\partial \delta_R)/m$
Z	—	Force along Z axis, lbs
Z_{i_T}	—	$(\partial Z/\partial i_T)/m$
Z_q	—	$(\partial Z/\partial q)/m$
Z_u	—	$(\partial Z/\partial u)/m$
Z_w	—	$(\partial Z/\partial w)/m$
Z_α	—	$(\partial Z/\partial \alpha)/mV$
$Z_{\Delta\beta}$	—	$(\partial Z/\partial \Delta\beta)/m$
$Z_{\Delta N}$	—	$(\partial Z/\partial \Delta N)/m$
α_F	—	Fuselage angle of attack, degrees
β	—	Angle of sideslip, degrees
β_N	—	Main prop blade angle ($N = 1$ to 4), degrees
β_{T_P}	—	Tail prop blade angle, degrees
$\Delta\beta$	—	Change in main prop blade angle $(\beta_1 + \beta_2 + \beta_3 + \beta_4)/4$, degrees

Δ_{i_T} -   Change in unit horizontal tail deflection, degrees

ΔN -   Change in propeller RPM, rpm

Δn_Z - $(n_Z - 1)$

δ_A -   Aileron deflection, $(\delta_{A_{LT}} - \delta_{A_{RT}})/2$, degrees

δ_β -   Differential prop pitch, $\{(\beta_1 + \beta_2) - (\beta_3 + \beta_4)\}/4$, degrees

δ_F -   Flap deflection, degrees

δ_R -   Rudder deflection, degrees

ϕ -   Bank angle, degrees

ρ -   Density

σ -   Density ratio, ρ/ρ_o

θ -   Pitch attitude, degrees

SUMMARY

A wind tunnel-flight test data correlation program, under contract to the Air Force Flight Dynamics Laboratory, was begun on 21 June 1965. The objective of the program was to assess the degree of correlation attainable and to establish the problem areas where present wind tunnel testing techniques and correction techniques appear to be inadequate.

Wind tunnel data obtained from tests of three models of the XC-142A airplane in four different size test sections could not be satisfactorily correlated. These tests differed in model configurations, methods of establishing test conditions, measurement and control of thrust, selection of propeller blade angles, and roughness of model surfaces. Disagreements in the data due to these differences were never resolved because of the interaction of several factors that affected the data. Although these tests did not provide the specific data needed for this study, they identified certain problem areas. The scope of the investigation was expanded to include three additional tests, performed with the same model, but in different size test sections of the same tunnel. The results of these tests indicated that with proper equipment and techniques, valid V/STOL wind tunnel data can be acquired.

The flight data used in the study were obtained from the Contractor's Category I test program. The objective of this flight test program was primarily to perform a qualitative evaluation of the airplane rather than to obtain the quantitative data desired for aerodynamic analysis purposes. The flight data available were not of suitable quality to allow a high degree of confidence in inverse solutions for aerodynamic derivatives. Controls fixed maneuvers, which would have eliminated the predominant effect of control effectiveness in low speed flight and enabled more accurate determination of the basic airframe characteristics, were not available. It is recommended that future programs include a critical review of the instrumentation system and flight maneuvers in order to obtain the best possible data for determining the low speed flight aerodynamic characteristics.

SECTION II

INTRODUCTION

The capability to predict accurately the aerodynamic characteristics of V/STOL airplanes has not been refined sufficiently to provide the degree of confidence desirable for future design studies. Historically, in the design of conventional aircraft, engineering aerodynamics has relied on three phases; theory, wind tunnel testing, and flight test confirmation. Engineering confidence has rested on the completed cycle of these aspects. However, many V/STOL concepts have failed in the development stages and much of the desired engineering information or verification has not been obtained. One result has been the basic V/STOL technology lack of complete aerodynamic information cycles on which to base future design studies. The most promising opportunity for closing the data gap appeared to lie in research programs closely coordinated with systems in the final development stages. Since a large quantity of wind tunnel data were acquired in different tunnels with models of the XC-142A, this airplane presented a promising source for the correlation of wind tunnel and flight test data.

An investigation, under contract with the Air Force Flight Dynamics Laboratory, was undertaken to correlate the aerodynamic stability and control characteristics derived from XC-142A flight test data with corresponding characteristics determined from wind tunnel tests. At the time the study was initiated, several wind tunnel tests were completed and flight tests of the XC-142A airplane were in progress. Models of the XC-142A, a four-propeller tilt-wing V/STOL airplane, had been tested in the NASA Ames 40 x 80-foot full scale tunnel, the NASA Langley 30 x 60-foot free flight tunnel, the 17-foot section of the NASA Langley subsonic tunnel, the 7 x 10-foot and 21 x 23-foot sections of the VAD subsonic tunnel, and the Princeton University track facility.

The primary purpose of the investigation was to assess the degree of correlation attainable and to establish the problem areas where present wind tunnel testing techniques and correction techniques appear to be inadequate. It was hoped that the knowledge gained from this investigation would be sufficiently broad in application that the data requirements for future V/STOL developments could be defined.

The program was divided into three phases to identify the major areas of activity. The first phase involved the collection and correlation of data available from wind tunnel tests conducted in support of the aircraft development program. The next phase covered the collection of flight test data and extraction of the pertinent aerodynamic parameters from the Contractor's Category I flight tests of the XC-142A airplane. The final phase was the comparison of the wind tunnel and flight test data. However, after the first two phases were completed, it became apparent that the desired degree of correlation could not be attained with the available wind tunnel data. Also, the flight data available were not of suitable quality to allow a high degree of

confidence in inverse solutions for aerodynamic derivatives. Because of these unexpected results, the program effort was redirected toward improving the wind tunnel data correlation. In essence, another phase was added, which consisted of the collection and correlation of data obtained from wind tunnel tests conducted specifically for this program.

It should be emphasized that the inability to achieve good correlation for this program does not necessarily detract from the usefulness of the data for design and research purposes. However, it should also be pointed out that the results of this program indicate the design and research engineers need to be well acquainted with the test conditions and techniques used in order to properly use the data. As a specific example, satisfactory correlation was not obtained because of differences in propeller blade angles used by the various facilities; however, for design purposes the data have to be extrapolated to full scale and the particular "starting point" is not important.

This report describes the work performed under Contract AF 33(615)-2897 and presents the results obtained.

SECTION III

CORRELATION OF WIND TUNNEL DATA
ACQUIRED FOR AIRCRAFT DEVELOPMENT

The first phase of the program was intended to resolve any differences that existed in the wind tunnel data, obtained from the various facilities, before attempting to correlate wind tunnel and flight test data. In the beginning, the wind tunnel wall effects were expected to be the most significant factor in determining the degree of correlation attained. As the program progressed, it became apparent that certain other factors were just as significant.

Although a very large amount of testing was collectively performed, only a few runs were made by each facility during which the model configurations were similar enough for direct comparison. Furthermore, some of these runs were not suitable for comparison because of differences in test conditions. Since this study was undertaken after the wind tunnel tests were completed and the original contract did not permit additional testing, data specifically obtained for correlation purposes were never available.

1. TEST APPARATUS AND PROCEDURES

Although five models of the XC-142A airplane were tested in six different size test sections, only three of the facilities (four test sections) produced data that were suitable for the correlation program. Photographs of all the models installed in the test sections are shown in Figures 1 through 6. A comparison of the model geometry (increased to full scale) and airplane geometry is presented in Table I.

a. NASA AMES TESTS

Ames tested a 0.6 scale model in the 40 x 80-foot wind tunnel (Reference 1). Four tests were conducted; two were out of ground effect and two were in ground effect. The wing incidence angle was varied from 0 to 90 degrees. Tufts were attached to the model during almost all of the runs and sketches of the surface flow characteristics were drawn. A few photographs of the tufts were also obtained.

The model was mounted on a three support system using an external balance system to measure the aerodynamic forces and moments. Ground effect data were obtained using a fixed ground board. Each of the three-bladed propellers was driven by a 250 horsepower variable frequency electric motor. The motors were operated in parallel from a single power supply and rotated at approximately the same speed. The propeller speed was varied from 750 to 1550 RPM (+ 15 RPM). The majority of the testing was performed with a propeller blade angle setting of 10 degrees; however, a few runs were made with the following blade angle settings:

4

| INBOARD PROPELLERS | 20 | 12 | 14 | 14 | 14 | 22.5 | 6 | 14 |
| OUTBOARD PROPELLERS | 20 | 18 | 6 | 14 | 0 | 22.5 | 6 | OFF |

The blade angles were fixed during a run. During two of the tests, two of the propellers were instrumented with strain gage balances that measured the propeller thrust, torque, normal force, side force, pitching moment and yawing moment. The balances rotated with the propellers. The nacelles were moved approximately 10 inches aft of the normal location when the balances were installed. Discrepancies in the data obtained with these balances were never resolved and the data were not available for the correlation program. A powered tail rotor was used during the last two tests. The blade angle was set at 10 degrees and the thrust was measured with a strain gage balance.

The propeller thrust characteristics were obtained from propellers-on and propellers-off runs with the wing at zero incidence and the fuselage at -2 degrees, to approximate a zero lift condition. The tunnel dynamic pressure and propeller speed were varied for a range of thrust coefficients (T'_c) at 10 and 14 degrees propeller blade angle. With the propellers removed, a model drag coefficient was determined. This value of drag coefficient (sign reversed) was added to the propellers-on data to estimate thrust coefficient. These data were used to establish the nominal thrust coefficient for each run regardless of the wing incidence angle.

The normal procedure for conducting a run consisted of establishing a nominal thrust coefficient by setting the required combination of tunnel dynamic pressure and propeller speed; these values were then maintained essentially constant as the model attitude was varied. The dynamic pressure was allowed to vary slightly during a run, to avoid the difficulty and loss of time involved in maintaining a constant value. The coefficients were computed using the measured dynamic pressure for each data point. Both pitch and yaw runs were made. The tunnel dynamic pressure was varied from 0 to 10 PSF.

Tunnel wall effects corrections were not applied to the data. No corrections were applied to the data to account for the effects of the model support system for the out of ground effects tests. During the ground effect tests, the supports were not housed in wind shields and runs were made with the model removed to determine the tare loads on the supports. These corrections were applied to the data. The model weighed approximately 25,500 pounds and weight tare corrections were applied to the data.

b. NASA LANGLEY TESTS

(1) 7 x 10-Foot Tunnel (Modified 15.7 x 17-foot V/STOL Test Section)

Langley tested a 1/11-scale model in the modified 15.7 x 17-foot section of the 7 x 10-foot subsonic tunnel (Reference 2). Four tests were conducted; one out of ground effect and three in ground effect. The wing incidence angle was varied from 0 to 90 degrees. Tufts were attached to the model during almost all of the runs and photographs of the surface flow characteristics were obtained.

The model was mounted on a horizontal sting support using an internal strain gage balance to measure the aerodynamic forces and moments. Ground effect data were obtained using a fixed ground board during one test and using a moving belt ground board, with the belt moving and stationary, during the other two tests. Each of the four-bladed propellers was driven by a 7 1/2 horsepower variable frequency electric motor. The motors on one side of the wing were operated in parallel from one power supply and the motors on the opposite side were operated in parallel from another power supply. This permitted the two pairs of motors to be operated at different speeds while maintaining the same speed for the motors in a pair within $\pm$ 15 RPM. The propeller speed was maintained constant at either 7000 or 7500 RPM, except during asymmetric thrust runs. The majority of the testing was performed with a fixed propeller blade angle setting of 12 degrees. A few runs were made with a blade angle setting of 8 degrees. The blade angles were set with the propellers in a bench jig, but when they were installed on the model, they did not develop the same thrust for the same rotational speed. Therefore, the blade angles were altered by an iterative process until the same thrust was developed by each propeller. The final blade angles were not measured and, therefore, must be regarded as nominal values. The propeller forces were measured with internal four-component strain gage balances. Propeller thrust, normal force, pitching moment and torque were measured for the propellers on one side of the wing and thrust, side force, yawing moment, and torque for the propellers on the other side.

The propeller thrust characteristics were also obtained by performing runs with the propellers on and off the model with the wing and fuselage at zero angle of attack. The tunnel dynamic pressure was varied while maintaining a constant propeller speed to obtain a range of thrust coefficients (C_{T_s}). With the propellers removed, a model drag coefficient was determined. This value of drag coefficient (sign reversed) was added to the propellers-on data to estimate thrust coefficient. These data were used to establish the nominal thrust coefficient for each run, regardless of the wing incidence angle.

The normal procedure for conducting a run consisted of establishing a nominal thrust coefficient by setting the required tunnel dynamic pressure and propeller speed (7000 or 7500 RPM); the dynamic pressure and propeller speed were then maintained constant as the model attitude was varied. Both pitch and yaw runs were made. The tunnel dynamic pressure was varied from 0 to 10 PSF.

Tunnel wall effect corrections were not applied to the data. No corrections were applied to the data to account for the interference effects of the model support system. The model weighed approximately 175 pounds and weight tare corrections were applied to the data. During the out of ground effect test, the model was rolled 90 degrees to eliminate the weight tare in the model longitudinal forces.

6

(2) <u>30 x 60-Foot Tunnel</u>

Langley also tested a 1/9-scale model in the 30x 60-foot tunnel (Reference 3). The majority of the test was devoted to free-flight testing the model but a few runs were made to obtain static force data. The wing incidence angle was varied from 0 to 90 degrees. The model was dynamically scaled. The propellers were interconnected by a system of shafts and gear boxes and were driven by a pneumatic motor. During the free-flight testing, the pneumatic and electric power and control signals were supplied to the model through a flexible trailing cable which was made up of wires and light plastic tubes. During the static force testing, the model was mounted on a sting support and the aerodynamic forces were measured with an internal strain gage balance.

The free-flight testing consisted of slow constant-altitude transitions and simulated descending-flight conditions at low transition speeds. The results were mainly qualitative and consisted of pilots' observations and opinions of the behavior of the model. The force testing was made to help document some of the aerodynamic, stability and control characteristics of the model. The procedure for conducting the force runs consisted of setting the fuselage at zero angle of attack, varying the propeller rotational speed and the tunnel dynamic pressure until the longitudinal force was zero, and then varying the model attitude with the propeller speed and tunnel dynamic pressure held fixed. Propeller thrust was not determined during the test.

c. PRINCETON UNIVERSITY TESTS

A 0.10 scale model was tested in the Princeton dynamic model track facility (Reference 4). The primary purpose of the test was to determine the dynamic stability characteristics of the model; however, a few static force runs were also made. Four wing incidence angles were tested; 40, 60, 70, and 90 degrees.

The model was dynamically scaled. The four main propellers and tail rotor were interconnected by a system of flexible shafts and gear boxes and driven with a five horsepower electric motor. The model had electrically driven collective pitch change on each of the propellers. The collective pitch system was arranged so that the left and right propellers were separately controlled, thus providing differential collective pitch for roll trim. Wing incidence, flaps, ailerons, and the horizontal tail were power operated so that full transition runs could be made with required programming of all items.

The model was mounted on a boom which was attached to a servo-driven carriage that traveled on a 750-foot track. The operation of the carriage-track system consisted of flying the dynamically scaled model in an enclosed area, and following the natural motions of the model with a slaved carriage, thereby providing a frame of reference for measuring the time histories of the motion. Positioning servo-mechanisms operating on the error signal (the difference between the model position and the carriage position) caused the carriage to follow the model without restraining the motion of the model.

Static testing was performed by commanding the carriage movement in accordance to pre-selected velocity profiles or programming angle of attack changes while driving the carriage at constant velocities. During the static testing, the model was rigidly attached to the carriage and the aerodynamic forces were measured with strain gage balances. Propeller thrust was adjusted at the beginning of each run to obtain trim conditions with the fuselage at zero angle-of-attack; however, the thrust was not measured.

d. VAD TESTS

A 0.11 scale model was tested in the 7 x 10-foot and modified 21 x 23-foot V/STOL test sections of the VAD low speed wind tunnel (References 5 through 10). Six tests were conducted: one in ground effect and five out of ground effect. This model was also tested in an open air hover facility (References 11 and 12). The wing incidence angle was varied from 0 to 90 degrees during these tests. Tufts were attached to the model during almost all of the runs and photographs of the surface flow characteristics were obtained.

During tests in the 7 x 10-foot section, the model was mounted on a two-support system and the aerodynamic forces were measured with an external beam balance system. During tests in the 21 x 23-foot section and hover facility, the model was mounted on a single-support and the aerodynamic forces were measured with an internal strain gage balance. Ground effect data were obtained by varying the height of the model above the floor in the 21 x 23-foot section and the hover facility. Each of the four-bladed main propellers were driven by a 25 horsepower hydraulic motor. The three-bladed tail rotor was driven by a 10 horsepower hydraulic motor. The motors were individually controlled such that the speed of each motor could be varied between 0 and 10,000 RPM (18,000 RPM for the tail rotor). The accuracy in setting and controlling the speed was approximately ±30 RPM. The majority of the testing was performed with a fixed nominal blade angle of 14 degrees. A few runs were made with the outboard propellers set at a nominal 14 degrees and the inboard propellers set at 10 degrees. A defect in the manufacture of the blade angle setting devices caused an error in the blade angles. The right propellers (viewed from behind the model) had an error of 1.33 degrees and the left propellers had an error of 3.83 degrees. For a nominal blade angle setting of 14 degrees, the actual angles were 15.33 degrees for the right and 17.83 degrees for the left propellers. This condition existed during the propeller calibration and all tests except the last. The tail rotor blade angle settings were -20, 0, and +20 degrees. A device to measure the propeller thrust, normal force and pitching moment was fabricated; however, data obtained with the device were insufficiently accurate to justify its use. The thrust of each propeller was measured with a strain gage balance that incorporated a sliding, splined shaft which isolated the propeller shaft from the motor in the thrust direction. The tail rotor thrust and pitching moment were measured using a two-component strain gage balance located in the tail rotor boom.

The thrust characteristics of each propeller and the tail rotor (removed from the model) were obtained from tests in both the 7 x 10- and 21 x 23-foot test sections (Reference 13). A hydraulic motor and its housing were mounted on a sting support in the 21 x 23-foot section and on a two strut tandem support in the 7 x 10-foot section. Thrust was measured for several blade angles over a range of tunnel dynamic pressures and propeller rotational speeds. Most

8

of the runs were made with the propeller disk plane perpendicular to the free
stream flow. The thrust coefficients $(C_{T,s})$ obtained from these calibration
runs were used to set the tunnel dynamic pressure and propeller speed for all
of the model test runs, regardless of the wing incidence angle.

The normal procedure for conducting a run consisted of establishing a
nominal thrust coefficient by setting the required combination of tunnel
dynamic pressure and propeller speed; the model attitude was then varied with
the tunnel dynamic pressure and propeller speed held constant. Both pitch and
yaw runs were made. The tunnel dynamic pressure was varied from 0 to 40 PSF in
the 7 x 10-foot section and from 0 to 2.81 PSF in the 21 x 23-foot section.

Tunnel wall effect corrections, using the classical method (Reference
14) were applied to the data obtained in the 7 x 10-foot section, but not to the
data obtained in the 21 x 23-foot section. Corrections, obtained experimentally,
were applied to the data obtained in the 7 x 10-foot section to account for the
effects of the model support system. No corrections were applied to the data
obtained in the 21 x 23-foot section or hover facility to account for the effects
of the support system. The model weighed approximately 650 pounds and weight
tare corrections were applied to the data for all tests.

2. DATA COMPARISONS

Variations in test techniques, data reduction methods, and definition of
terms used by the different facilities prevented direct comparisons of the data.
Considerable manipulation of the data was necessary before useful comparisons
were possible. The data from the various facilities were assembled and reviewed
in order to select test runs suitable for comparison. The primary purpose of
the Langley free-flight tests and the Princeton track tests was to determine
the dynamic characteristics of the model. While a very limited amount of static
force data was also obtained in the two tests, correlation of these data was not
possible because propeller thrust was not measured. Basic data suitable for
correlation were available from tests at Ames, Langley, and VAD for wing/flap
combinations, ranging from cruise configuration $(0^\circ/0^\circ)$ to low speed STOL config-
uration $(40^\circ/60^\circ)$. These data were reduced to coefficient form using uniform
data reduction methods. The aerodynamic coefficients were based on the free
stream dynamic pressures. Tunnel wall corrections, using the classical method
(Reference 14) were applied only to the VAD 7 x 10-foot test section data.
Correlation of the longitudinal characteristics was attempted first, and because
of the degree of correlation attained, it was not considered advisable to con-
tinue with the lateral-directional characteristics. Comparisons of both pro-
pellers-off and propellers-on data are discussed in the following paragraphs.

a. PROPELLERS-OFF

Comparisons of propellers-off data from each of the facilities are
presented in Figure 7. The lift curve slopes are in good agreement. The maximum
lift for Langley and VAD is in fair agreement for the flaps up configuration,
when corrected for Reynolds number effect. There is considerable difference in
the increase in lift with flap deflection obtained from Langley and VAD (data
not available from Ames). The larger increase in lift with flap deflection
obtained by VAD is, at least in part, due to the use of grit on the model to
increase the local effective Reynolds number, discussed later. The angle of
attack for maximum lift and the zero-lift drag are not in good agreement.

9

b. PROPELLERS-ON

Comparisons of the propellers-on data from each of the facilities are presented in Figures 8 through 14. It was not possible to make comparisons of data from all three facilities together; therefore, each of the figures compares data from two of the facilities.

(1) Langley and VAD

Data for a wing/flap configuration of $0^{\circ}/0^{\circ}$ and nominal thrust coefficients of 0.05 and 0.07, are presented in Figure 8. The lift curve slope is slightly larger for VAD than Langley. The VAD maximum lift is only slightly greater than for the propellers-off case, but the Langley lift continues to increase without evidence of stall. This disagreement may be caused by the difference in thrust coefficient; as these data indicate, the thrust coefficient increases more rapidly with angle of attack for Langley than VAD. However, the drag is also larger for Langley than VAD. Because of these disagreements, the pitching moment comparison is meaningless.

Comparison of a $20^{\circ}/60^{\circ}$ wing/flap configuration for a nominal thrust coefficient of 0.6 is presented in Figure 9. The slopes of the lift curves are in good agreement. The maximum lift and associated angle of attack are not consistent. Part of this discrepancy can be explained by the differences in the thrust coefficients for these runs. The shapes of the drag and pitching moment curves are similar for the two facilities but different in magnitude. VAD used grit on the model to increase the local effective Reynolds number during all runs with the flap deflected. Additional comparisons of the $20^{\circ}/60^{\circ}$ configuration for nominal thrust coefficients of 0.7 and 0.8 showed the same general trends.

A comparison of the $20^{\circ}/60^{\circ}$ configuration cross-plotted to obtain data at a constant actual thrust coefficient (not nominal), is shown in Figure 10. The shapes and slopes of the curves are in good agreement; however, the magnitudes are not. The lift is consistently higher and drag lower for the VAD data.

Comparison of a wing/flap configuration of $40^{\circ}/60^{\circ}$ for a nominal thrust coefficient of 0.9 is shown in Figure 11. The propeller blade angles for the two Langley runs are different, 8 and 12 degrees. The slope of the lift curve and maximum lift from VAD agree well with the Langley 8 degree blade angle run, but the agreement is poor with the 12 degree run. The opposite is true with the thrust coefficients. The thrust coefficients for VAD agree well with the Langley 12 degree blade angle run and the agreement is poor with the 8 degree run. The drag and moment comparisons are meaningless because of the lift and thrust differences.

(2) Langley and Ames

Comparison of a wing/flap configuration of $0^{\circ}/0^{\circ}$ for a nominal thrust coefficient of 0.4, is presented in Figure 12. The lift curves are in fairly good agreement, although the Ames data indicate a slightly greater slope. The drag curves are in fair agreement, which indicates the actual thrust coefficients were about the same. The difference in the thrust coefficient curves probably represents the difference in methods of determining thrust, which is discussed later. The moment curves are also in fairly good agreement considering the agreement of lift and drag.

10

Comparison of the 20°/60° wing/flap configuration, for a nominal thrust coefficient of 0.59, is presented in Figure 13. Again, the slopes of the lift curves are in good agreement. The angles of attack for maximum lift are in fair agreement, but the lift values from Langley are greater than Ames throughout the angle of attack range. The shapes of the drag and moment curves are similar, but the magnitudes are not in very good agreement. Again, there is considerable difference in the thrust coefficient curves.

(3) Ames and VAD

Comparison of a 30°/60° wing/flap configuration, for a nominal thrust coefficient of 0.84, is shown in Figure 14. The slopes of the lift curves are in good agreement, but the VAD lift values are larger throughout the angle of attack range. The angle for maximum lift, the drag curves, and thrust coefficients are in fair agreement. The scatter in the Ames thrust coefficient data is caused by the variation in tunnel dynamic pressure. Comparison of the moment curves is meaningless because of the differences in lift and drag. The leading edge flap was set at 90 degrees on the VAD model and 80 degrees on the Ames model.

3. DISCUSSION OF RESULTS

An unexpected result of the correlation program was the finding that certain controllable factors contributed as much difficulty in correlating the data as the tunnel wall effects. Many factors were found to affect the correlation. Some of the factors possibly represent the state-of-the-art, such as the tunnel wall effects; while other factors are readily controllable, such as the test techniques. The factors contributing to the lack of agreement in the data can be grouped into five main categories: model configurations, data reduction, propeller characteristics, special test techniques, and wind tunnel corrections.

a. MODEL CONFIGURATIONS

Model configurations became a factor by the use of three different models without completely common geometric characteristics. Differences existed in the basic models, as well as the configurations tested. A summary of the more significant differences in the basic models (from Table I) were as follows:

Ames: Larger wing area, geometric wing twist, larger chord, smaller horizontal tail, no dorsal, no gear pods, nacelles were not contoured, three-bladed propellers, inboard propellers were not tilted.

Langley: Had propeller spinners, inboard propellers were not tilted, no tail rotor.

VAD: Had propeller spinners.

Some of the differences existed because of fabrication costs and others because of the airplane configuration changes after the models were constructed and these changes were not incorporated in all the models.

Each test was conducted for specific purposes such as stability and control, performance, slat optimization, and improved descent capability. Because of these different objectives, a wide variation of model configurations were tested. Only a few runs were made by each facility during which the model configurations were similar enough for direct comparison of the data. It was impossible to evaluate the effects of the differences in model configurations because of the presence of other factors, discussed subsequently, that simultaneously affected the data.

b. DATA REDUCTION

Data reduction became a factor in the correlation by the lack of a common base for comparing data from the various tests. Conventional airplane force coefficients are based on the free stream dynamic pressure. However, since these coefficients approach infinity as the hover condition is approached, it has become the practice of some facilities to base the coefficients on the slipstream dynamic pressure for V/STOL tests. The definition of the dynamic pressure, used in reducing the data to coefficient form, was different for each facility. Ames selected the tunnel dynamic pressure. Langley selected the slipstream dynamic pressure (which varied during a run because the thrust varied with model attitude). VAD selected a nominal slipstream dynamic pressure, based on the average thrust and tunnel dynamic pressure at zero angle-of-attack. Therefore, a constant value was used in the data reduction for each run. These differences in the definition of the dynamic pressure prevented a direct comparison of the data. A comparison of data reduced by the different methods is presented in Figure 15. The maximum lift coefficient and corresponding angle-of-attack are shown to be affected by the method of data reduction. Differences in data reduction methods did not prevent the eventual correlation of the data, of course, but additional computations were required.

The difference in definition of thrust coefficient ($C_{T,s}$ and T'_c) also prevented a direct comparison of data. Although conversion from one definition to another is quite simple, another calculation is necessary.

c. PROPELLER CHARACTERISTICS

Propeller characteristics have a pronounced effect on the aerodynamic forces on a tilt-wing V/STOL airplane because almost all of the wing is submerged in the propeller slipstream. Consequently, measurement of all the propeller forces and moments are desirable, but measurement of thrust is essential.

Langley and VAD measured the thrust of each propeller directly. Ames determined thrust from propellers-on and propellers-off runs, using data obtained from the main balance. This method actually provides the net thrust, including slipstream drag and other factors, and is only applicable for the condition measured, zero lift and cruise configuration. For a small angle-of-attack range, this method may be satisfactory; however, for a tilt-wing configuration, the angle-of-attack range is too large for it to be considered acceptable. Data, for which the thrust was measured directly, indicated a large increase in thrust with increase in angle of attack for values of thrust coefficient ($C_{T,s}$) between 0 and 0.6. The variation of thrust with angle of attack is significant up to a thrust coefficient of about 0.95. Determination

12

of thrust by this method has the further disadvantage of providing only the total (net) thrust rather than the thrust of each propeller.

The propeller data from both Langley and VAD (Figures 16 and 17) indicated a different thrust for each propeller, whereas the thrust should have been uniform. The reason for this variation is not known; it could be caused by the accuracy of setting the propeller speed, variation in tunnel flow conditions, accuracy in thrust measurement, or other such variables. Assuming that the variation in thrust between propellers is not caused by the measuring accuracy, a difference in the distribution of thrust could account for part of the disagreement between two runs that are otherwise similar. Ames reported (Reference 1) that, for the same total thrust, operating with more thrust on the inboard propellers than on the outboard propellers, increased the maximum lift coefficient and descent capability. As an example of the magnitude of the variation in spanwise thrust distribution, during one Langley run, the average thrust coefficient ($C_{T,s}$) was 0.02 and the individual thrust coefficients were -0.09, +0.20, -0.02, and -0.05. While the spanwise distribution of thrust may be significant in the aerodynamic coefficients, no attempt was made by any of the facilities to maintain the same thrust distribution from run to run other than to establish a particular propeller speed and tunnel dynamic pressure.

Each facility used nominal values of thrust coefficient as the basis for establishing the test conditions for a run. However, the methods of determining nominal thrust were different. Ames and Langley obtained the variation of nominal thrust coefficient with tunnel dynamic pressure and propeller speed from propellers-on and propellers-off runs, with the wing and fuselage at zero angle of attack. VAD obtained this variation from propeller-nacelle alone runs, with the thrust axis at zero angle of attack. These data were used to establish the test conditions for a desired nominal thrust coefficient for all wing/flap combinations. As a result of this procedure, the actual thrust coefficient values were not the same and a direct comparison was usually not possible. Only a limited amount of data was available to permit cross-plotting the data to obtain information at the same thrust coefficient.

The XC-142A airplane propellers operate at constant speed with varying blade angle, whereas the wind tunnel tests were conducted by varying the propeller speed with a fixed blade angle. The usual practice for conventional propeller driven aircraft has been to match the model and airplane propeller advance ratio using two-blade angles; one for low speed and one for high speed. This, of course, is not economically practical for tilt-wing tests as numerous blade angles would be required. Consequently, each facility conducted the majority of runs with a single blade angle. The nominal blade angles were 10, 12, and 14 degrees for Ames, Langley, and VAD, respectively.

Ames and Langley conducted a few runs (Reference 2) to determine the effect of using different blade angles. Langley reported that reducing the propeller blade pitch angle from 12 to 8 degrees made a significant improvement in the descent capability. The data from Langley and VAD did not show the same variation of thrust coefficient with angle of attack. As indicated in Figure 18, the rate of change of thrust with angle of attack increased with a decrease in blade angle. Also, the propeller forces and moments represent a significant percentage of the total forces and moments applied to the model.

13

Sufficient data were not available to determine the effect of blade angle on the propeller forces and moments. Since only Langley was successful in measuring all of the propeller forces and moments, comparisons of these parameters were not possible.

Since these propeller characteristics have been shown to produce such a pronounced effect on data correlation, they must be similar during data acquisition to attain a satisfactory degree of correlation. The thrust must be accurately measured and controlled to produce similar thrust coefficients and thrust distributions. Also, the propeller blade angles must be selected on the same basis to assure the same slipstream characteristics and propeller forces and moments.

d. SPECIAL TEST TECHNIQUES

Test techniques are always pertinent to the acquisition of reliable data, and this appears to be especially true of V/STOL data to be used in any correlation studies. In the tests providing data for this correlation study, the normal procedure for acquiring data was similar for each facility. Each facility, however, used certain unique test techniques that affected the data correlation. The most significant of these were the way flow visualization was provided and the manner in which control of local Reynolds number was maintained.

One of the main purposes of wind tunnel tests of a tilt-wing configuration is the investigation of the wing stall characteristics. In order to obtain a visual indication of the flow separation pattern, tufts were attached to the model wings during almost all the runs. The tufts were not attached to the models in the same manner or in the same locations. The tufts on the VAD model were attached with spanwise lengths of tape that produced small chordwise steps in the contour of the upper surface of the wing at each row of tufts. During some of the runs with the tufts attached in this manner, the leading edge of the tape lifted somewhat and caused the tape to act as a spoiler. The tufts on the Langley model were attached with chordwide lengths of tape that produced a small streamwise step at each tuft. Ames attached each tuft individually with a small piece of tape. Also, the tuft spacing differed for each model at the various facilities primarily because of the method of attaching the tufts. Yet, the effect of tufts on force data were not fully known since only a few runs were made for this purpose. The tufts generally caused an increase in drag and a decrease in lift. However, tufts were accepted in these tests because of their value in providing flow visualization.

Another technique was the control of the local effective Reynolds number. VAD used Carborundum grit to control boundary layer transition and improve the flap effectiveness. The grit was attached by a thin layer of lacquer to the lower surface of the wing and on the flaps. The pattern of the grit was not the same for the various flap deflections. This technique was not used on the Ames or Langley model and can account for some of the discrepancies in the lift curves. As shown in Figure 7, VAD increased the flap effectiveness significantly by increasing the local effective Reynolds number. These differences in test techniques are considered major factors in preventing the attainment of the desired degree of correlation.

14

e. WIND TUNNEL CORRECTIONS

Several corrections are typically applied to the basic wind tunnel
data to account for the conditions that exist in the tunnel, but not in free
air. These corrections consist of the various tares, model support system
effects, and tunnel wall effects.

The tares are caused by temperature changes, model weight, pressurized
tubing, and similar factors. These tares are usually small and readily deter-
mined. However, with the lower tunnel dynamic pressure associated with V/STOL
testing, the tare loads can represent a significant percentage of the total
measured load. It was assumed that these tares were correctly evaluated and
did not affect the data correlation.

The conventional low speed tunnel model support system, using an
external balance, have a drag load (tare) and affect the free air flow about
the model (interference). Support systems using internal balances have only
the interference effects. The models were supported in a different manner in
each facility. The effects of the model support system were determined only
for the VAD model in the 7 x 10-foot section. It was not known to what extent
the other model supports affected the data correlation.

Wind tunnel wall effects for V/STOL airplanes cannot be adequately
determined by the same methods used for conventional airplanes. The theore-
tical methods to calculate V/STOL wind tunnel wall corrections (References 15
and 16) require a large range of thrust coefficients to permit cross-plotting
the data. Sufficient data were not available to make a proper evaluation of
these tunnel wall corrections. The magnitude of the tunnel wall effects depends
on the size of the model relative to the size of the test section. The relation-
ship between the model size and test section size for the Ames, Langley, and
VAD tests is shown in Figure 19. Large wall effects would be predicted for the
Ames tunnel and the VAD 7 x 10-foot section. Small wall effects would be
predicted for the Langley tunnel and the VAD 21 x 23-foot section. Furthermore,
the magnitude of the corrections for the latter two test sections should be
about the same. However, comparison of data from these sections (Figure 10)
indicates a significant difference in both lift and drag coefficients,
apparently attributable to other factors.

One of the problems associated with testing V/STOL models is the
accurate measurement of dynamic pressure when the dynamic pressure is a
very low value. For propeller-driven models, the ratio of the slipstream
to tunnel dynamic pressure must be large. Therefore, the maximum tunnel
dynamic pressure is determined by the limitation of either the model motors
or the tunnel drive system. The limitation of the model motors, of course,
is determined by the allowable motor size. The tunnels that have been
modified to provide a second larger test section, the purpose of which is to
reduce the effects of the tunnel walls, use the same drive system. Therefore,
the maximum dynamic pressure obtainable in this section is considerably less
than in the smaller section. The tunnel dynamic pressure variation with
nominal thrust coefficient for the Ames, Langley, and VAD tests is shown in

15

Table II. Each facility tested at values of dynamic pressure below 2.0 PSF. The accuracy of measuring the dynamic pressure with a typical micromanometer is about 0.05 PSF (0.01 inches of water). Therefore, at the lower values of dynamic pressure, instrument limitations should introduce a significant error and the errors may be additive when comparing data from two facilities.

TABLE I   COMPARISON OF AIRPLANE/MODEL GEOMETRY

WING	XC-142	Ames 0.6 Scale	Langley (Force) 1/11 Scale	VAD 0.11 Scale	Princeton 1/10 Scale	Langley (Free Flight) 1/9 Scale
Area, sq ft	534.37	545.83	534.82	534.38	534.38	534.6
Span, ft	67.55	67.50	67.47	67.50	67.50	67.5
Aspect Ratio	8.53	8.35	8.53	8.53	8.53	8.53
Taper Ratio	0.61	0.55	0.61	0.61	0.61	0.61
Sweepback of L.E., degrees	6.48	6.67	6.50	6.48	6.50	0.48
Sweepback of 1/4 chord, degrees	4.13	4.70	4.13	4.13	4.10	4.13
Sweepback of T.E., degrees	0	-1.30	0	0	0	0
Dihedral Angle, degrees	-2.12	-2.12	-2.70	-2.12	-2.10	-2.12
Geometric Twist, degrees	0	3.70 Washout	0	0	0	0
Root Chord, ft	9.83	10.44	9.83	9.83	9.83	9.83
Tip Chord, ft	6.0	5.74	6.0	6.0	6.0	6.0
Mean Geometric Chord						
Length, ft	8.072	8.319	8.072	8.072	8.072	8.072
Spanwise Location From B.L. O, ft	15.51	15.25	15.50	15.50	15.50	15.50
Location of L.E. From Nose of Fuselage, ft	235.47	240.55	235.18	235.47	235.47	235.47

TABLE I COMPARISON OF AIRPLANE/MODEL GEOMETRY (Continued)

WING (Cont.)		XC-142	Ames 0.6 Scale	Langley (Force) 1/11 Scale	VAD 0.11 Scale	Princeton 1/10 Scale	Langley (Free Flight) 1/9 Scale
Airfoil Section		63-318	23017 Mod LE	63-318	63-318	63-318	63-318
Wing Pivot Location Fuselage Station		274.5	274.04	274.44	274.50	274.50	274.50
Water Line		157.0	160.0	156.0	157.0	157.0	157.0
LEADING EDGE SLATS							
Spanwise Location, % Semispan							
Inboard, Root		44.98	43.6	44.13	45.0	45.0	45.0
Tip		68.90	68.3	69.13	68.0	69.0	69.0
Outboard, Root		11.3	10.0	10.0	11.3	11.3	10.0
Tip		11.3	10.0	10.0	11.3	11.3	10.0
Area, Inboard (Each), Sq Ft		10.34	10.0	9.9	9.95	10.3	9.5
Outboard (Each), Sq Ft		2.56	2.77	2.4	2.6	2.6	2.75
Slat L.E. Location From Wing L.E.,	Inboard, Root	15.88	16	16	16	16	16
	Tip	9.08	9	9	9	9	9
% Wing Chord	Outboard, Root	11.0	9	9	11	11.0	11
	Tip	11.0	9	9	11	11.0	11

TABLE I COMPARISON OF AIRPLANE/MODEL GEOMETRY (Continued)

LEADING EDGE SLATS (Cont.)		XC-142	Ames 0.6 Scale	Langley (Force) 1/11 Scale	VAD 0.11 Scale	Princeton 1/10 Scale	Langley (Free Flight) 1/9 Scale
Slat Gap, Between	Inboard, Root	4.85	5	5	5	5	5
T.E. of Slat and	Tip	4.27	5	4	4	4	4
Wing Upper Surface,	Outboard, Root	4.0	4	4	4	4	4
% Wing Chord	Tip	4.0	4	4	4	4	4
Vertical Distance of	Inboard, Root	3.0	3	3	3	3.0	3
Slat Nose Ref. Point	Tip	1.09	3	0.5	1.0	1.1	1.1
Below Wing Chord	Outboard, Root	0	0	0	0	0	0
Plane, % Wing Chord	Tip	0	0	0	0	0	0
TRAILING EDGE FLAPS (DOUBLE SLOTTED)							
Flap Span,	Inboard, Root	15.43	15.06	14.51	15.05	15.20	15.04
% Wing	Tip	35.74	35.39	37.15	36.55	34.50	36.5
Semispan	Center, Root	43.60	43.62	43.37	42.47	44.55	42.5
	Tip	78.25	78.19	79.95	79.26	77.20	79.2
	Outboard, Root	86.08	86.42	85.87	85.18	87.10	85.1
	Tip	98.92	100.0	99.0	99.0	99.70	99.0
Flap Chord, In Flap Chord Plane, % Wing Chord		33.0	33.0	33.0	33.0	33.0	33.0

TABLE I   COMPARISON OF AIRPLANE/MODEL GEOMETRY (Continued)

TRAILING EDGE FLAPS (DOUBLE SLOTTED) (Cont.)			XC-142	Ames 0.6 Scale	Langley (Force) 1/11 Scale	VAD 0.11 Scale	Princeton 1/10 Scale	Langley (Free Flight) 1/9 Scale
Flap Area, In		Inboard	19.09	19.95	21.30	20.15	19.05	20.10
Flap Chord Plane,		Center, Including Ail.	29.00	29.15	30.50	30.80	27.20	30.60
(One Side), Sq Ft		Outboard, Including Ail.	9.10	9.16	9.18	9.68	8.85	9.75
Vane Span,		Inboard, Root	15.53	15.06	14.51	15.05	15.20	15.05
% Wing		Tip	35.66	35.39	37.15	36.55	34.50	36.5
Semispan		Center, Root	43.69	43.63	43.37	42.47	44.55	42.5
		Tip	78.00	78.19	79.95	79.26	77.20	79.2
		Outboard, Root	86.26	86.42	85.87	85.16	87.10	85.1
		Tip	98.94	100.0	99.0	99.0	99.70	99.0
Vane Chord, In Vane Chord Plane % Wing Chord			15.4	15.4	15.4	15.4	15.4	15.4
Vane Area, In		Inboard	9.24	9.80	10.43	9.90	8.86	9.87
Vane Chord Plane		Center	13.55	13.60	14.25	14.40	12.7	14.29
(One Side), Sq Ft		Outboard	4.09	4.29	4.29	4.51	4.14	4.55

20

TABLE I COMPARISON OF AIRPLANE/MODEL GEOMETRY (Continued)

TRAILING EDGE FLAPS (DOUBLE SLOTTED) (Cont.)		XC-142	Ames 0.6 Scale	Langley (Force) 1/11 Scale	VAD 0.11 Scale	Princeton 1/10 Scale	Langley (Free Flight) 1/9 Scale
Vane Orientation	L.E. (Forward)	0.68	0.65	0.65	0.70	0.69	.69
Flap Ext. 60°, Measured From Wing T.E. 77.3% Chord, % Wing Chord	Upper Surface (Below)	1.99	2.0	2.0	2.04	2.0	2.0
	Deflection, Degrees	30.9	31	31	30	31	31
Flap Orientation,	L.E. (Forward)	4.53	4.5	4.53	4.50	4.5	4.5
Ext. 60°, Measured From Vane T.E., % Wing Chord	Upper Surface (Below)	3.39	3.4	3.42	3.44	3.4	3.4
AILERONS, PLAIN							
Spanwise Location % Wing Semispan	Center, Root	43.30	43.62	43.37	42.47	44.55	42.5
	Tip	78.40	78.19	79.95	79.26	77.20	79.2
	Outboard, Root	86.03	86.42	85.87	85.18	87.10	85.1
	Tip	99.61	100.0	99.0	99.0	99.70	99.0
Chord, Aft of Hinge Line, % Wing Chord		25.0	25.0	25.0	25.0	25.0	25.0
Area, Aft. of Hinge Center		22.28	22.10	23.1	23.31	20.6	23.2
Line (One Side) Soft Outboard		7.11	6.93	6.95	7.85	6.70	7.39

TABLE I COMPARISON OF AIRPLANE/MODEL GEOMETRY (Continued)

UNIT HORIZONTAL TAIL	XC-142	Ames 0.6 Scale	Langley (Force) 1/11 Scale	VAD 0.11 Scale	Langley (Force) 1/11 Scale	Princeton 1/10 Scale	Langley (Free Flight) 1/9 Scale
Area, Sq Ft	163.5	140.0	163.5	163.6	163.5	140.0	163.5
Span, Ft.	31.14	26.67	31.16	31.14	31.14	26.67	31.14
Aspect Ratio	5.93	5.08	5.93	5.93	5.93	5.08	5.68
Taper Ratio	0.5	0.5	0.5	0.5	0.5	0.5	0.50
Sweepback of L.E., Degrees	12.66	14.7	12.66	12.66	12.66	14.7	12.6
Sweepback of 1/4 Chord, Degrees	9.57	11.0	9.57	9.58	9.57	11.0	9.5
Sweepback of T.E.	0.0	0.0	0.0	0.0	0.0	0.0	0.0
Dihedral Angle (Root Chord at B.L.O. To Tip Chord)	0.0	0.0	0.0	0.0	0.0	0.0	0.0
Geometric Twist, Degrees	0.0	0.0	0.0	0.0	0.0	0.0	0.0
Root Chord, Ft.	7.0	7.0	7.0	7.0	7.0	7.0	7.0
Tip Chord, Ft.	3.5	3.5	3.5	3.5	3.5	3.5	3.5
Mean Geometric Chord							
Length, Ft.	5.44	5.44	5.44	5.44	5.44	5.44	5.44
Spanwise Location From B.L.O., Ft.	6.92	5.93	6.92	6.92	6.92	5.93	6.92
Fuselage Station of L.E.	549.67	545.4	549.72	549.67	549.72	545.5	546.5

22

TABLE I COMPARISON OF AIRPLANE/MODEL GEOMETRY (Continued)

	XC-142	Ames 0.6 Scale	Langley (Force) 1/11 Scale	VAD 0.11 Scale	Princeton 1/10 Scale	Langley (Free Flight) 1/9 Scale
VERTICAL TAIL (Cont.)						
Mean Geometric Chord (Continued)						
Height Above W.L. 100 ($i_t=0$) Inches	110.0	105.0	109.5	110.0	105.0	110.0
Tail Arm, l_n/c (1/4 chord wing to 1/4 chord tail MGC)	3.07	3.91	3.06	3.07	3.02	3.02
Airfoil Section Root	0015	0015	0015	0015	0015	0015
Tip	0012	0012	0015	0012	0012	0012
Hinge Line % Root Chord (Tail)	31.55	36.50	33.38	31.55	32.4	29.76
% MGC (Tail)	11.99	18.37	14.15	11.99	13.0	10.44
Height Above W.L. 100, Inches	108.0	105.0	109.5	108.0	105.0	105.5
Fuselage Station	557.5	557.4	559.0	557.5	554.0	553.4
VERTICAL TAIL						
Area (Including Rudder) Sq Ft	130.0	129.7	130.0	130.0	129.8	130.4
Span, Inches	187.5	187.0	187.5	187.0	187.0	187.0
Aspect Ratio	1.88	1.87	1.88	1.87	1.87	1.87
Taper Ratio	0.25	0.25	0.25	0.25	0.25	0.25
Sweepback of L.E., Degrees	32.6	32.7	32.6	32.6	32.6	32.6
Sweepback of 1/4 Chord, Degrees	26.0	25.7	26.0	26.0	26.0	26.0

TABLE I COMPARISON OF AIRPLANE/MODEL GEOMETRY (Continued)

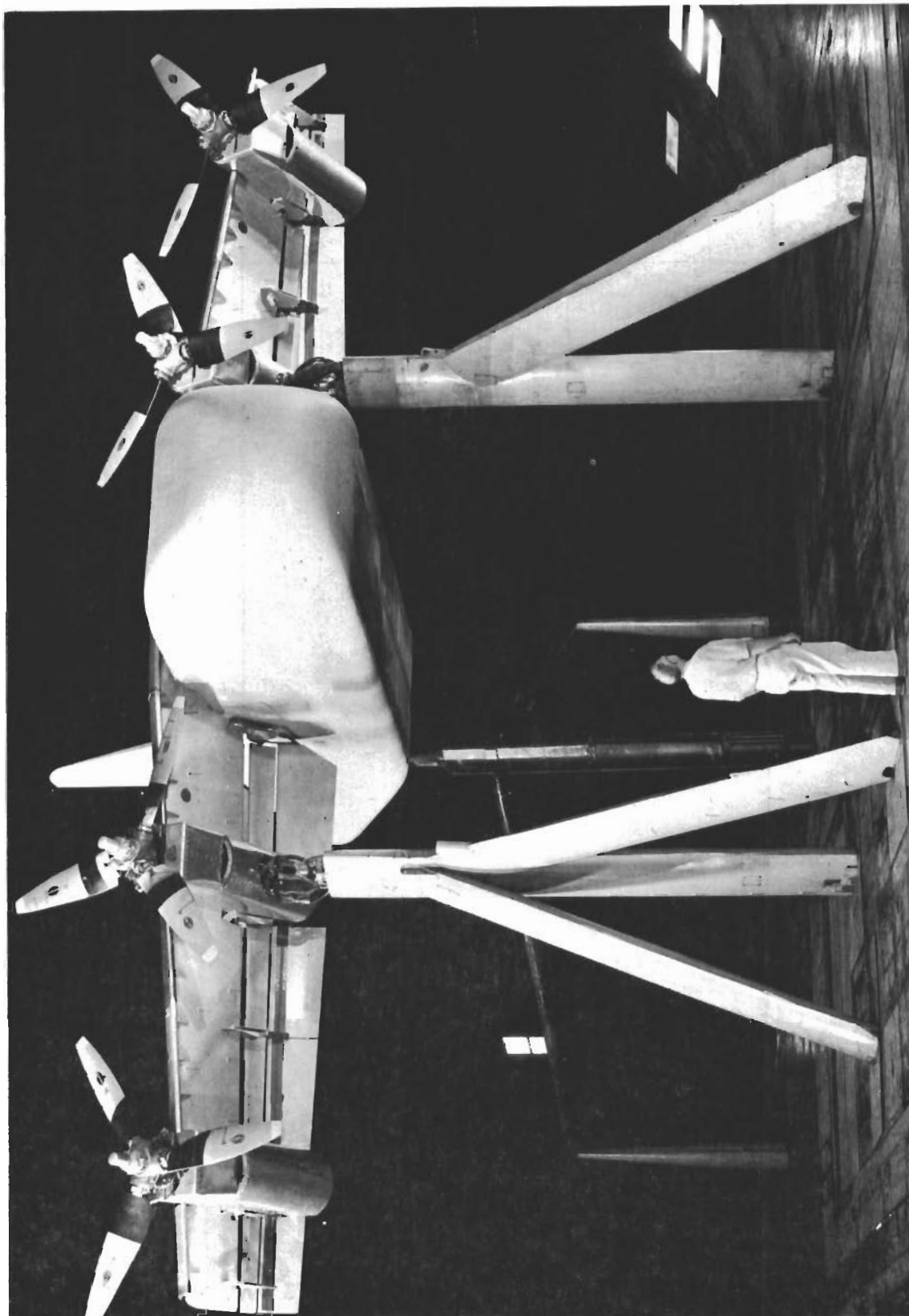| VERTICAL TAIL (Cont.)		XC-142	Ames 0.6 Scale	Langley (Force) 1/11 Scale	VAD 0.11 Scale	Princeton 1/10 Scale	Langley (Free Flight) 1/9 Scale
Sweepback of T.E.		0	0	0	0	0	0
Root Chord, Inches		159.84	160	160	160	160	160
Tip Chord, Inches		39.96	40	40	40	40	40
Mean Geometric Chord							
Length, Inches		111.96	112	112	112	112	112
Spanwise Distance From W.L. 100, Inches		122.52	122.33	122.5	122.5	122.5	122.5
Fuselage Station of L.E.		498.0	499.0	498.0	498.0	498.0	498.0
Tail Arm, l_T/c(1/4 M.G.C. to 1/4 tail M.G.C.)		2.65	2.57	2.67	2.65	2.65	2.58
Airfoil Section	Root	0018	0018	0018	0018	0018	0018
	Tip	0012	0012	0012	0012	0012	0012
RUDDER (PLAIN)							
Spanwise Location, % Vertical Tail Span	Root	41.6	0	None	41.0	12.8	39.4
	Tip	100	100	None	100	100	100
Chord, % Vertical Tail Chord	Root	40	33	None	39	33	40.5
	Tip	40	33	None	39	33	40.5
M.G.C. (Inches)		32.16	36.84	None	31.2	28.44	33.1

TABLE I COMPARISON OF AIRPLANE/MODEL GEOMETRY (Continued)

	XC-142	Ames 0.6 Scale	Langley (Force) 1/11 Scale	VAD 0.11 Scale	Princeton 1/10 Scale	Langley (Free Flight) 1/9 Scale
RUDDER (PLAIN) (Cont.)						
Area, Aft. of Hinge Line, Sq Ft	22.82	42.76	None	22.75	35.3	24.4
Dorsal	Yes	No	Yes	Yes	Yes	Yes
FUSELAGE						
Length, Ft.	50.0	50.83	50.0	50.0	50.0	50.0
Maximum Height, Ft.	10.38	10.25	10.34	10.6	10.58	10.21
Maximum Width, Ft.	9.25	9.17	9.17	9.20	9.25	9.18
Maximum Cross-Sectional Area, Sq Ft	92.0	90.0	91.0	93.5	94.0	90.0
Gear Pods	Yes	No	Yes	Yes	Yes	Yes
MAIN PROPELLERS						
Diameter, Ft.	15.625	15.5	15.5	15.5	15.5	15.5
Number of Blades	4	3	4	4	4	4
Activity Factor, Per Blade	86.0	121.3	91	91	91	91
Integrated Design Lift Coefficient	0.475	0.493	-	-	-	-
Area (Each) Sq Ft	191.75	188.6	188.6	188.6	188.6	188.6
Tilt of Thrust Line — Inboard (Relative to Wing Chord Pl.)	-2° 6'	0	0	-2° 6'	0	0
Tilt of Thrust Line — Outboard (Relative to Wing Chord Pl.)	0	0	0	0	0	0

25

TABLE I COMPARISON OF AIRPLANE/MODEL GEOMETRY (Concluded)

MAIN PROPELLERS (Cont.)	XC-142	Ames 0.6 Scale	Langley (Force) 1/11 Scale	VAD 0.11 Scale	Princeton 1/10 Scale	Langley (Free Flight) 1/9 Scale
Spinners	No	No	Yes	Yes	No	No
TAIL ROTOR						
Diameter, Ft.	8.167	7.95	None	8.0	8.33	8.01
Number of Blades	3	3	--	3	3	3
Activity Factor Per Blade	145	--	--	172	117	145
Integrated Design Lift Coefficient	0	0	--	0	0	0

TABLE II TUNNEL DYNAMIC PRESSURE VALUES

THRUST COEFFICIENT $C_{T,s}$	DYNAMIC PRESSURE PSF			
	VAD 7 X 10	VAD 21 X 23	LANGLEY 15 X 17	AMES 40 X 80
0	40	2.81	10	10
.2	30	2.81	7.8	---
.4	--	2.81	5.7	6
.5	18	2.81	---	---
.6	6	2.81	3.8	6
.8	6	2.81	2.9	5.0
.9	---	2.0	1.0	1.7
.96	---	1.4	.4	---
1.0	---	0	0	0

FIGURE 1

INSTALLATION OF 0.6 SCALE MODEL IN THE AMES 40 X 80 FOOT WIND TUNNEL

28
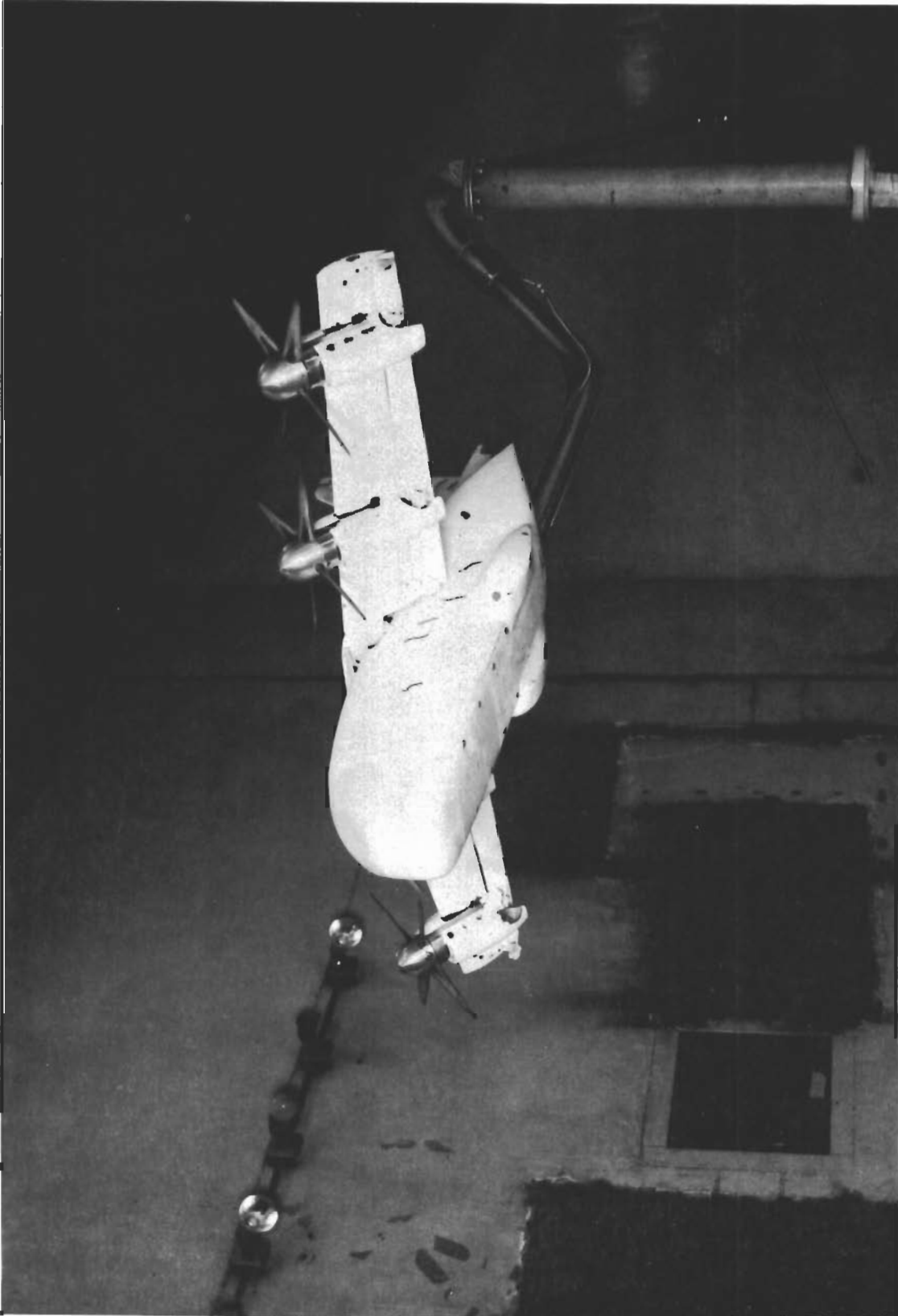
FIGURE 2

INSTALLATION OF 1/11 SCALE MODEL IN THE 17 FOOT TEST SECTION OF THE LANGLEY SUBSONIC TUNNEL

FIGURE 3

INSTALLATION OF 0.11 SCALE MODEL IN THE 7 X 10 FOOT TEST SECTION OF THE VAD SUBSONIC TUNNEL

30
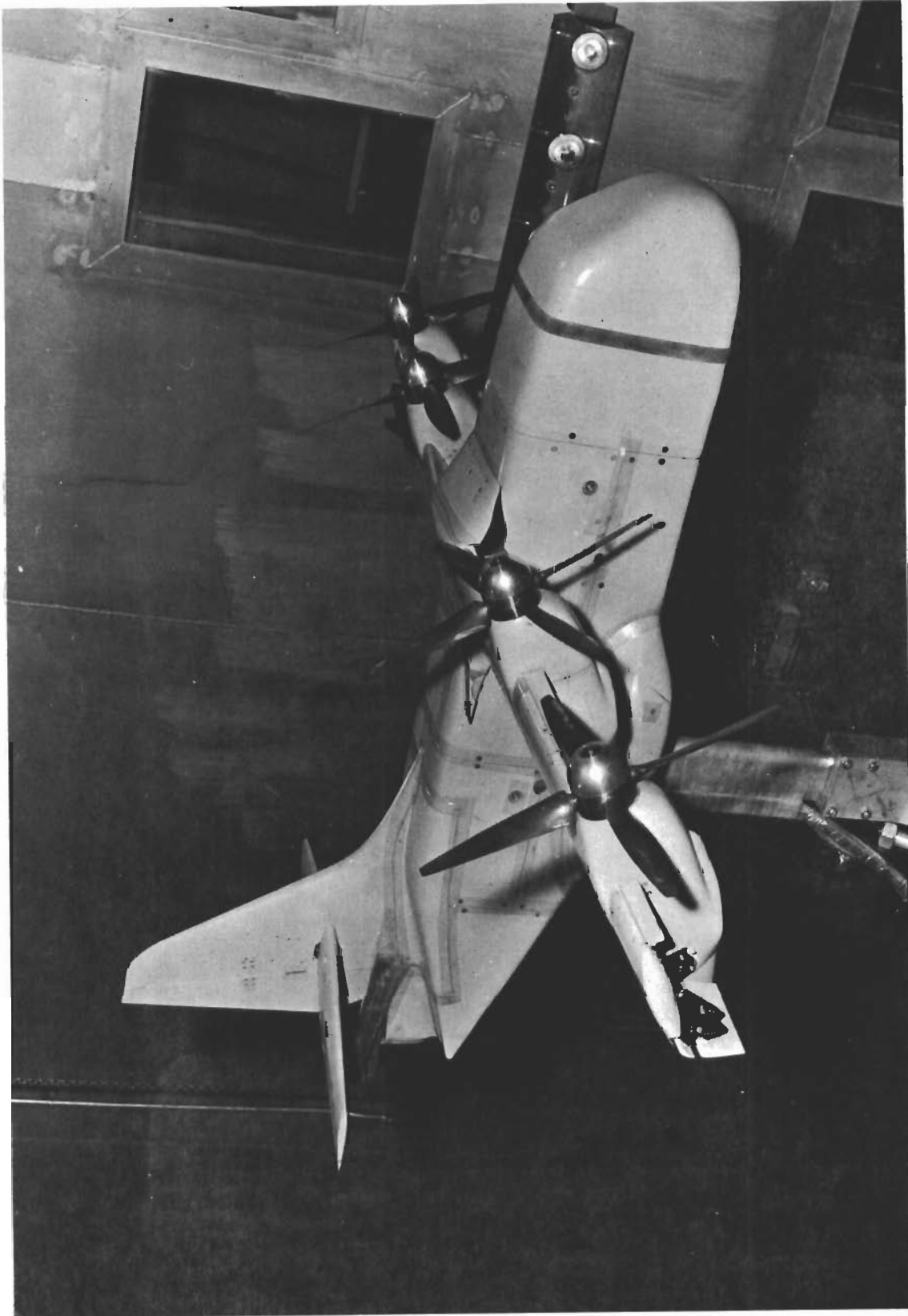
FIGURE 4

INSTALLATION OF 0.11 SCALE MODEL IN THE 21 X 23 FOOT TEST SECTION OF THE VAD SUBSONIC TUNNEL
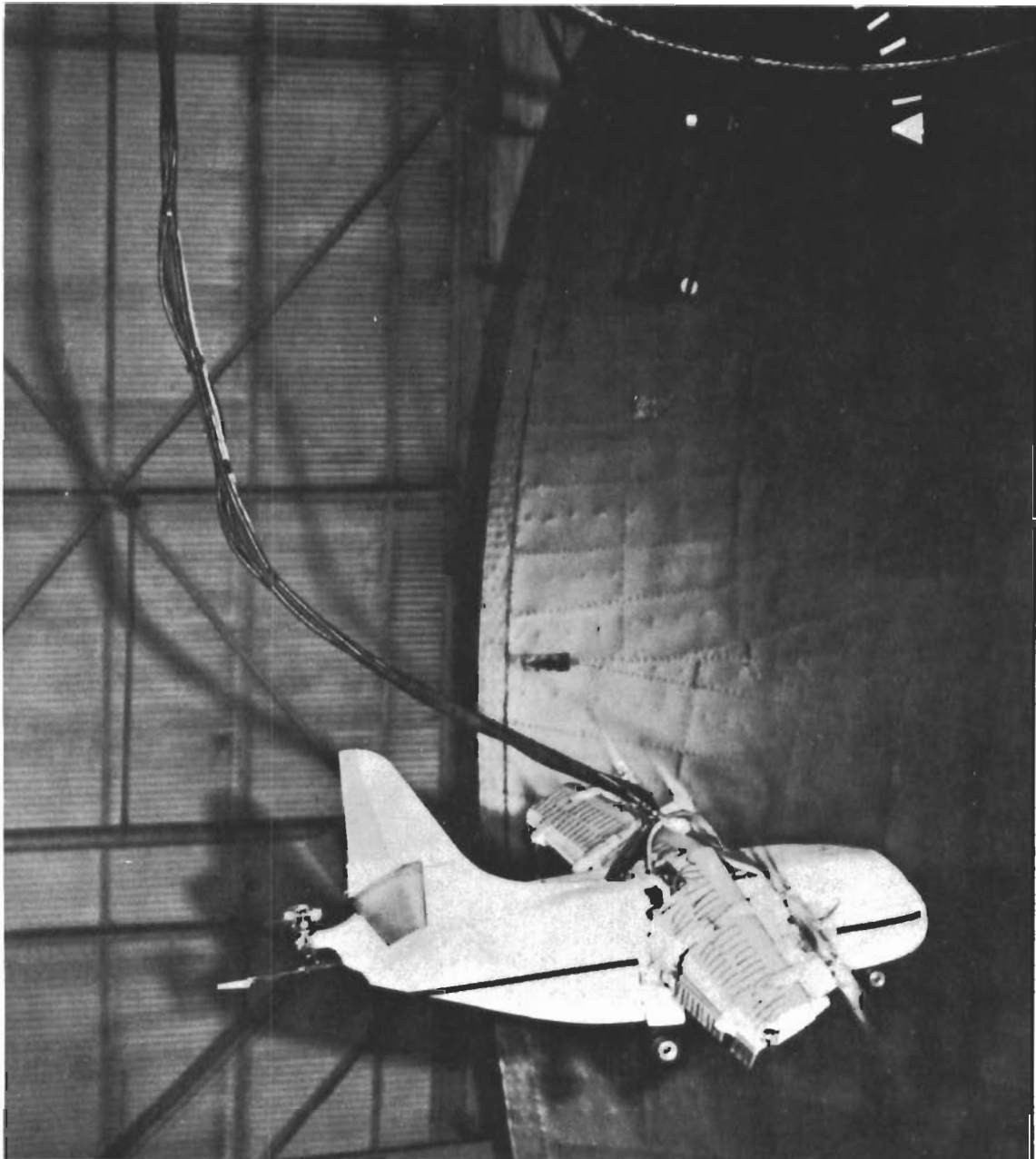
FIGURE 5

INSTALLATION OF 1/9 SCALE MODEL IN THE
LANGELEY 30 X 60 FOOT FREE FLIGHT TUNNEL

FIGURE 6

INSTALLATION OF 0.10 SCALE MODEL IN THE
PRINCETON DYNAMIC MODEL TRACK FACILITY

33
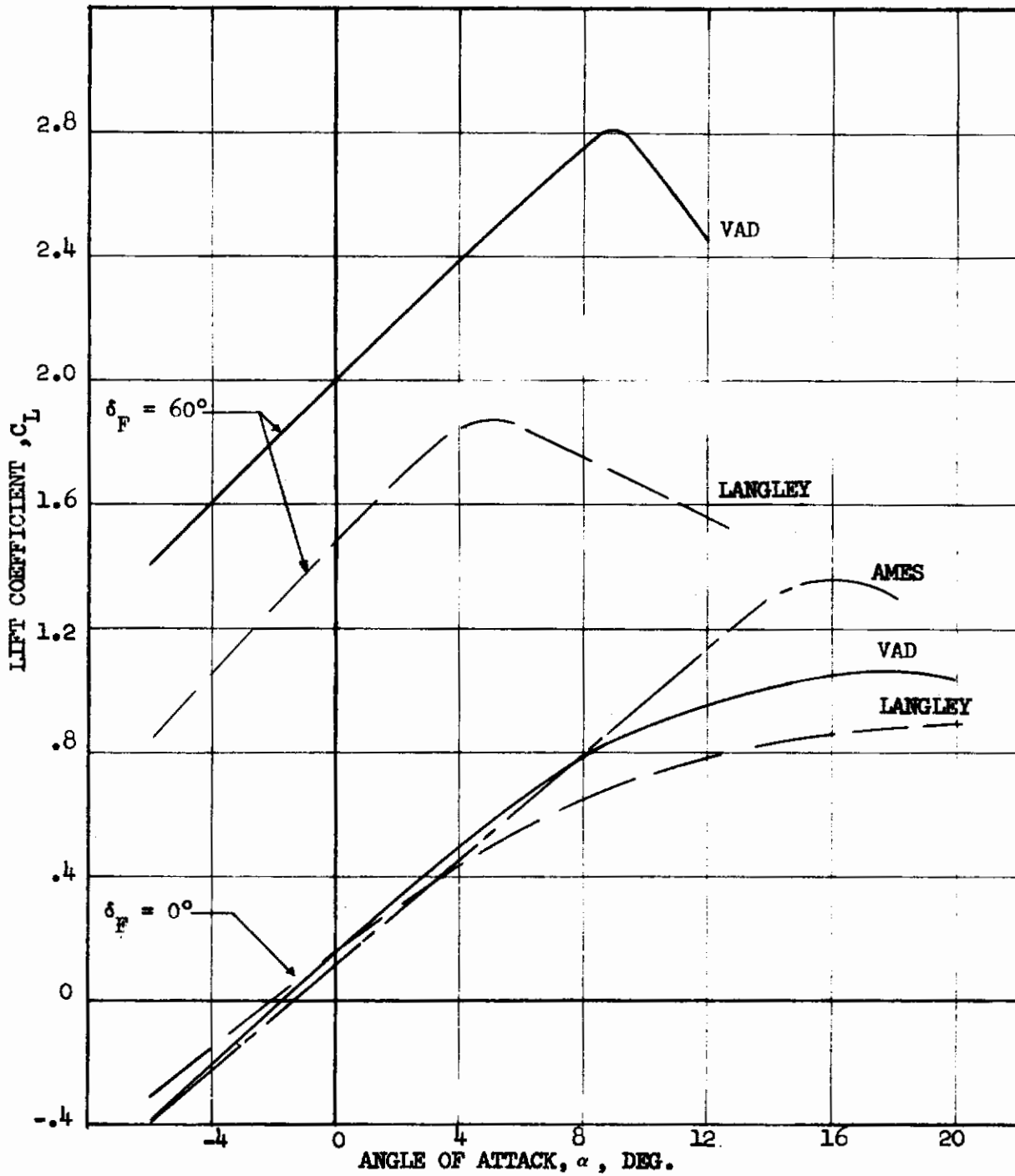
FIGURE 7   COMPARISON OF AMES, LANGLEY, AND VAD DATA (PROPELLERS OFF)

34
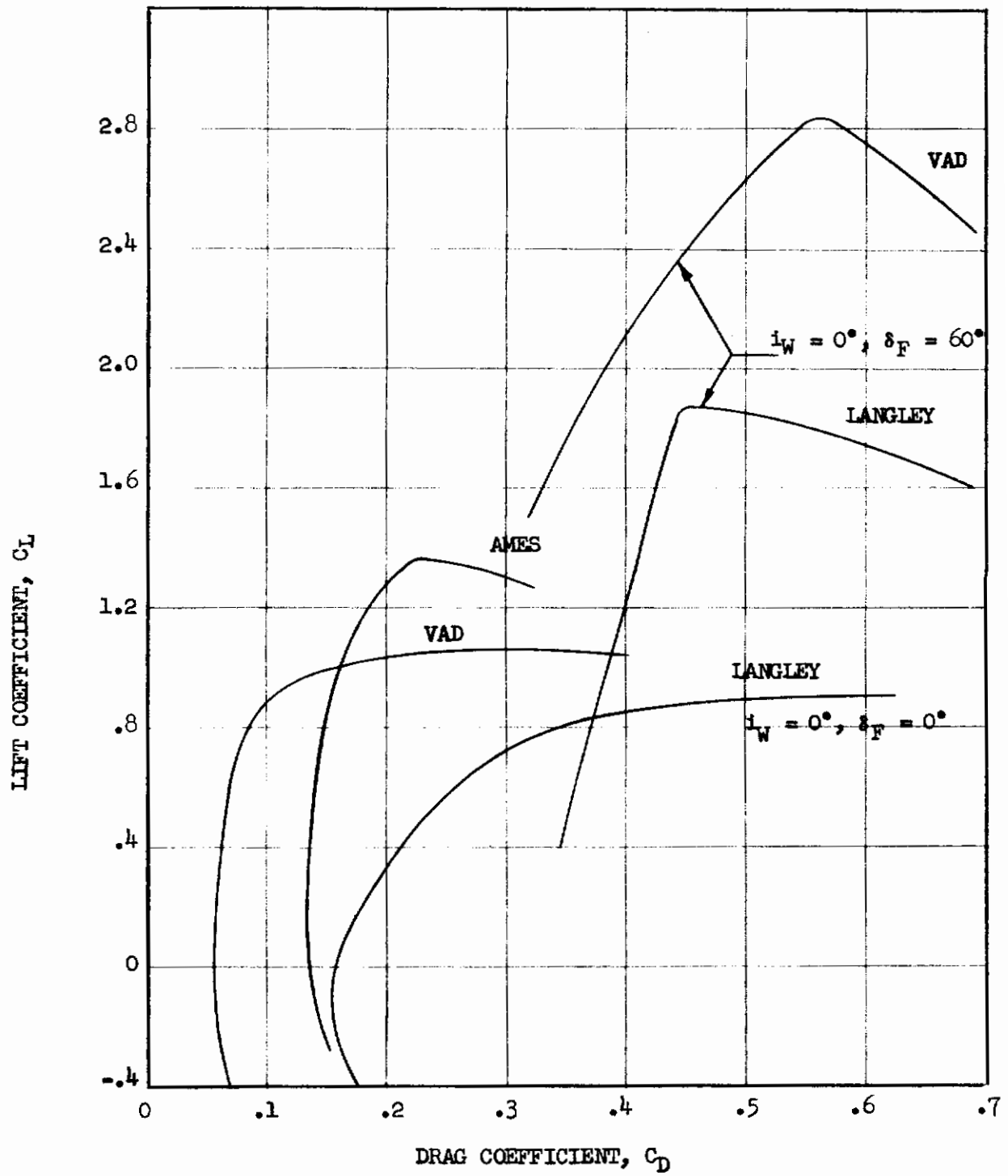
(b) C_L vs C_D

FIGURE 7 (CONCLUDED)

35

$i_W = 0°$, $\delta_F = 0°$

○ VAD, $\beta = 40°$, NOMINAL $C_{T,S} = 0.05$
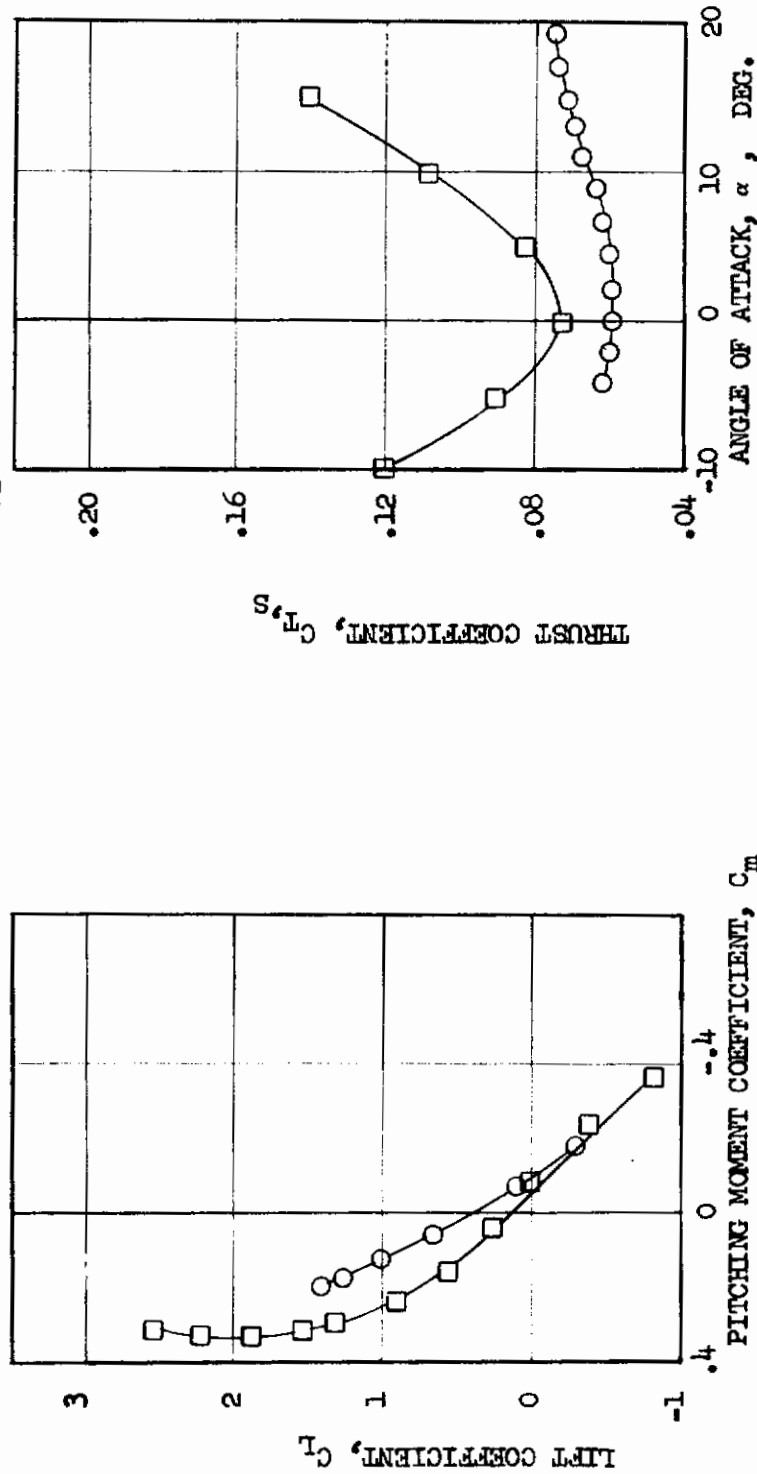
□ LANGLEY, $\beta = 8°$, NOMINAL $C_{T,S} = 0.07$
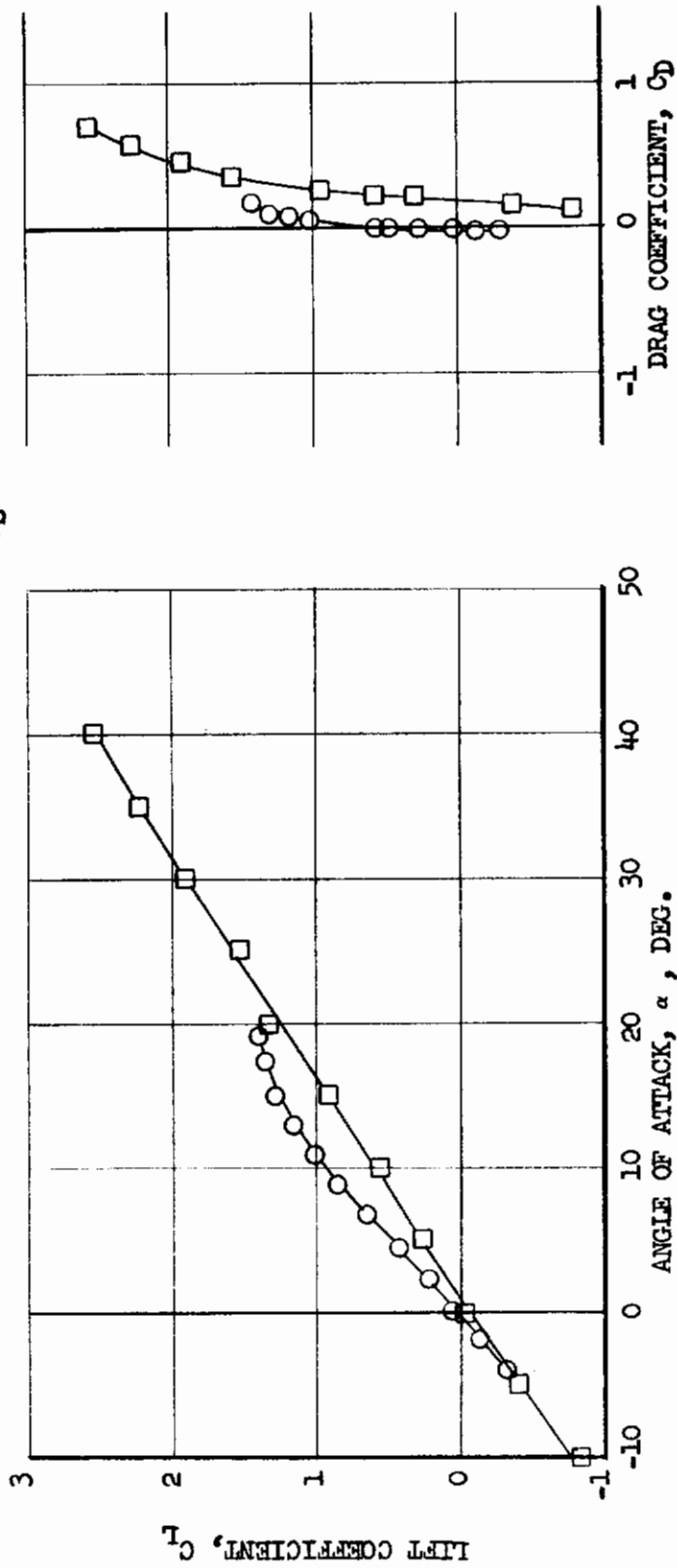
(a) C_L vs α and C_L vs C_D

FIGURE 8 COMPARISON OF LANGLEY AND VAD CRUISE CONFIGURATION DATA

$i_W = 0°$, $\beta = 0°$, $\delta_F = 0°$

○ VAD, $\beta = 40°$, NOMINAL $C_{T,S} = 0.05$

□ LANGLEY, $\beta = 8°$, NOMINAL $C_{T,S} = 0.07$

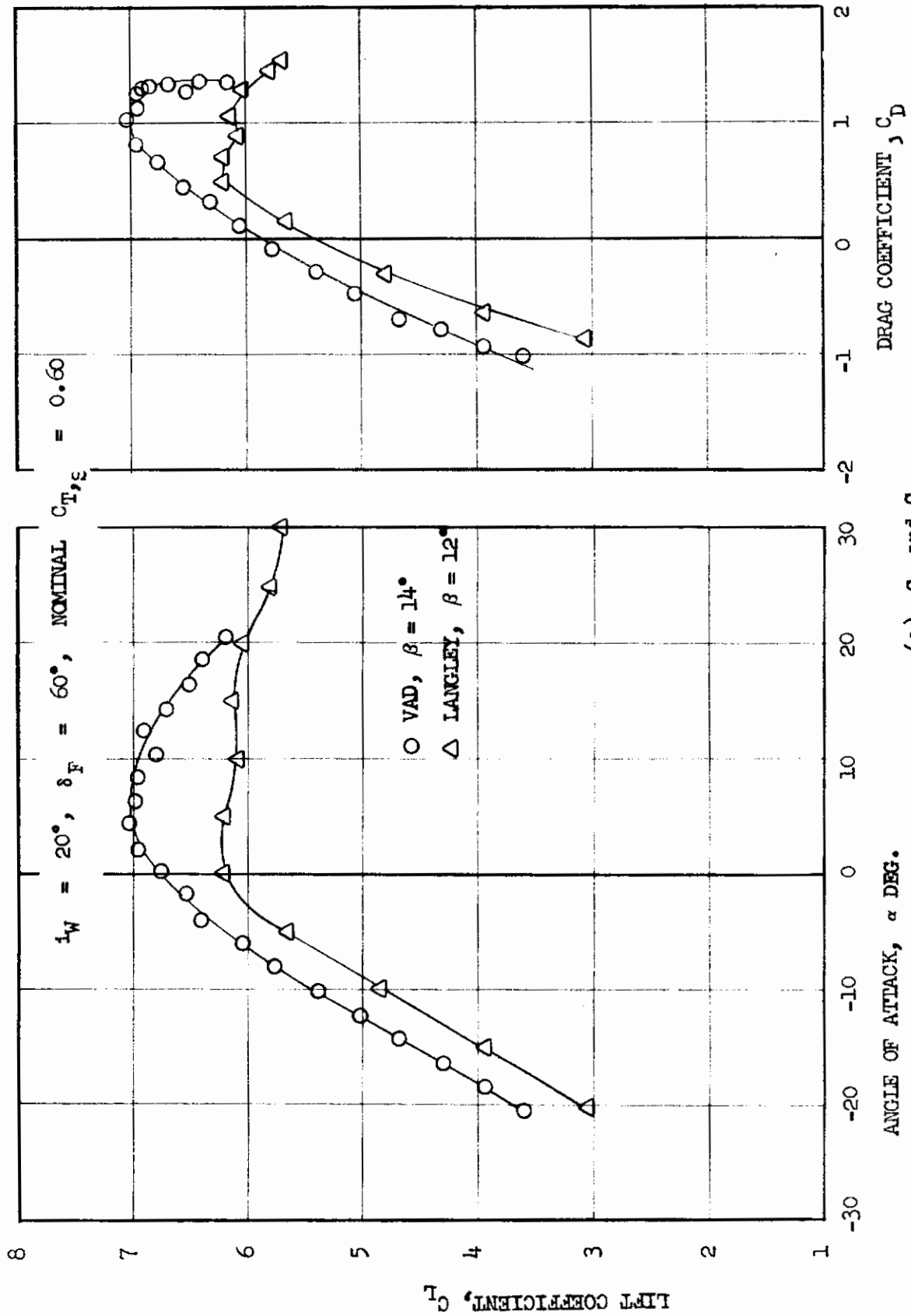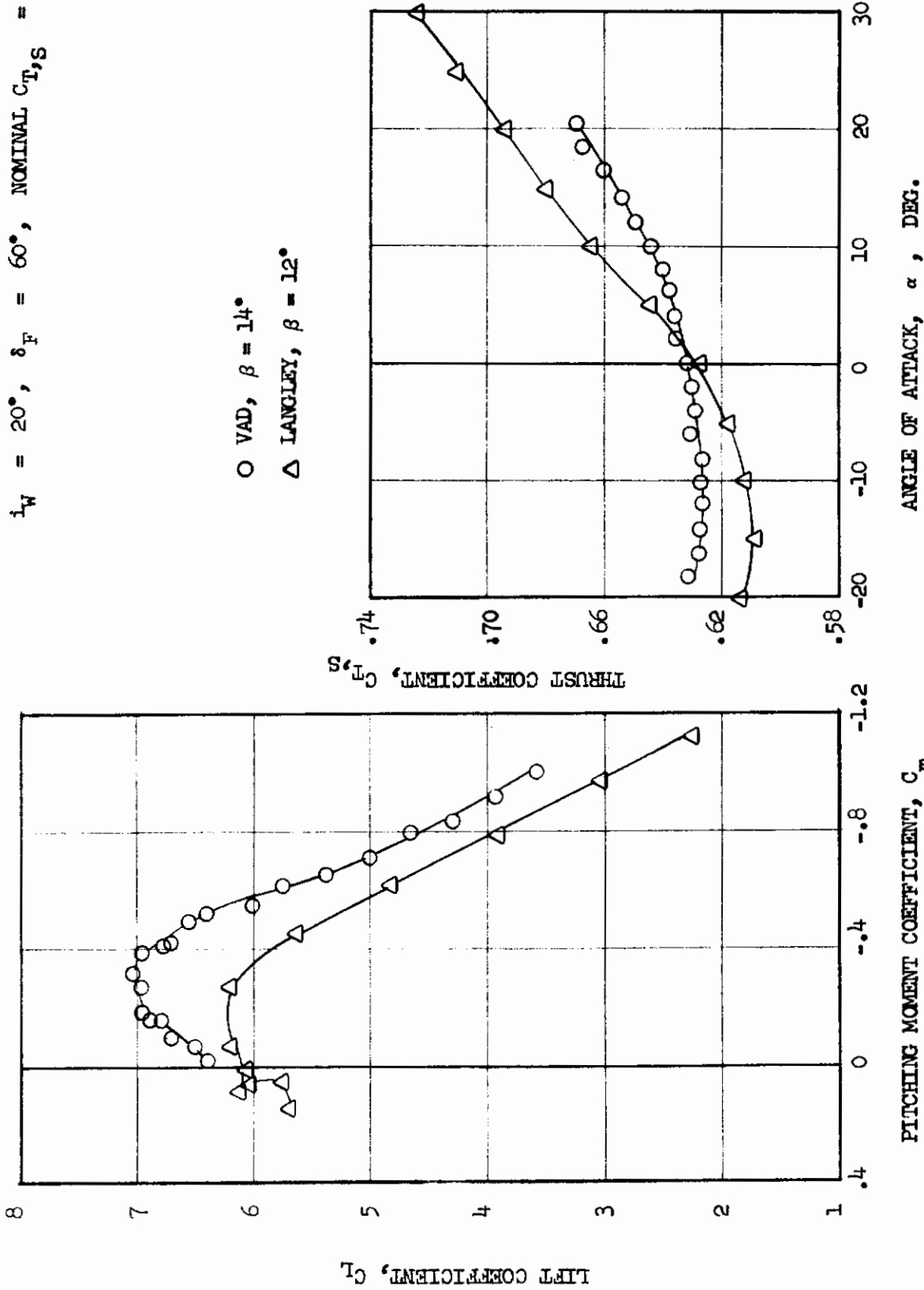(b) C_L vs C_m and $C_{T,S}$ vs α

FIGURE 8 (CONCLUDED)

37

FIGURE 9   COMPARISON OF LANGLEY AND VAD STOL CONFIGURATION DATA ($i_W = 20°$)

(a) C_L and C_D

$i_W = 20°$, $\delta_F = 60°$, NOMINAL $C_{T,S} = 0.60$

○ VAD, $\beta = 14°$

△ LANGLEY, $\beta = 12°$

ANGLE OF ATTACK, α, DEG.

THRUST COEFFICIENT, $C_{T,S}$

PITCHING MOMENT COEFFICIENT, C_m

LIFT COEFFICIENT, C_L

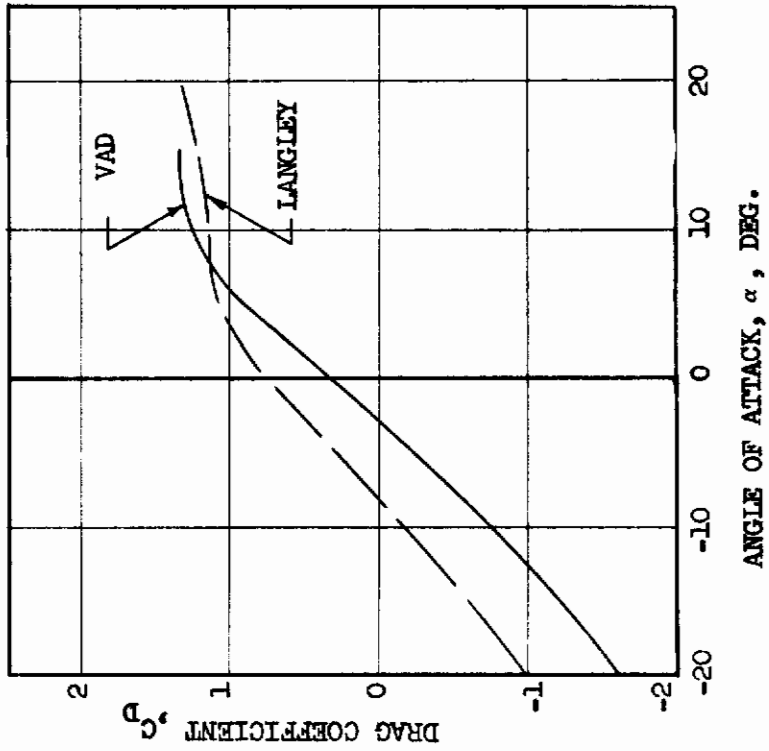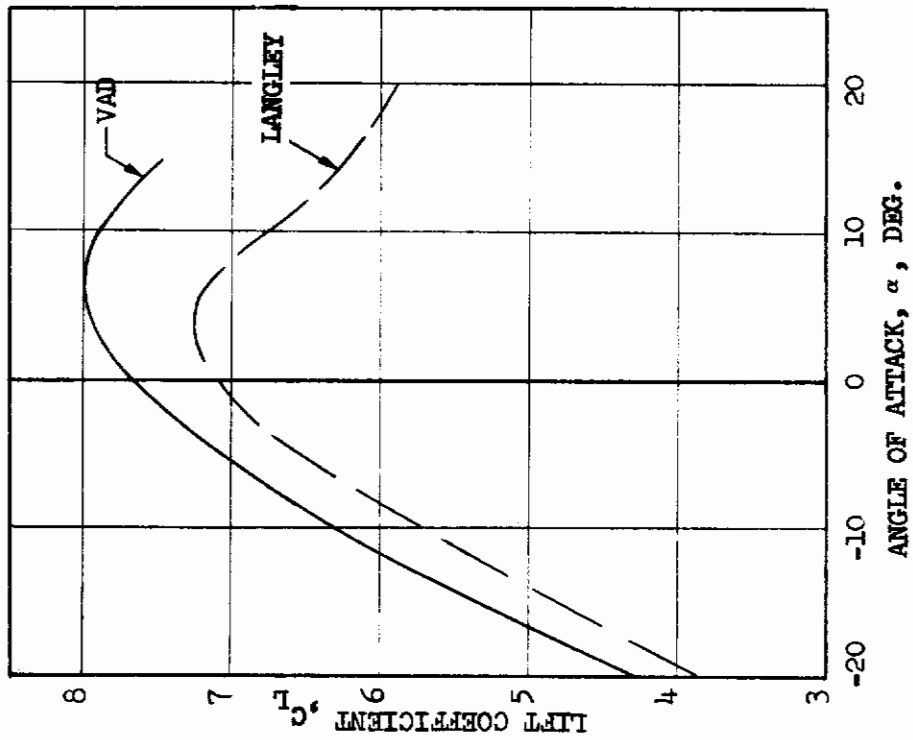(b) C_L vs C_m and $C_{T,S}$ vs α

FIGURE 9 (CONCLUDED)

39

FIGURE 10 COMPARISON OF LANGLEY AND VAD CONSTANT THRUST DATA

$i_W = 40°$, $\delta_F = 60°$, NOMINAL $c_{T,S} = 0.9$
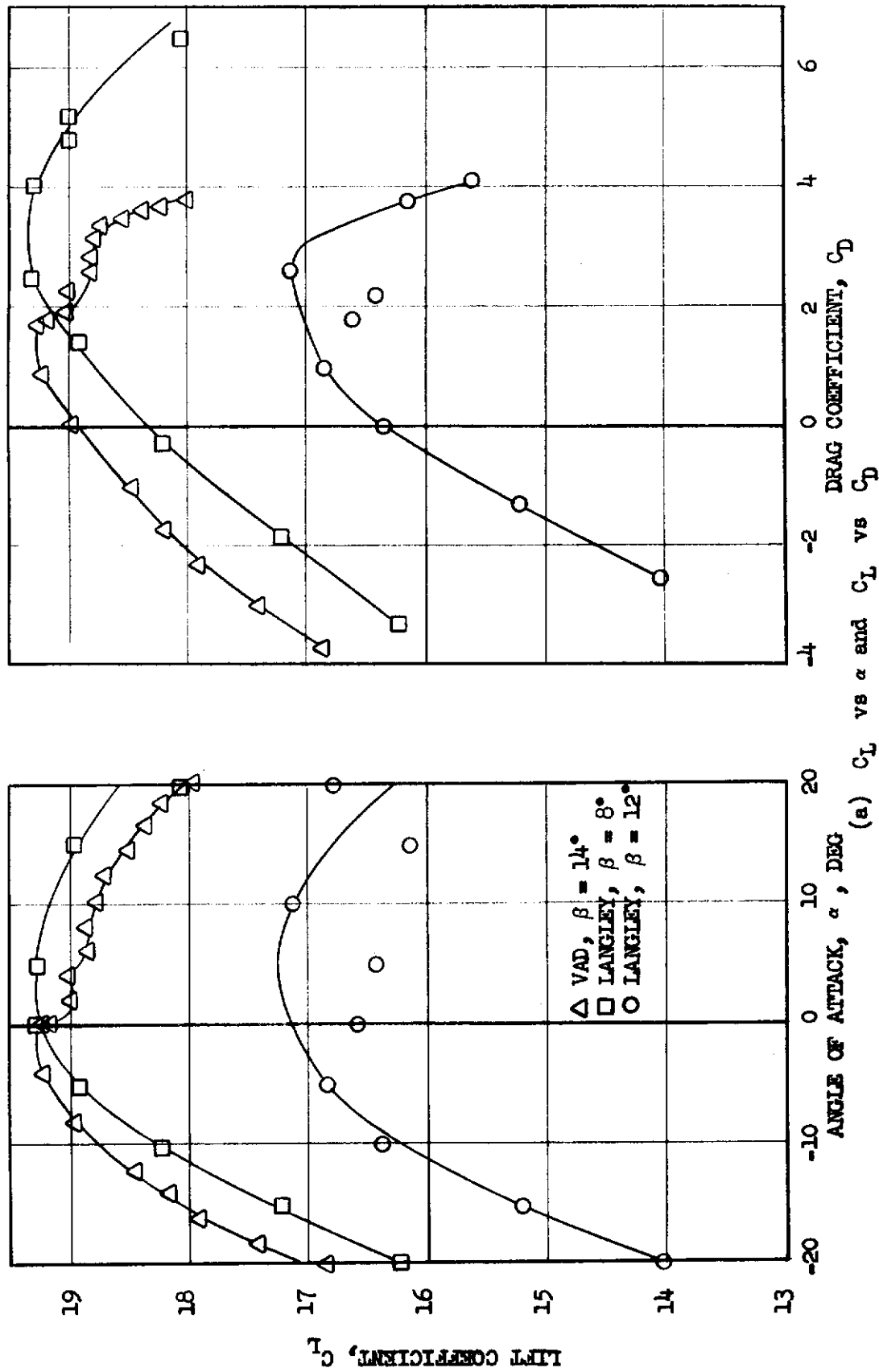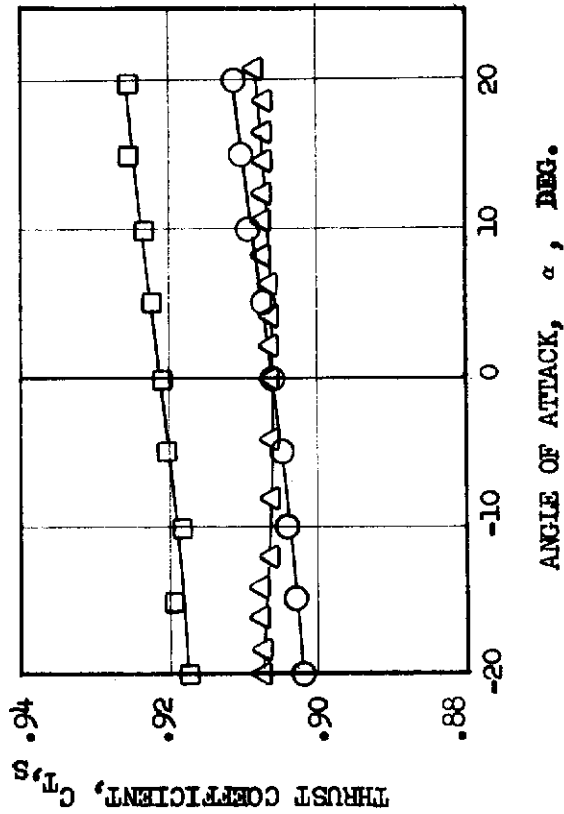

(a) C_L vs α and C_L vs C_D

FIGURE 11 COMPARISON OF LANGLEY AND VAD STOL CONFIGURATION DATA ($i_W = 40°$)
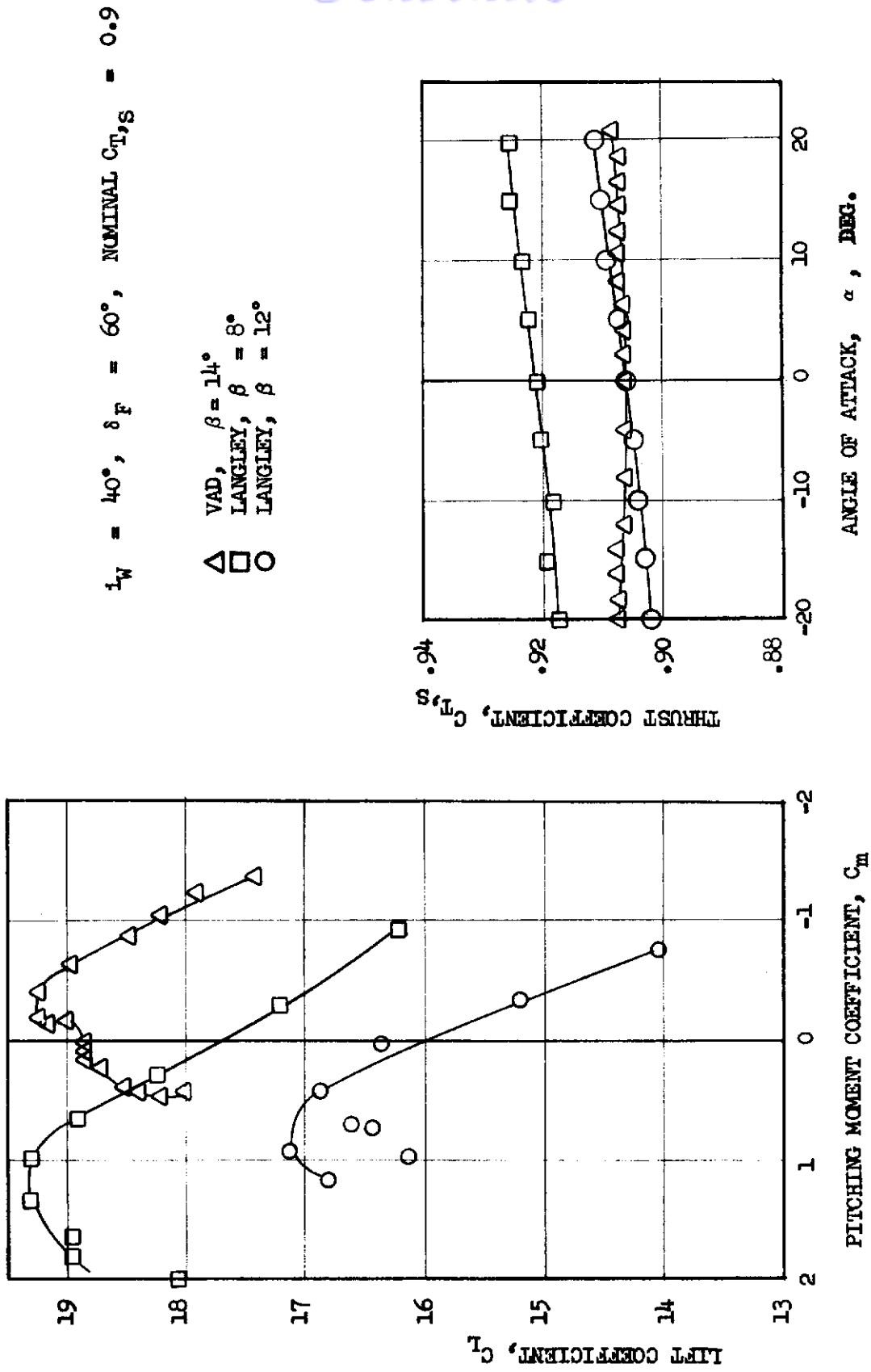
(b) C_L vs C_m and $C_{T,S}$ vs α

FIGURE 11 (CONCLUDED)
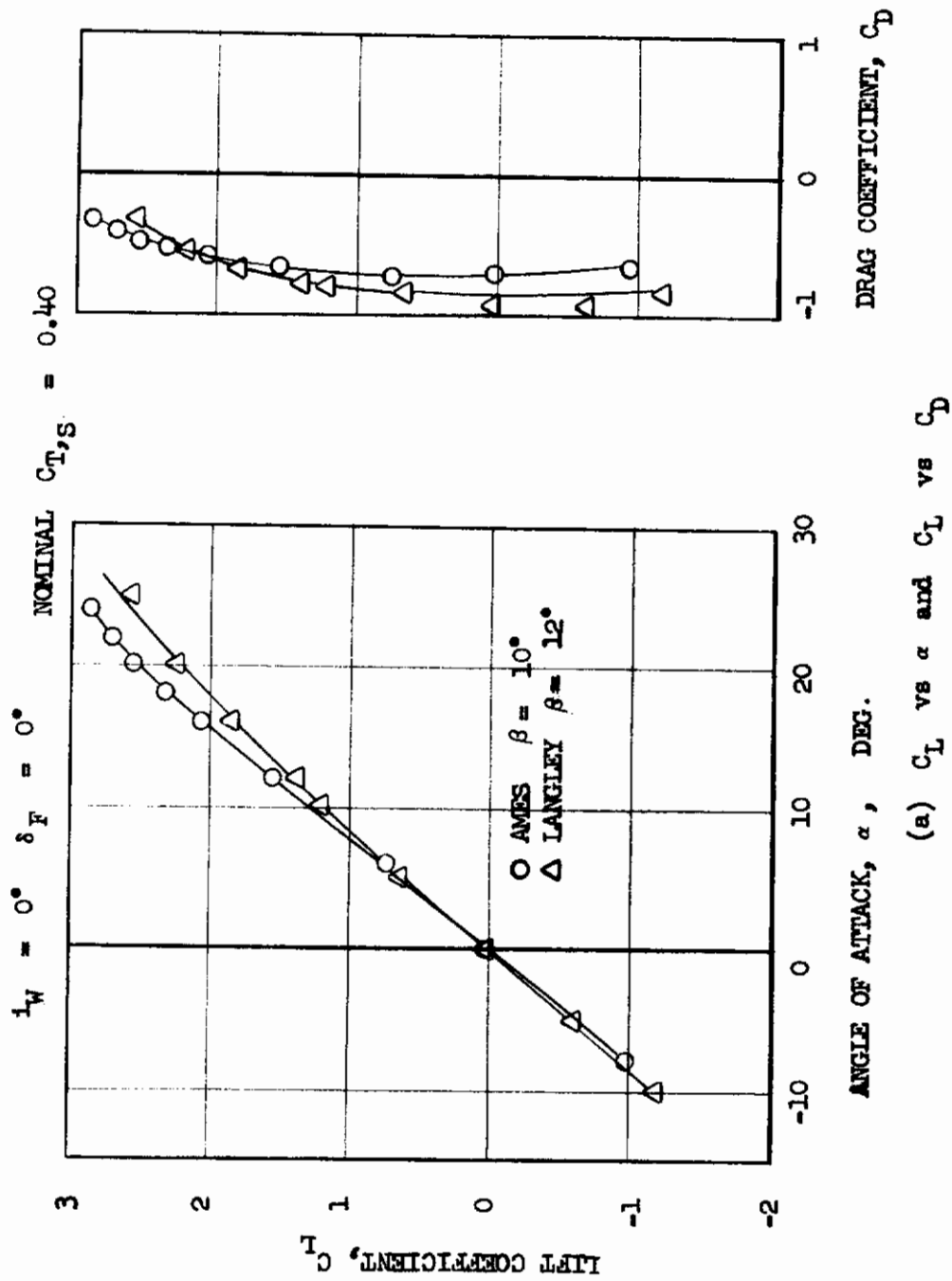
FIGURE 12 COMPARISON OF LANGLEY AND AMES CRUISE CONFIGURATION DATA

(a) C_L vs α and C_L vs C_D

43

$i_W = 0°, \quad \delta_F = 0°, \quad$ NOMINAL $C_{T,S} = 0.40$
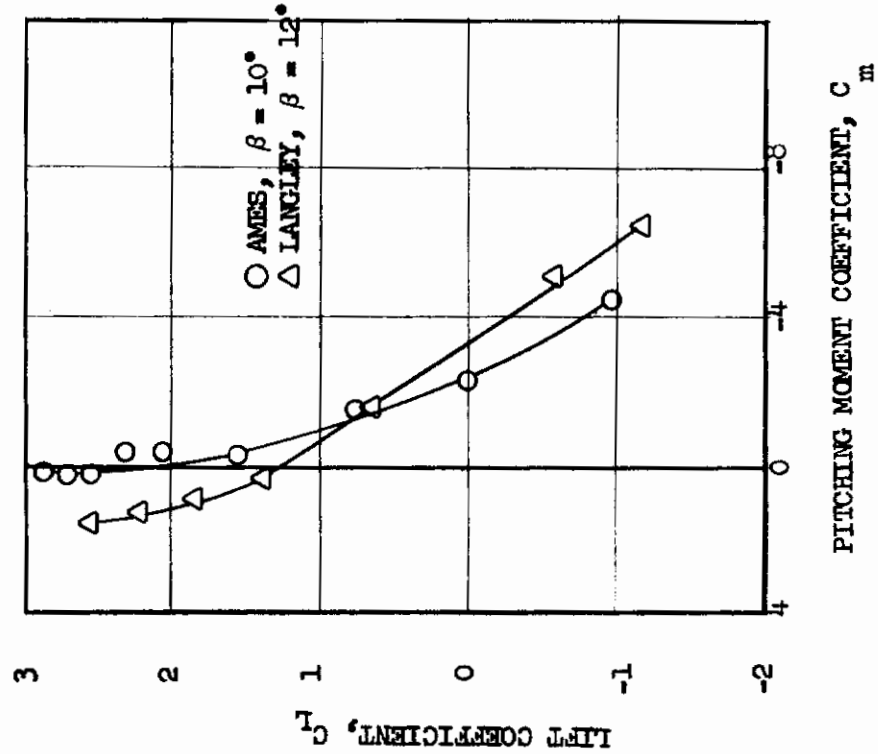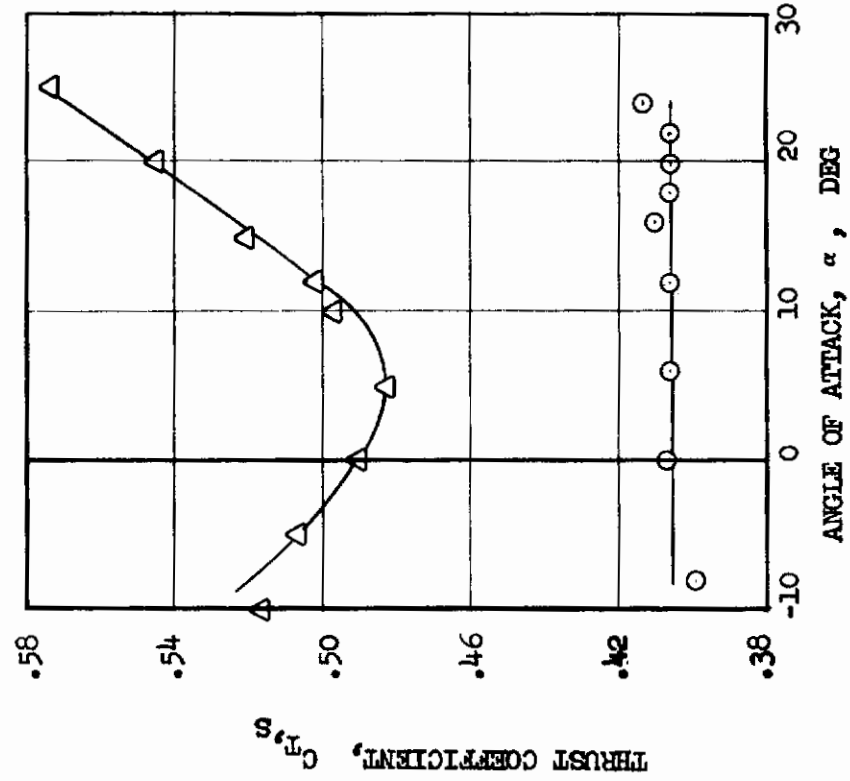
(b) C_L vs C_m and $C_{T,S}$ vs α

FIGURE 12 (CONCLUDED)

44
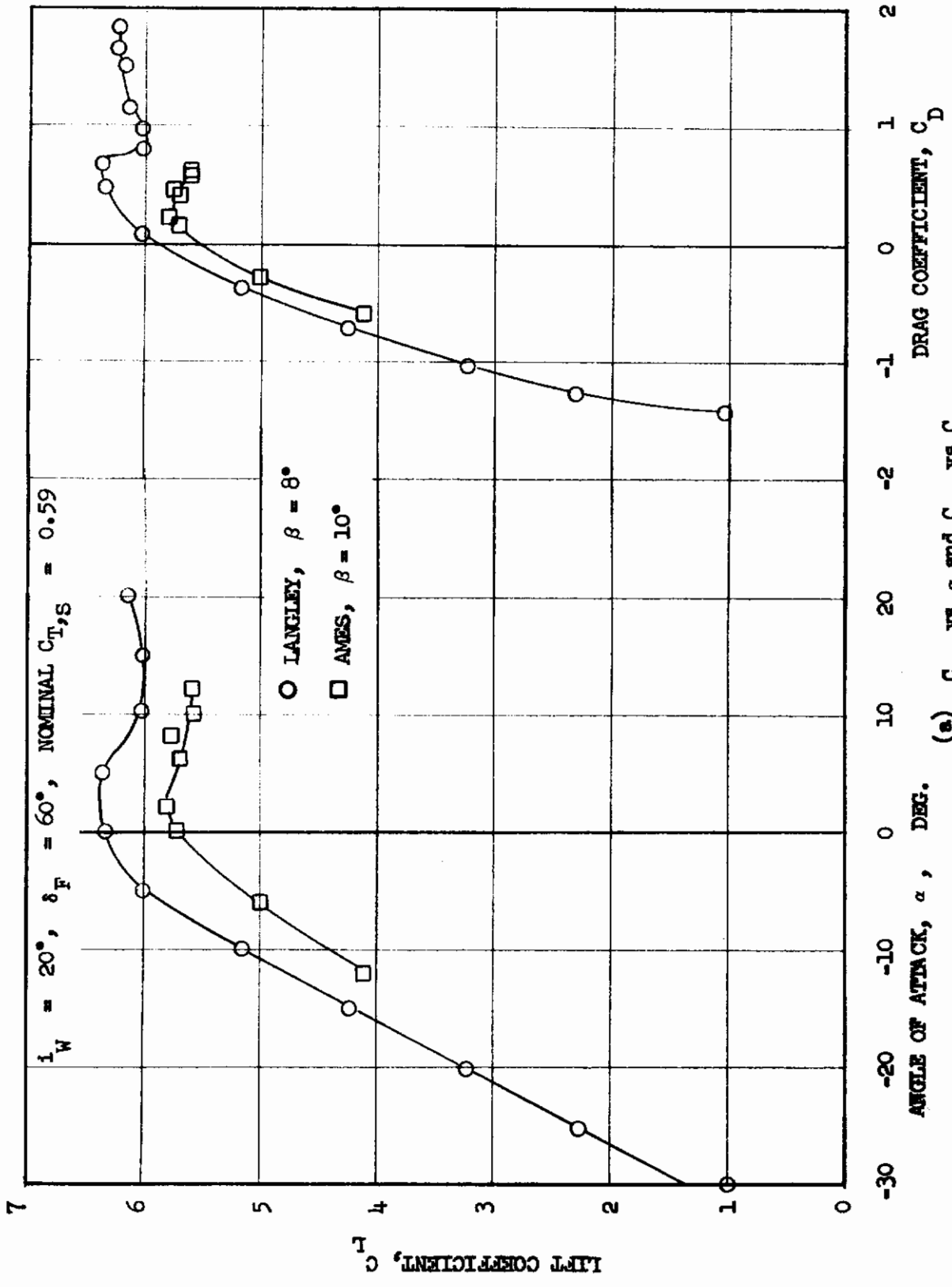
FIGURE 13 COMPARISON OF LANGLEY AND AMES STOL CONFIGURATION DATA

(a) C_L vs α and C_L vs C_D

$t_W = 20°$, $\delta_F = 60°$, NOMINAL $C_{T,S} = 0.59$

○ LANGLEY, $\beta = 8°$

□ AMES, $\beta = 10°$
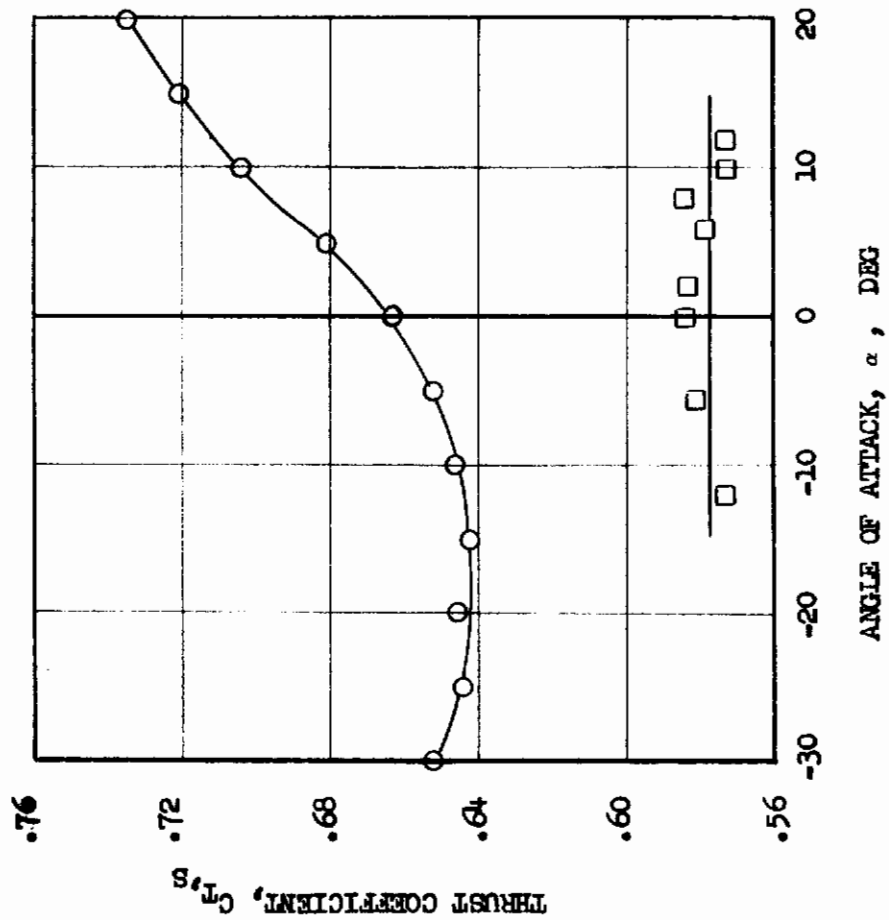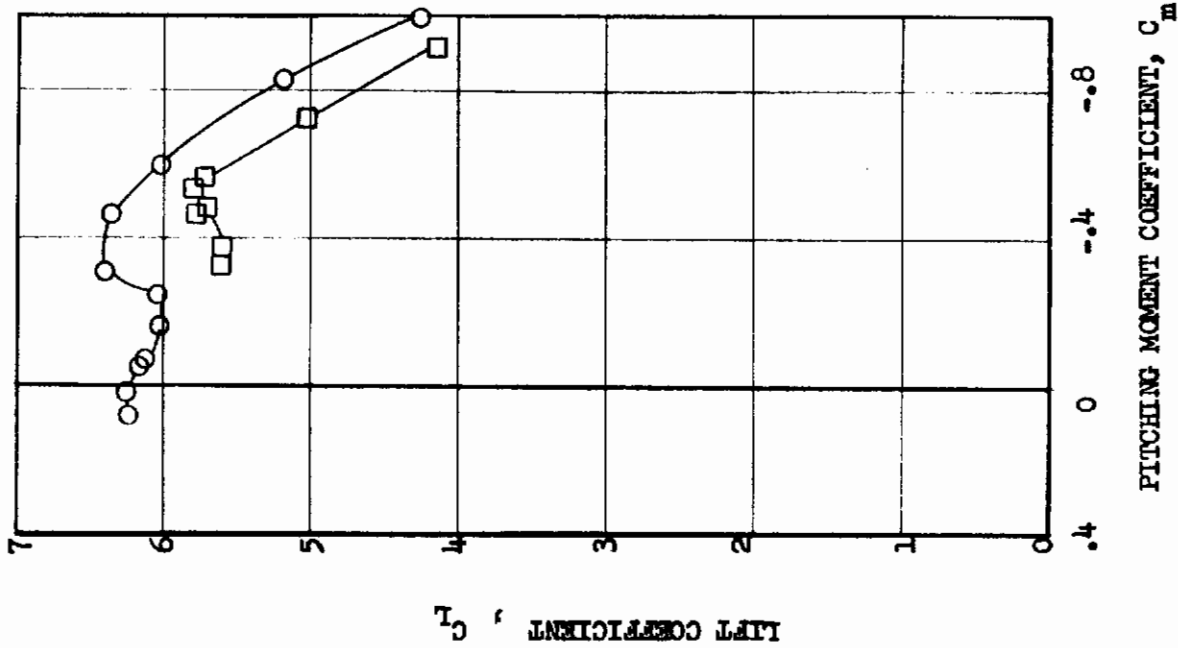
(b) C_L vs C_m and $C_{T,S}$ vs α

FIGURE 13 (CONCLUDED)

46
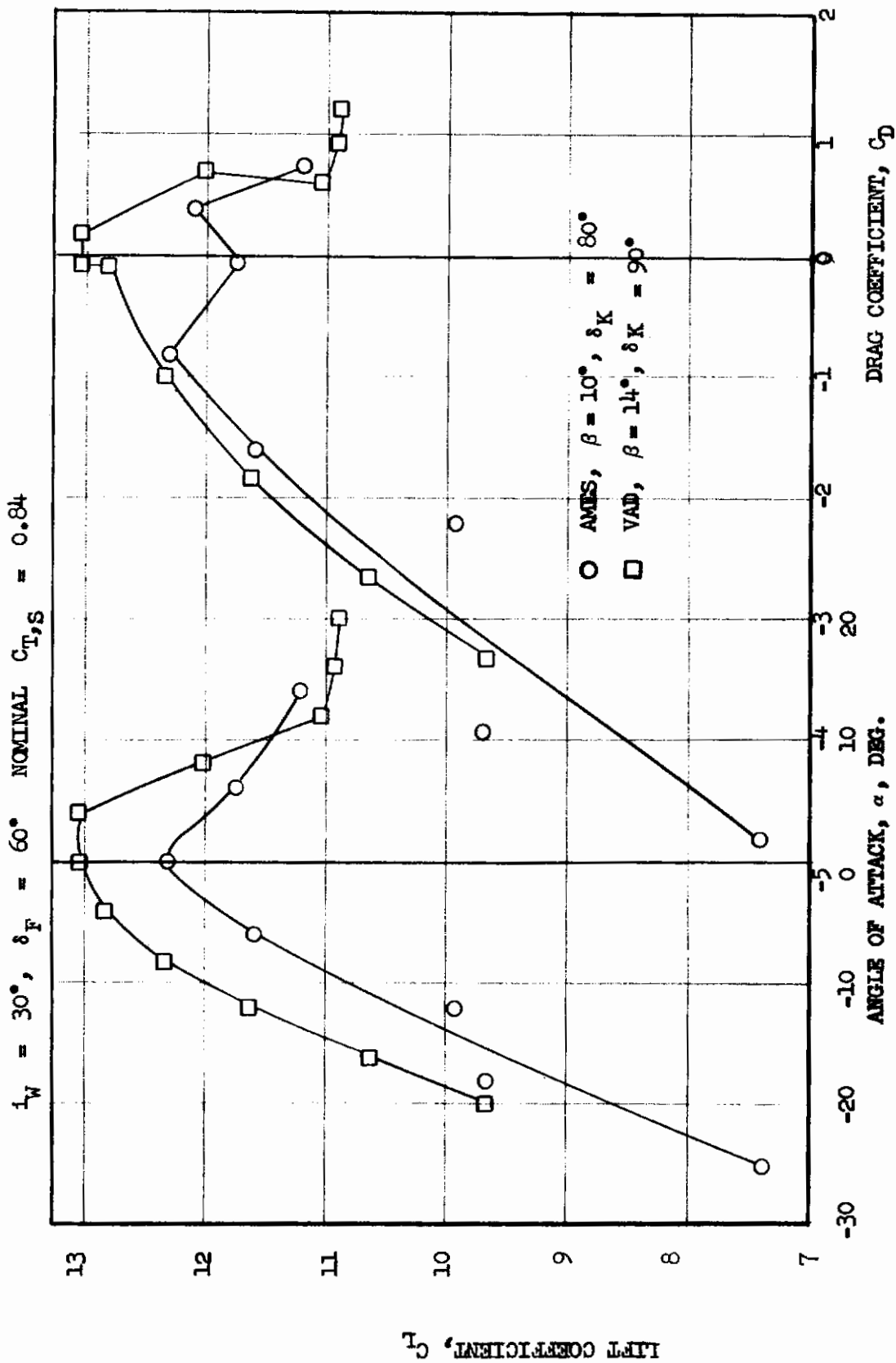
FIGURE 14 COMPARISON OF AMES AND VAD STOL CONFIGURATION DATA

(a) C_L vs α and C_L vs C_D

$i_W = 30°$, $\delta_F = 60°$ NOMINAL $C_{T,S} = 0.84$

47

$i_W = 30°$, $\delta_F = 60°$, NOMINAL $C_{T,S} = 0.84$

$\bigcirc$ AMES, $\beta = 10°$, $\delta_K = 80°$

$\square$ VAD, $\beta = 14°$, $\delta_K = 90°$

THRUST COEFFICIENT $C_{T,S}$

.92

.88

.84

.80

ANGLE OF ATTACK, α, DEG.

-30   -20   -10   0   10   20

PITCHING MOMENT COEFFICIENT, C_m

0   -1   -2   -3

LIFT COEFFICIENT, C_L

13   12   11   10   9   8   7
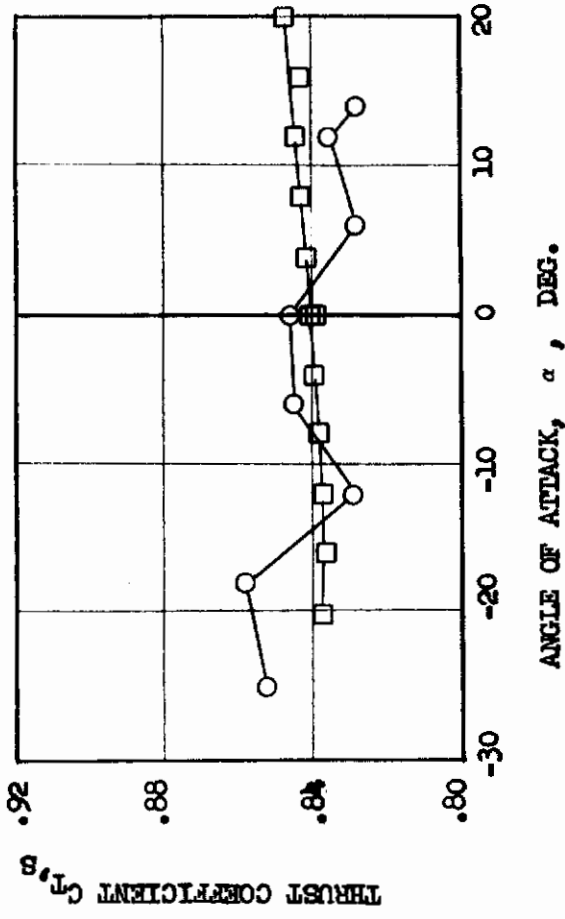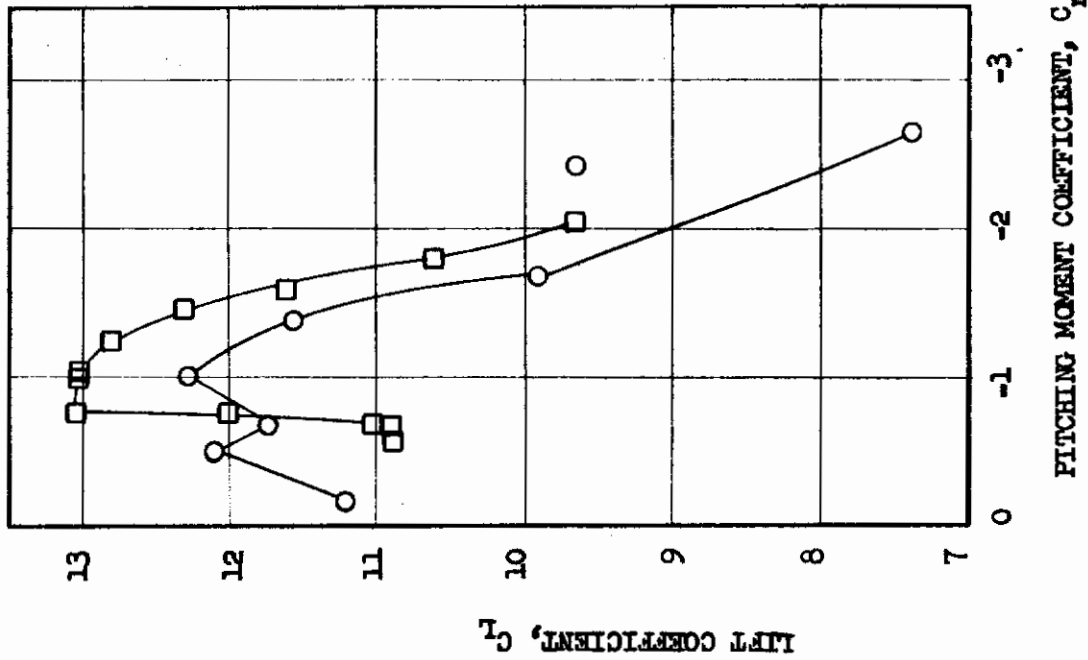
(b) C_L vs C_m and $C_{T,S}$ vs α

FIGURE 14 (CONCLUDED)

48
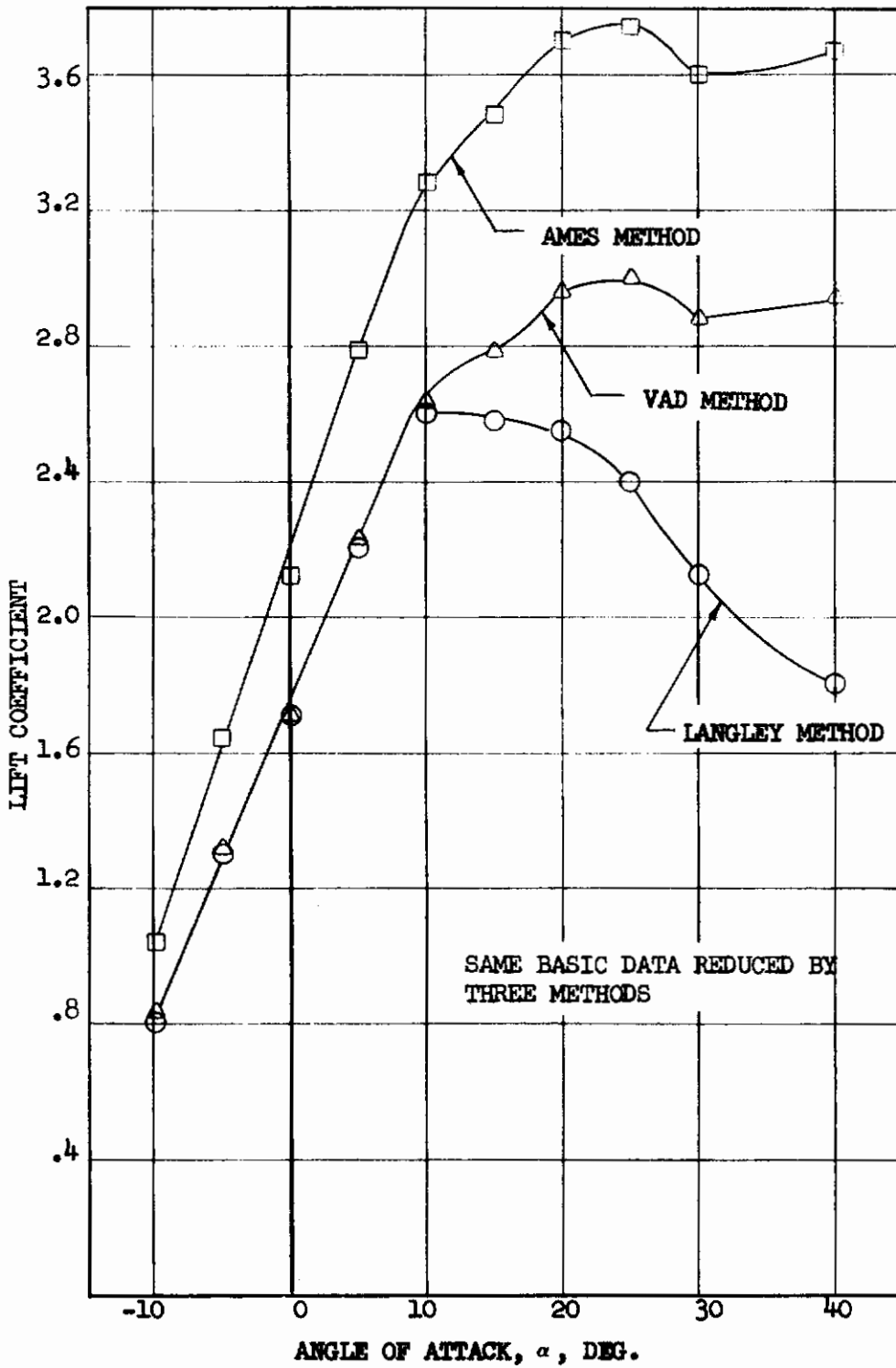
FIGURE 15 DATA REDUCED BY DIFFERENT METHODS

49

$i_W = 0°,$ $\alpha = 0°,$ $\beta = 12°$
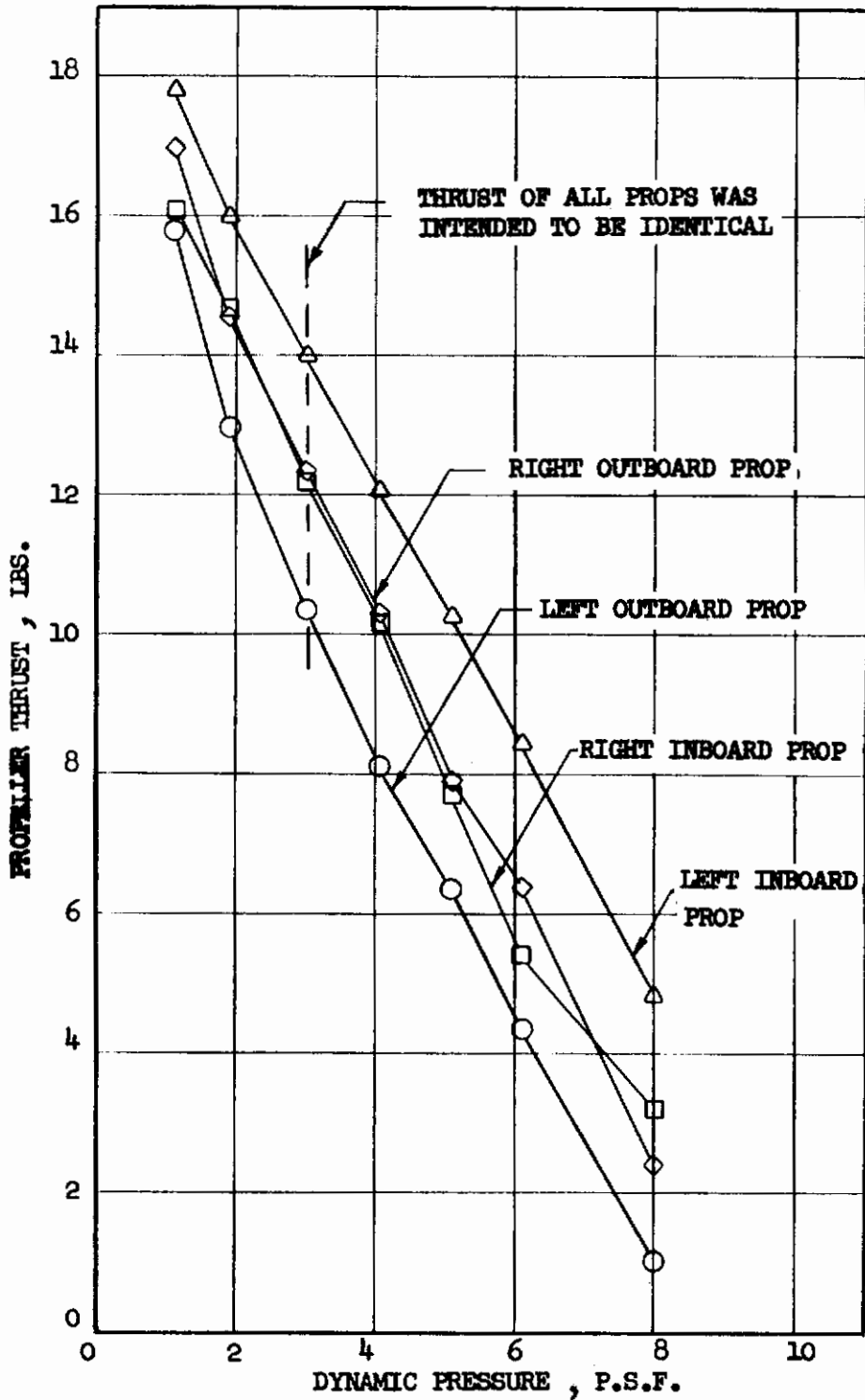
FIGURE 16 LANGLEY PROPELLER THRUST VARIATION

50

$\quad \omega = 0°, \quad \delta_F = 60°, \quad \alpha = 0°, \quad \beta = 14°$
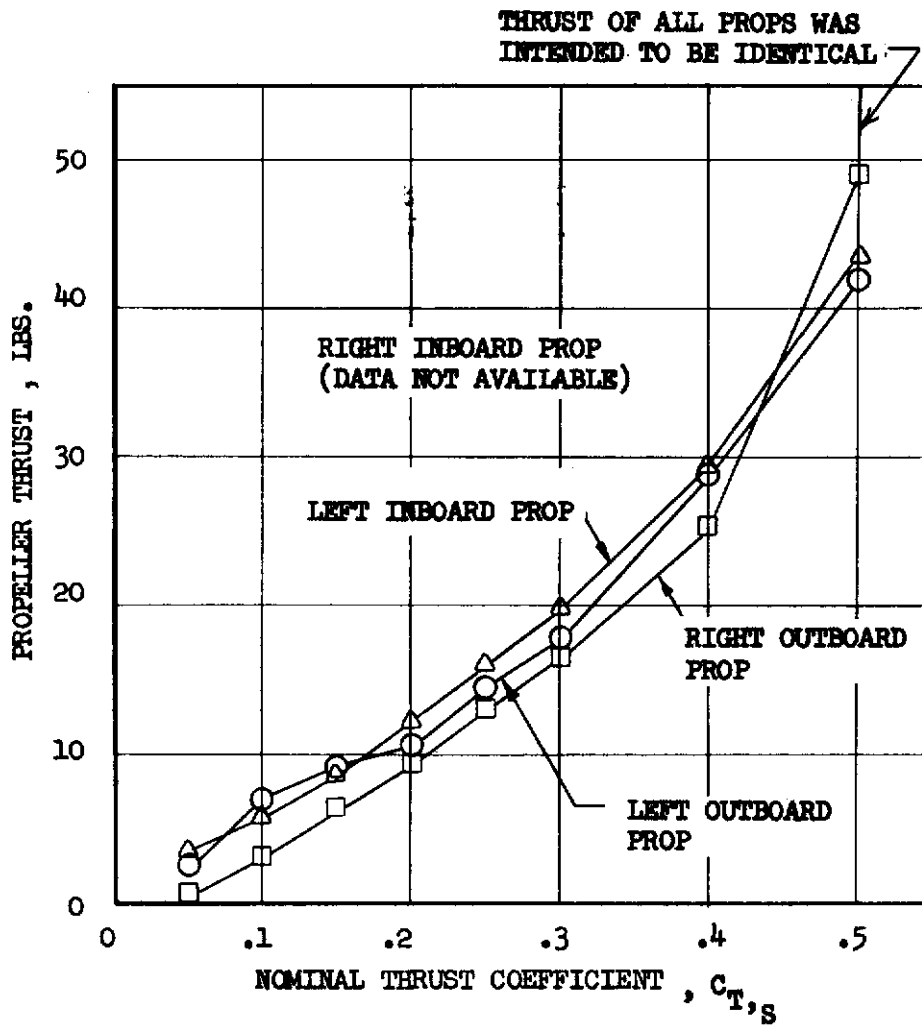
FIGURE 17 VAD PROPELLER THRUST VARIATION
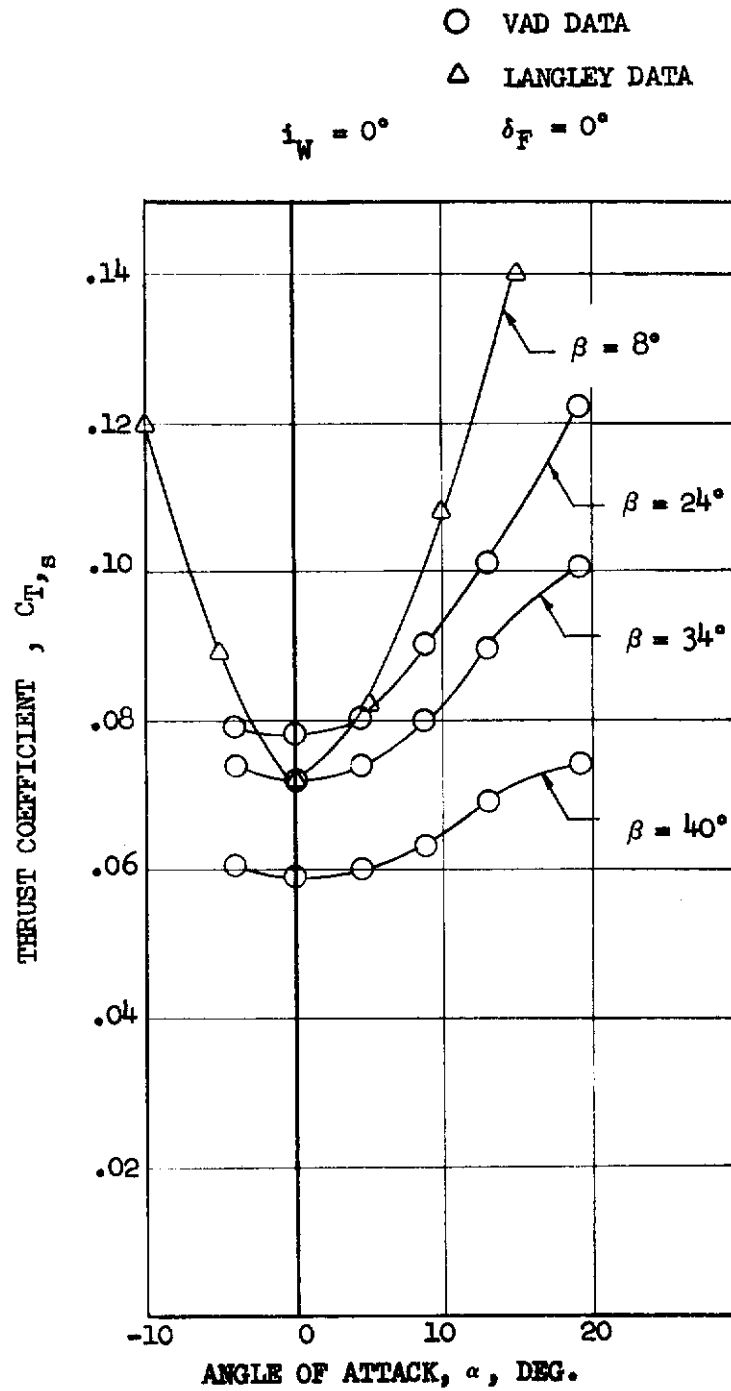
FIGURE 18 VARIATION OF THRUST WITH ANGLE-OF-ATTACK

VAD 21' X 23'

VAD 7' X 10'

LANGLEY 17'

AMES 40' X 80'
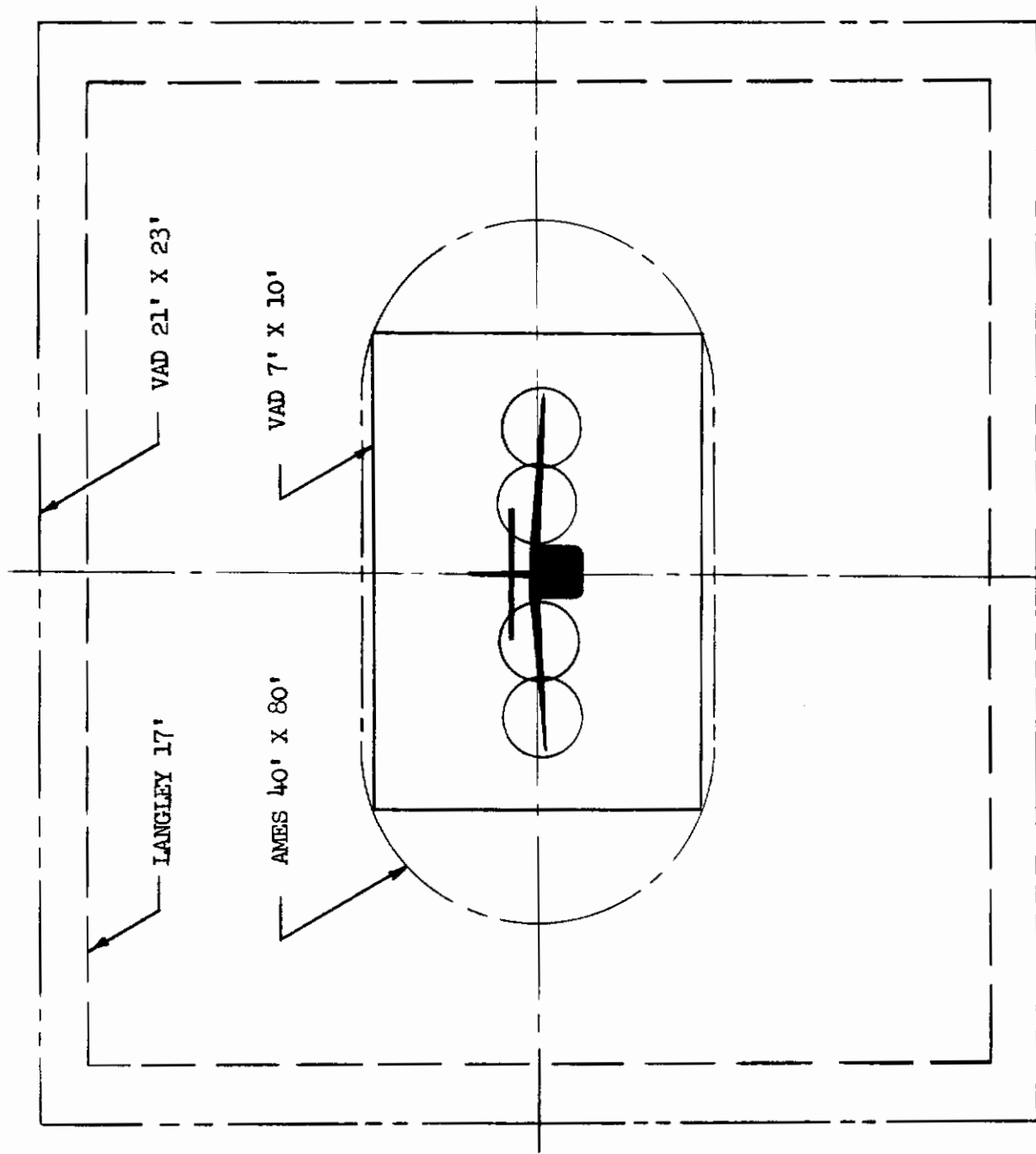
FIGURE 19 MODEL SIZE RELATIVE TO TEST SECTION SIZE

53

SECTION IV

CORRELATION OF WIND TUNNEL DATA
ACQUIRED FOR DEFINITION OF V/STOL TEST REQUIREMENTS

Although the wind tunnel tests performed to obtain aircraft design data did not provide the specific data needed for this study, they certainly identified some factors important to the acquisition of data suitable for correlation purposes. The inability to perform a valid data correlation was caused primarily by the lack of data from similar model configurations and test conditions. The scope of the investigation was eventually expanded to include three additional tests, performed with the same model but in different size test sections. These tests were intended to avoid practically all the differences that existed during the previous tests and provide data that could be used to establish test requirements for future V/STOL wind tunnel programs.

1. TEST APPARATUS AND PROCEDURES

It was recognized that considerable emphasis must be placed on obtaining accurate data and on the rigid control of test parameters, particularly thrust, in order to achieve the program objectives. These requirements were high-lighted during the analysis of the data obtained from the previous wind tunnel tests. To satisfy these requirements, improvements were made in the model instrumentation and data recording system.

a. MODEL

The VAD 0.11 scale XC-142A model was used for these tests. The basic model is described in Section III. Prior to the beginning of these tests, several modifications were made to the model. These modifications, which did not affect the aerodynamic characteristics, were as follows:

(1) The single component propeller balances that measured thrust were replaced with five-component balances that measured propeller thrust, normal force, pitching moment, side force, and yawing moment. With the use of these balances the propeller rotational speed could be measured and controlled to within $\pm$ 2 RPM.

(2) The wing incidence bracket that allowed setting the wing incidence from 0 to 90 degrees in 10 degree increments was replaced with a remotely controlled wing actuator that permitted the wing incidence to be varied from 0 to 90 degrees during a run. The wing incidence angle could be set to within $\pm$ 0.10 degree.

54

(3) The fuselage angle-of-attack measurement was improved with the installation of electrolytic bubble levels. These levels were attached to a plate and mounted inside the model. Each level was set to a predetermined angle to provide an angle-of-attack range of $\pm$ 20 degrees in 2 degree increments. The accuracy of setting the fuselage angle-of-attack was $\pm$ 1 minute.

b. TEST SECTIONS

The tests were performed in the three test sections of the VAD low speed wind tunnel. The following is a brief description of these sections.

The rectangular 7 X 10-foot test section is 16 feet long and operates at atmospheric pressure. The dynamic pressure range for the test in this section was approximately 3.0 to 50 PSF. An internal strain gage balance was used to measure the aerodynamic forces on the model during the test runs for which the wing incidence was varied while maintaining a constant fuselage angle-of-attack. An external beam balance was used for all other runs.

The rectangular 15 X 20-foot test section was constructed after the aircraft development tests were completed. The section is 39 feet long and is located upstream of the 7 X 10-foot section in a tandem arrangement. This section operates at a slight positive static pressure which varies with tunnel speed. The dynamic pressure range for the test in this section was approximately 0.5 to 7.0 PSF. An internal strain gage balance was used to measure the aerodynamic forces on the model.

The rectangular 21 X 23-foot test section is 35 feet long (at the centerline) and is located upstream of the 15 X 20-foot section between two corners of the return passage. This section also operates at a slight positive static pressure which varies with tunnel speed. The dynamic pressure range for the test in this section was approximately 0.5 to 3.0 PSF. An internal strain gage balance was used to measure the aerodynamic forces on the model.

c. TESTS

The objectives of these tests were to obtain data that would be suitable for evaluating the wind tunnel wall corrections, correlating with data obtained from NASA Langley tests, and defining significant V/STOL test parameters. Complete descriptions of these tests and the data acquired are presented in References 17, 18, and 19.

Data for evaluating the tunnel wall corrections were obtained from each of the test sections using the same model configuration, support system, balance system, recording system and test procedures. The normal procedure of varying the model fuselage angle of attack while maintaining a fixed wing incidence was not practical for the wing angle of attack range desired for these data. Therefore, the data for evaluating the tunnel wall corrections

55

were obtained from runs for which the fuselage angle was constant and the wing incidence angle was varied. While this procedure may not be best for obtaining design data, it provides a suitable means of obtaining data to investigate tunnel wall effects. The procedure for conducting these runs consisted of establishing a nominal thrust coefficient by setting the required combination of tunnel dynamic pressure and propeller speed; the wing incidence angle was then varied from 0 to 90 degrees while maintaining constant tunnel dynamic pressure and propeller speed. The thrust coefficient range for these runs was from 0 to 0.975 in the 15 X 20- and 21 X 23-foot sections and from 0 to 0.75 in the 7 X 10-foot section. The maximum thrust coefficient in the 7 X 10-foot section was limited by the minimum controllable dynamic pressure in that section. Runs were made with the horizontal tail at zero incidence and with the horizontal tail removed. The wing leading edge slats and trailing edge flaps were in the retracted position. During this phase of each test, tufts were attached to the test section floor and side walls to detect any recirculation or tunnel flow reversal that might occur at the higher wing incidences and thrust coefficients.

Model configurations and test conditions were selected from the NASA Langley tests and simulated in each of the VAD test sections. One possibly significant configuration detail remained different, however, the inboard propellers on the VAD model were tilted down approximately two degrees and on the Langley model they were not. Tufts were attached to the model wing using the Langley method. Model configurations and average thrust coefficients for wing/flap combinations of 0°/0°, 20°/60°, and 40°/60°, corresponding to the Langley tests, were duplicated. Matching the individual propeller thrust coefficients of the Langley tests was not attempted. The procedure for conducting these runs consisted of matching the Langley thrust value at zero angle of attack by setting the required combination of tunnel dynamic pressure and propeller speed; the dynamic pressure and propeller speed were then maintained constant while the model attitude was varied.

Several parameters were individually varied during the tests to determine which parameters have a significant effect on test results. Since the previous wind tunnel tests indicated the propeller blade pitch angle affected the aerodynamic characteristics of the model, this parameter was further investigated during these tests. Model configurations with propeller blade pitch angles of 4, 8, 12, and 14 degrees were tested. Data were obtained during the test in the 7 X 10-foot section for evaluating flow continuity corrections (Reference 20). The dynamic pressure was measured in the proximity of the model with four pitot-static tubes. The tubes were located outside of the propeller slipstream. The free stream dynamic pressure was established in the normal manner and either the propeller thrust coefficient or model angle of attack was varied. Reynolds number effects were investigated during the tests in the 7 X 10- and 15 X 20-foot sections. Data were obtained from runs during which the propeller thrust coefficient was the same but the free stream dynamic pressure was different.

A few runs were repeated during the tests to obtain an indication of the instrumentation accuracy. Data obtained from repeat runs in the 15 X 20-foot section are shown in Figure 20. Based on repeat runs, the instrumentation accuracy was approximately $\pm$ 1.0 pounds for lift, $\pm$ 0.5 pounds for drag, $\pm$ 0.5 foot-pounds for pitching moment, and $\pm$ 0.25 pounds for the thrust of each propeller.

2. DISCUSSION OF RESULTS

Since it was found that many of the factors contributing to the lack of agreement in the data from the previous tests were controllable, every effort was made to avoid such problems with the data obtained during these tests. However, significant differences between data obtained from the three test sections remain.

During the analysis of the data obtained from the three sections, it became apparent that although the characteristics of the data were quite similar, the magnitude of the data from the 21 X 23-foot test section was consistently less than either the 7 X 10- or 15 X 20-foot sections. An extensive study was made of the possible causes of this discrepancy, but no strict resolution was achieved. There are numerous factors that could conceivably cause the difference in the data, but only one was found that would bring the data into better agreement throughout the wing incidence range and thrust coefficient range. The apparent reason for the discrepancy in the data is that the test section dynamic pressure used to reduce the data to coefficient form, which was determined from a free test section survey, was not the same as the average dynamic pressure acting on the model during the test. It is believed that the discrepancy could be eliminated with an accurate dynamic pressure survey in the region occupied by the model.

For the propellers-off runs, an error in dynamic pressure of about 10-15 percent (0.09 inches of water) would bring the data into good agreement. A somewhat higher error, about 25 percent, is needed for the propellers-on runs. Of course, an error in the dynamic pressure for the other two sections would bring those data into agreement with the 21 X 23-foot section data. However, the very uniform flow in these two sections makes this possibility an unlikely prospect.

As a consequence of the dynamic pressure uncertainty, the absolute value of coefficient data obtained in the 21 X 23-foot section is unknown; and, therefore, these data were not considered in some of the analysis. However, the characteristics of the data not affected by the dynamic pressure, such as angle for maximum lift, were considered in the analysis.

a. TUNNEL WALL EFFECTS

The large wake deflection angles of V/STOL models in some test sections result in wake impingement on the wind tunnel walls in the region near the model causing relatively large, wall induced, flow deflection angles. The classical wall correction methods are not applicable to V/STOL models because of the assumption, in the derivation of the theory, that the model wake is not

57

deflected. Mr. H. H. Heyson, of the NASA Langley Research Center, developed a method (Reference 15) for correcting the data for the effects of the tunnel walls that takes into account the deflection of the model wake. However, previous attempts to correlate wind tunnel data obtained from a single model tested in different size test sections (References 21, 22, and 23), using this method, did not provide satisfactory results. Generally, the corrections were adequate for correcting the lift and drag to free air conditions only in the intermediate angle-of-attack range and the pitching moment corrections were in the wrong direction. The method was later modified (Reference 24) to improve the pitching moment correction. Essentially, the modification amounted to using an "effective" wake deflection angle (measured from the horizontal) which was one-half that used in the original method. It was recognized that with this modification, the method would not be applicable for hovering or very low forward speeds. However, it was believed that limitations on the minimum speed at which tests can be made in a meaningful fashion in wind tunnels (when recirculation occurs) would be encountered before the failure of the correction method.

The theoretical relations of Reference 15 and the "effective" wake angle modification were incorporated into a data correction routine and applied to the basic data from each test section. The calculation procedure consisted of three basic steps. First, the effective wake deflection angle was calculated from the lift, drag and tunnel flow measurements. Second, the wall interference factors were calculated for that wake angle, tunnel geometry and model location. The third operation consisted of converting the interference factors into wall induced angle-of-attack and dynamic pressure change and correcting the various aerodynamic parameters accordingly. Since the tunnel dynamic pressure was used in reducing the data to coefficient form, all model force and moment coefficients were affected by the change in dynamic pressure.

An indication of the relative magnitude of the tunnel wall corrections for the different test sections is shown in Table III. The corrections were obtained from runs for which the nominal thrust coefficient was 0.5 at the beginning of the run. The magnitudes of the corrections are very nearly in the same ratio as the test section areas.

The longitudinal force and moment coefficient data, corrected for the effects of the tunnel walls, are presented in Figure 21. Data comparisons cannot be made at constant thrust coefficients at the very low values because of the manner in which the runs were conducted. Although the thrust coefficient was near zero at the beginning of a run, because the tunnel dynamic pressure and propeller speed were held constant, the thrust coefficient increased with increase in wing incidence to about 0.6 at a wing incidence of 90 degrees.

The net effect of the wind tunnel wall corrections for the wing incidence runs is very small as shown in Figure 22, although the correction to each parameter is quite large. The effect of the corrections is different for the wing incidence runs and the angle-of-attack runs as shown in Figure 23. The exact reason is not known; however, for the wing incidence runs, the model behaves as a pure tilt wing (no flap deflection) and for the angle-of-attack runs, the model behaves more as a deflected thrust model. The different lift-drag relationships for these two configurations appear to be the reason for the difference in tunnel wall corrections.

58

The corrections appear to be adequate for correcting the lift data from the 7 x 10-foot section up to about a thrust coefficient of 0.7 and wing incidence of 30 degrees (zero flap deflection). Above these values there is an abrupt loss in lift in the 7 x 10-foot section data. The drag data are in good agreement up to a wing incidence of about 40 degrees. Above this wing incidence, the agreement progressively gets worse. The pitching moment coefficient shows about the same characteristics, but it is shifted throughout the wing incidence range.

The good agreement of the data from 7 x 10- and 15 x 20-foot sections may only be fortuitous in that the dynamic pressure survey, discussed later, indicated the actual dynamic pressure was considerably higher than indicated by the clear tunnel calibration. In other words, the data may actually be shown for the wrong thrust coefficient and these compensating errors may only apply to this particular model. In any event, the tunnel wall corrections would not improve the agreement because their net effect is small.

The model force data do not give any indication of flow breakdown or recirculation effects, although the tufts in the 15 x 20-foot section indicated recirculation for the 0.975 thrust coefficient run above a wing incidence of about 60 degrees. This was indicated by the tufts adjacent to the model on the sidewalls pointing straight up. At about 70 degrees wing incidence, the tufts on the floor were pointing forward, indicating flow breakdown. It appears that the beginning of recirculation effects can be identified in the thrust measurements. As indicated in Figure 24, the thrust on the inboard propeller is shown to drop off sharply at a wing incidence of 60 degrees. The same trend is indicated by the thrust measurements taken in the 21 x 23-foot section, although the tufts did not show a definite indication of recirculation. As shown in the figure, the sharp reduction in thrust occurred at a wing incidence of about 70 degrees and a thrust coefficient of 0.95 in the 15 x 20-foot section. Data were not obtained for a thrust coefficient of 0.95 in the 21 x 23-foot section. There was no indication of recirculation effects in either of the sections at a thrust coefficient of 0.90. These indications might not be as apparent if the runs were conducted at a constant thrust coefficient unless the change in propeller speed required to maintain a constant thrust coefficient was sufficient to indicate recirculation.

It was hoped that the information obtained from these tests could be used to establish the practical limits of model configuration (i.e., wing/flap) and test condition variations with model/test section size ratio. However, because of the conflicting indication produced by the aerodynamic data, tuft observation and propeller thrust, it does not appear to be feasible.

b. DATA COMPARISONS FOR SIMILAR CONFIGURATIONS AND TEST CONDITIONS

(1) Propellers-off

Several runs were made in each of the test sections with the propellers removed. The primary reason for these runs was to determine the data repeatability without the presence of thrust effects. However, at

the low dynamic pressure values for most of these runs, the levels of the aerodynamic forces were very small. As a consequence, there were appreciable differences in the magnitudes of the force coefficients and also a large mount of scatter in the drag and pitching moment coefficient data. Comparisons of the propellers-off data are not shown because good agreement could be obtained by the selection of certain runs (from several repeat runs) and also very poor agreement could be obtained by the selection of other runs. The conclusion drawn from the analysis of these data is that propellers-off data should not be acquired in low speed sections, such as the VAD 15 x 20- and 21 x 23-foot test sections.

(2) Propellers-on

The data presented are for a constant thrust coefficient, obtained from cross-plots of the force coefficient versus thrust coefficient. Data for only one value of the thrust coefficient are shown for each model configuration because the results were very similar for other thrust coefficients and would not materially add to the discussion. Pitching moment data from the Langley tests are not shown because the data are not available for the same center-of-gravity location as the VAD data. However, since lift and drag have a strong influence on pitching moment, comparisons of these parameters provide a good indication of what could be expected from pitching moment comparisons.

Data for the cruise configuration (wing/flap combination of $0°/0°$) for a constant thrust coefficient of 0.20 are presented in Figure 25. The slope of the lift curve is in good agreement except for the 21 x 23-foot section, which is low. The angle for zero lift is in good agreement except for the 15 x 20-foot section, which indicates a more negative angle of about three-fourths degree. The drag coefficient is in fair agreement except for the Langley data, which shows a higher drag throughout the angle-of-attack range. The pitching moment comparison shows good agreement for the two large sections, whereas in the 7 x 10-foot section the pitching moment has about the same slope but is shifted; also, it shows no slope change for the higher angles-of-attack near stall.

Data for the STOL configuration (wing/flap combination of $20°/60°$) for a constant thrust coefficient of 0.70 are presented in Figure 26. The lift curve slope is in good agreement for all test sections. The angle for maximum lift is about the same for each test in the VAD tunnel, but the angle in the Langley tunnel is about four degrees lower. The magnitude of the data from both the VAD 21 x 23-foot section and the Langley tunnel appears to be low. The VAD drag coefficient data are in fairly good agreement except for the higher angles-of-attack. The Langley data are lower in magnitude through most of the angle-of-attack range. The pitching moment slope is very similar, but the curves are shifted in the order of the test section area.

Data for another STOL configuration (wing/flap combination of $40°/60°$) for a constant thrust coefficient of 0.70 are presented in Figure 27 for the VAD tests. The characteristics of the lift curves are very similar. The data from the 21 x 23-foot section is low (because of the dynamic pressure used in reducing the data), but otherwise the agreement

60

is remarkable. The drag and pitching moment is also in good agreement up to the stall angle. Data for the same configuration, but for a thrust coefficient of 0.80, is shown in Figure 28 for the Langley tests and the VAD 21 x 23-foot section. As shown in this figure, the lift agreement is good for the lower angles-of-attack, but the Langley data indicate wing stall at about -10 degrees whereas the VAD data indicate stall to occur at about -4 degrees. The drag coefficient data are not in agreement.

(3) Possible Causes of Disagreement

Several reasons for the differences in the data obtained in the Langley tests and VAD tests are possible. One reason could be the tilt of the inboard nacelles. As shown in Figure 29, the thrust variation with angle-of-attack is not the same for the inboard and outboard propellers. The data shown in this figure are typical for all VAD runs. Whether the difference in characteristics is caused by the tilt of the inboard propellers or some other effect, such as fuselage interference, is not known.

Another reason for the lack of agreement could be in the accuracy in determining and controlling thrust. As shown in Table IV, the accuracy in measuring or controlling thrust at the beginning of a Langley run was about three or four pounds; whereas, for the special VAD tests, the accuracy was well within one-half pound. The thrust levels are different for the two tests because the model scales were different and the test dynamic pressures the same. The variation of thrust with angle-of-attack is also different for the two tests. Although there is considerable difference in the thrust of each propeller, the average thrust coefficients are very similar. No attempt was made to duplicate the thrust of individual propellers of the Langley tests, only the average thrust for zero angle-of-attack was duplicated. To simulate all variables would have resulted in a mammoth test program.

Model configurations could also account for some of the disagreements. Although every effort was made to simulate the Langley configurations, differences still existed; furthermore, the accuracy in setting the various slat and flap deflections could result in disagreements.

As a last consideration, the accuracy of the test dynamic pressure value used in reducing the data to coefficient form could account for some of the differences in data. At low values of test dynamic pressure, instrumentation limitations can cause errors, as discussed in Section III. Also, the method of deriving an average test section dynamic pressure from the test section survey can affect the value obtained.

Although there are some differences in the data obtained in the Langley and VAD tests, so are there differences in the data obtained in the three VAD test sections. In general, the agreement is considered acceptable. The exceptions point out the fact that V/STOL wind tunnel testing is still relatively new and emphasizes the continual need for improving test techniques.

c. **SIGNIFICANT TEST PARAMETERS**

Wind tunnel test requirements are obviously much more stringent for V/STOL models than for conventional models. In order to define the test requirements for future V/STOL tests, several parameters were investigated to assess their importance in acquiring valid data. The following paragraphs present the results of this study.

(1) **Propeller Effects**

Propeller thrust is a fundamental parameter in the determination of aerodynamic forces on a tilt wing airplane; therefore, knowledge of the magnitude of thrust is essential to correlating data from different tests. Since the wing angle-of-attack range is large (and can exceed 90 degrees), using the standard procedure of maintaining a constant propeller speed results in a variation of thrust with angle-of-attack that is extremely large. As shown in Figure 30, for a fixed blade angle, constant tunnel dynamic pressure and constant propeller speed, the average thrust coefficient varies from zero at zero wing incidence to about 0.55 at a wing incidence of 90 degrees. The rate of change of thrust coefficient with wing incidence is shown to decrease with increase in thrust coefficient, but it continues to be significant to a thrust coefficient between 0.9 and 0.95.

In addition to accurately measuring and controlling thrust, it is also important to simulate the slipstream rotation, as shown in Figure 31. For the cruise configuration, the propeller blade pitch angle has a significant effect on the aerodynamic force data. The effect is even more pronounced for the STOL configuration. These data indicate that misleading information can result if only one propeller blade pitch angle is used for all transition tests. It appears that the conventional model testing practice of matching the airplane advance ratio should be adopted for V/STOL wind tunnel tests.

The conventional model testing procedure of maintaining a constant propeller rotational speed during a run has carried over to V/STOL testing. Since the propeller thrust must now be measured, this procedure is no longer advisable. Because of the variation of thrust with angle-of-attack, when the propeller speed is constant, the main balance data must be cross-plotted to obtain data at a constant thrust coefficient. Furthermore, although the tunnel dynamic pressure is maintained constant during a run, the tunnel air temperature may vary because heat is added by the tunnel fan and model propellers. This change in tunnel air temperature alters the tunnel velocity and model propeller thrust. It is virtually impossible to repeat a run at the same thrust, with constant propeller speed, when the tunnel temperature variation for each run is different. A comparison of data for a constant thrust coefficient, obtained from cross-plots and from a run for which the thrust was held constant, is presented in Figure 32. Based on this comparison, the final result is not dependent upon which of these two methods is used to acquire the data. It seems a more suitable procedure for conducting propeller driven model tests is to vary the propeller speed, such that the propeller thrust is maintained constant.

The propeller hub moments, usually negligible for conventional airplanes, are significant at the high angles of incidence encountered by V/STOL airplanes. The propeller hub moment combined with the propeller normal force represents a major part of the total airplane pitching moment, as shown in Figure 33. The aerodynamic design engineer needs to know the contribution of each component to the total aerodynamic characteristics of the airplane. Therefore, it becomes essential to measure all propeller forces and moments.

(2) Test Section Dynamic Pressure

The measurement of the test section dynamic pressure becomes uncertain if the model is large relative to the test section. The usual method of establishing the test dynamic pressure is to relate the clear test section average dynamic pressure to the difference between two static pressures; one measured in the plenum (or large section), and the other at the entrance to the test section. For an unpowered model test, a flow continuity correction is included in the data reduction to account for the effect of the model on the dynamic pressure. The presence of the model decreases the effective test section area and, therefore, the dynamic pressure in the region of the model is increased. With a propeller driven V/STOL model and its high thrust, the mass flow through the propellers can represent a large percentage of the mass flow through the test section. Reference 20 presents a method for correcting the test dynamic pressure for the effects of the propeller slipstream at zero angle-of-attack. Correction methods have not been developed that will account for the effect of the model thrust on the test section dynamic pressure through the large angle range associated with a V/STOL model.

Dynamic pressure measurements were taken in the vicinity of the model, outside the slipstream, during the test in the 7 x 10-foot section. The location of the pitot-static tubes, with relation to the model and test section walls, is shown in Figure 34. The data presented in Figure 35 were obtained from runs for which the wing incidence and flap deflection were zero. Two observations are apparent: the pitot-static measurements are higher than the clear test section indication, and the pitot-static measurements increase with angle-of-attack. The average of the four pressures is shown in this figure. Generally, the No. 1, No. 2 and No. 3 probes showed an increase in dynamic pressure with increase in angle-of-attack, and the No. 4 probe showed a decrease in pressure. However, the data obtained with the probes leave some doubt because of the interference of the model flow field on the probes. Since the test section dynamic pressure is used to establish the thrust coefficient and to reduce the data to coefficient form, serious errors can result if the dynamic pressure is not accurately determined. It seems that further study of the effects of model propulsion systems on test dynamic pressure is appropriate.

(3) Scale Effect

Small scale model tests are usually conducted at Reynolds numbers considerably lower than for the full scale aircraft. Consequently, there is concern about scale effects. One of the main concerns

is the effect of Reynolds number on lift coefficient. With a model that has the wing almost completely submerged in the propeller slipstream, such as the XC-142A model, the turbulence in the slipstream would be expected to diminish the scale effects. This appears to be true for the cruise configuration (no flaps or slats) as shown in Figure 36. The data shown in this figure were obtained in the 7 x 10-foot section at dynamic pressures of 6.0, 9.0, and 15 PSF, corresponding to free stream Reynolds numbers (based on the wing MGC) of 4.1, 5.0, and 6.05 x 10^5, respectively. These runs were made by varying the wing incidence with the fuselage at zero angle-of-attack. The slipstream Reynolds numbers were only slightly higher because of the relatively low thrust coefficients for these runs. The Reynolds number effect for the STOL configuration is fairly large, as shown in Figure 37. The data shown were obtained in the 15 x 20-foot section for a wing/flap combination of 20°/60° with leading edge slats at a thrust coefficient of 0.64. The dynamic pressure was 2.81 and 3.84 PSF, corresponding to free stream Reynolds numbers of 2.8 and 3.27 x 10^5, respectively. The slipstream Reynolds numbers were 4.63 and 5.43 x 10^5. The scale effect shown for this configuration may be due to the double-slotted flaps and slats, because the Reynolds number for these components would be much lower than for the wing. Since scale effects cannot always be predicted, it is recommended that the investigation of these effects be included in every V/STOL wind tunnel program.

(4) Effect of Tufts

No particular effort was made to evaluate the effect of tufts during this program because of the large number of runs involved in such an investigation. Runs were made in the 15 x 20-foot section with tufts on and off for a wing/flap configuration of 20°/60° and a thrust coefficient $(C_{T,s})$ of 0.64. The results of these runs are presented in Figure 38. It is apparent that a significant effect was achieved when tufts were used. As shown by the repeat runs for the propellers-off configuration (Figure 39), which were the first runs of the test, it appears that the tuft effect varies with time. Or, more specifically, when the tufts are first installed and are in good clean condition, they have a certain effect on the data, but as the tufts become frayed and knotted or otherwise deteriorated, their effect on the data changes. This would lead one to conclude that the effect of tufts on the data cannot be accounted for by making only a few runs with the tufts removed. If the condition of the tufts causes their effects to be different, the manner in which they are installed (the orientation of the hold down tape, for example) would certainly be expected to produce different effects.
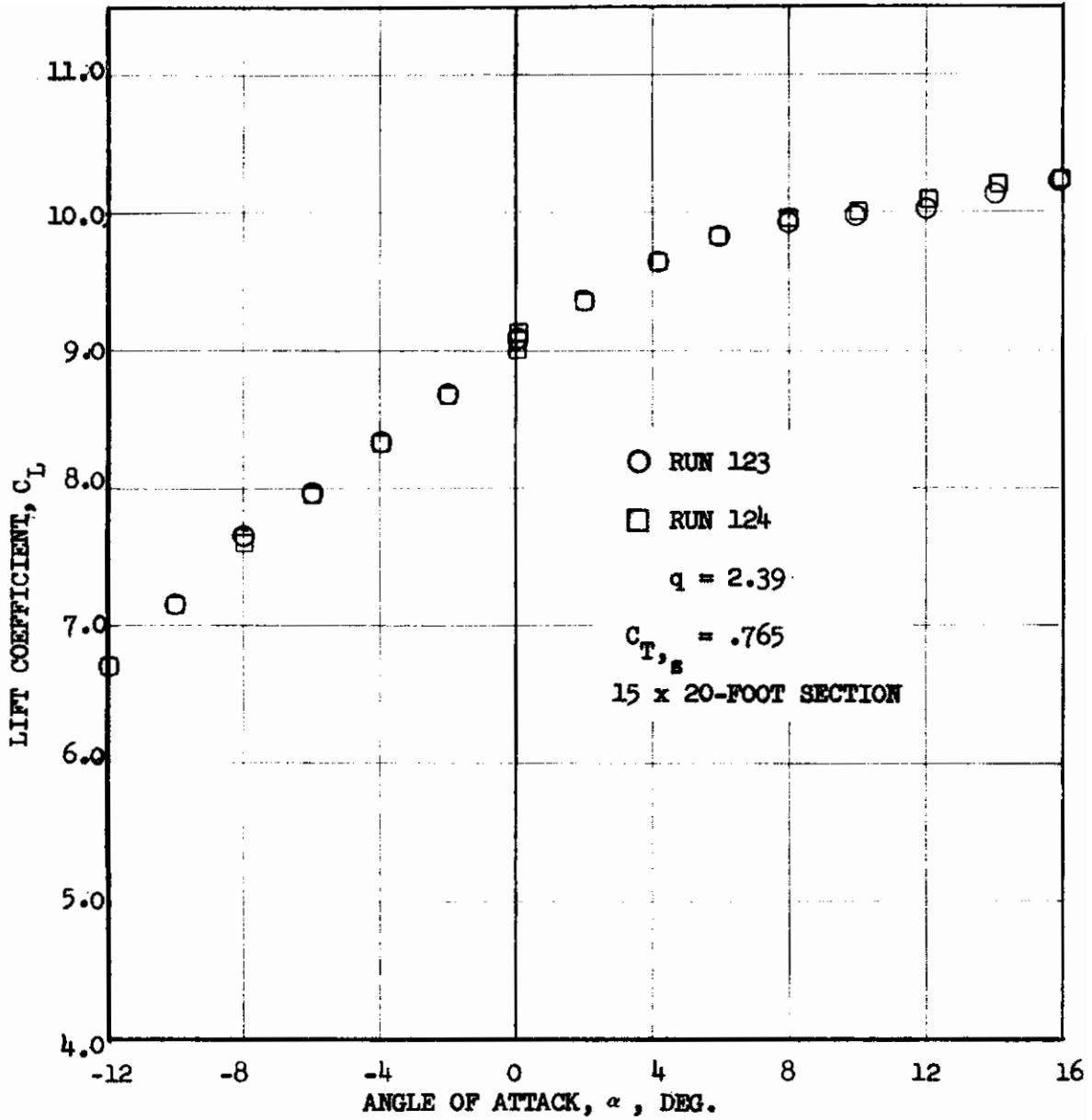
TABLE III RELATIVE MAGNITUDE OF TUNNEL WALL CORRECTIONS

Wing Incidence Degrees	Correction to Angle-of-Attack - Degrees		
	7 X 10	15 X 20	21 X 23
0	0.41	0	0
10	1.05	0.13	0.07
20	1.50	0.24	0.14
30	1.87	0.32	0.19
40	2.25	0.42	0.24
50	2.59	0.50	0.28
60	2.82	0.59	0.33
70	3.04	0.66	0.36
80	3.21	0.72	0.38
90	3.41	0.75	0.40

TABLE IV - COMPARISON OF LANGLEY AND VAD PROPELLER THRUST

Angle of Attack (Degrees)	PROPELLER THRUST - POUNDS				Average Thrust Coefficient	Test
	Left Outboard	Left Inboard	Right Inboard	Right Outboard		
-10	7.05	11.27	8.77	9.16	.515	
-5	6.35	10.50	9.48	8.61	.506	
0	6.11	9.74	8.60	8.22	.489	
5	5.98	8.98	8.61	8.18	.482	Langley
10	6.58	9.19	9.57	8.32	.497	
15	7.63	9.75	10.51	8.94	.519	
20	8.57	10.50	11.45	10.23	.545	
-6	11.91	11.74	12.03	11.92	.488	
-4	11.74	11.56	11.83	11.76	.484	
0	11.52	11.34	11.58	11.58	.479	
4	11.57	11.43	11.58	11.60	.480	VAD
8	11.86	11.62	11.84	11.88	.485	
12	12.30	12.09	12.31	12.31	.495	
16	12.95	12.65	13.09	13.05	.508	
20	13.75	13.72	14.11	13.90	.530	

O RUN 123

□ RUN 124

$q = 2.39$

$C_{T,s} = .765$

15 x 20-FOOT SECTION

LIFT COEFFICIENT, C_L

ANGLE OF ATTACK, α , DEG.

(a) C_L vs α

FIGURE 20   REPEATABILITY, RUN TO RUN
IN VAD 15 x 20-FOOT TEST SECTION

67

O   RUN 123

□   RUN 124

$q = 2.39$

$c_{T,_s} = .765$

15 x 20-FOOT SECTION

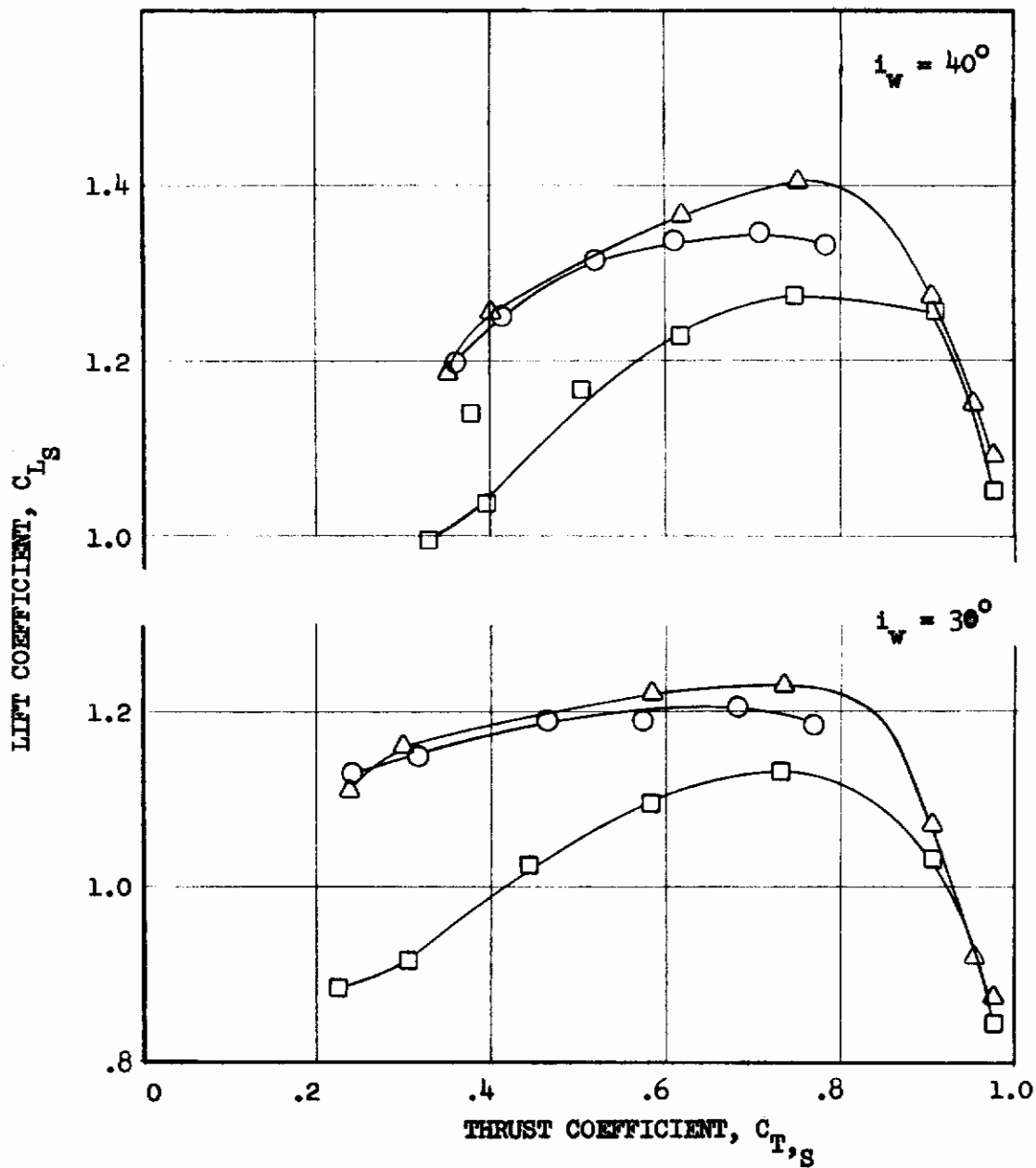c_D vs α

ANGLE OF ATTACK, α , DEG.
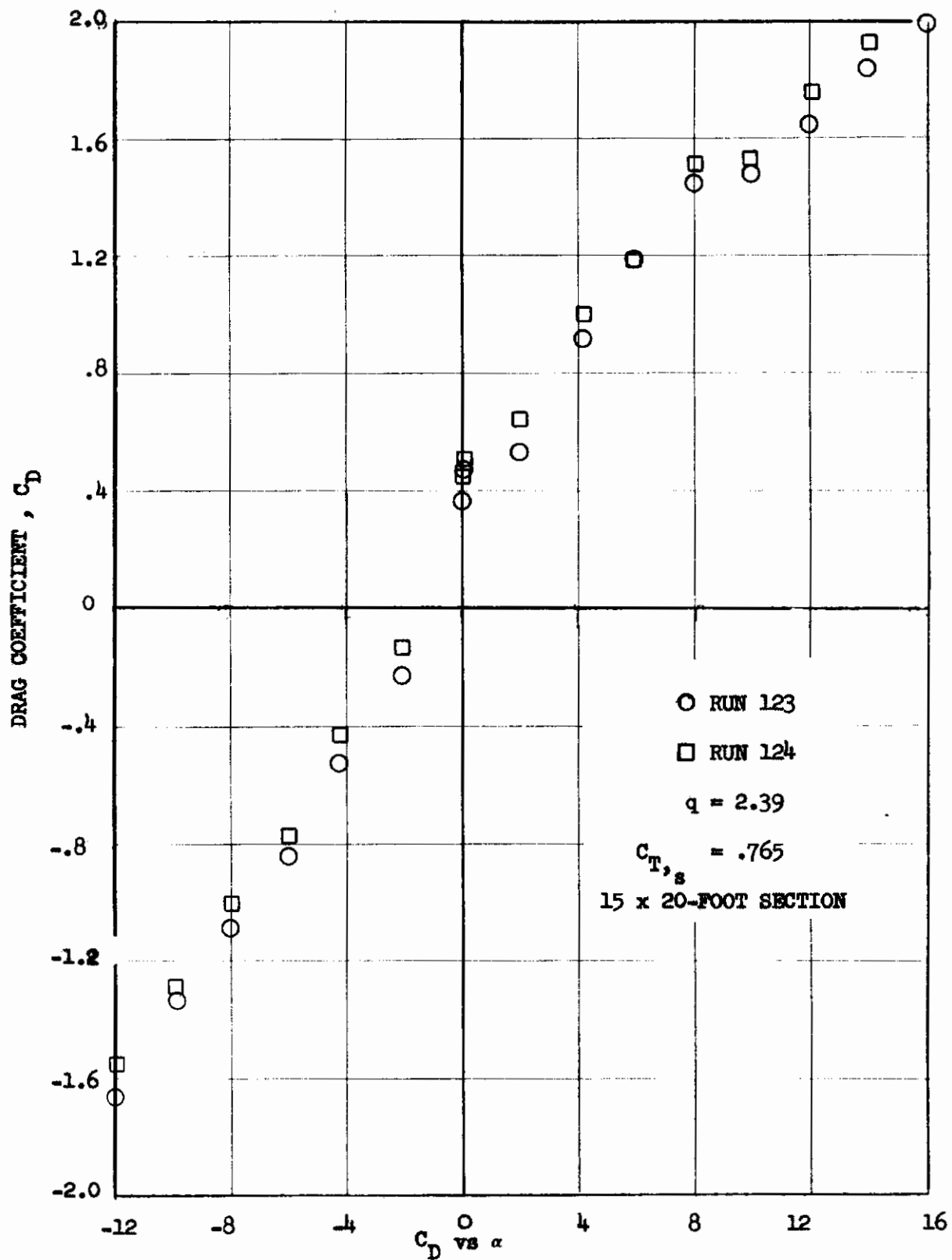
FIGURE 20 (CONCLUDED)

68
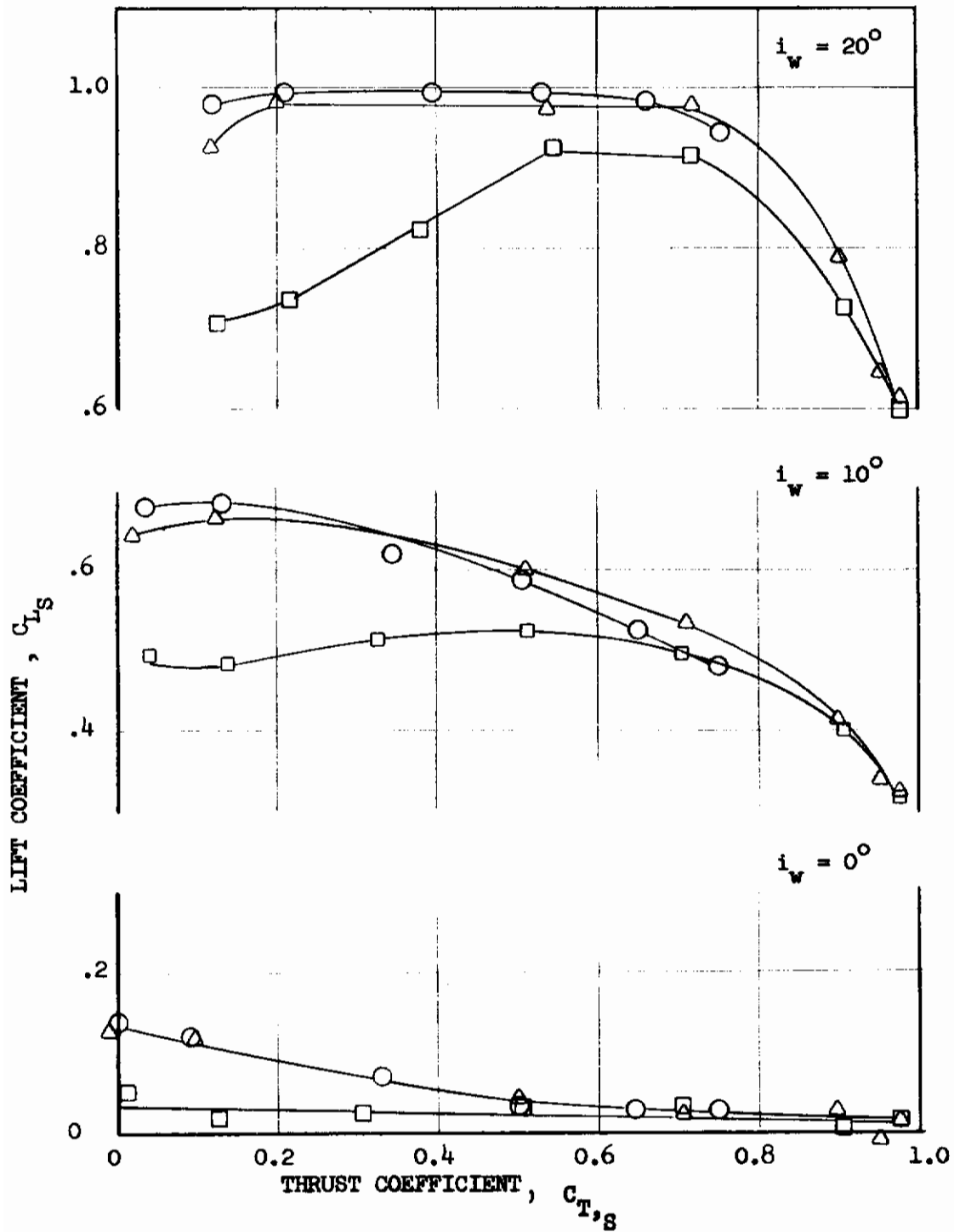
○ 7 X 10 , △ 15 X 20 , □ 21 X 23

(a) C_{L_S}, $i_w = 0°$, $10°$, AND $20°$

FIGURE 21   COMPARISON OF DATA FROM THREE DIFFERENT SIZE
TEST SECTIONS, CORRECTED FOR WALL EFFECTS

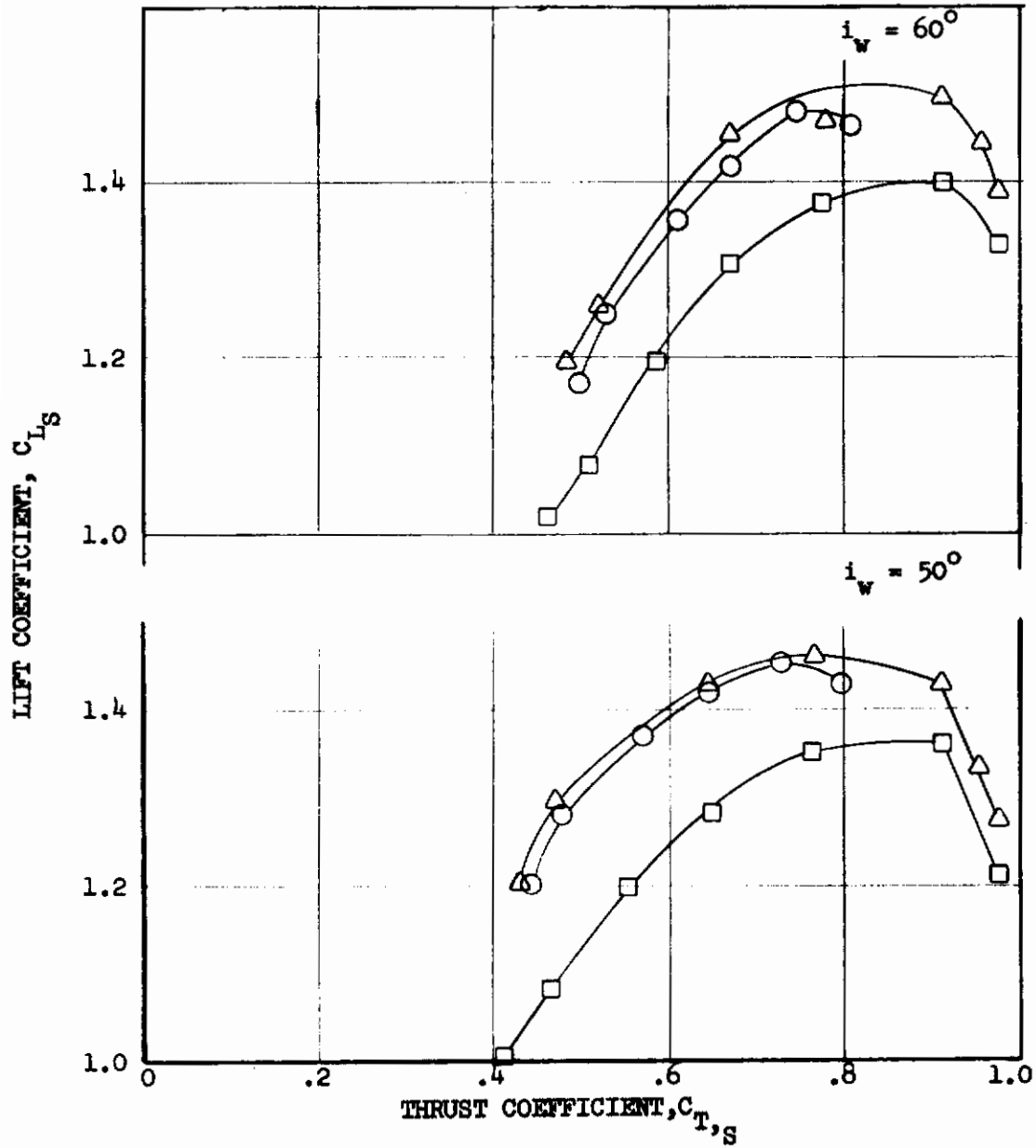$\bigcirc 7 \times 10, \triangle 15 \times 20, \square 21 \times 23$

(b) C_{L_S}, $i_w = 30°$ AND $40°$

FIGURE 21 (CONTINUED)

$\bigcirc$ 7 X 10 , $\triangle$ 15 X 20 , $\square$ 21 X 23

(c) C_{L_S} , i_w = 50° AND 60°

FIGURE 21 (CONTINUED)

71

○ 7 X 10 , △ 15 X 20 , □ 21 X 23

$i_w = 80^\circ$

$i_w = 70^\circ$

LIFT COEFFICIENT, C_{L_S}

THRUST COEFFICIENT, $C_{T,S}$
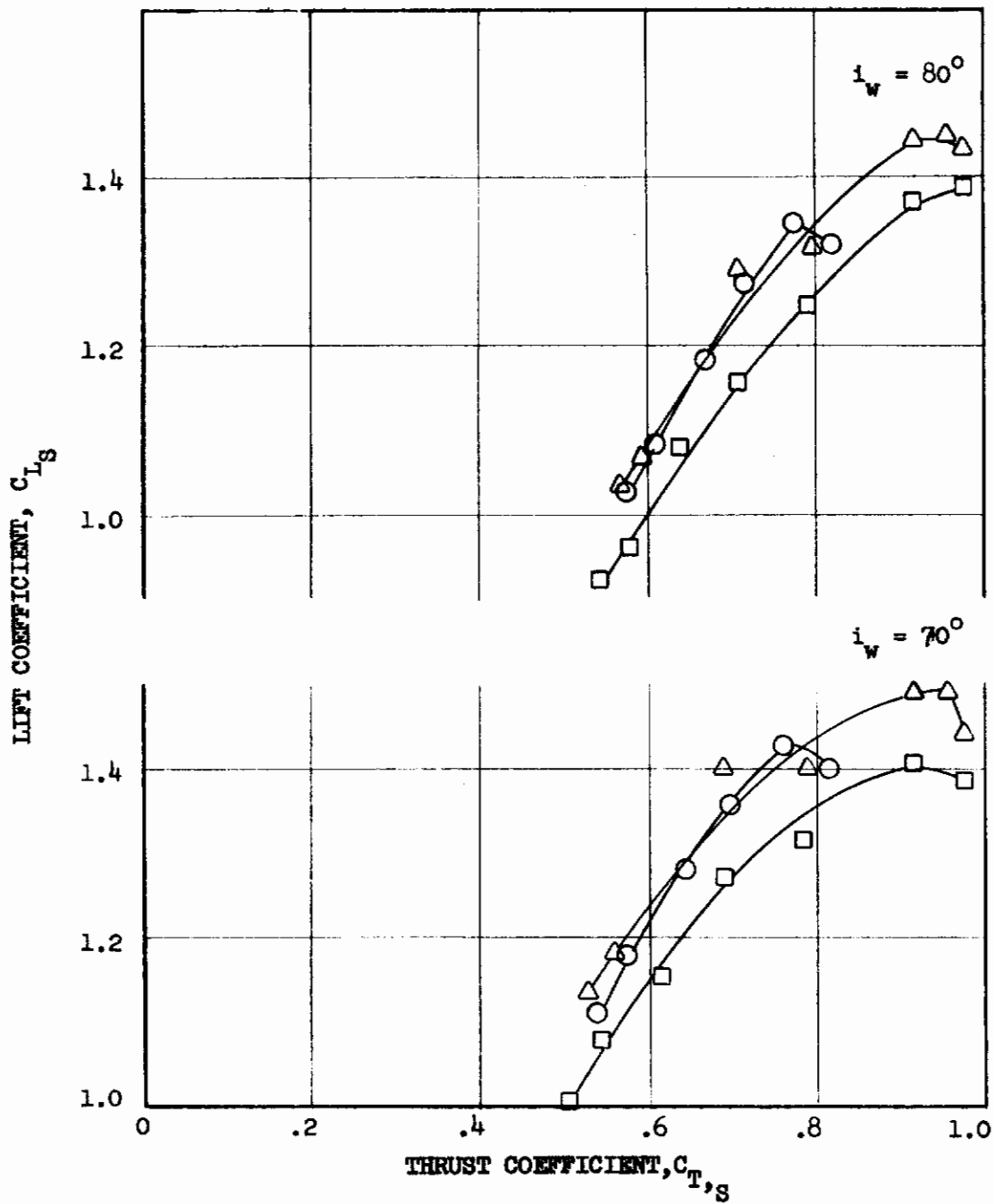
(d) C_{L_S} , $i_w = 70^\circ$ AND 80°

FIGURE 21 (CONTINUED)

○ 7 X 10 , △ 15 X 20 , □ 21 X 23
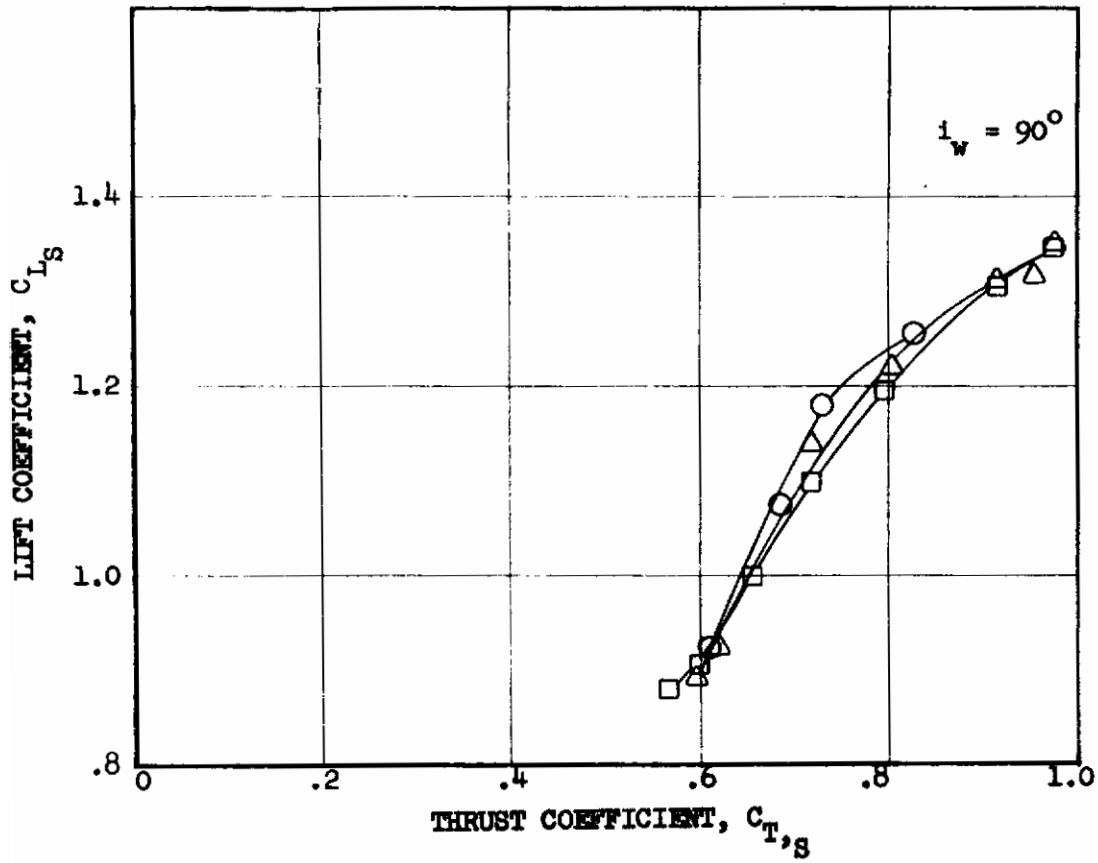

(e) c_{L_S} , $i_w = 90°$

FIGURE 21 (CONTINUED)

73

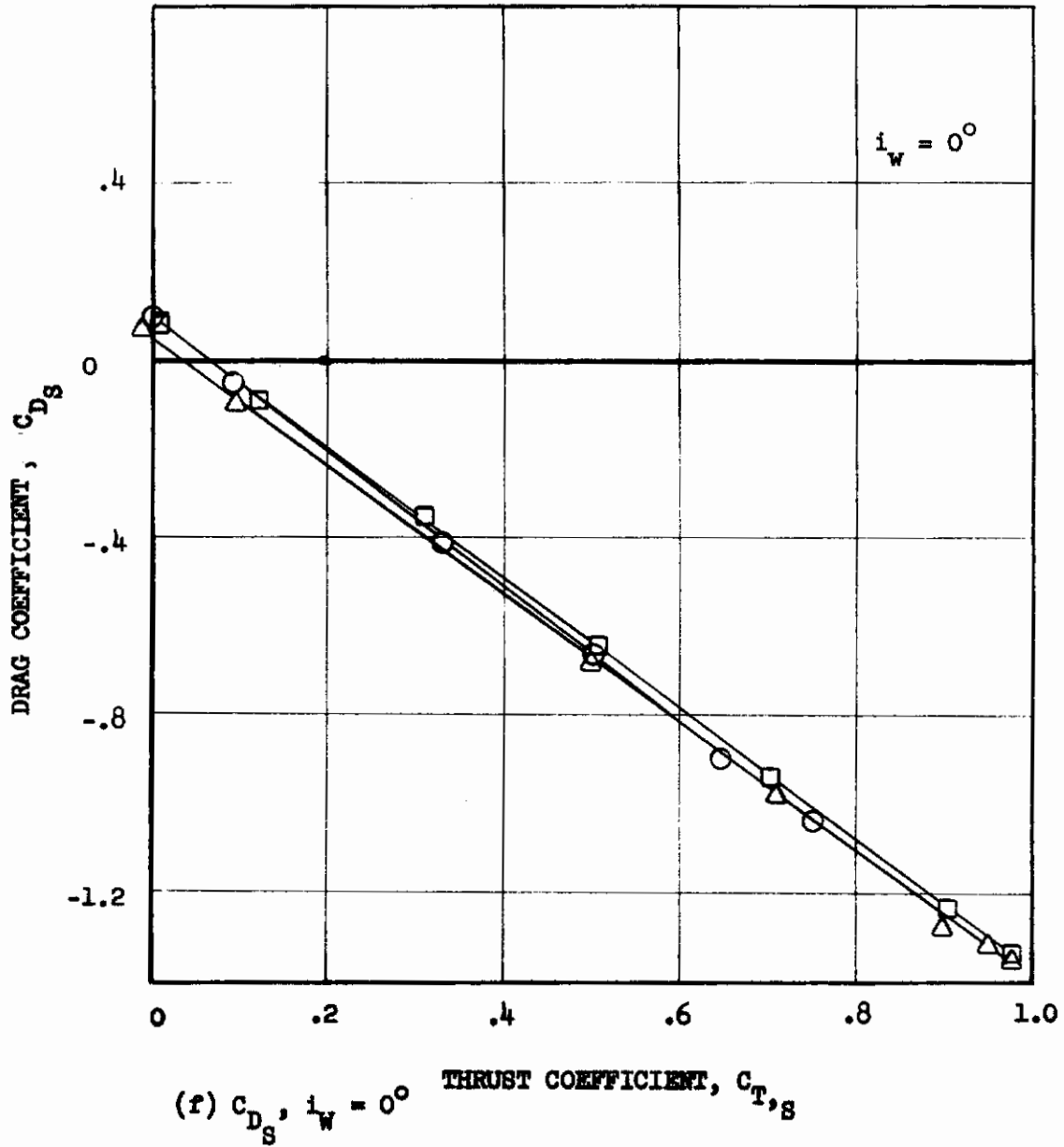$\bigcirc$ 7 X 10 , $\triangle$ 15 X 20 , $\square$ 21 X 23

(f) C_{D_S}, $i_W = 0^\circ$

FIGURE 21 (CONTINUED)

$\bigcirc$ 7 X 10 , $\triangle$ 15 X 20 , $\square$ 21 X 23

$i_W = 10^{\circ}$

DRAG COEFFICIENT C_{D_S}

.4

0

-.4

-.8

-1.2

0   .2   .4   .6   .8   1.0

THRUST COEFFICIENT, $C_{T,s}$

(g) C_{D_S}, $i_W = 10^{\circ}$

FIGURE 21 (CONTINUED)

75

$\bigcirc$ 7 X 10 , $\triangle$15 X 20 , $\square$ 21 X 23

$i_W = 20^\circ$

DRAG COEFFICIENT, C_{D_S}

.4

0

-.4

-.8

-1.2

0 .2 .4 .6 .8 1.0

THRUST COEFFICIENT, $C_{T,S}$
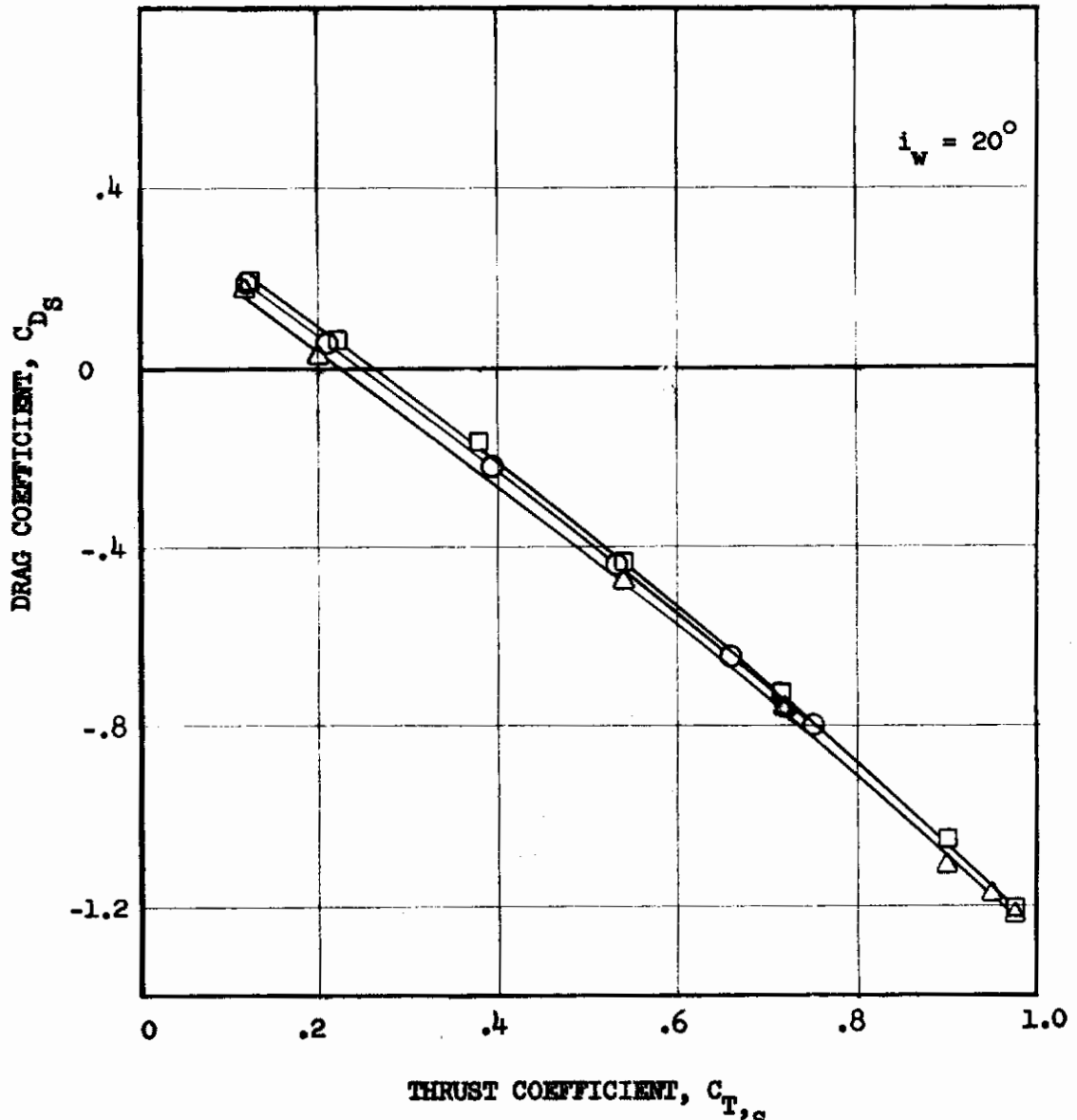
(h) C_{D_S} , $i_W = 20^\circ$

FIGURE 21 (CONTINUED)
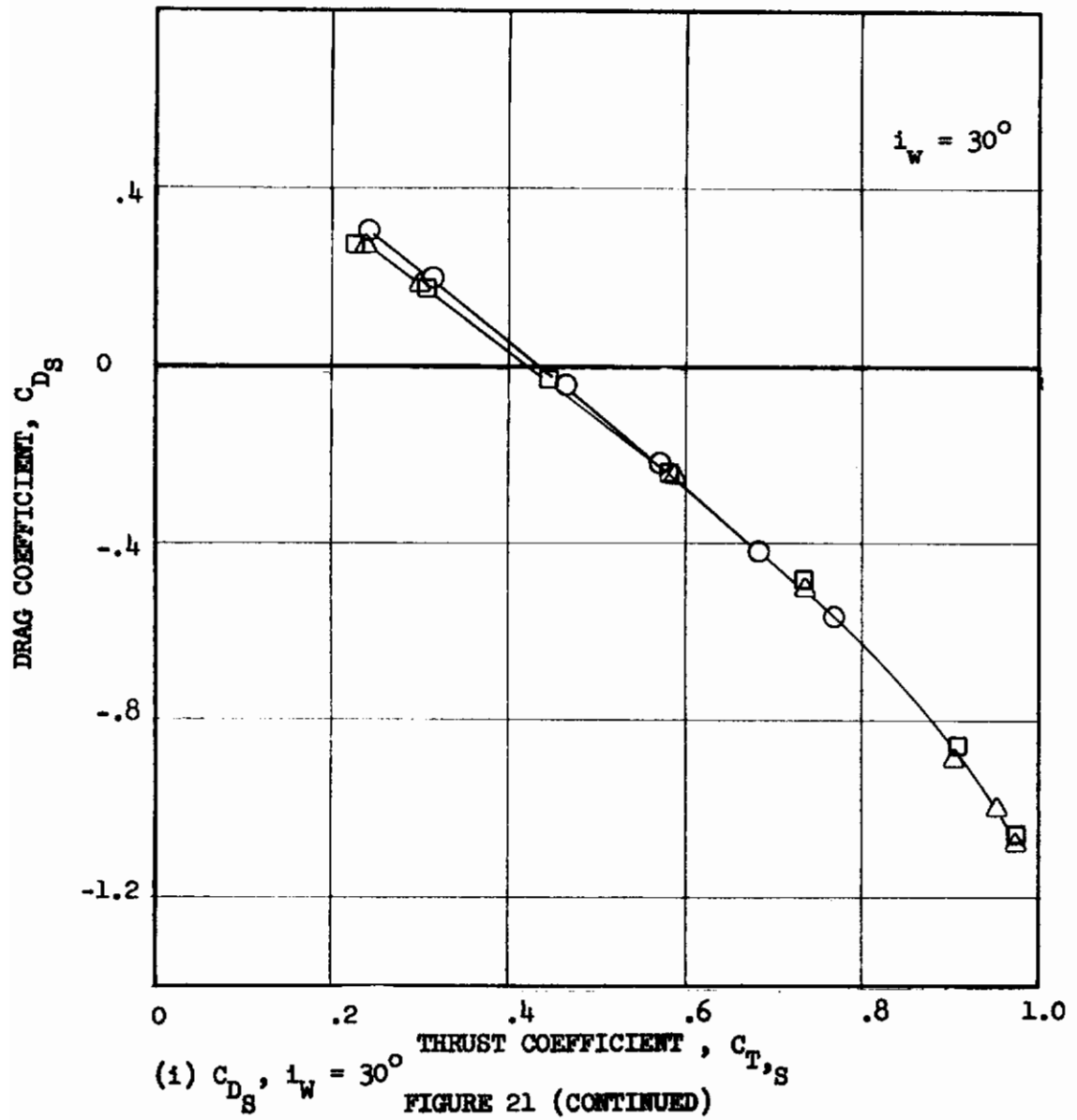
76

$\bigcirc$ 7 X 10 , $\triangle$ 15 X 20 , $\square$ 21 X 23

$i_w = 30^{\circ}$

(i) C_{D_S}, $i_W = 30^{\circ}$

FIGURE 21 (CONTINUED)

77

(j) C_{D_S}, $i = 40°$ AND $50°$

FIGURE 21 (CONTINUED)

78

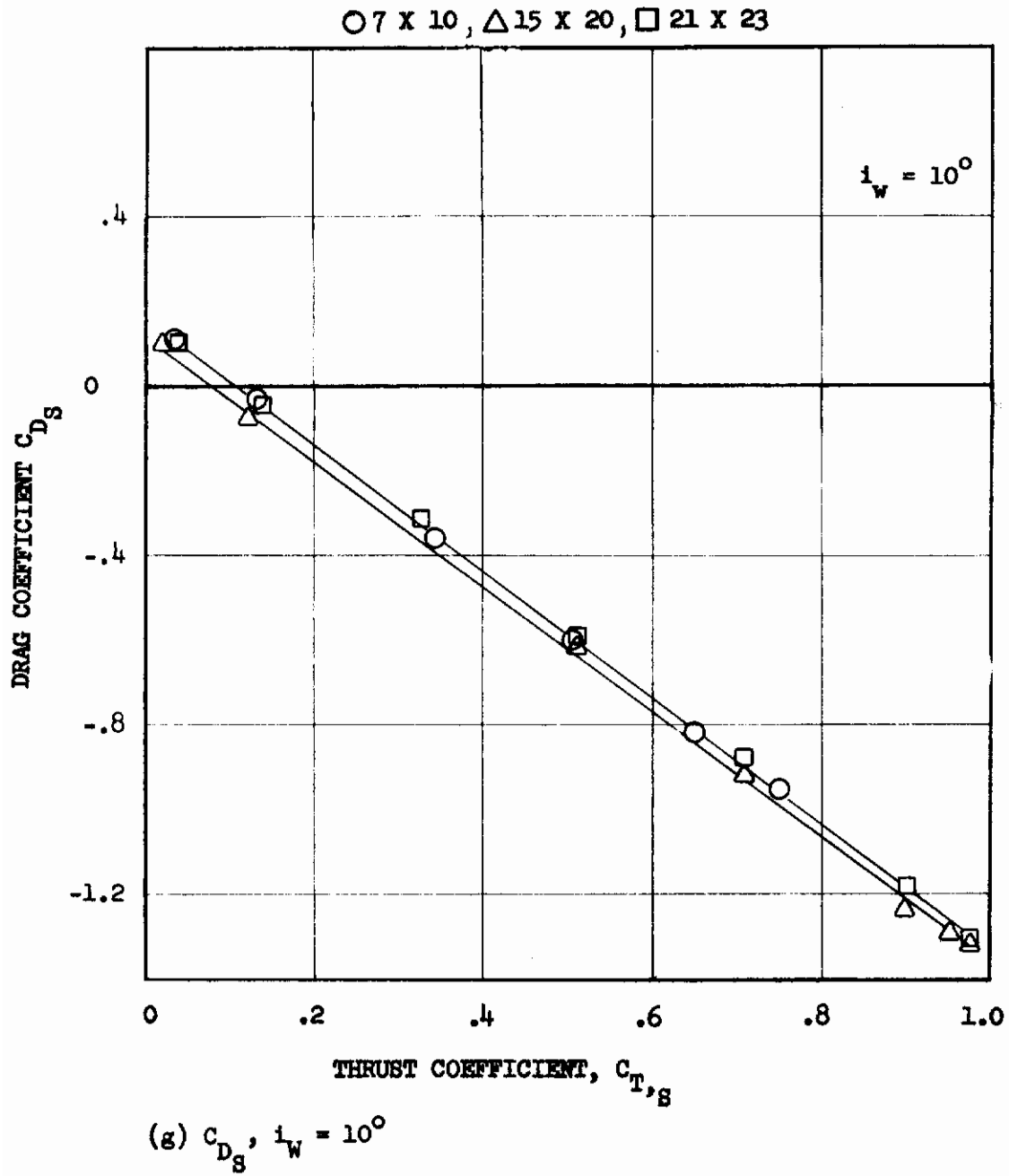O 7 X 10, $\triangle$ 15 X 20, $\square$ 21 X 23

(k) C_{D_S}, $i_W = 60°$ AND $70°$

FIGURE 21 (CONTINUED)

79

O 7 X 10, △ 15 X 20, □ 21 X 23

$i_w = 90^\circ$

$i_w = 80^\circ$

DRAG COEFFICIENT, C_{D_S}

THRUST COEFFICIENT, $C_{T,S}$

(1) C_{D_S}, $i_w = 80^\circ$ AND 90°

FIGURE 21 CONTINUED)

80

○ 7 X 10 , △ 15 X 20 , □ 21 X 23

(m) C_{M_S}, $i_W = 0°$ AND $10°$
FIGURE 21 (CONTINUED)

81

(n) C_{M_S}, $i_W = 20°$ AND $30°$

FIGURE 21 (CONTINUED)

82

O 7 X 10, △ 15 X 20, □ 21 X 23

(o) C_{M_S}, i_W = 40° AND 50°

FIGURE 21 (CONTINUED)

83

○ 7X10, △ 15X20 , □ 21X23

$i_W = 70°$

$i_W = 60°$

PITCHING MOMENT COEFFICIENT, C_{M_S}

THRUST COEFFICIENT , $C_{T,S}$

(p) C_{M_S} , $i_W = 60°$ AND $70°$

FIGURE 21 (CONTINUED)

84

O 7X10, △ 15X20, □ 21X23

$i_W = 90°$

$i_W = 80°$

PITCHING MOMENT COEFFICIENT, C_{M_S}

.4

.2

0

.2   .4   .6   .8   1.0

THRUST COEFFICIENT , $C_{T,S}$

(q) C_{M_S}, $i_W = 80°$ AND $90°$

FIGURE 21 (CONCLUDED)

85
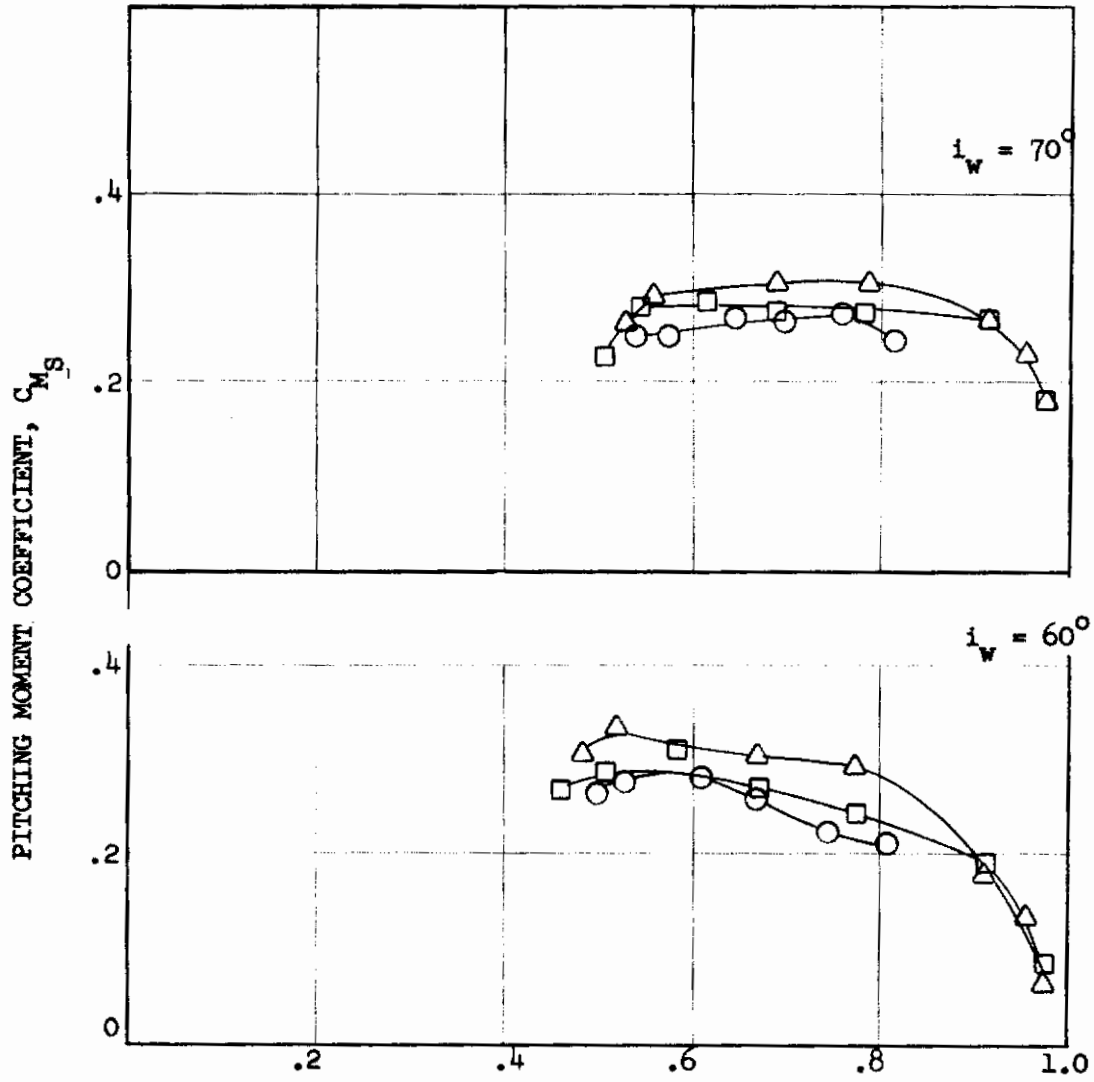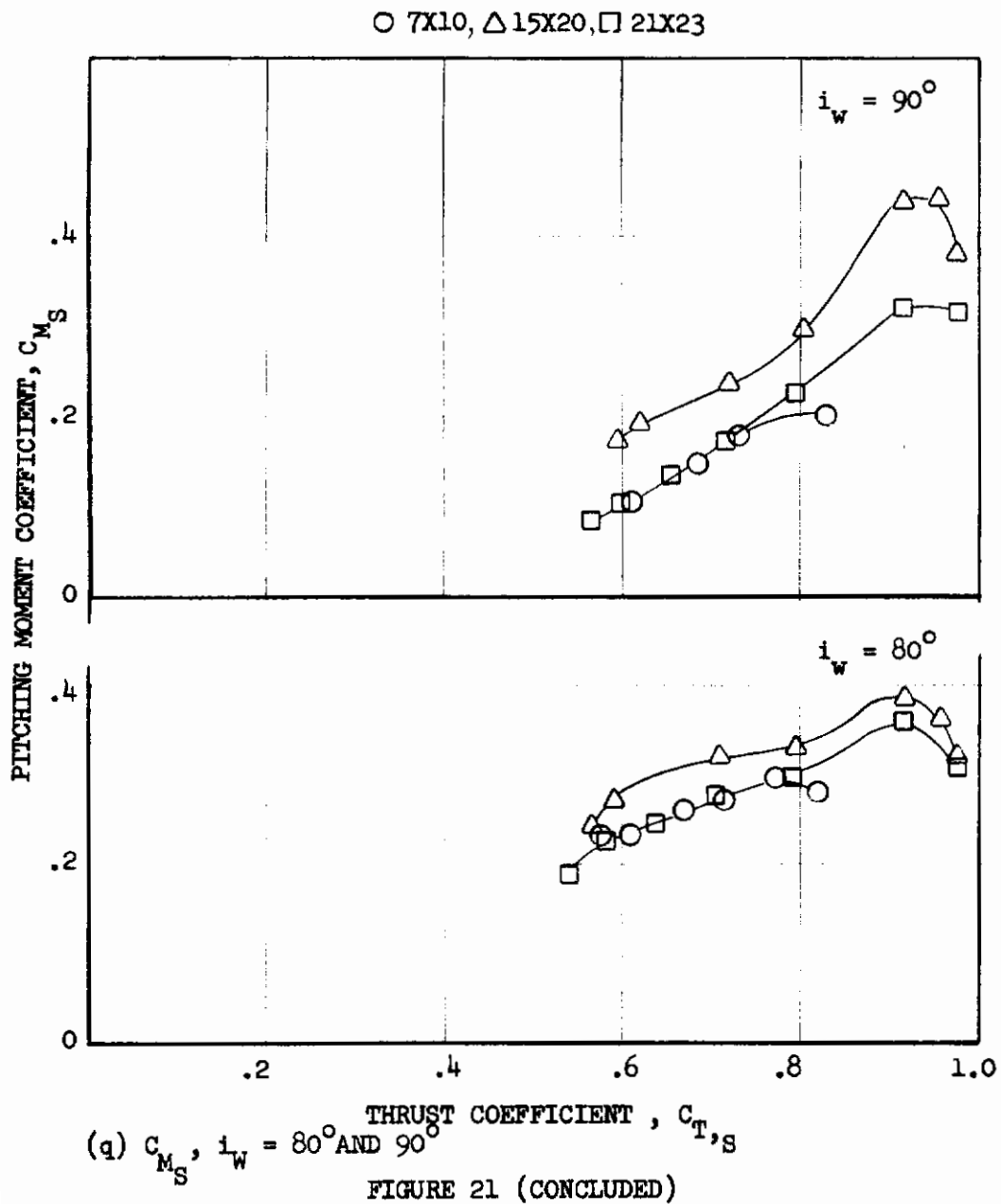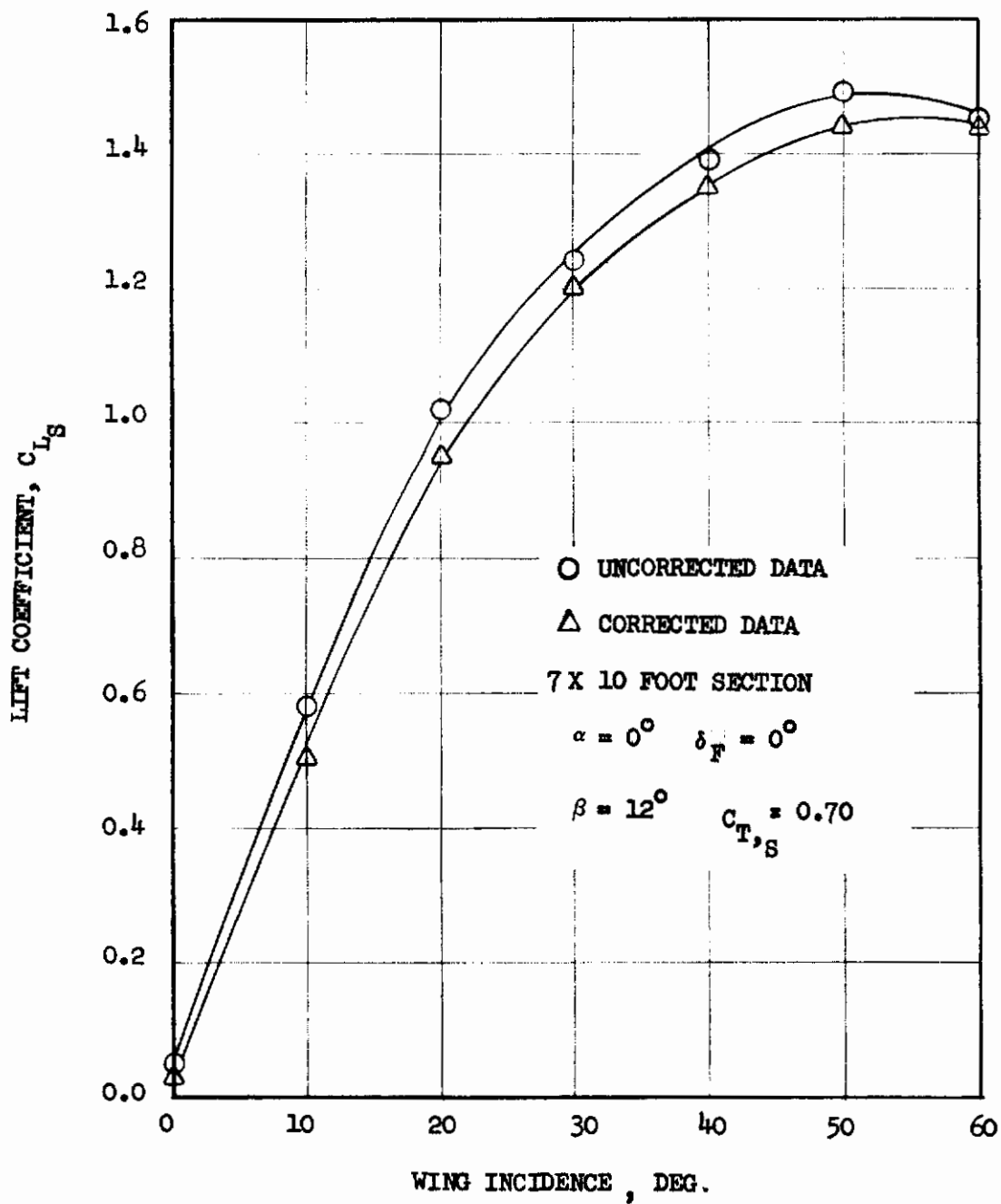
FIGURE 22   EFFECT OF TUNNEL WALL CORRECTIONS FOR
WING INCIDENCE RUNS

86
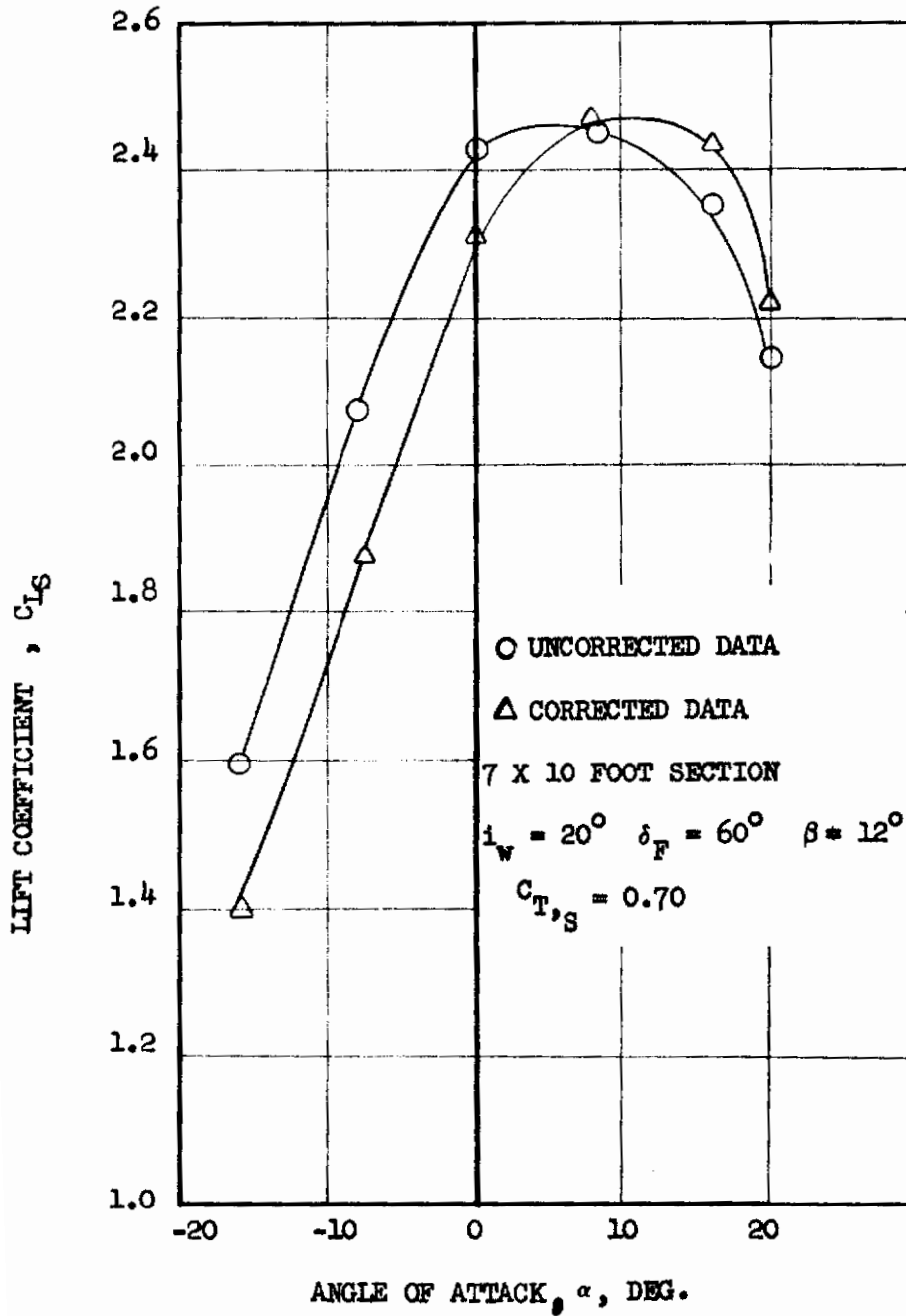
FIGURE 23   EFFECT OF TUNNEL WALL CORRECTIONS FOR
ANGLE-OF-ATTACK RUNS

87
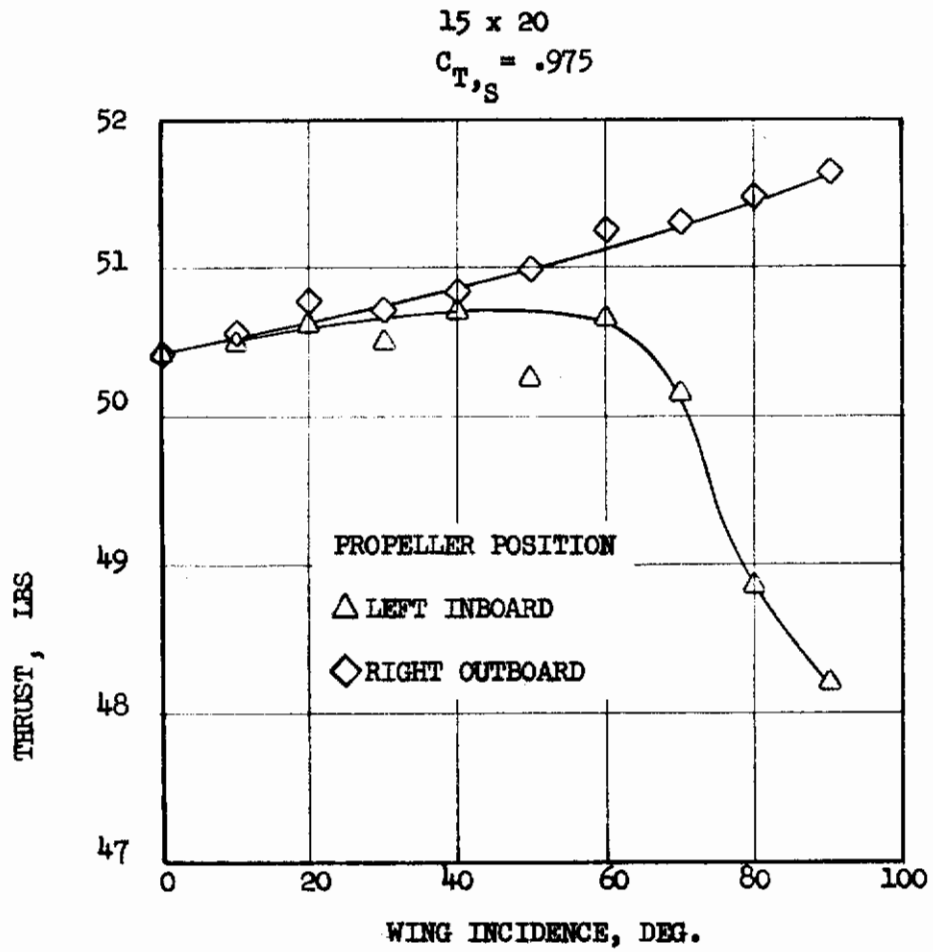
15 x 20

$C_{T,S} = .975$

(a) $C_{T,S} = 0.975$ (15 x 20)

FIGURE 24   EFFECT OF RECIRCULATION ON PROPELLER THRUST

88

21 x 23

$$c_{T,S} = .975$$

PROPELLER POSITION

○ LEFT OUTBOARD

△ LEFT INBOARD

◇ RIGHT OUTBOARD

□ RIGHT INBOARD

WING INCIDENCE, DEG.
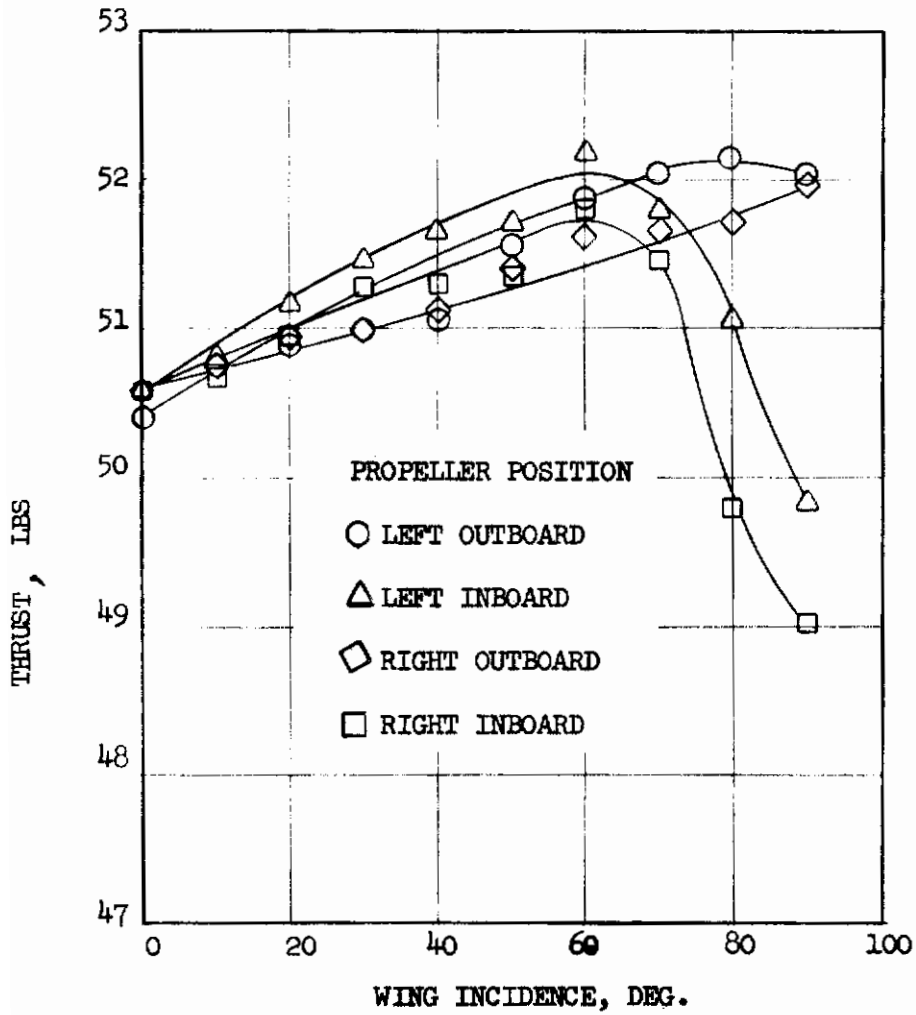
(b) $c_{T,S} = 0.975$ (21 x 23)

FIGURE 24 (CONTINUED)

89

15 x 20

$$C_{T,S} = .95$$

PROPELLER POSITION

△ LEFT INBOARD

◇ RIGHT OUTBOARD

WING INCIDENCE, DEG.
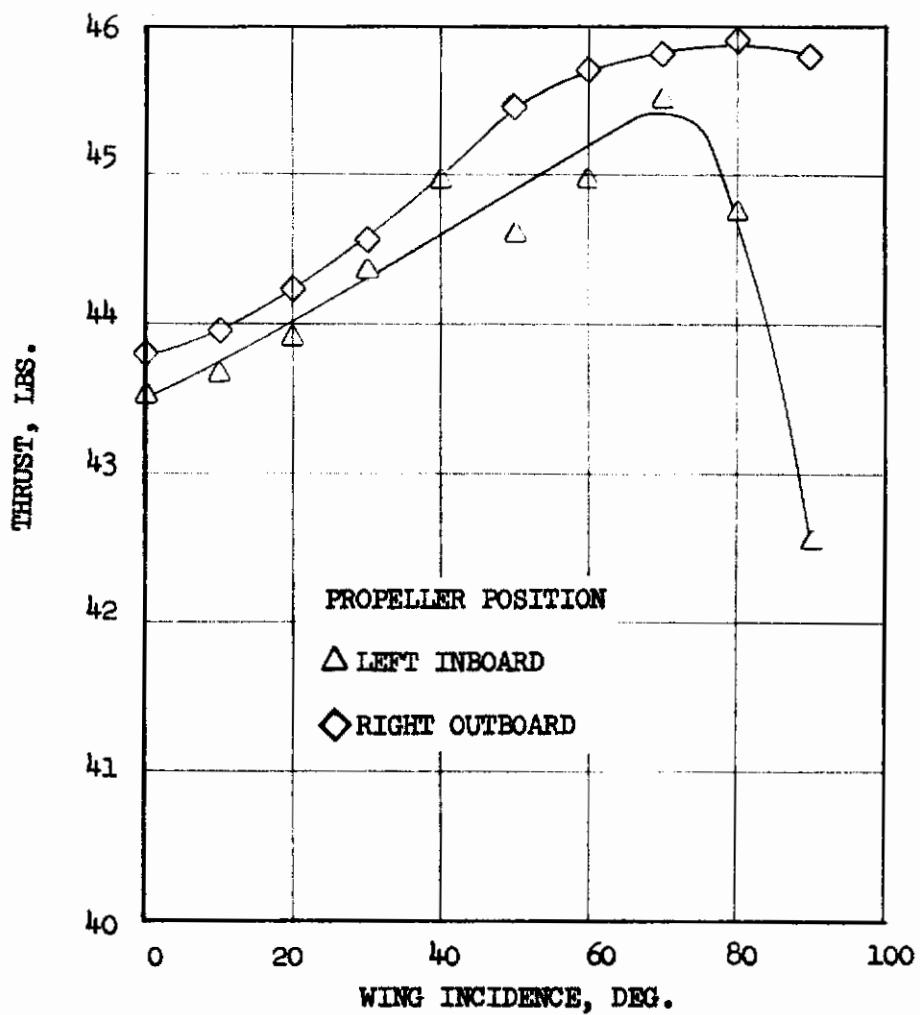
(c) $C_{T,S} = 0.95$ (15 x 20)

FIGURE 24 (CONCLUDED)

$i_w = 0^{\circ}$, $\delta_F = 0^{\circ}$, $\beta = 12^{\circ}$, $C_{T,S} = .20$
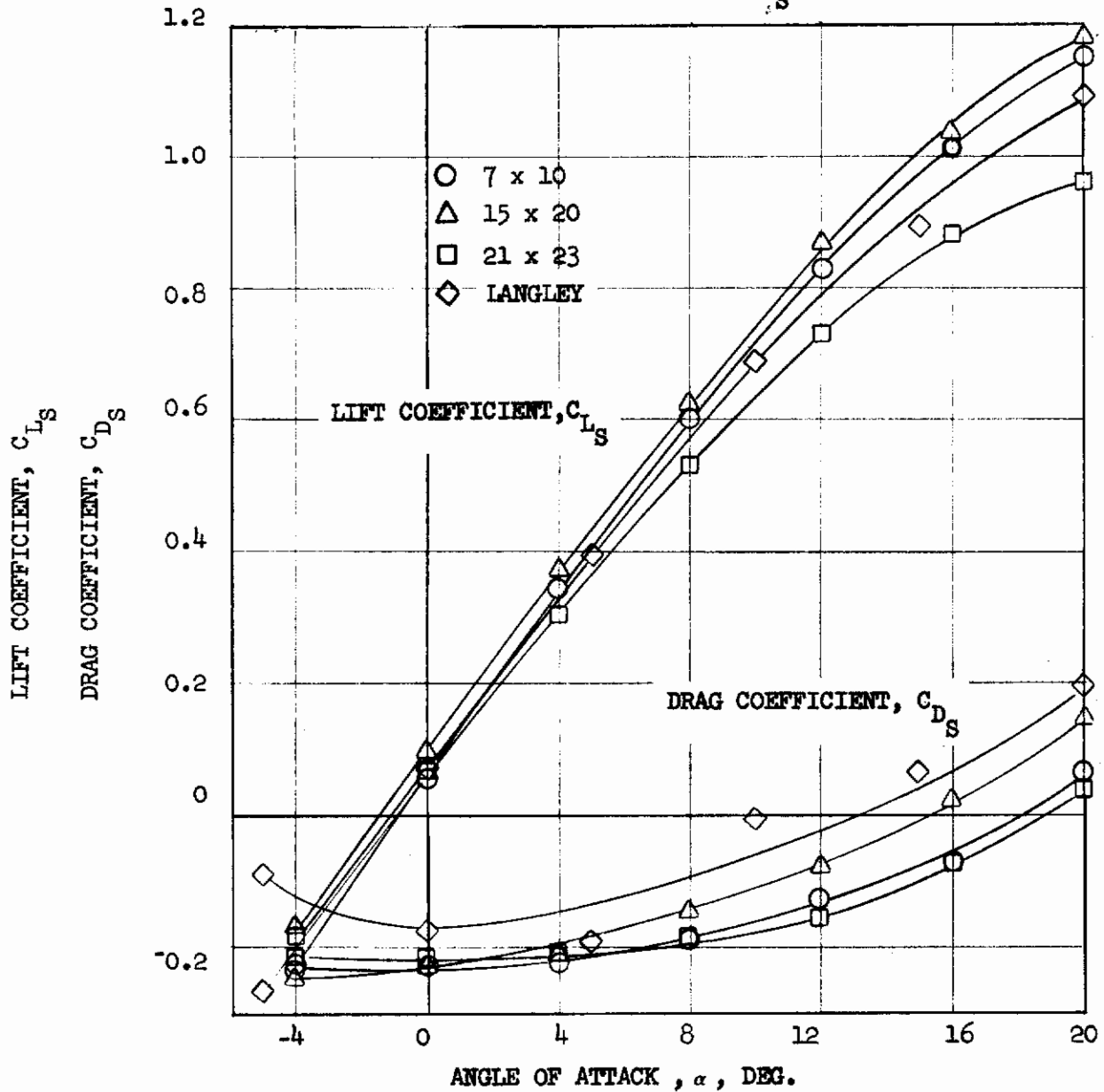
(a) C_{L_S} and C_{D_S} vs α

FIGURE 25   COMPARISON OF CRUISE DATA FROM VAD AND LANGLEY

91

$$i_W = 0^\circ, \delta_F = 0^\circ, \beta = 12^\circ, C_{T,S} = .20$$

(b) C_{M_S} vs α

FIGURE 25 (CONCLUDED)

$$i_W = 20°, \ \delta_F = 60°, \ \beta = 12°, \ C_{T,_S} = .70$$

(a) C_{L_S} vs α
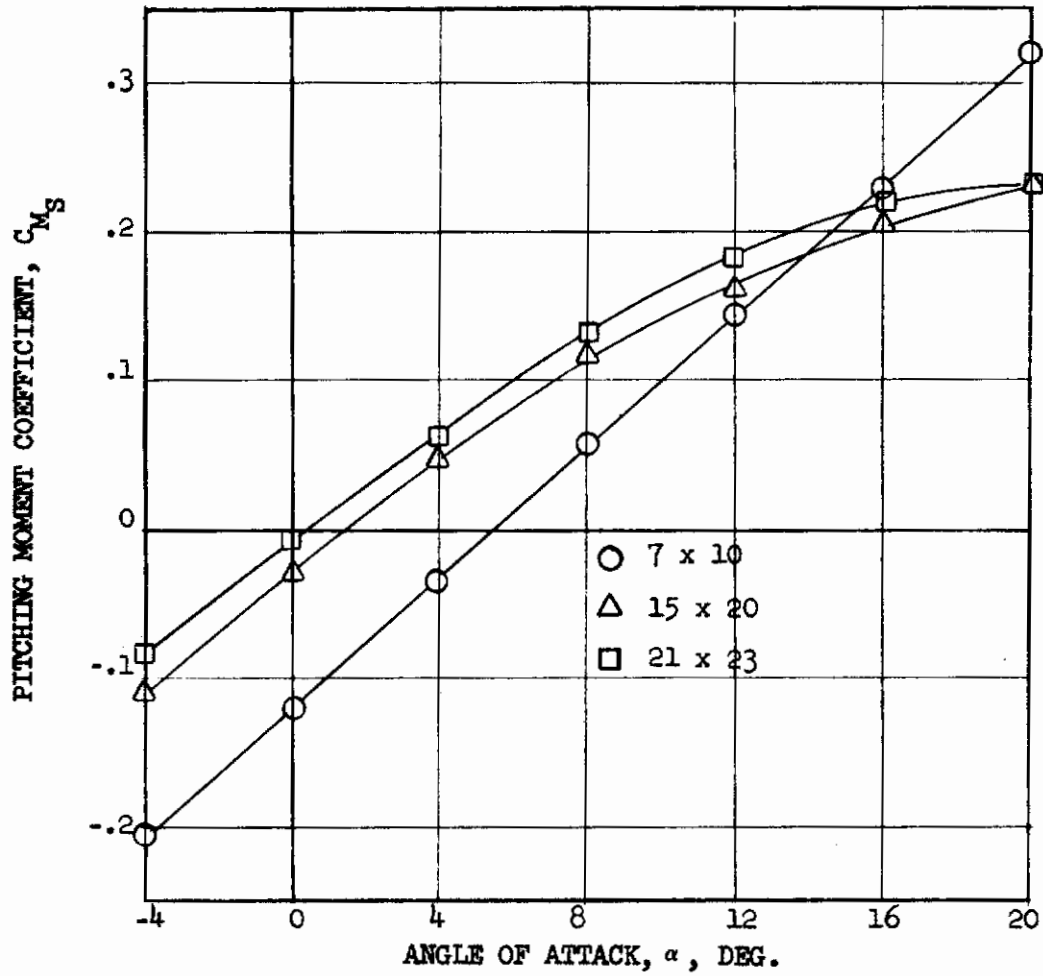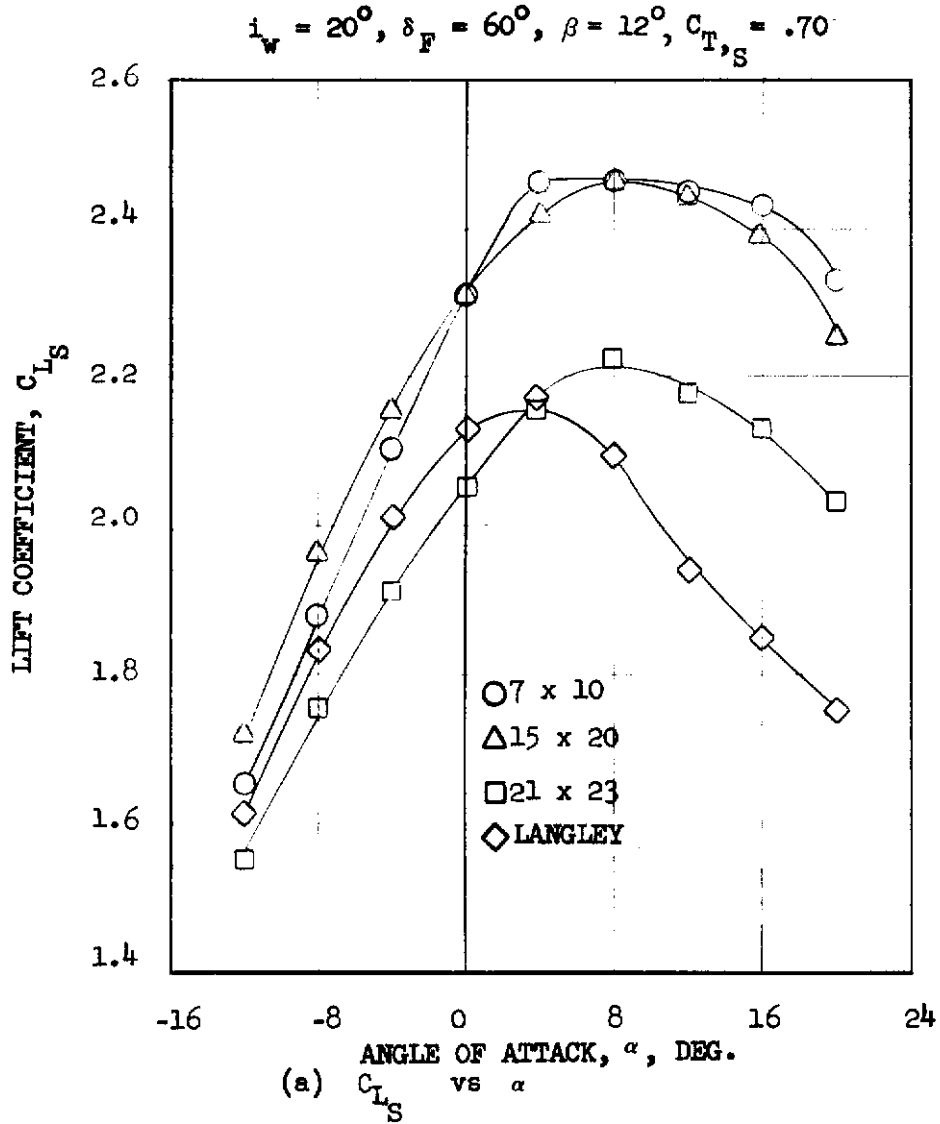
FIGURE 26   COMPARISON OF STOL ($i_W = 20°$)
CONFIGURATION DATA FROM
VAD AND LANGLEY

93

$i_w = 20^\circ, \delta_F = 60^\circ, \beta = 12^\circ, C_{T,S} = .70$

(b) C_{D_S} vs α

FIGURE 26 (CONTINUED)

94

$i_w = 20^\circ, \delta_F = 60^\circ, \beta = 12^\circ, C_{T,s} = .70$

(c) C_{M_S} vs α

FIGURE 26 (CONCLUDED)

$i_W = 40^\circ$, $\delta_F = 60^\circ$, $\beta = 12^\circ$, $C_{T,S} = .70$

(a) C_{L_S} vs α
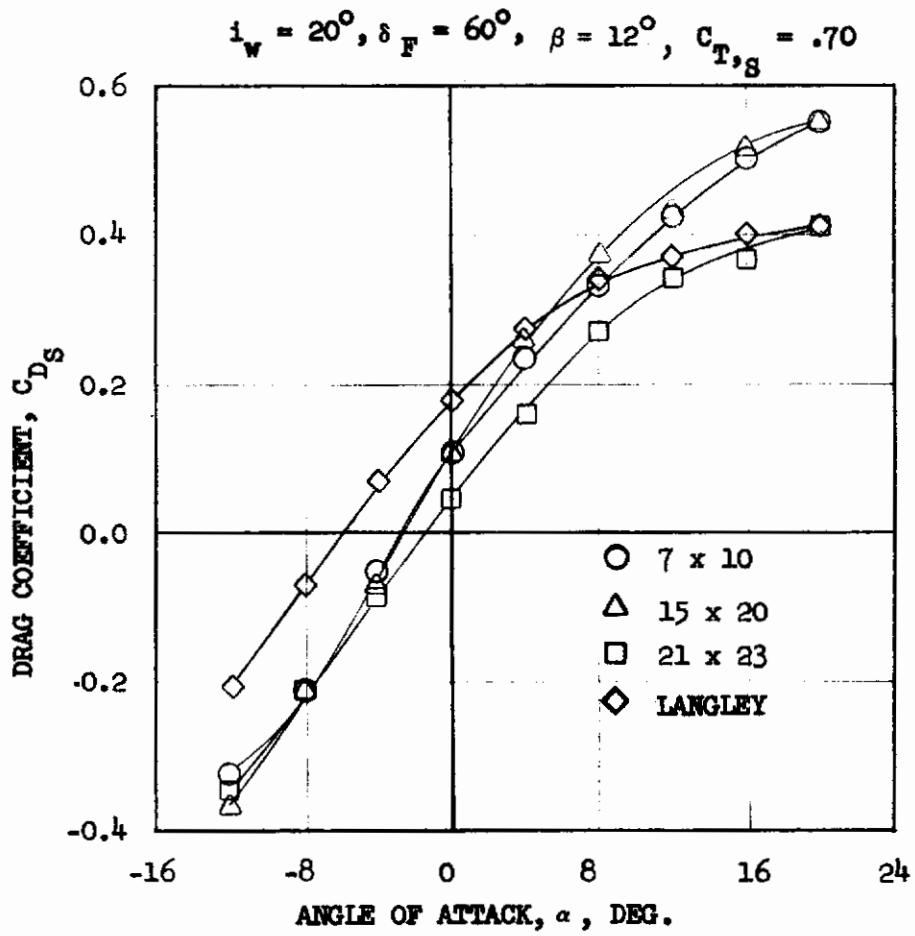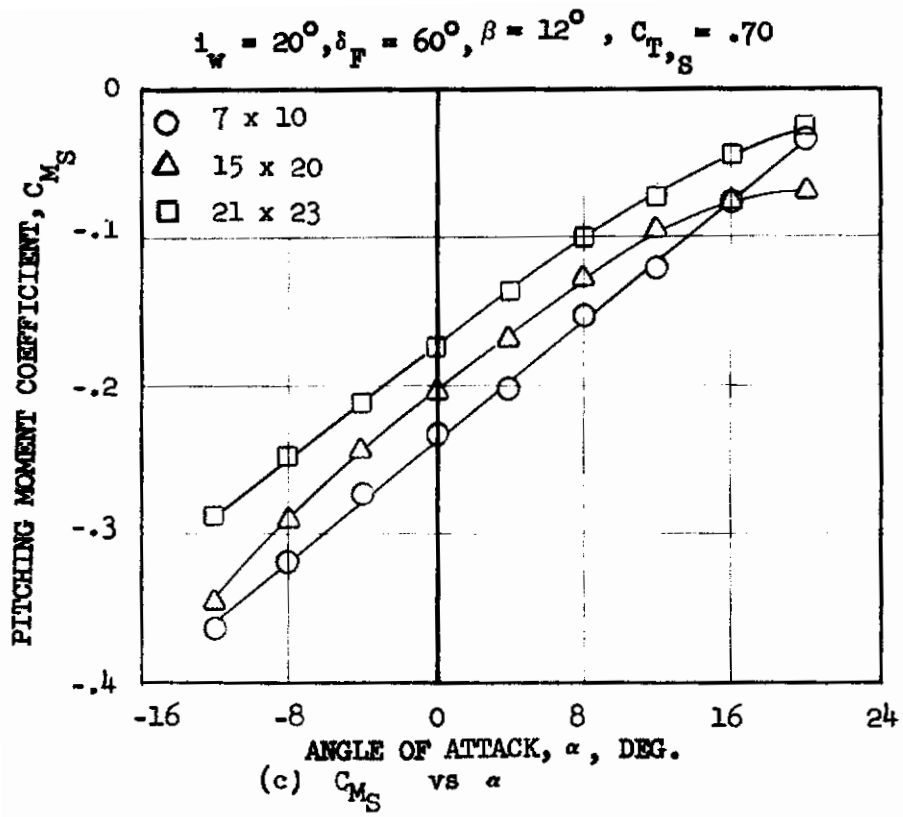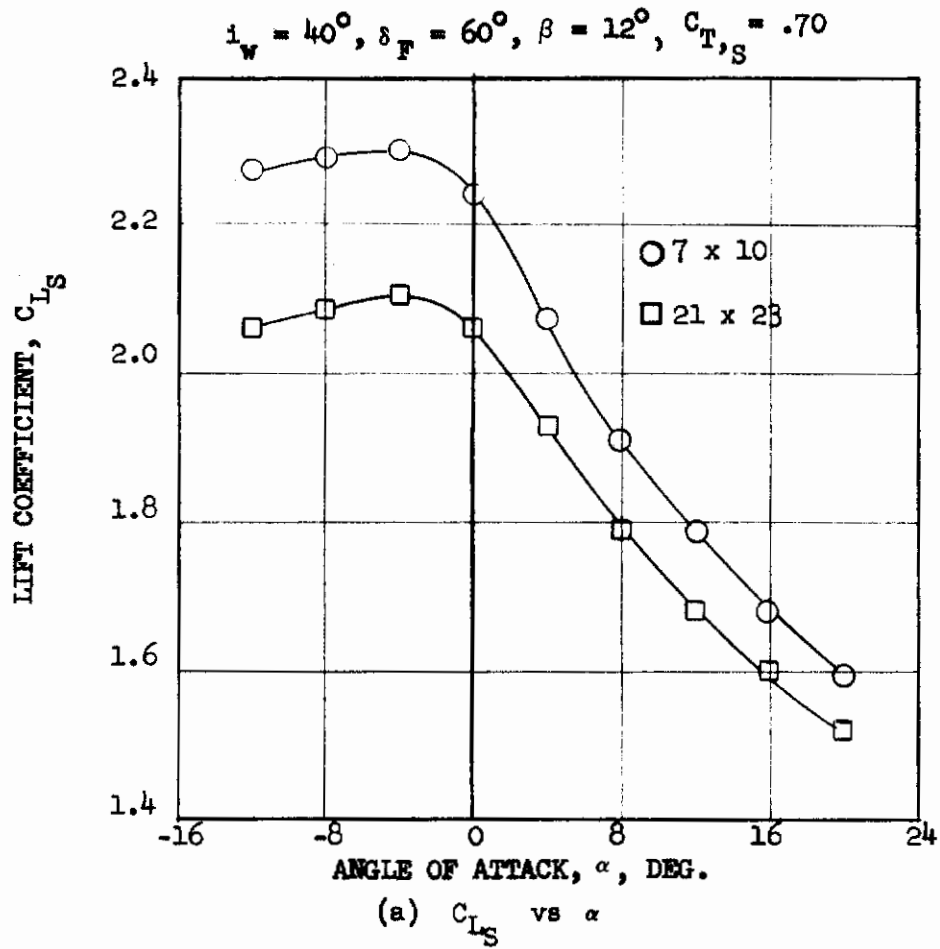
FIGURE 27   COMPARISON OF STOL ($i_W = 40^\circ$)
CONFIGURATION DATA FROM VAD
TEST SECTIONS

96

$i_W = 40°$, $\delta_F = 60°$, $\beta = 12°$, $C_{T,S} = .70$

(b) C_{D_S} vs α

FIGURE 27 (CONTINUED)

97

$i_w = 40°, \delta_F = 60°, \beta = 12°, C_{T,S} = .70$

(c) C_{M_S} vs α

FIGURE 27   (CONCLUDED)

$$i_W = 40°, \delta_F = 60°, \beta = 12°, C_{T,S} = .80$$

(a) C_{L_S} vs α
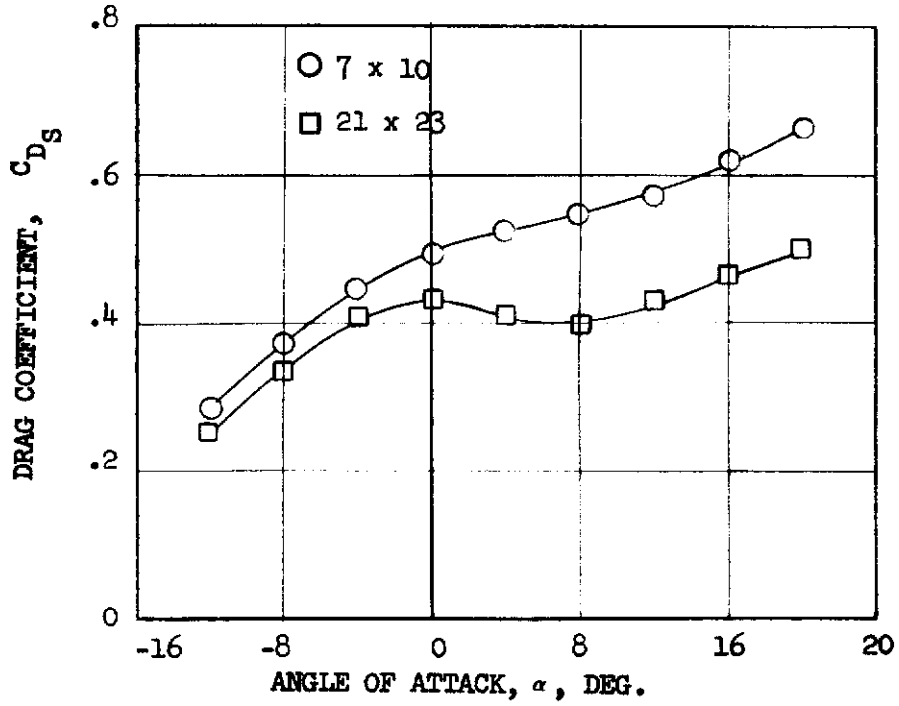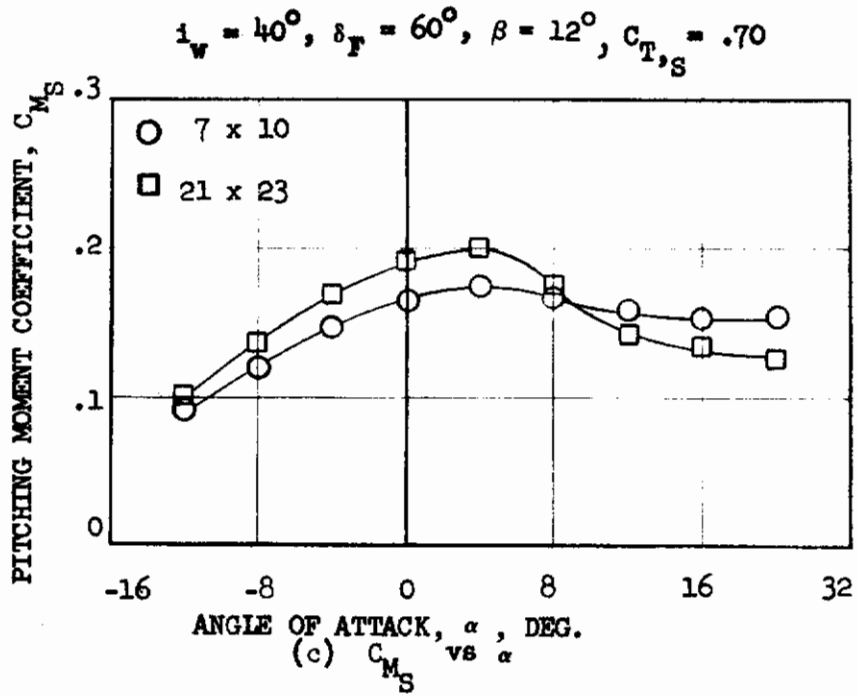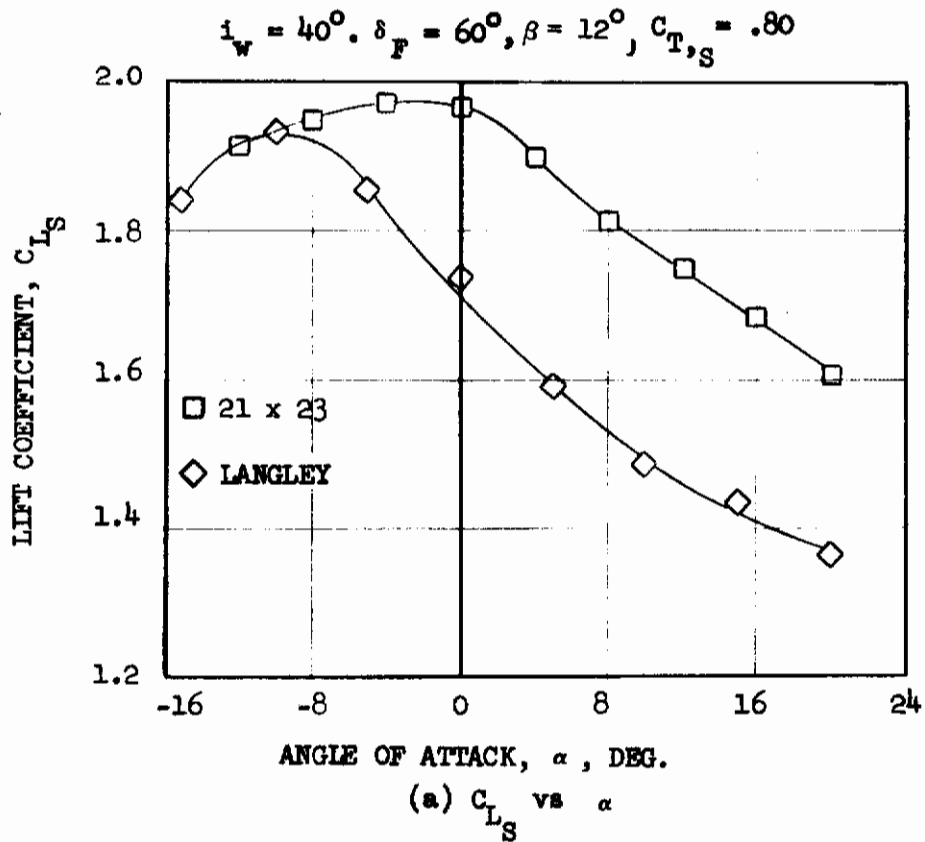
FIGURE 28   COMPARISON OF STOL (i_W = 40°)
CONFIGURATION DATA FROM VAD
AND LANGLEY

99

$$i_W = 40°, \, \delta_F = 60°, \, \beta = 12°, \, C_{T,S} = 0.80$$

☐   21 x 23

◇   LANGLEY
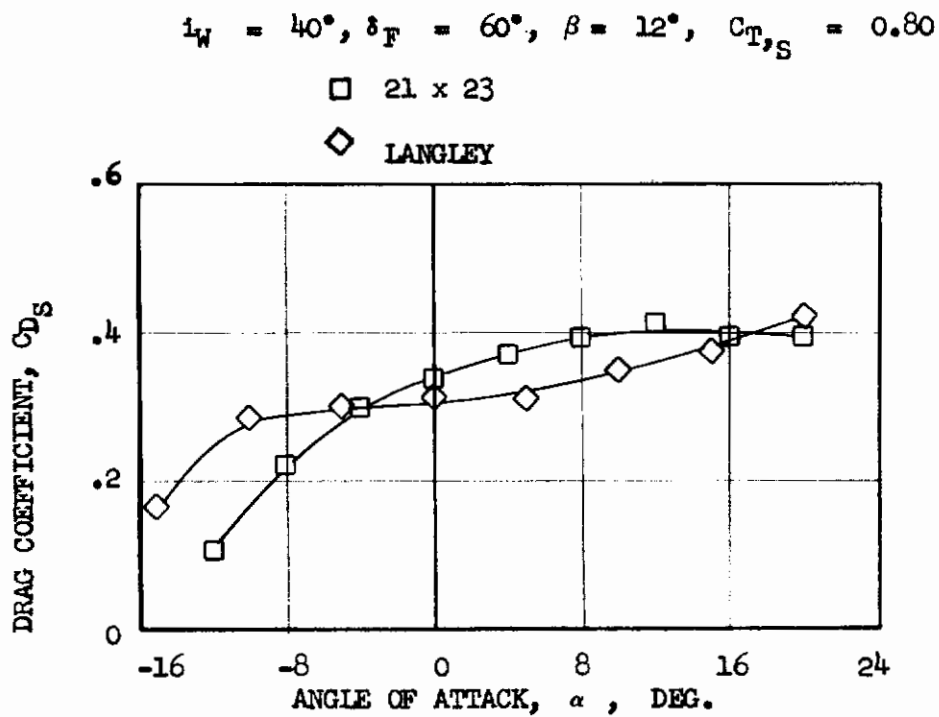
(b) C_{D_S} vs α

FIGURE 28   (CONCLUDED)

21 x 23

$$C_{T,S} = .70$$
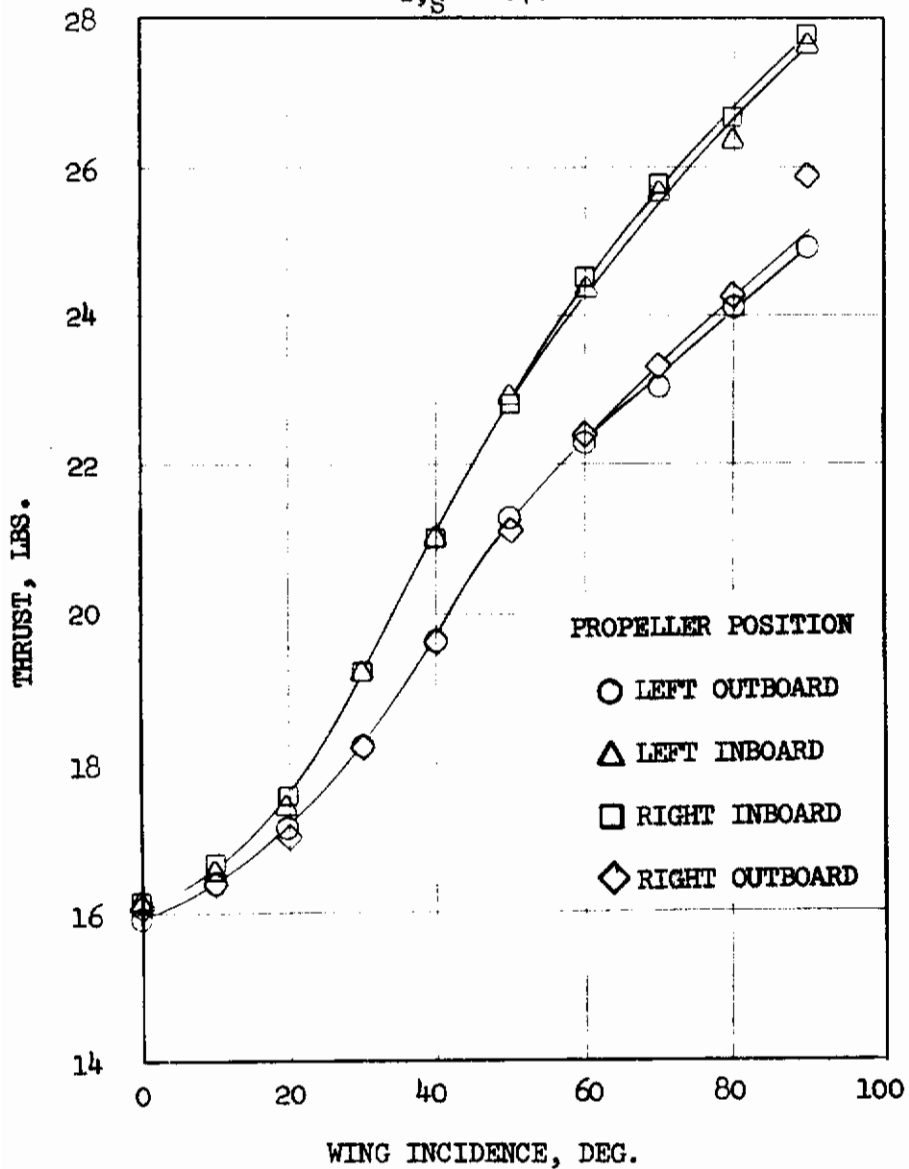
FIGURE 29   COMPARISON OF INBOARD AND OUTBOARD
PROPELLER THRUST VARIATION

101

15 x 20
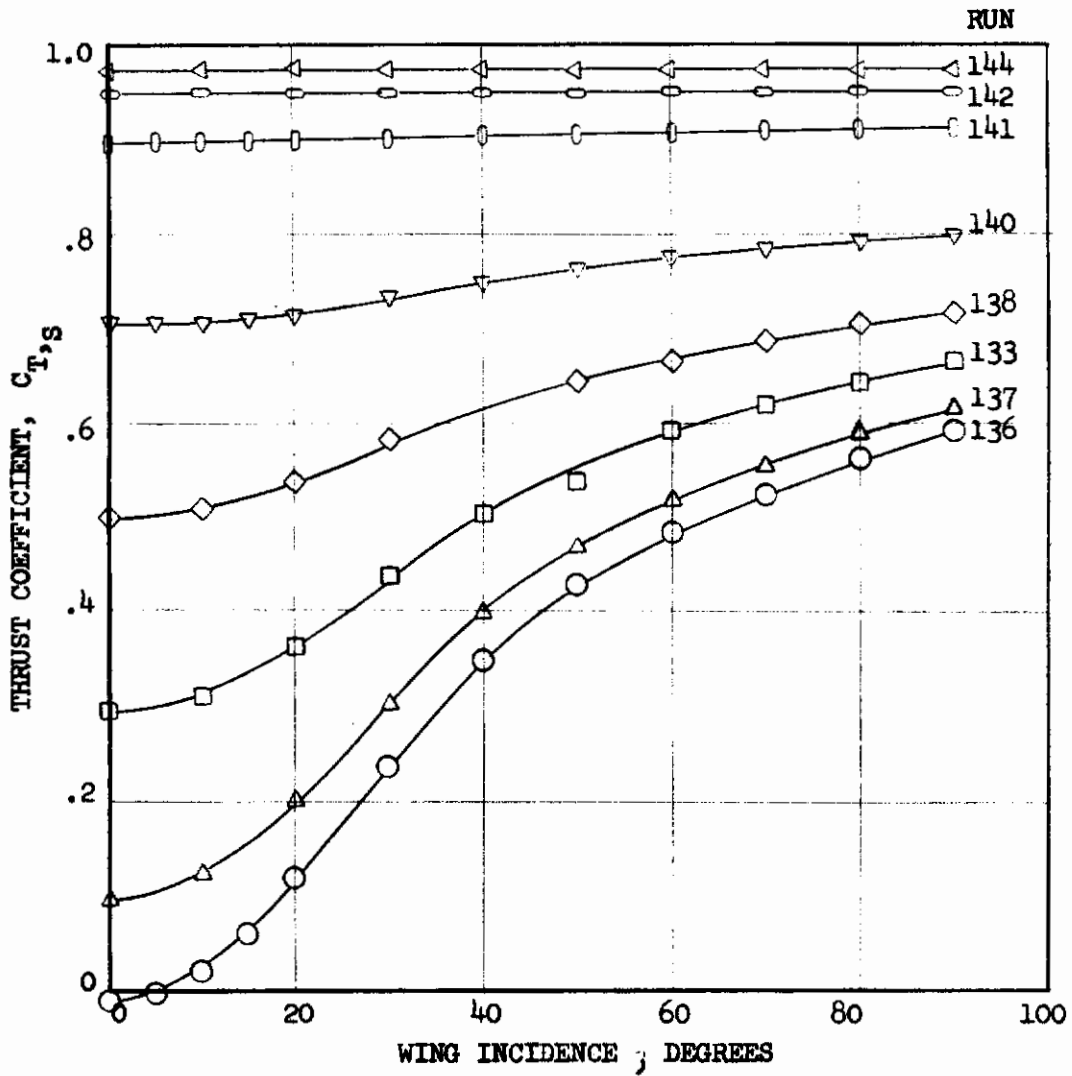
FIGURE 30   EFFECT OF WING INCIDENCE ON THRUST COEFFICIENT

$i_w = 0°$, $_F = 0°$, $C_{T,_S} = .20°$

C_{L_S}

C_{D_S}

○ $\beta = 4°$
△ $\beta = 8°$
□ $\beta = 12°$

ANGLE OF ATTACK, α, DEG.
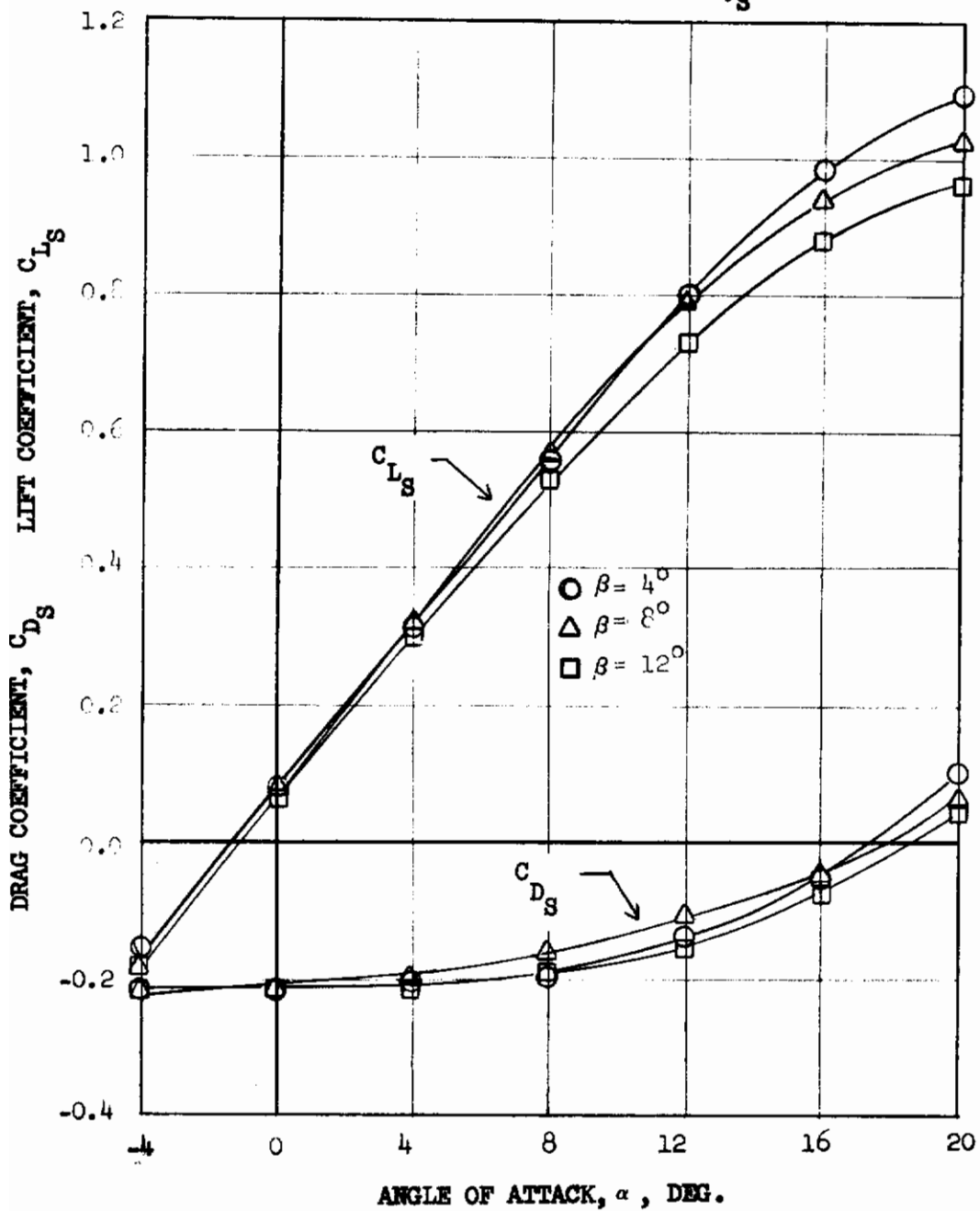
(a) CRUISE CONFIGURATION

FIGURE 31 EFFECT OF PROPELLER BLADE
PITCH ANGLE

103
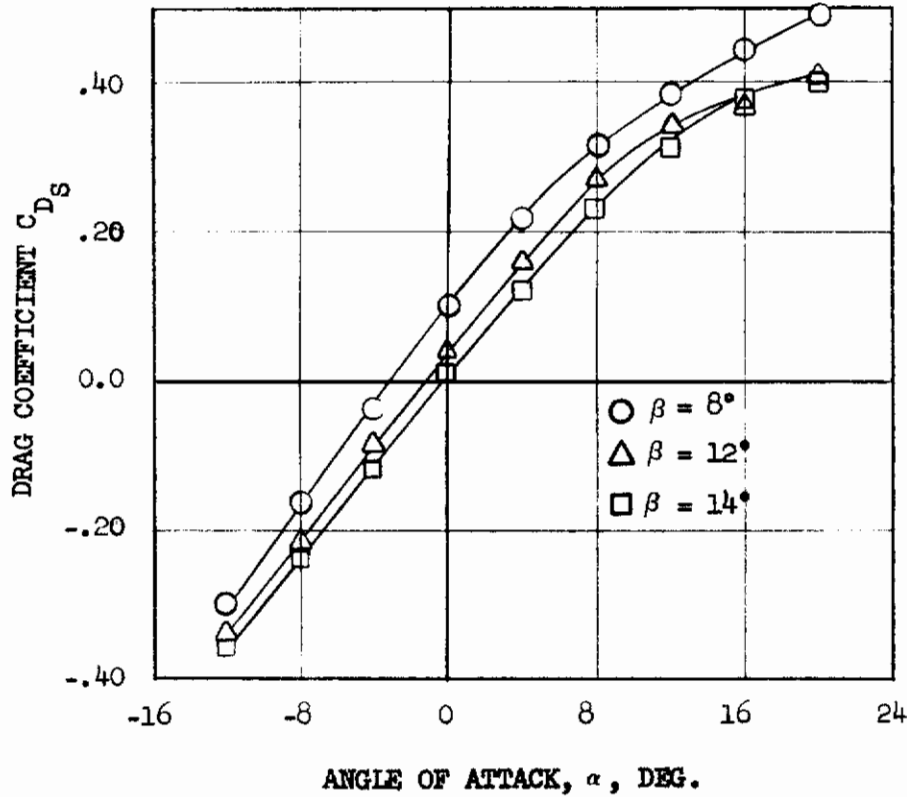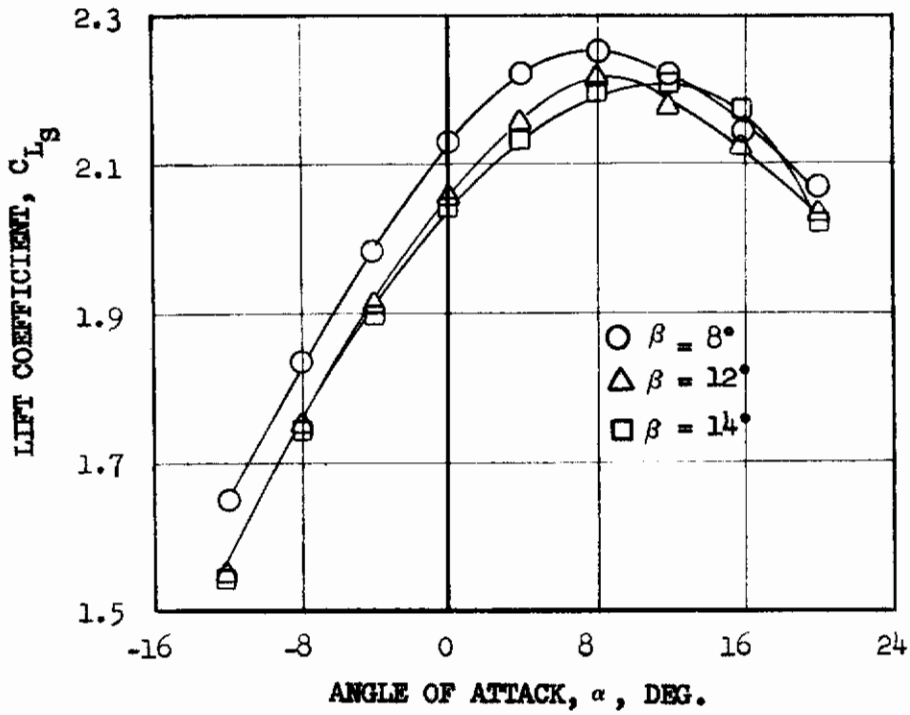
(b) STOL CONFIGURATION

FIGURE 31 (CONCLUDED)

$\beta = 12^{\bar{o}}, \; i_w = 0^o, \; \delta_F = 0^o$

$C_{T,s} = 0.49$

$(\; 7 \times 10 \;)$

○ CONSTANT THRUST RUN

△ CROSS-PLOTTED DATA

ANGLE OF ATTACK, α, DEG.

LIFT COEFFICIENT, C_{L_S}
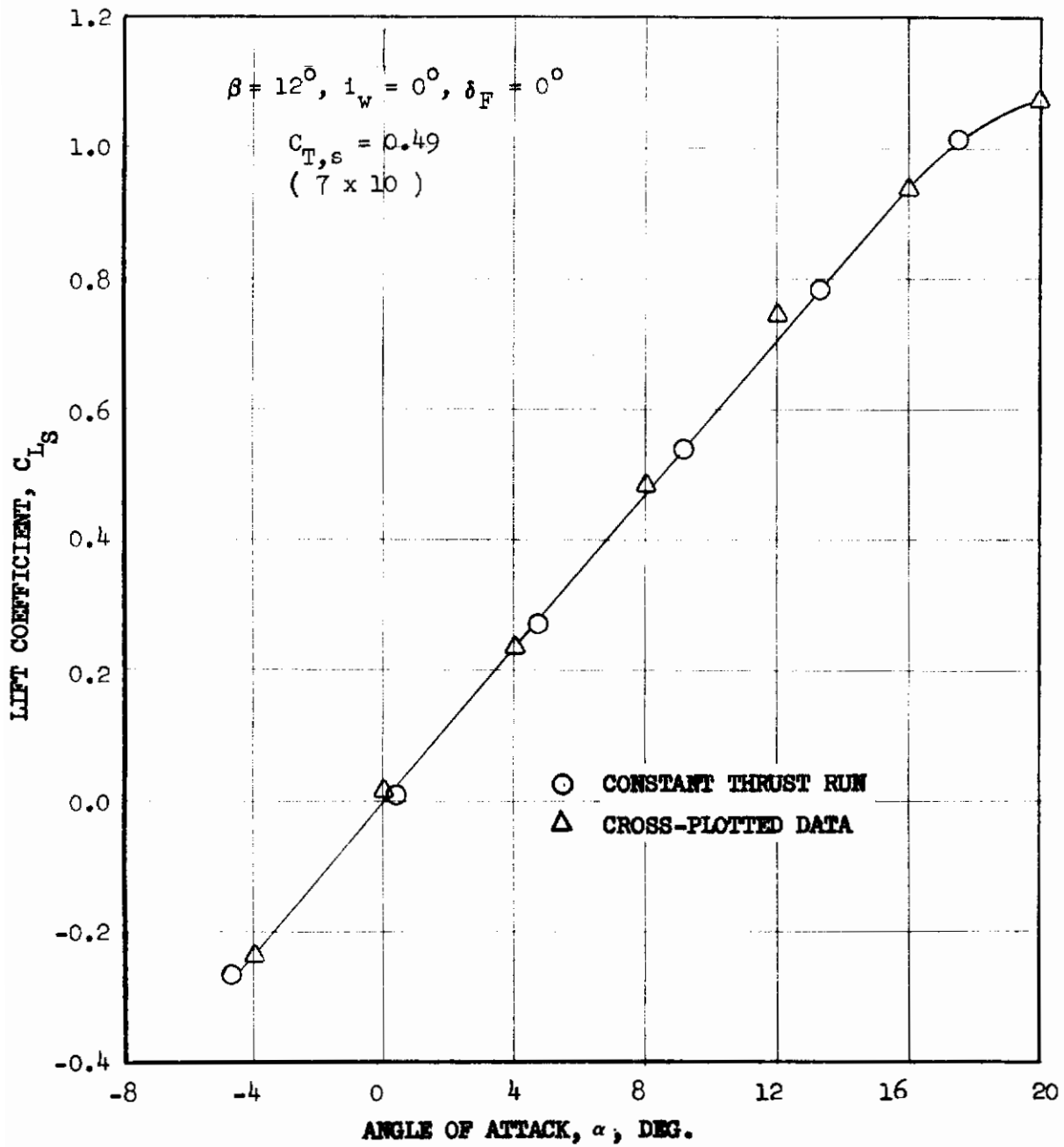
FIGURE 32 COMPARISON OF CONSTANT THRUST DATA
OBTAINED BY DIFFERENT METHODS

105
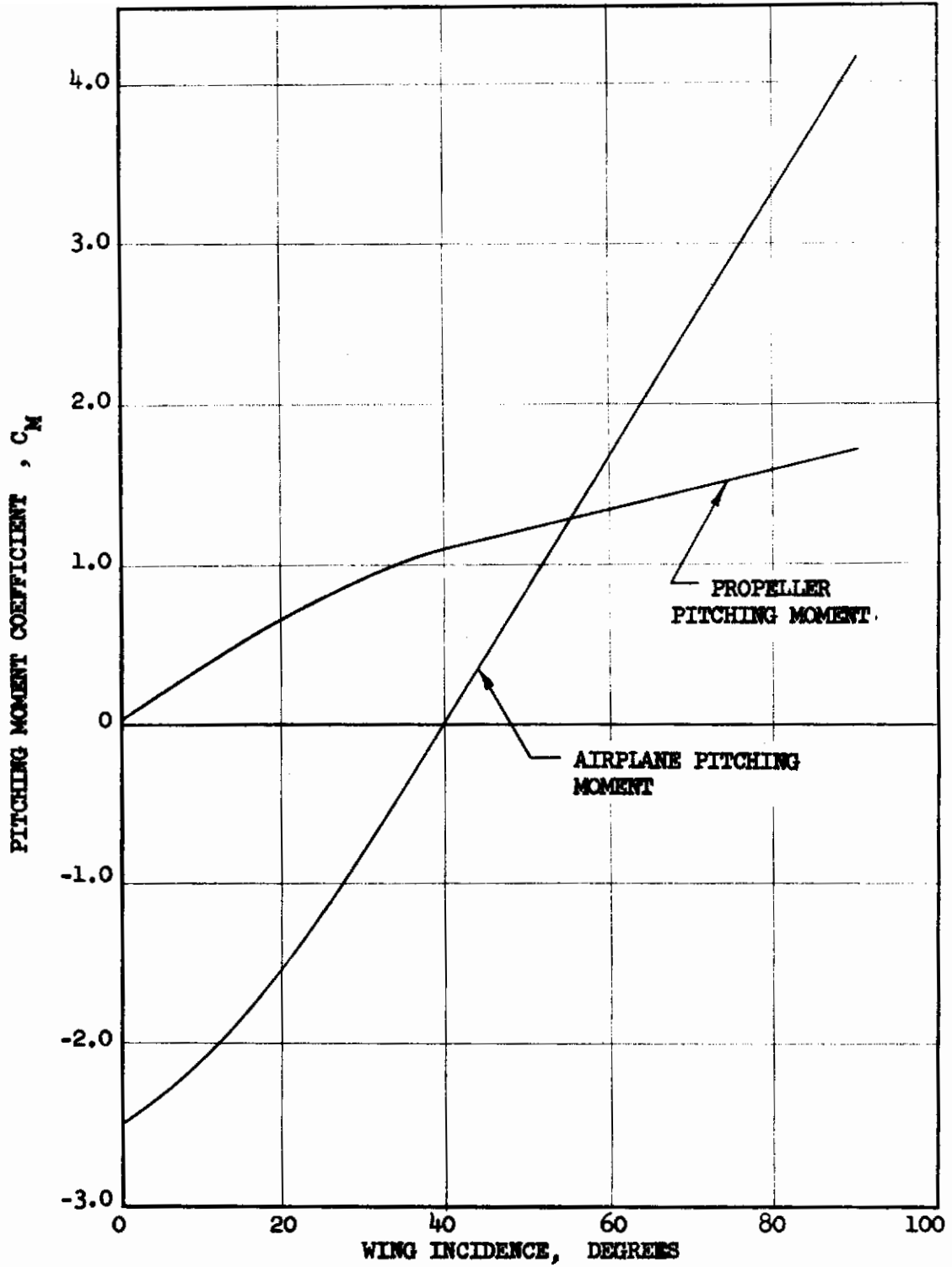
FIGURE 33   COMPARISON OF PROPELLER PITCHING MOMENT WITH AIRPLANE
PITCHING MOMENT

106

PITOT-STATIC TUBES

#1

#2

#3

#4

7 x 10-foot TEST SECTION
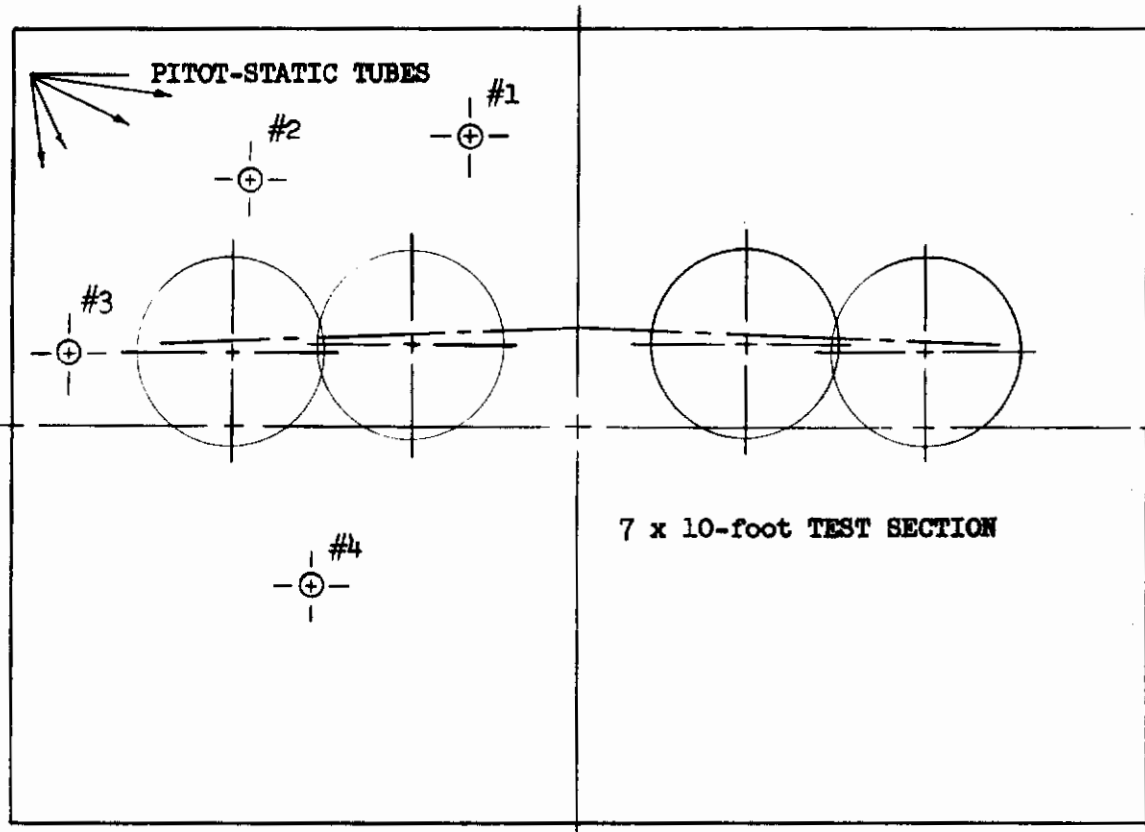
FIGURE 34   PITOT-STATIC TUBE INSTALLATION

(7 x 10)

$\beta = 12^{\circ}$, $i_w = 0^{\circ}$, $\delta_F = 0^{\circ}$ $c_{T,S} = 0.30$

CLEAR TEST SECTION
DYNAMIC PRESSURE

$c_{T,S} = 0.49$

DYNAMIC PRESSURE
NEAR MODEL

CLEAR TEST SECTION
DYNAMIC PRESSURE

$c_{T,S} = 0.70$

CLEAR TEST SECTION
DYNAMIC PRESSURE

AVERAGE DYNAMIC PRESSURE, P S F

ANGLE OF ATTACK, α, DEG.
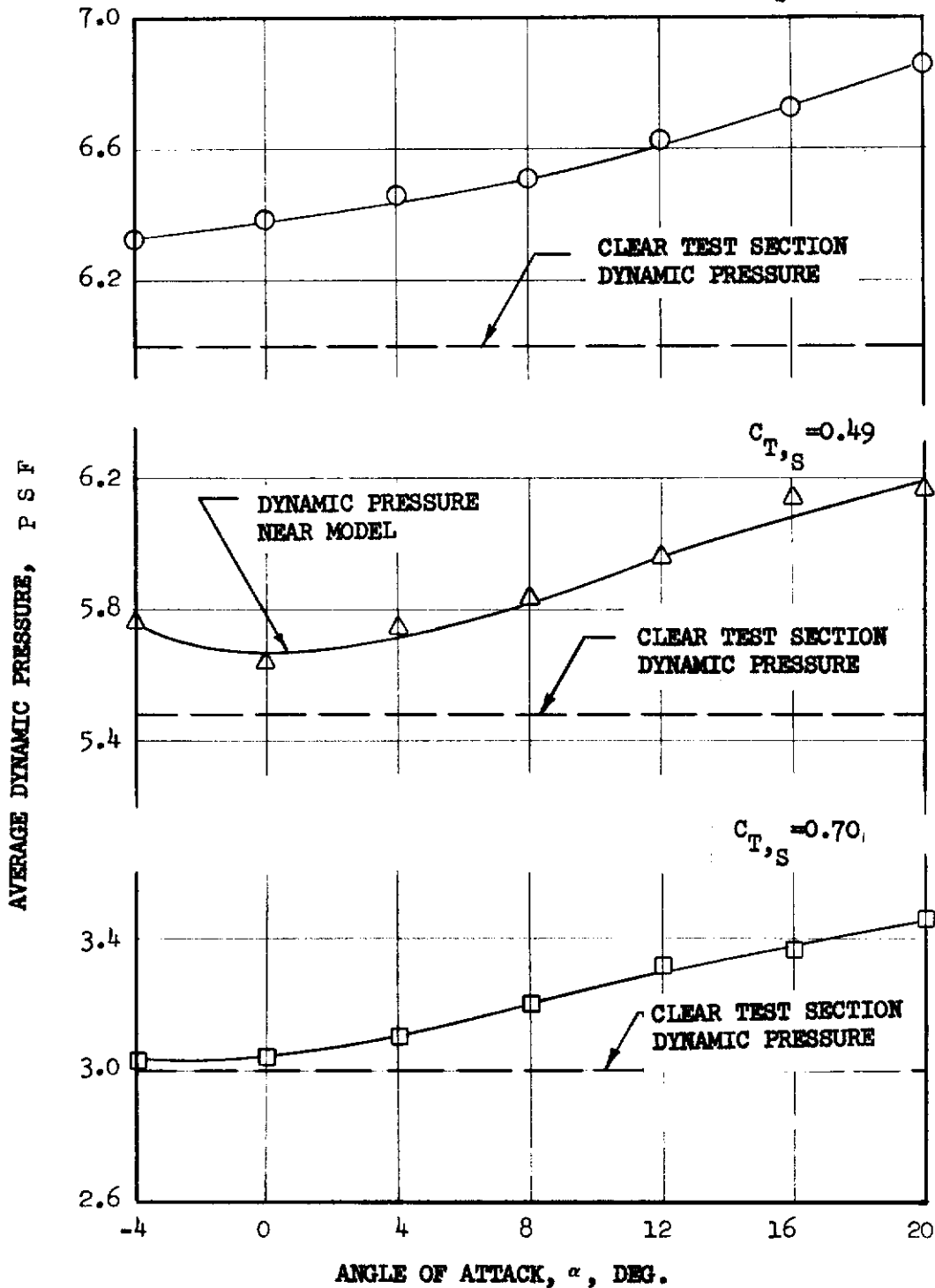
FIGURE 35   COMPARISON OF DYNAMIC PRESSURE
DETERMINED BY TWO METHODS

108

$\beta = 12^{0} \quad \alpha = 0^{0}$

$C_{T,s}(\text{nominal}) = 0.10$

(7×10)

Legend:
- ○ q = 6.0 PSF
- △ q = 9.0 PSF
- □ q = 15.0 PSF

LIFT COEFFICIENT, C_{L_s}

WING INCIDENCE, DEG.
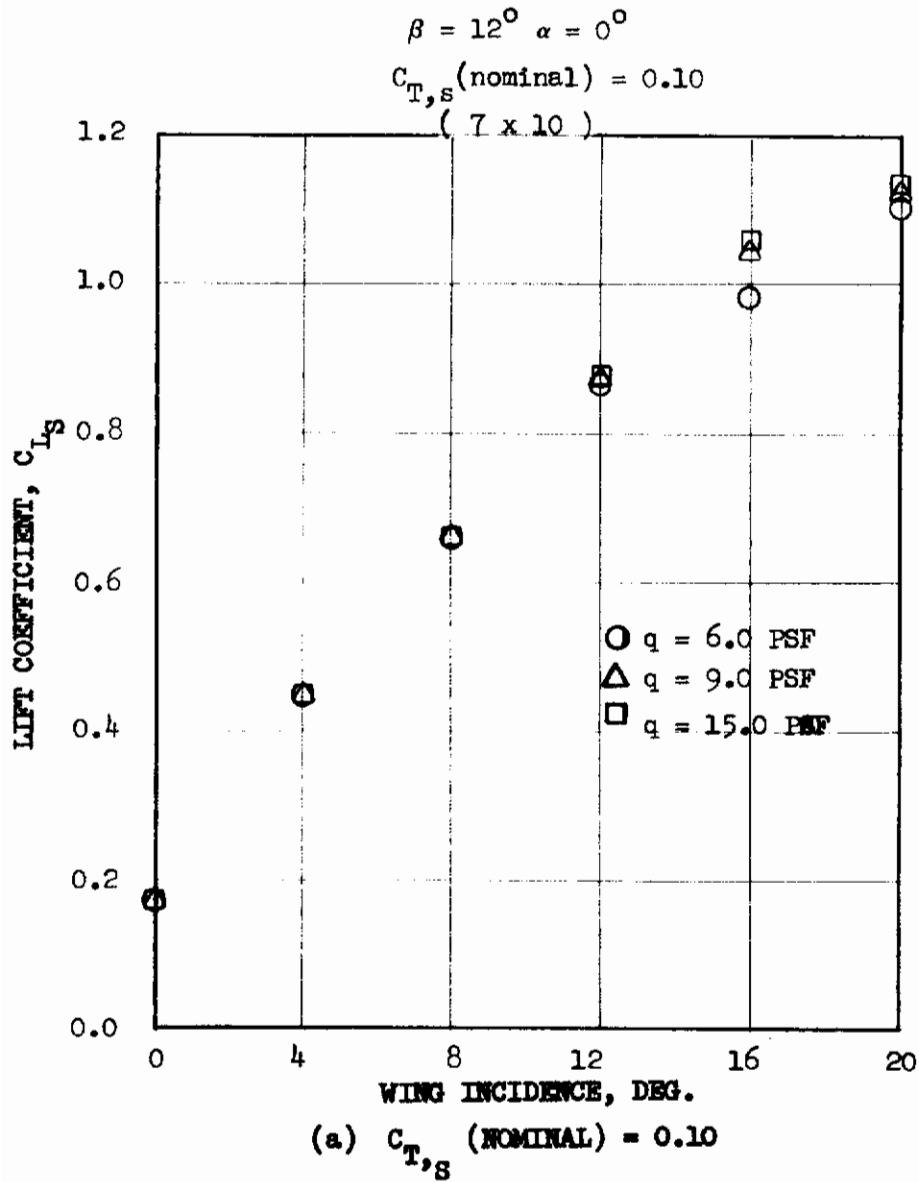
(a) $C_{T,s}$ (NOMINAL) = 0.10

FIGURE 36 EFFECT OF REYNOLDS NUMBER,
CRUISE CONFIGURATION

$\beta = 12^{\circ}$ $\alpha = 0$
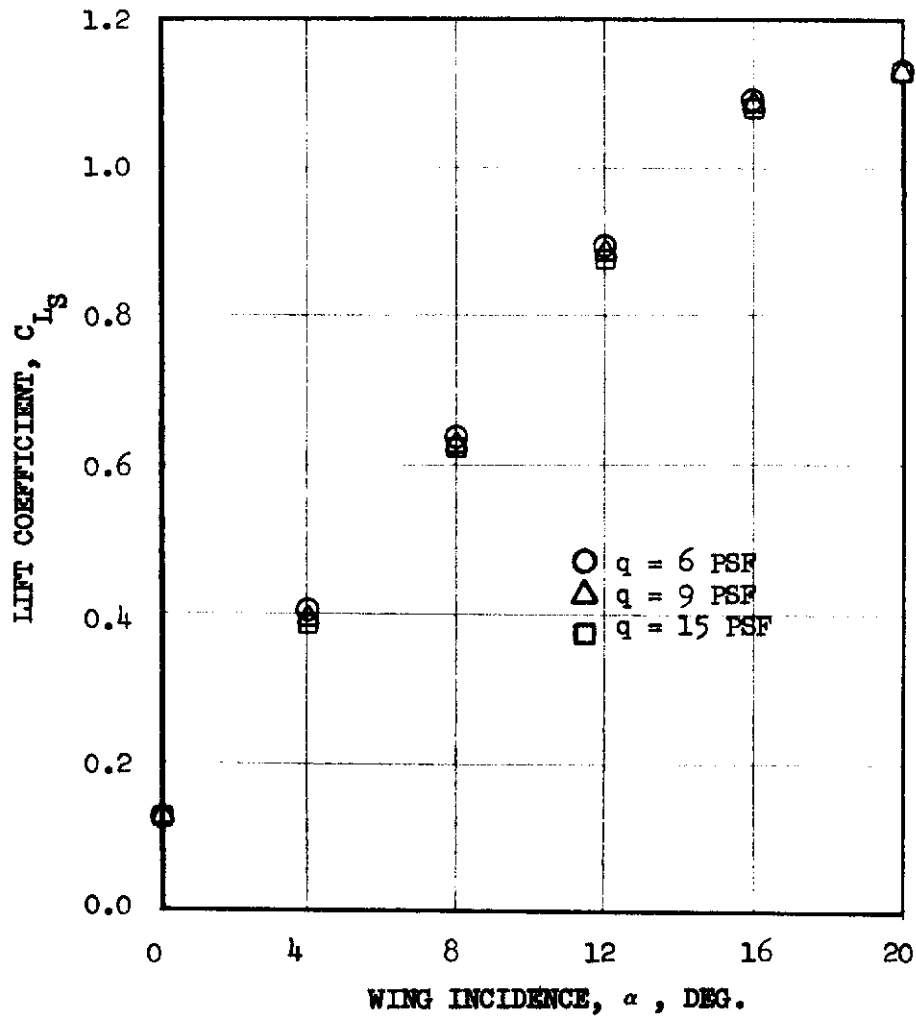
(b) C_{T_S} (NOMINAL) = 0.30

FIGURE 36 (CONCLUDED)
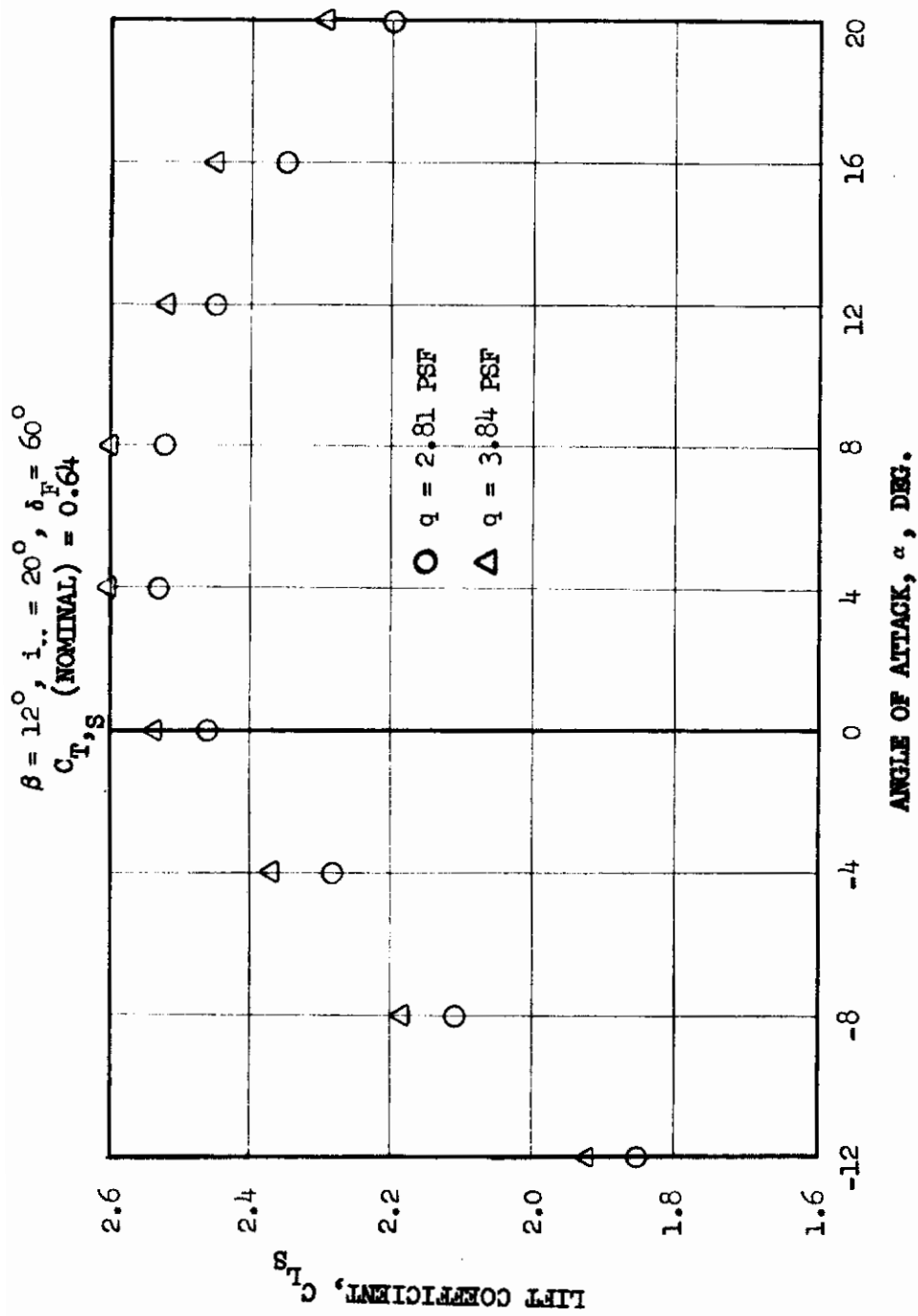
FIGURE 37   EFFECT OF REYNOLDS NUMBER,
STOL CONFIGURATION

$\beta = 12^\circ$, $i_{..} = 20^\circ$, $\delta_F = 60^\circ$
$c_{T,S}$ (NOMINAL) = 0.64

O q = 2.81 PSF
△ q = 3.84 PSF

ANGLE OF ATTACK, α, DEG.

LIFT COEFFICIENT, c_{L_S}

111

$\beta = 12^{\circ}$, $i_w = 20^{\circ}$, $\delta_F = 60^{\circ}$

$c_{T,S}$ (NOMINAL) $= 0.64$

(15 x 20)

△ TUFFS ON

O TUFFS OFF

LIFT COEFFICIENT C_{L_S}

ANGLE OF ATTACK, α , DEG.
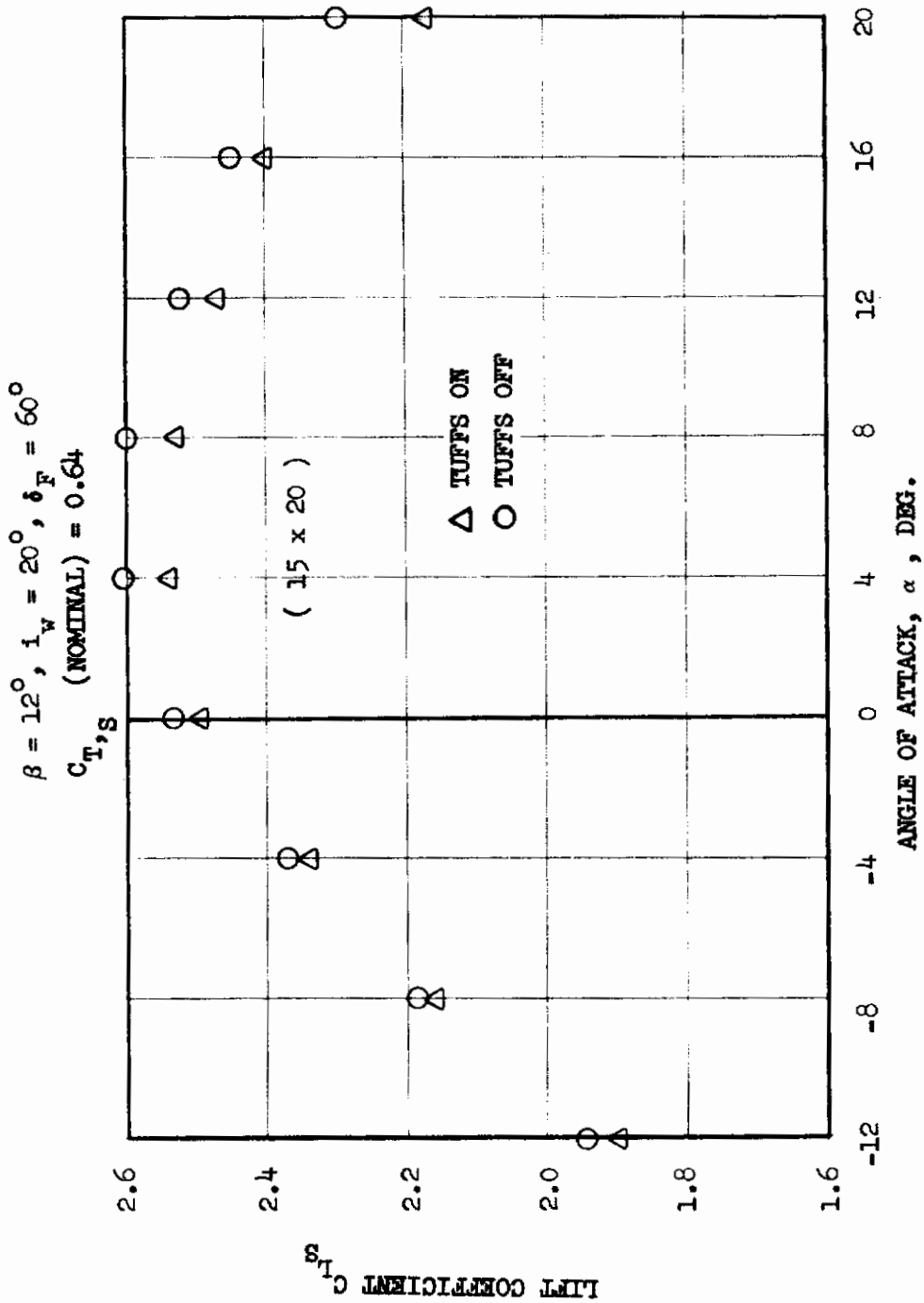
FIGURE 38 EFFECT OF TUFFS,
STOL CONFIGURATION

112

(21 x 23)

$i_w = 0^o$, $\delta_F = 0^o$, $q = 3.0$
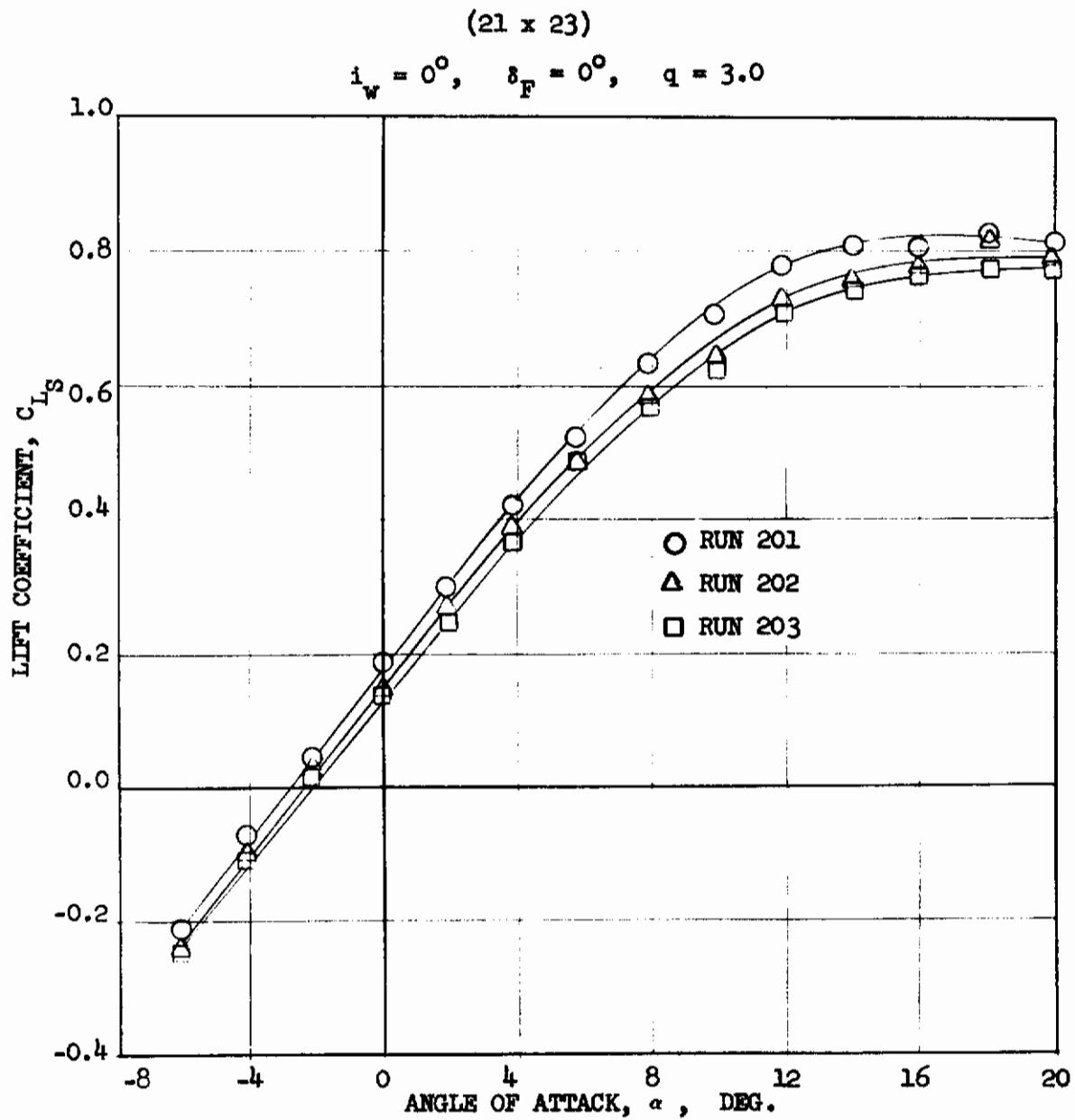
FIGURE 39   EFFECT OF TUFTS,
            CRUISE CONFIGURATION

SECTION V

EXTRACTION OF AERODYNAMIC CHARACTERISTICS
FROM FLIGHT DATA

The extensive flight test evaluation program for the XC-142A airplanes offered an opportunity to extract stability and control derivatives and other basic characteristics which could be used for comparison with wind tunnel characteristics of the XC-142A models. The flight test program was primarily planned for qualitative evaluation of the airplane, but a few flight maneuvers were performed specifically for obtaining data that would be suitable for stability derivative extraction. The direction of special flight testing was not a prerogative of this program, although it was recognized that the quantitative test data necessary for satisfactory extraction of aerodynamic characteristics might be unavailable in many cases.

1.   FLIGHT DATA AVAILABLE

The flight data available for the study was obtained from the Contractor's Category I test program. The flight maneuvers performed in hover and transition flight were dominated by the influence of the control effectiveness used to force the maneuver and to stabilize the airplane. Free oscillation maneuvers with controls fixed were not performed as this type of testing was not within the scope of the flight evaluation program. In general, the tests performed consisted of pilot controlled maneuvers aimed at pilot evaluation of the handling qualities of the airplane.

2.   FLIGHT INSTRUMENTATION

The Category I flight test program provided instrumentation in the No. 1 and No. 2 XC-142A airplanes (Figure 40) sufficient in terms of the necessary variables measured for the purposes of this program. Less extensive instrumentation was installed in the No. 3 airplane, but it provided enough information for analysis in some special cases. The airborne data recording was accomplished with a pulse duration modulation (PDM) tape system, camera coverage of cockpit control panels, and pilot and co-pilot verbal reports. The sampling rate of the PDM system was 10/sec. and 20/sec. In some cases (certain flights), multiple gyro instrumentation, with different sensitivities, was available by recording stabilization system gyro signals, as well as the instrumentation gyro measurements. This multiple instrumentation provided comparison checks in these cases.

The particular variables generally available and required for performance, stability, and control analyses were:

> (1)   Aileron position, left outboard
> Aileron position, left center section
> Aileron position, right outboard
> Aileron position, right center section

(2)   Main propeller blade angle, No. 1
         Main propeller blade angle, No. 2
         Main propeller blade angle, No. 3
         Main propeller blade angle, No. 4

(3)   Tail propeller blade angle

(4)   Propeller RPM

(5)   Unit horizontal tail position, small range
         Unit horizontal tail position, large range

(6)   Rudder position

(7)   Wing position

(8)   Flap position, left outboard
         Flap position, left center section
         Flap position, left inboard
         Flap position, right outboard
         Flap position, right center section
         Flap position, right inboard

(9)   Engine shaft torque, No. 1
         Engine shaft torque, No. 2
         Engine shaft torque, No. 3
         Engine shaft torque, No. 4

(10)   Pitch rate

(11)   Roll rate

(12)   Yaw rate

(13)   Pitch attitude

(14)   Roll attitude

(15)   Heading

(16)   Longitudinal acceleration at c.g.

(17)   Normal acceleration at c.g.

(18)   Lateral acceleration at c.g.

(19)   Angle-of-attack, nose boom vane

(20)   Angle of sideslip, nose boom vane

(21)   Airspeed, nose boom pitot tube

(22)   Altitude, nose boom pitot tube

In general, the flight data obtained during the program exhibited a relatively low signal to noise ratio, especially in the data obtained from earlier flights. As the program progressed, the quality of the flight data was improved somewhat by selecting gyro and accelerometer locations so as to isolate them as nearly as possible from aircraft vibration and electrical noise. Because of the relatively low sample rates employed (20 samples per second, maximum), it was not possible to determine the true frequency content of the noise. In theory, samples must be taken at twice the highest frequency component contained in the data in order to avoid the loss of information, and in practice, even higher sample rates are required. Because the sampling rate was too low to completely recover the entire frequency content of the noise, the filtering algorithms employed in smoothing the data were not strictly mathematically correct. However, the filtering of the data did produce smooth fairings through the data points which helped to reduce the scatter in the extracted stability derivatives.

Additional inaccuracy in the XC-142A flight test data is attributed to the large range over which many of the variables must be measured. Since the sensitivity of most instruments varies inversely with the range of measurement, the accuracy of the measurement of such variables is necessarily reduced. For example, propeller pitch angles range from about -4° up to 56° for normal control and to 76° when feathered. However, differential propeller control in transition must be determined in fractions of degrees. The unit horizontal tail (UHT) incidence range is a similar case requiring a 50° range in transition flight and only a few degrees in range over the cruise flight envelope. Dual sensor instrumentation was provided as an attempt to solve the UHT problem, but additional blade angle instrumentation was not provided.

The measurement of airspeed provided by the nose boom system was checked against ground camera determined speeds and by comparison with a helicopter system while being paced through the lower speed range of transition. Results indicated the nose boom system was accurate to within one knot above 30 knots and to within two knots in the 20 to 30 knots airspeed range. The system was unreliable below 20 knots.

3. DATA ANALYSIS METHODS

a. LEAST SQUARES METHOD

The method referred to herein as the least squares method consists of fitting a mathematical model to the flight data where the criteria for obtaining the fit is the minimization of the squared error between the flight data and the model response. The assumed aerodynamic representation or model must consider only those variables which are excited independently during that maneuver. General equations of motion representing the first order aerodynamic effects for the XC-142A are defined in Appendix I. These equations are for uncoupled longitudinal and lateral-directional motion which was assumed for this analysis.

All of the flight variables in the equations were available from the usual flight instrumentation for the XC-142A, with the exception of the angular accelerations. These accelerations had to be determined by differentiating the angular rates obtained from rate gyros. The actual differentiation

116

was performed by either a central difference method (Stirling's formula) or by numerical digital derivative-smoothing filters as an integral part of an IBM 7090 digital computer routine for the least squares computations.

It is well known that differentiation of a signal which contains high frequency noise components results in a reduction of signal to noise ratio. Therefore, it would have been more desirable to use actual measurements of the angular accelerations had such data been available.

A description of the mathematics involved in the least squares derivative extraction process is presented in Appendics I and II. In Appendix I, the equations of motion that were fitted to the XC-142A flight test data are developed; and in Appendix II, the least squares normal equations for the stability derivatives are derived. The normal equations are simply a set of simultaneous linear algebraic equations where the stability derivatives are the unknowns and the constant coefficients are computed from the flight test time history data using the equations of Appendix II. The variables that were not excited during a particular maneuver, and those that were considered proportional to another variable, were eliminated from this general set-up by input specifications to the computer for each set of data. These normal equations also contain a constant coefficient which represents the total bias that may result from errors in selecting a set of trim or null values of the flight variables from which perturbations are taken for a particular maneuver. This term is not significant in itself, but without its inclusion in the solution, very large errors may result in the coefficients determined.

The digital computer routine used for the least squares solutions was checked by determining solutions for "exact" time histories of assumed linear models obtained from established inverse Laplace routines. A comparison of the original or assumed aerodynamic coefficients with the least squares solutions was satisfactory to three or more significant digits for the important derivatives, the less significant derivatives being slightly less accurate. The fact that the computed time histories were determined by single precision arithmetic would account for this difference. Single precision arithmetic was utilized in the least squares routine used in this program since aerodynamic models with six or fewer coefficients were selected. Higher order models might have required some investigation of double precision arithmetic, but the quality of the flight data generally did not merit more elaborate aerodynamic representation.

The least squares method lends itself readily to the type of flight data that were generally available for this study; i.e., continuously controlled maneuvers. In fact exagerated maneuvers, in which all variables affecting the aerodynamics of the vehicle are excited, are desirable when this method is to be applied.

b.   NUMERICAL FILTERING

The flight data were processed through a numerical or digital filtering routine (on an optional basis) prior to the least squares analysis due to their apparent high frequency noise and/or vibration content. The numerical

filters were defined in the same manner as the "Martin-Graham" type described in Reference 25. A summary of the equations for definition of these filters is included in Appendix III of this report. A general discussion on the application of these filters is contained in Reference 26.

The effect of filters with various cut-off frequencies and roll-off bandwidths was evaluated in terms of the corresponding effect on the least squares solutions for the aerodynamic derivatives for particular sets of flight data. Solutions were obtained using unfiltered data for a basis of comparison. The relatively low sampling rate (10/sec. and 20/sec.) of the flight data system prevented any determination of the true frequency content of the data. Depending on the flight maneuver, filters with cut-off frequencies of one or two cps were necessary to "improve" the least squares solutions in most cases. This judgement was based on comparison of the consistency of results for several separate maneuvers performed at identical flight conditions. For example, three sets of data from the same flight and the same test condition might yield completely uncorrelated solutions when using unsmoothed data. By filtering the data, some reasonable consistency of solutions could be obtained. In general, the use of these smoothing filters was necessary on this basis although the application of low cut-off frequency filters to data with very abrupt control inputs was avoided whenever possible. The validity of the use of filters for smoothing as well as differentiating the XC-142A flight data cannot be justified in any strict manner, but only in that more consistent results were obtained with their use. It should be noted that the results presented later in this report indicate generally lower values of the aerodynamic derivatives in comparison to predicted levels in some cases. This may indicate some undesired attentuation of the data due to use of filters too low in cut-off frequency. This effect could be avoided only by increasing the sampling rate of the data system so that higher cut-off frequency filters could be used.

c.   ANALOG DUPLICATION

The trial and error method of duplication of flight time history data, using an analog computer, was used for analyzing some longitudinal, cruise configuration flight data. The particular flight maneuvers were pilot-forced sinusoidal oscillations. The unit horizontal tail (UHT) time history was generated for the computer input forcing function. Computer output recordings of pitch attitude and rate, normal acceleration, and angle-of-attack were matched to the flight measured time histories by adjustment of the aerodynamic derivatives as required.
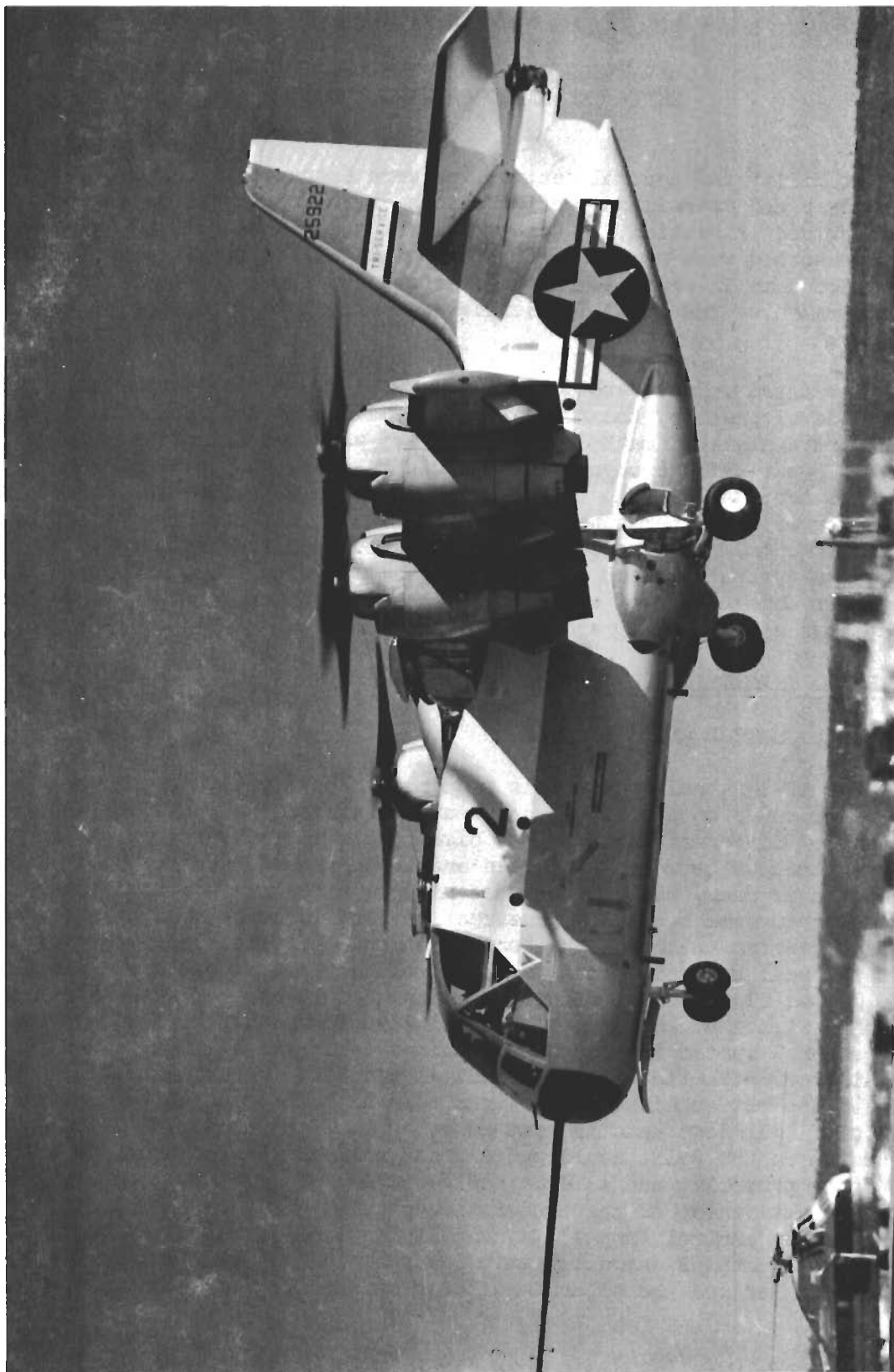
FIGURE 40

NO. 2 XC-142A IN HOVER FLIGHT

SECTION VI

COMPARISON OF FLIGHT TEST RESULTS WITH
ESTIMATES BASED ON WIND TUNNEL DATA

The stability and control derivatives were extracted from the flight
data, in hover and transition configurations, by means of the least squares
method described in Section V. Both the least squares method and the analog
duplication method were used to extract longitudinal derivatives from cruise
configuration data in order to compare the results from the two methods.
Estimated values of the stability derivatives are shown in each case for
comparisons.

The estimated values were derived from wind tunnel tests conducted during
design and development of the XC-142A. In arriving at the estimated values,
the Princeton analytical method (Reference 27) was used extensively to derive
equivalent "power-off" aerodynamic coefficients from the "power-on" wind
tunnel model test data. This approach is necessary to remove the direct
propeller forces and moments which differ from the full scale propeller
forces and moments. It also permits analysis of individual control
effectiveness (propellers and ailerons for various wing, flap and power
settings) for development of aerodynamic characteristics for the flight test
power settings and wing/flap and control programming.

1. HOVER AND TRANSITION DERIVATIVES

a. ROLL CONTROL EFFECTIVENESS

The XC-142A roll control is sequenced mechanically through the
transition maneuver to accomplish a gradual change in the principal source of
roll control. Differential propeller blade angle is the primary roll control
for wing incidences between 90 degrees and 10 degrees. For wing incidence
less than ten degrees, the ailerons become more effective for roll control,
and propeller control becomes more effective for yaw control as the wing and
flaps are converted to the cruise configuration. Differential propeller blade
angle in the roll control system is not completely phased out above the 0 degree
wing, 10 degree flap configuration. The design roll control gearing relations
are shown in Figure 41 as a function of wing incidence for reference. Since
the roll control system interconnect gearings establish a linear dependence
between aileron deflection and differential propeller blade angle, it is not
possible to separate their contributions to roll control using a least squares
analysis of flight test data in most cases. (It might be possible in certain
situations where the pilot could put in both roll and yaw control, such that
the resulting propeller and aileron deflections would not be proportional.)
The total effectiveness of the integrated controls for pure roll control in-
puts (and no yaw control inputs) is actually most desirable to evaluate the
airplane's roll control characteristics; but since most of the wind tunnel
data available defined the separate aileron and differential thrust control

effectiveness, a direct correlation of the combined effectiveness cannot be made.

It would have been convenient to base roll control effectiveness on some deflection in the control system common to both the propellers and ailerons, such as a point in the system between the stabilization actuators and the integrated controls phasing mechanism. This would be similar to a control derivative based on control stick deflection, but would include stabilization inputs and thus correspond to surface deflections (neglecting system dynamics). The desirable result of such a control derivative would be that it would provide a more normal or standard base and an indication of the actual roll effectiveness would be apparent from the derivative. However, an approach of this type would have involved some accounting for the control system's dynamic characteristics downstream of the measured deflection point. This fact would make such an approach undesirable for defining aerodynamic characteristics, since it would further complicate the already difficult inverse solution problem. Instrumentation was not included in the airplane for measuring such a deflection point in the control system, but the objective of this discussion is to point out the problems associated with forming desirable definitions for the control effectiveness derivatives of a blended control system in general, and the XC-142A roll control system in particular.

The total roll control derivatives extracted from the flight data were based on differential propeller control deflections throughout the transition range. Corresponding derivatives based on aileron deflections were defined for the lower wing incidence range only (aileron roll control derivatives become indeterminate at high wing incidences). In terms of the individual control surface derivatives, the extracted roll parameters may be represented in the following forms:

$$L^*_{\delta_\beta} \doteq L_{\delta_\beta} + L_{\delta_A} (\delta_A/\delta_\beta)$$

$$N^*_{\delta_\beta} \doteq N_{\delta_\beta} + N\delta_A (\delta_A/\delta_\beta)$$

$$L^*_{\delta_A} \doteq L_{\delta_A} + L_{\delta_\beta} (\delta_\beta/\delta_A)$$

$$N^*_{\delta_A} \doteq N_{\delta_A} + N_{\delta_\beta} (\delta_\beta/\delta_A)$$

The basic restriction involved in selecting flight maneuvers for defining these parameters is that only roll control inputs can be applied during the maneuver. Yaw control (from both pilot and stabilization inputs) must be zero or constant. The assumption that the differential propeller controls and the aileron controls are linearly dependent requires that the surface control system actuators have similar response times. Any difference in response characteristics would probably lie within the data accuracy in the case of the XC-142A.

121

Roll control maneuvers consisting of continuous rolling through a +10 to +15° bank angle range were performed in the Category I program with the yaw stabilization system deactivated (turned off) and the roll stabilization system operative (insignificant to the data analysis). The maneuvers performed in 0° to 30° wing configurations were of good quality in that yaw control inputs were all and fairly rapid roll control was applied. The lease squares extractions of $L^*_{\delta_\beta}$ and $L^*_{\delta_A}$ from these data were summarized in

Figures 42 and 43 along with estimated values derived from wind tunnel data. The corresponding extractions of $N^*_{\delta_\beta}$ and $N^*_{\delta_A}$ are summarized in Figures 44 and

45. The numbers with the points correspond to the point numbers in Table V which defines the various flight test conditions. Generally good agreement is indicated for the primary rolling effectiveness in Figures 42 and 43 and reasonable agreement is also indicated for the yaw due to roll control derivatives in Figures 44 and 45.

b. YAW CONTROL EFFECTIVENESS

Yaw control in transition configurations is developed by a combination of aileron deflection, differential propeller blade angle and rudder deflection. Since the three control surfaces do not move independently, it is not possible to extract the yaw control stability derivatives separately. Instead, the least squares analysis yields the following typical combinations of the derivatives given below.

$$L^*_{\delta_R} \doteq L_{\delta_R} + L_{\delta_\beta} \, (\delta_\beta/\delta_R) + L_{\delta_A} \, (\delta_A/\delta_R)$$
$$N^*_{\delta_R} \doteq N_{\delta_R} + N_{\delta_\beta} \, (\delta_\beta/\delta_R) + N_{\delta_A} \, (\delta_A/\delta_R)$$

Since the rudder actually moves even in hover, it is convenient to base the yaw control derivative extractions on its deflection, and the resulting derivative provides a good indication of the true effectiveness over the complete transition regime. The design directional control gearings δ_β/δ_R and δ_A/δ_R are defined in Figure 46 for reference. The extracted values of $N^*_{\delta_R}$ and $L^*_{\delta_R}$ are plotted with estimated values for comparison in Figures 47 and 48. The numbers placed along side the data points denote the reference flight conditions which are summarized in Table V. The comparison of $N^*_{\delta_R}$, flight extracted vs estimated, appears reasonably good over the transition range of wing incidence.

c. SIDESLIP DERIVATIVES

The sideslip angle derivatives, N_β and L_β, were extracted from the same maneuvers used to evaluate yaw and roll control effectiveness for configurations with wing incidence less than 35 degrees. The sideslip angle available was measured by a vane located on the nose boom installed on the test airplanes. This vane-measured slip angle was corrected for the effect of yaw rate by the formula:

$$\beta = \beta_{vane} - \ell \, (r/V)$$

where ℓ is the length from the vane to the c.g. of the airplane.

The extracted values of N_β and L_β , along with estimates, are plotted in Figures 49(a) and 50(a) to show the variation with airspeed. The same values are plotted against wing incidence in Figures 49(b) and 50(b). The comparison shown is obviously very poor, particularly for N_β, and this is attributed to the insufficient accuracy of the flight data for determining the lower order aerodynamic effects in the speed range below 100 knots.

d. ROLL AND YAW DAMPING DERIVATIVES

The roll and yaw damping derivatives, L_p and N_r , extracted along with the control effectiveness and sideslip derivatives are summarized in Figures 51 and 52. These derivatives appear to be consistently lower than predicted levels, but little confidence can be attached to the comparison for these reasons: (1) On a percentage basis, the effect of the aerodynamic damping is considerably lower than moments generated by the control surfaces during pilot forced maneuvers. As might be expected, the least squares method tends to extract the strongest aerodynamic contributions with the greatest accuracy. (2) The generally lower level may have been caused by the arbitrary use of smoothing filters which possibly attenuated the measured airplane responses, especially since the cut-off frequences of the filters were so low (1 or 2 cps).

e. ANGLE-OF-ATTACK DERIVATIVES

The angle-of-attack derivatives, Z_α and M_α , were not evaluated in the low wing transition regime due to the absence of suitable flight data. The high noise or vibration content in the normal accelerometer instrumentation prevented any confident extraction of Z_α from dynamic maneuvers. Suitable dynamic maneuvers in which pitch rate and acceleration were of sufficient quality and excitation (amplitude) to determine M_α were unavailable also. An indication of the airplane lift slope can be obtained from Figure 53. The lift coefficient shown in the figure was calculated at various points in time during very slow stall approach maneuvers. The maneuvers were performed at a fixed throttle or power setting by pulling the nose of the airplane up slowly and allowing airspeed to decrease accordingly. The lift coefficient includes the effect of the tail and tail propeller control, plus any variation of thrust due to the variation of airspeed and governor (constant RPM) controlled blade angle due to airspeed reduction during the maneuvers. It is impossible to separate these effects during this type maneuver from the data available. The estimated value of the thrust coefficient, C_{T_s}, is also plotted in the figure. Pilot remarks denoting buffet onset points and buffet intensity are noted per pilot comments during the tests.

2. CRUISE CONFIGURATION DERIVATIVES

Some special longitudinal flight maneuvers were performed in the Category I program to define longitudinal stability characteristics in the cruise configuration. These maneuvers were sinusoidal oscillations in pitch performed at 8000 feet altitude at airspeeds of 215, 235, 250 and 270 knots EAS. At each airspeed, the pilot forced oscillations of approximately 0.3 and 0.5 cycles per second. Similar maneuvers were performed at both 17% and 25% center of gravity positions. Additional instrumentation, including a pitch

rate gyro and normal and longitudinal accelerometers, were installed to provide improved data for these tests (only). An oscillograph recorder was installed also for providing continuous data recordings in addition to the standard sampled data system recordings. The type of maneuvers performed during the two flights made for these tests provided the best data available from the Category I program, but the derivative extractions from the least squares analysis indicated some inconsistencies most likely attributable to instrumentation errors. The most obvious of these is the difference in derivatives due to frequency as apparent in Figures 54 through 61. Reference test conditions for these results are recorded in Table VI.

The results of an analog duplication analysis of these same flight data are shown in Figures 54, 56, 58 and 60. This analog study was made independently of the least squares analysis and it reflects no effort to arrive at similar results. In fact, the two sets of results are not directly comparable as presented since those from the analog analysis represent the values which best fit both the 0.3 cps and the 0.5 cps maneuvers at each airspeed condition. It is not too surprising that the analog results more closely represent the trends if not the values of the estimated derivatives since an analog duplication uses the estimated values as a starting point. A best fit of the time histories is then obtained by "perturbating" the significant derivatives. Also the input and response time histories are faired before duplication is attempted. The least squares method, while more honest and unemotional since it does not require a knowledge of the estimated values, is much more strongly influenced by data inaccuracies and scatter.

3. THRUST REQUIRED IN GROUND EFFECT, HOVER

Model tests conducted at the NASA Langley Research Center with an XC-142A free flight model indicated a quite obvious cushioning effect as the controlled model was allowed to descend into the proximity of the ground. Some flight tests were made to determine the magnitude of this effect on the airplane. Results in terms of the required engine torque and propeller blade angle to hover were measured at several heights above the ground and are tabulated in Table VII. The indicated height above ground represents the tires-to-ground distance, and is only approximate as accurate height measurement was unavailable for these tests.

These data were obtained from the steady portions of extended hovers of some two minutes duration at each height, and represent arithmetic average values of the data. The blade angles and torques required were adjusted to a gross weight of 35,000 pounds and an RPM of 95% by means of isolated propeller test results. These adjusted values plotted in Figure 62 indicate a decrease in both torque and blade pitch required due to ground proximity, and it is assumed a corresponding trend in thrust required from the propellers would be realized if measurements were available.

Estimated thrust to weight ratio as a function of height above ground for these flight tests is summarized in Figure 62. The estimated thrust used to obtain this figure was calculated from ASD whirl rig data presented in Figure 67.

4. TRANSITION TRIM VARIABLES

A summary of the flight measured propeller blade angles, engine torque required, and pitch trim control requirements was made for representative wing-flap configurations spanning the transition flight regime of the XC-142A airplane. These data were selected from flight test trim points at zero pitch attitude with the flaps programmed for the landing configuration. This program provides flap deflections as a function of wing incidence. The actual data determined from flight are summarized in Table VIII and in Figures 63 and 64. The comparison of estimated trim airspeeds with flight measured values over the transition wing angle range shown in Figure 63 indicates general agreement. The estimated wing angle vs airspeed relation indicates a variation of about one knot per degree of wing angle at 40° wing and increases to greater than two knots per degree at 10° wing. Approximately the same variation in airspeed exists with fuselage attitude. These two significant effects, together with other minor effects, make the comparison in Figure 63 appear fairly good when the absolute accuracy of wing incidence and fuselage attitude instrumentation are considered.

The propeller system RPM, airplane center of gravity, and air density ratio, σ, defined in Table VIII, vary over a range too large to allow a direct comparison of propeller characteristics and pitch trim requirements against estimates made for nominal conditions. In order to obtain a comparison of propeller characteristics for consistent RPM settings and standard density, and to better indicate any areas of significant disagreement with predicted characteristics, it was assumed that the flight data could be adjusted to a nominal RPM of 95% at standard day atmosphere, sea level conditions. This adjustment was based on the assumption that thrust required for a given wing-flap configuration was primarily a function of equivalent airspeed, all other factors being negligible. Then an adjustment to blade angle was estimated due to the difference in true airspeed and RPM from the test condition to the base or standard condition. Using this adjusted blade angle, an estimated increment was made for the adjustment of torque required to the standard base.

These adjustments to blade angle and torque required were estimated on an incremental basis by use of the isolated propeller characteristics defined by ASD whirl rig tests and NASA Ames wind tunnel tests of the full scale propeller. These propeller characteristics are shown in Figures 67 and 68 for reference. The tests were made at or near zero inflow angles, but the modified advance ratio, $J \cos \Psi$, where Ψ was assumed to be the wing incidence angle, was used for entering these prop maps. No attempt was made to account for the effect of wing upwash on the inflow angle Ψ. Even so, the adjusted data should be reasonably valid in most cases since only minor changes or perturbations have been made to the actual data.

The resulting blade angle and torque values are summarized in Figures 65 and 66. Estimated curves are shown also for comparison purposes. These estimates are representative of lift, drag and thrust characteristics derived from wind tunnel data. Based on the thrust required estimate, the torque and

blade angle required were defined from the isolated propeller maps. The significant differences in blade angle and torque required appear in the 30° to 80° wing incidence range. An explanation for these differences is difficult to ascertain due to the three possible sources of error; i.e., (1) the wind tunnel determined lift, drag and thrust required, (2) the application of isolated propeller data, and (3) the flight measured data. Of these errors, the latter is probably less significant in this case.

The pitch trim requirements, UHT position and tail propeller blade angle, shown in Figure 64, have not been correlated with estimates due to the several factors affecting a valid comparison. The factors to be considered in such a comparison include: (1) both the horizontal and vertical center of gravity locations, (2) gross weight, (3) propeller RPM, and (4) air density for each test point.

5. DESCENT BOUNDARIES

Rate of descent characteristics of the XC-142A in the transition flight regime have been evaluated at several configurations in the wing incidence range of 0° to 40° with both the 60° (landing) flap program and the 30° (take-off) flap program. These evaluations consisted of determining the rate of sink at which buffet first occurs, and then increasing the rate of sink to determine the intensity of buffet and the limit rate of descent for acceptable handling qualities. These characteristics were determined by pilot observation and opinion via comments made during the tests. Some results for 60° flap configurations are recorded in Table IX. These results are plotted in Figure 69 along with the corresponding onset buffet boundary predicted from observed wing flow separation in model tests. Obviously, greater descent capability has been realized in flight than was predicted from these model tests by using the initial wing separation as a criterion.

TABLE V ROLL AND YAW CONTROL MANEUVERS IN TRANSITION AND HOVER

POINT NO.	AIRPLANE NO.	FLIGHT NO.	WING ANGLE (Deg)	FLAP ANGLE (Deg)	GROSS WEIGHT (Lb)	C.G. POSITION (% MGC)	TRIM VARIABLES					MANEUVER DESCRIPTION
							AIRSPEED EAS (Knots)	ALTITUDE (Ft)	PROP RPM (% Max)	PROP BLADE ANGLE (DEG)	TORQUE (% Max)	
22	1	48	0	27.0	36,700	24.3	140	2,140	90	20.3	37	Lateral stick inputs
23	1	48	0	27.0	36,700	24.3	140	2,140	90	20.6	38	Lateral stick inputs
24	1	48	0	27.0	36,820	24.3	140	1,930	91	20.6	37	Rudder pedal inputs
26	1	48	6.6	28.0	34,950	24.0	110	2,500	91	16.2	30	Rudder pedal inputs
25	1	48	10.0	30.8	35,000	23.6	92	2,580	92	13.0	25	Rudder pedal inputs
11	1	24	13.4	59.3	37,220	18.7	69	2,770	91	11.2	33	Lateral stick inputs
12	1	24	13.4	59.3	37,220	18.7	66	2,775	91	11.4	33	Lateral stick inputs
19	1	24	13.4	59.6	37,170	18.7	66	2,780	91	11.2	33	Rudder pedal inputs
13	1	24	13.1	59.4	36,820	18.7	72	2,800	92	12.0	35	Lateral stick inputs
14	1	24	23.3	61.1	36,720	18.1	48	2,800	92	11.4	42	Lateral stick inputs
15	1	24	23.3	61.1	36,720	18.1	49	2,770	92	12.2	47	Lateral stick inputs
16	1	24	23.3	61.1	36,720	18.1	52	2,850	92	12.3	45	Lateral stick inputs
20	1	24	23.0	61.2	36,620	18.0	51	2,750	92	11.0	38	Rudder pedal inputs
17	1	24	31.3	61.2	36,470	17.6	40	2,750	92	12.1	46	Lateral stick inputs
18	1	24	31.3	61.2	36,470	17.6	42	2,730	92	13.0	53	Lateral stick inputs
21	1	24	31.7	61.1	36,170	17.6	38	2,730	92	12.9	53	Rudder pedal inputs
10	3	41	65.0	25.0	34,785	16.1	22	140	94	13.1	67	Lateral stick inputs
9	3	41	67.0	22.0	34,885	16.1	22	160	94	13.6	64	Rudder pedal inputs
6	3	41	79.0	10.0	35,335	16.8	0	80	96	13.0	74	Rudder pedal inputs
8	3	41	79.0	10.0	35,335	16.8	0	100	96	13.3	74	Lateral stick inputs
7	3	41	79.0	10.0	35,335	16.8	0	120	96	13.1	74	Roll and yaw control
1	3	36	85.0	0	34,130	18.8	0	685	95	13.0	66	Yaw control
4	3	32	90.0	0	34,000	19.0	0	435	98	12.6	65	Yaw control
5	3	32	90.0	0	34,000	19.0	0	450	98	12.4	64	Yaw control
2	3	32	90.0	0	33,980	19.2	0	460	98	13.0	66	1/2 Pedal, 180 degree left turn
3	3	32	90.0	0	33,880	19.2	0	460	98	12.6	64	3/4 Pedal, 180 degree left turn
27	3	32	90.0	0	32,480	19.2	0	460	95	12.9	65	Roll control

127

TABLE VI REFERENCE CONDITIONS FOR LONGITUDINAL
MANEUVERS, CRUISE CONFIGURATION

(Airplane No. 1)

FLIGHT NO.	GROSS WEIGHT (Pounds)	C. G. (% MGC)	AIRSPEED EAS (Knots)	ALTITUDE (Feet)	PROP RPM % MAX	MANEUVER DESCRIPTION
50	37,650	16.97	214.0	7,947	75	Forced Sine @ .33 cps
50	37,600	16.96	217.6	7,900	75	" " @ .53 cps
50	37,530	16.95	234.5	7,932	75	" " @ .36 cps
50	37,450	16.95	235.0	7,944	75	" " @ .53 cps
50	37,250	16.93	252.0	7,983	75	" " @ .34 cps
50	37,200	16.92	251.0	8,002	75	" " @ .51 cps
50	37,000	16.91	270.0	8,011	75	" " @ .38 cps
50	36,950	16.90	270.0	8,066	75	" " @ .62 cps
50	36,650	25.03	213.5	7,925	75	" " @ .28 cps
50	36,570	25.04	213.5	7,975	75	" " @ .50 cps
50	36,450	25.04	235.0	7,886	75	" " @ .32 cps
50	36,400	25.04	233.0	8,032	75	" " @ .48 cps
51	37,700	25.0	252.0	7,998	75	" " @ .345 cps
51	37,650	25.01	251.3	7,928	75	" " @ .495 cps
51	37,400	25.01	269.0	7,965	75	" " @ .33 cps
51	37,350	25.01	271.7	7,896	75	" " @ .51 cps
51	36,650	25.0	211.0	7,811	75	" " @ .26 cps
51	36,630	25.0	213.0	7,860	75	" " @ .50 cps
51	36,530	25.0	234.0	7,950	75	" " @ .265 cps
51	36,450	25.0	233.0	7,946	75	" " @ .540 cps

TABLE VII   SUMMARY OF TEST DATA OBTAINED DURING
HOVER TESTS IN GROUND PROXIMITY

(Airplane No. 1, Flight No. 2)

HEIGHT ABOVE GROUND (Ft)	GROSS WEIGHT (Lb)	C. G. POSITION (% MAC)	WING ANGLE (Deg)	* MAIN PROP BLADE ANGLE	* RPM (% Max)	* ENGINE TORQUE (% Max)
2	34,350	18.9	84	13.9	94.3	68.4
5	34,200	18.9	86	14.0	94.1	69.3
10	34,100	18.9	86	14.1	94.3	69.8
20	33,800	18.9	86	14.25	93.6	70.0

* Average Values

TABLE VIII   SUMMARY OF TRIM VARIABLES IN TRANSITION CONFIGURATIONS
(STEADY LEVEL FLIGHT, ZERO FUSELAGE ATTITUDE)

POINT NO.	AIRCRAFT NO.	FLIGHT NO.	WING ANGLE (Deg)	FLAP ANGLE (Deg)	GROSS WEIGHT (Lb)	C. G. POSITION (% Max)	ALTITUDE (Ft)	DENSITY RATIO	AIRSPEED EAS (Knots)	PROP RPM (% Max)	ENGINE TORQUE (% MAX)	PROP BLADE ANGLE (Deg)	UHT ANGLE (Deg)	TAIL PROP BLADE ANGLE (Deg)
1	1	57	12	59	36,140	22.1	1,050	.964	72	89	31	11.4	3.8	-2
2	1	57	22	60	36,100	22.1	1,200	.961	52	89	37	10.9	11.5	-2.6
3	1	57	37	60	36,000	22.1	1,050	.964	33	91	56	13.0	23	1.5
4	1	20	33	60	35,120	21.1	2,075	.897	38	90	51	12.8	20.8	-1.0
5	1	20	29	60	34,820	21.2	2,020	.899	41	90	47	12.4	18.2	- .7
6	1	20	20	60	34,770	22.0	2,000	.900	49	90	34	10.5	11.6	-1.8
7	1	20	11	60	34,520	22.8	2,040	.903	66	91	31	10.8	4.7	-2.7
8	1	20	12	59	34,370	22.8	2,450	.894	75.5	93	30	11.7	4.8	-1.8
9	1	20	12	59	34,320	22.8	2,250	.899	73	90	26	10.9	4.7	-1.7
10	1	20	12	60	34,270	22.8	1,960	.910	67	93	30	10.6	4.5	-3.0
11	1	20	12	60	34,220	21.7	2,000	.907	68	93	30	10.6	4.6	-1.9
12	2	14	10	50	35,450	20.4	220	.998	67	95	31	9.5	2.7	-2.3
13	1	7	3	32	35,060	27.1	2,550	.910	108	90	30	16.9	- .5	-1.9
14	1	7	13	60	34,480	26.2	3,120	.900	62	91	33	12.6	5.5	-6.8
15	1	7	36	60	34,280	24.9	2,770	.906	29	92	49	13.2	25.5	.3
16	1	7	23	60	34,370	25.5	2,720	.909	48	90	37.5	12.0	14.5	-6.7
17	1	74	70	20	35,820	19.6	680	1.02	14*	95	70	13	30	6
18	1	74	55	46	36,220	19.6	665	1.02	15*	94	75	13	28	-3
19	1	74	45	60	36,620	19.6	655	1.02	20*	93	65	13	25	-6.5
20	1	2	86	0	33,800	18.9	--	.95	--	94	70	14.2	--	--

* Airspeed per ground camera data

TABLE IX   FLIGHT BUFFET AND DESCENT BOUNDARY TEST RESULTS

AIRPLANE NO.	FLIGHT NO.	WING ANGLE (Deg)	FLAP ANGLE (Deg)	GROSS WEIGHT (Lb)	AIRSPEED EAS (Knots)	RATE OF SINK (Ft/Min)
(Buffet Onset Points)						
2	28	11.5	56.2	36,000	59	1,300
2	28	17.5	57.5	35,900	54	1,000
2	29	17.8	58.3	35,500	51	910
2	28	22.8	57.6	35,700	47	950
2	29	27.5	58.4	35,500	41	700
2	29	33.3	58.5	35,500	36.5	650
2	29	35.6	58.4	35,300	32	680
(Limit Rate of Descent Points)						
1	24	17.0	61	35,900	59	1,920
1	24	21.4	61	35,800	52	1,530
1	24	30.5	61	35,700	44	1,500

(FULL STICK INPUT)
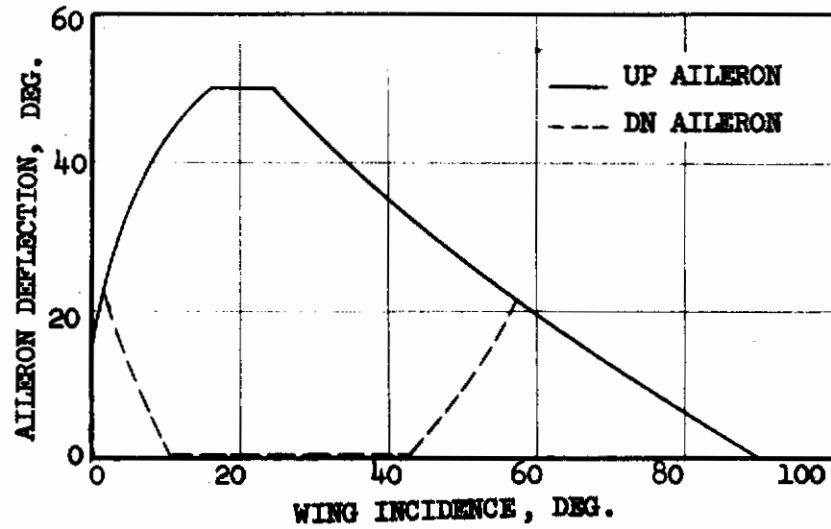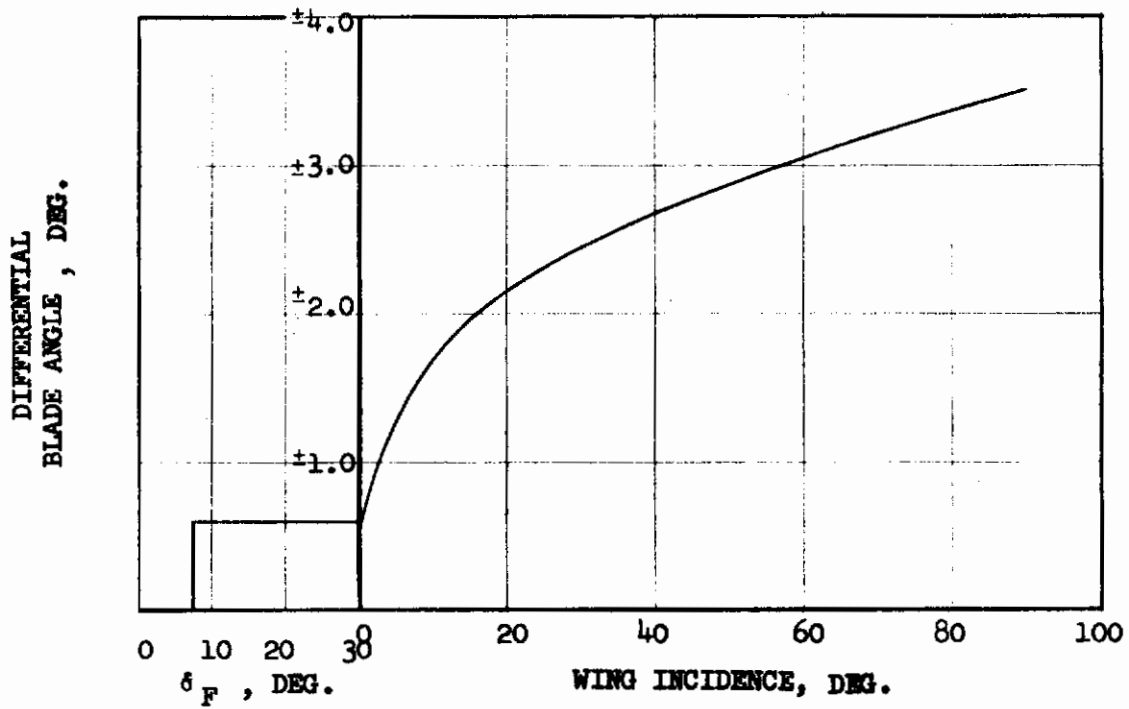
FIGURE 41 LATERAL CONTROL PROGRAMMING

132
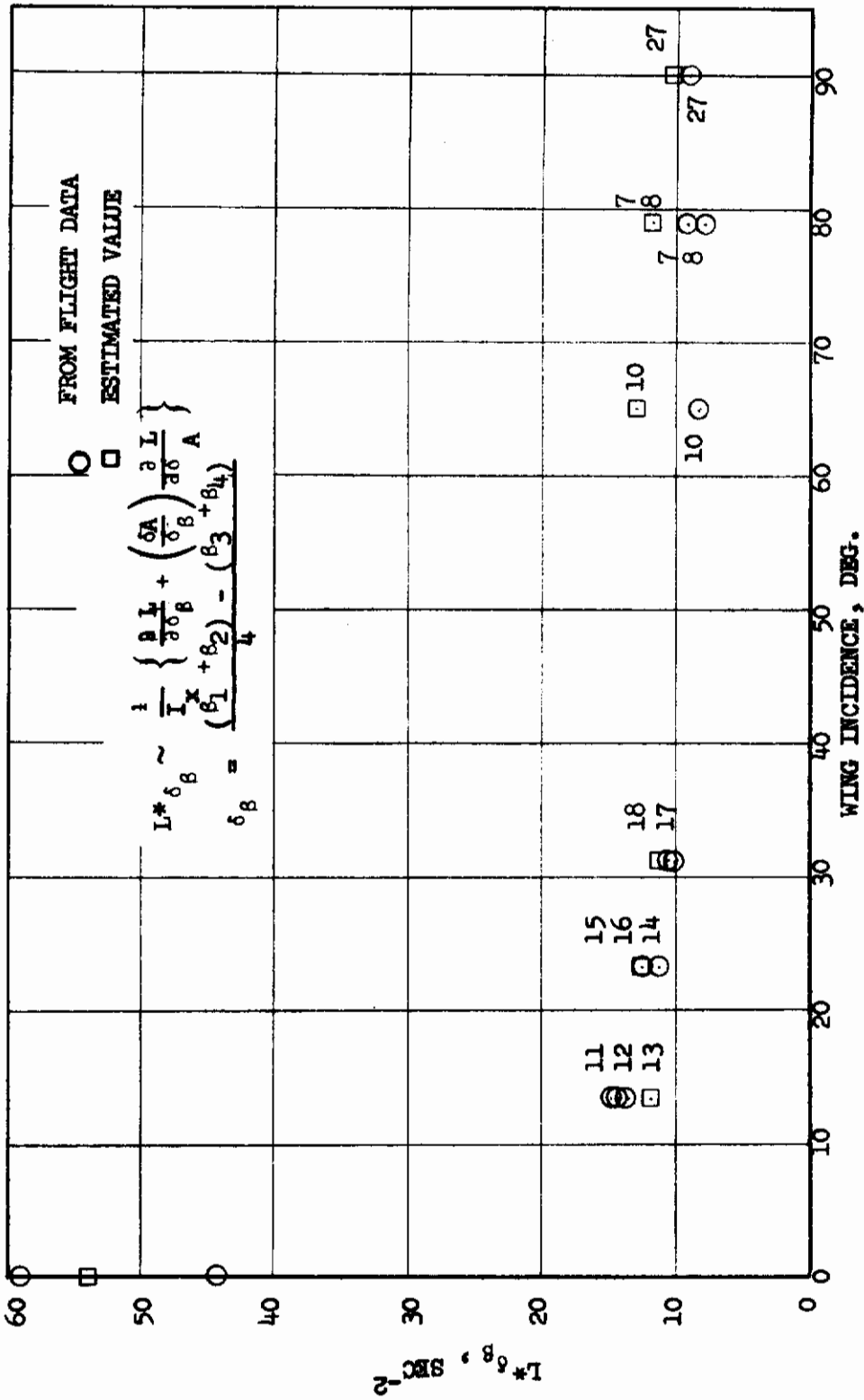
FIGURE 42 ROLL CONTROL EFFECTIVENESS, $L^*_{\delta_\beta}$

(BASED ON DIFFERENTIAL PROP PITCH)

FROM FLIGHT DATA

ESTIMATED VALUE

$$L^*_{\delta_\beta} \approx \frac{1}{I_x} \left\{ \frac{\partial L}{\partial \sigma_\beta} + \left(\frac{\partial A}{\sigma_\beta}\right) \frac{\partial L}{\partial \sigma} \right\}$$

$$\delta_\beta = \frac{(\beta_1 + \beta_2) - (\beta_3 + \beta_4)}{4}$$

WING INCIDENCE, DEG.

$L^*_{\delta_\beta}$, SEC^{-2}

(BASED ON AILERON)

$$L^*_{\delta_A} \sim \frac{1}{Ix}\left\{ \frac{\partial L}{\partial \delta_A} + -\frac{\delta \beta}{\delta_A}\frac{\partial L}{\partial \delta_\beta}\right\}$$

$$A = \left(\frac{\delta_{A_{LT}} - \delta_{A_{RT}}}{2} \right)$$

DOWN $\delta_{A_{LT}}$ OR $\delta_{A_{RT}}$ IS POSITIVE
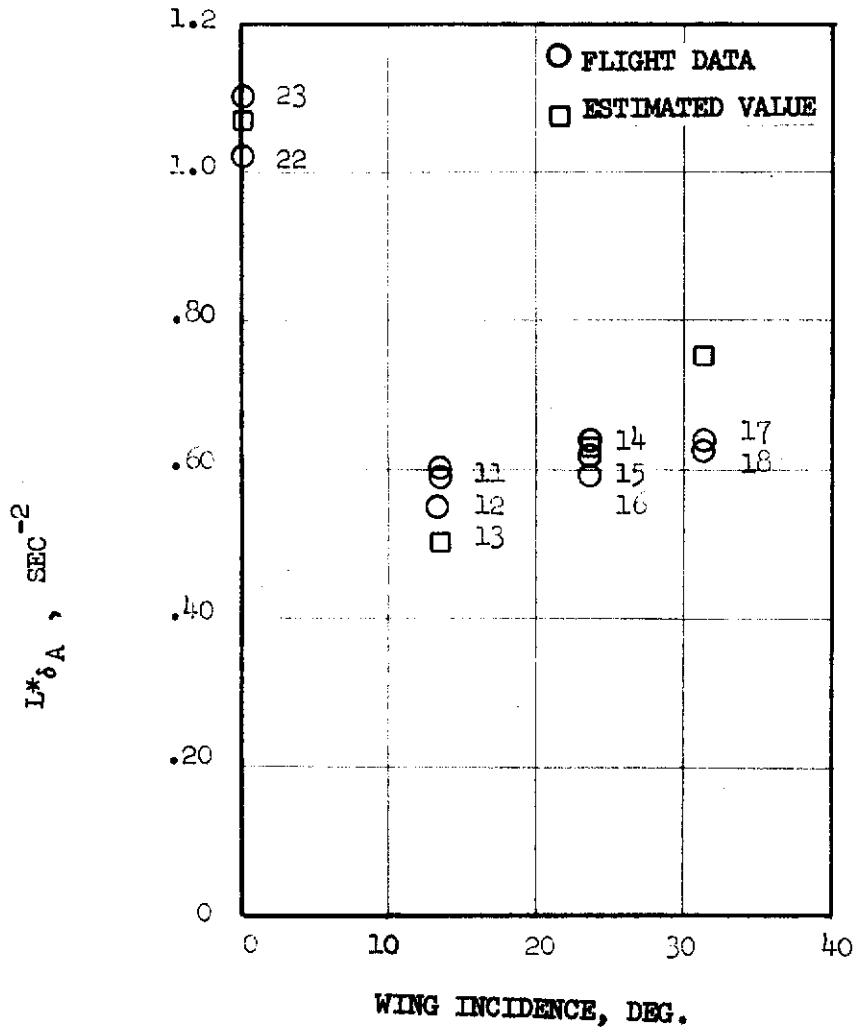
FIGURE 43 ROLL CONTROL EFFECTIVENESS, $L^*_{\delta_A}$

134
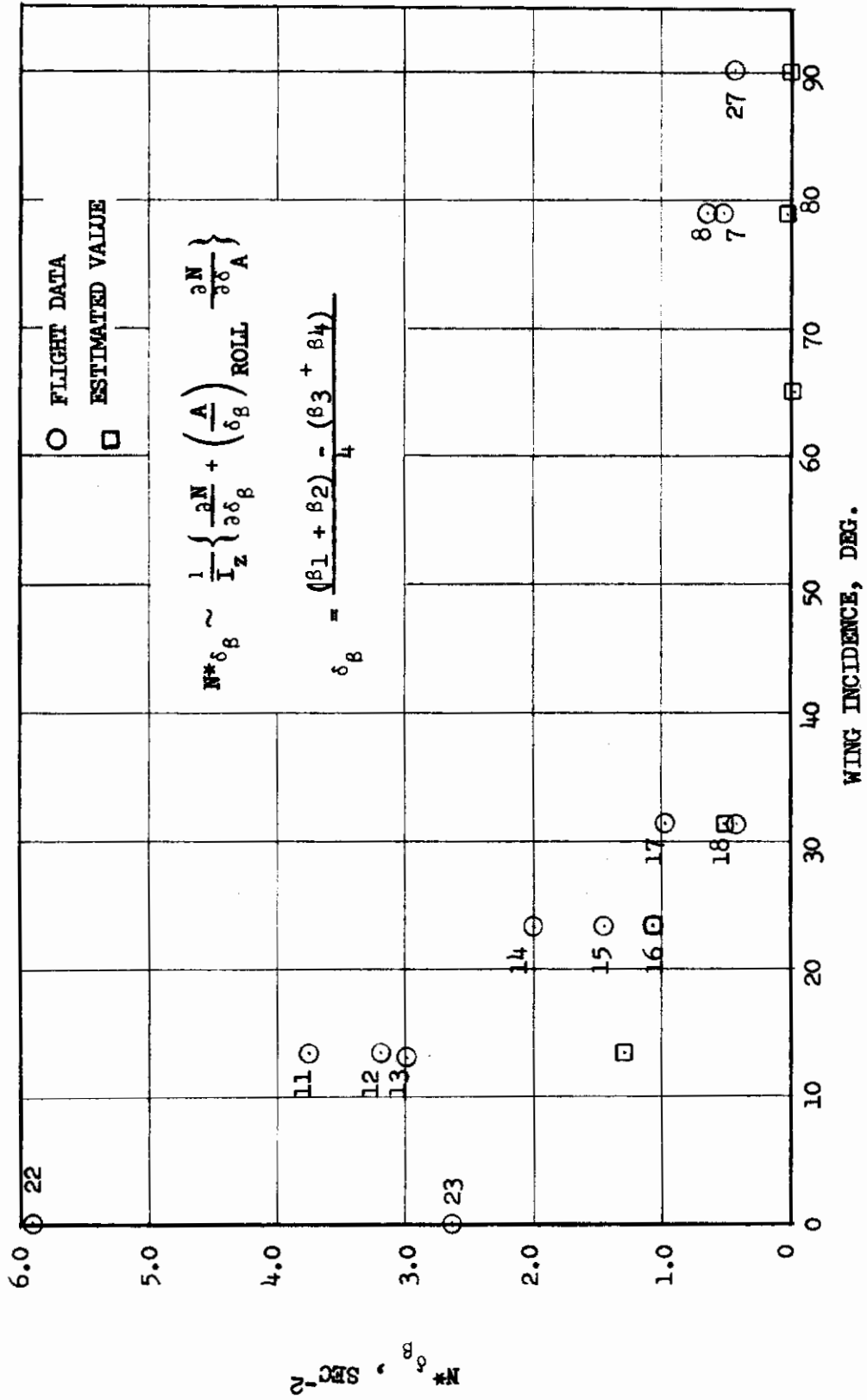
FIGURE 44 YAW DUE TO ROLL CONTROL, $N^*_{\delta_\beta}$

Legend:
○ FLIGHT DATA
□ ESTIMATED VALUE

$$N^*_{\delta_\beta} \approx \frac{1}{I_z} \left\{ \frac{\partial N}{\partial \delta_\beta} + \left(\frac{A}{\delta_\beta}\right) \text{ROLL} \; \frac{\partial N}{\partial \delta_A} \right\}$$

$$\delta_\beta = \frac{(\beta_1 + \beta_2) - (\beta_3 + \beta_4)}{4}$$

Y-axis: $N^*_{\delta_\beta}$, SEC^{-2}

X-axis: WING INCIDENCE, DEG.

$$N^{*}_{\delta A} \sim \frac{1}{I_Z}\left\{\frac{\partial N}{\partial \delta_A} + \left(\frac{\delta \beta}{\delta A}\right)_{ROLL} \cdot \frac{\partial N}{\partial \delta_\beta}\right\}$$

$$A = \left(\frac{\delta_{A_{LT}} - \delta_{A_{RT}}}{2}\right)$$

DOWN $\delta_{A_{LT}}$ OR $\delta_{A_{RT}}$ IS POSITIVE
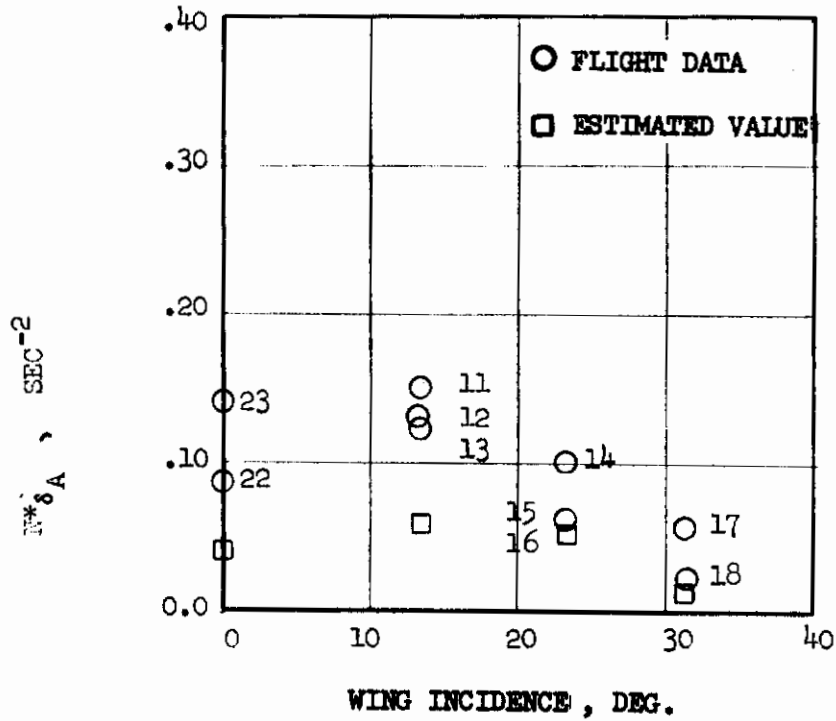
FIGURE 45   YAW DUE TO ROLL CONTROL, $N^{*}_{\delta_A}$

136

(FULL PEDAL INPUT)

NOTE: RUDDER DEFLECTION CONSTANT 27.5 DEG.
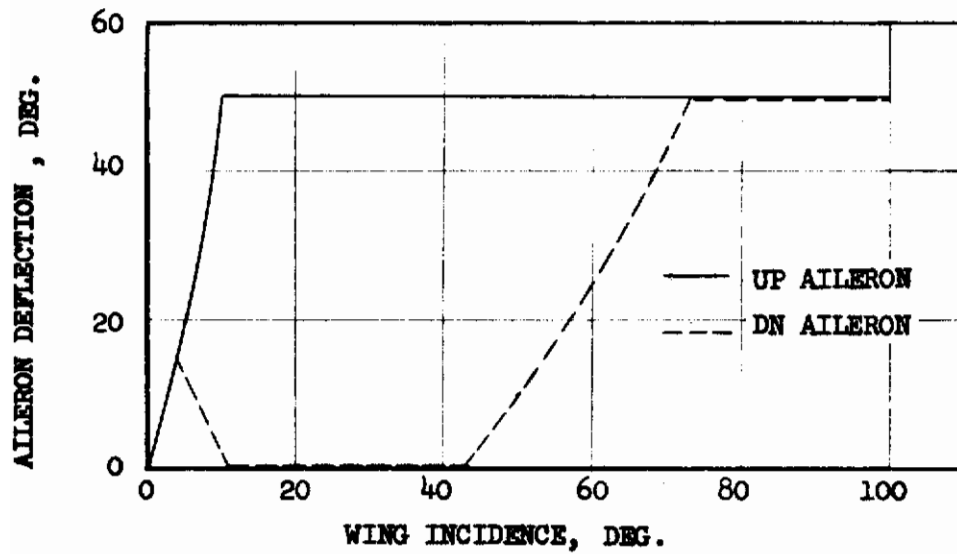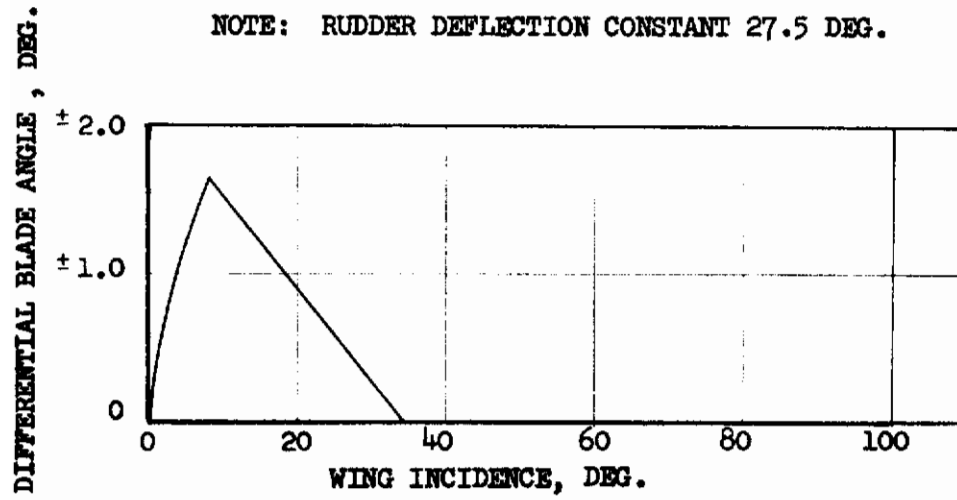
FIGURE 46   DIRECTIONAL CONTROL PROGRAMMING

$$N*_{\delta_R} \doteq \frac{1}{I_z} \left\{ \frac{\partial N}{\partial \delta_R} + \left(\frac{\delta A}{\delta R}\right)_{YAW} \frac{\partial N}{\partial \delta_A} + \left(\frac{\delta_B}{\delta_R}\right)_{YAW} \frac{\partial N}{\partial \delta_B} \right\}$$
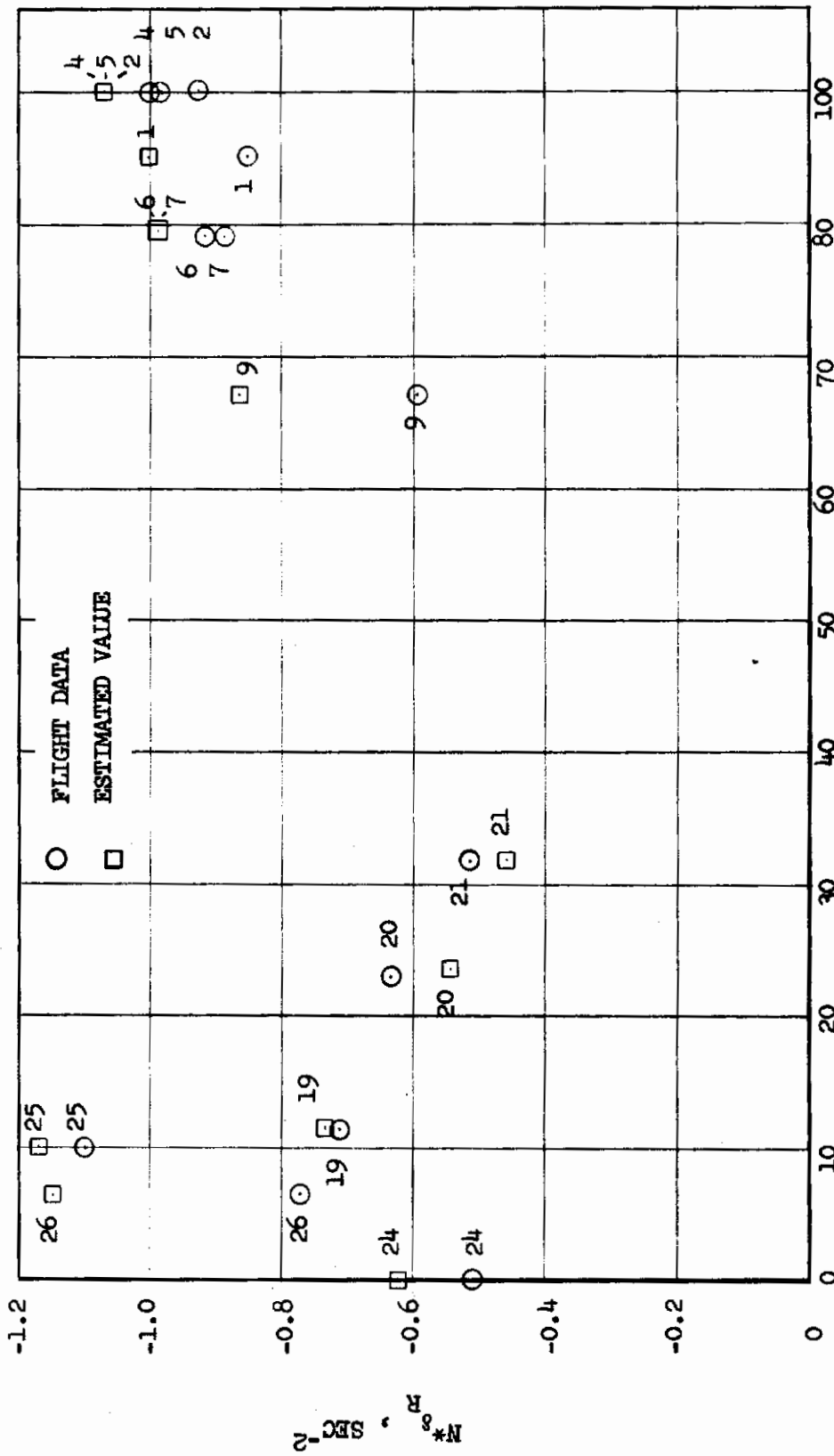
FIGURE 47 YAW CONTROL EFFECTIVENESS, $N*_{\delta_R}$

138

$$L*_{\delta_R} = \frac{1}{I_z} \left\{ \frac{\partial L}{\partial \delta_R} + \left(\frac{\delta_A}{\delta_R} \right)_{yaw} \frac{\partial L}{\partial \delta_A} + \left(\frac{\delta_B}{\delta_R} \right)_{yaw} \frac{\partial L}{\partial \delta_B} \right\}$$

○   FLIGHT DATA

□   ESTIMATED VALUE

WING INCIDENCE, DEG.

L*$_{\delta_R}$, SEC^{-2}
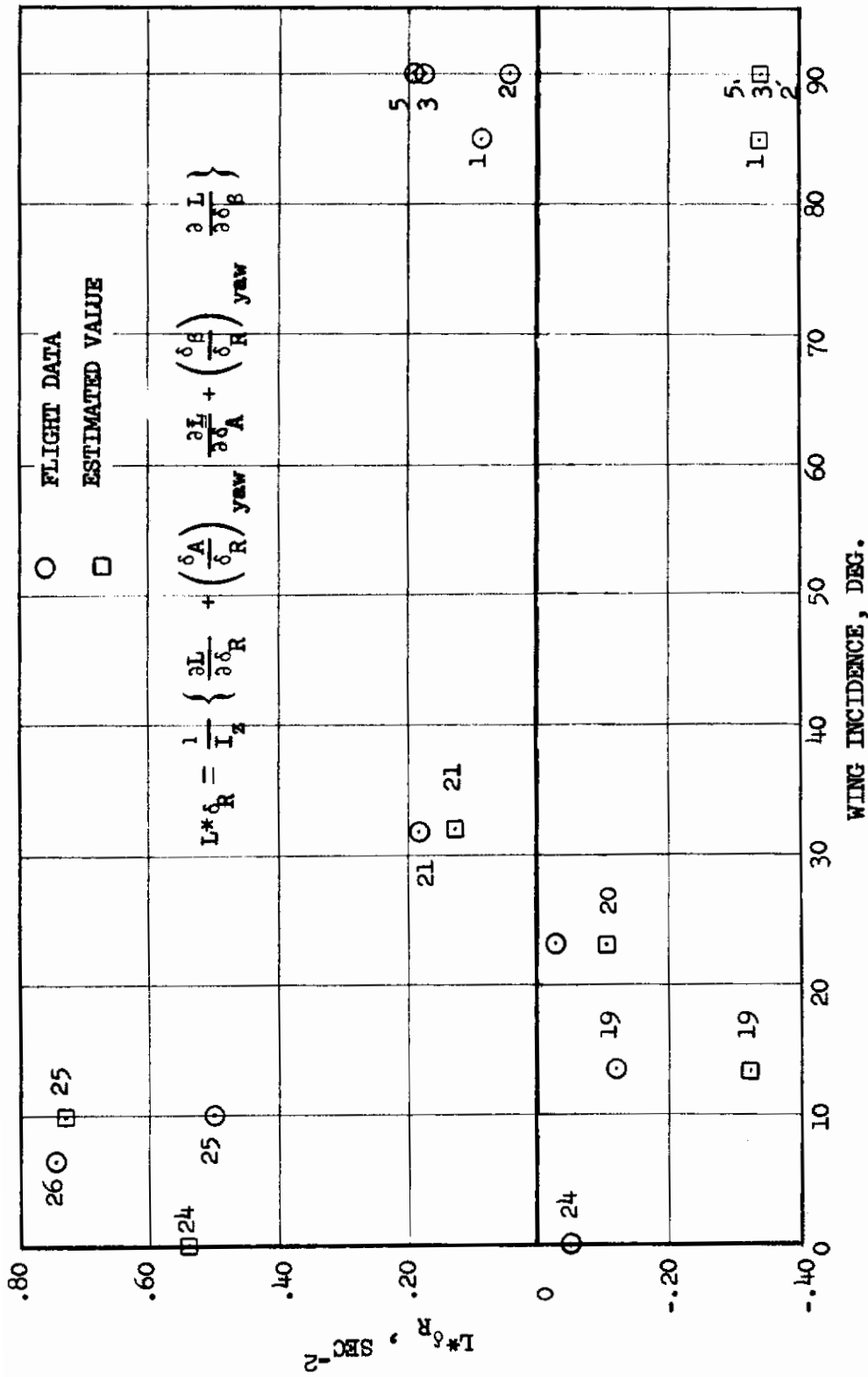
FIGURE 48   ROLL DUE TO YAW CONTROL, L*$_{\delta_R}$
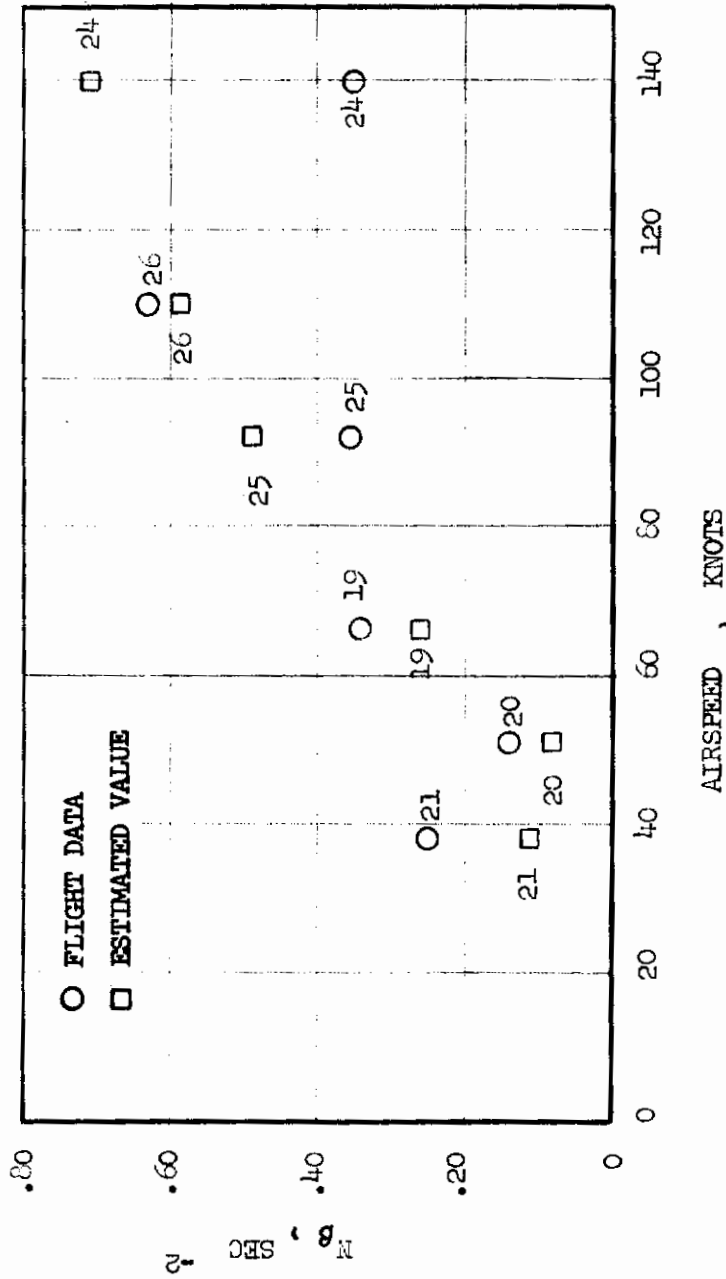
AIRSPEED , KNOTS

(a) N_β VS. AIRSPEED

FIGURE 49 DIRECTIONAL STABILITY PARAMETER, N_β

140
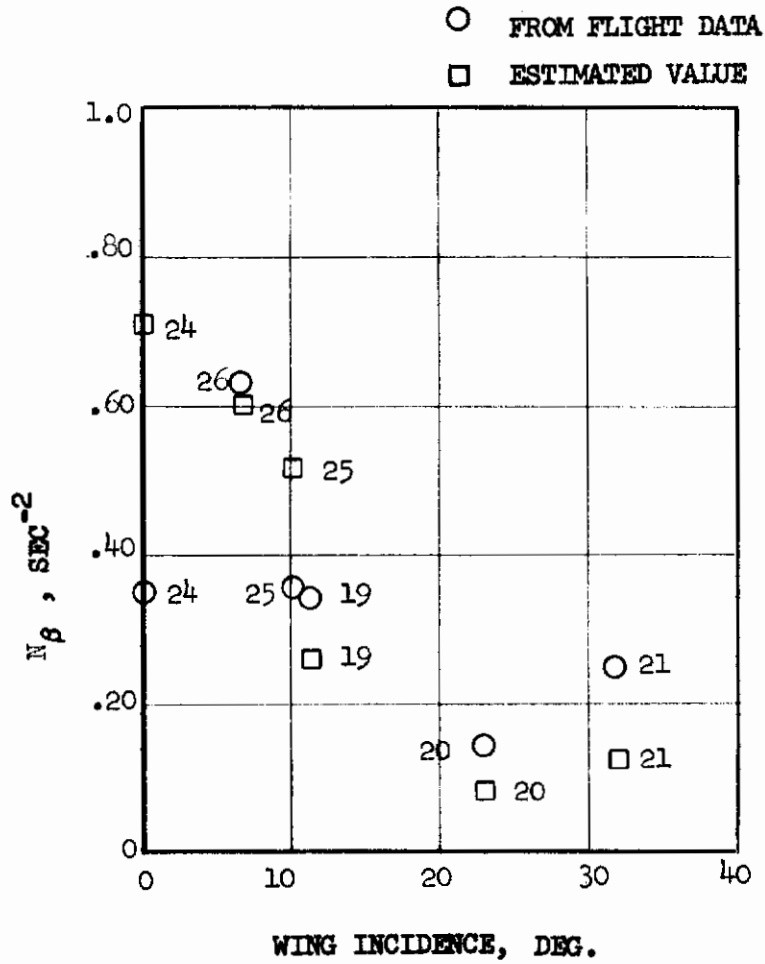
(b) N_β VS. WING INCIDENCE

FIGURE 49 (CONCLUDED)

141
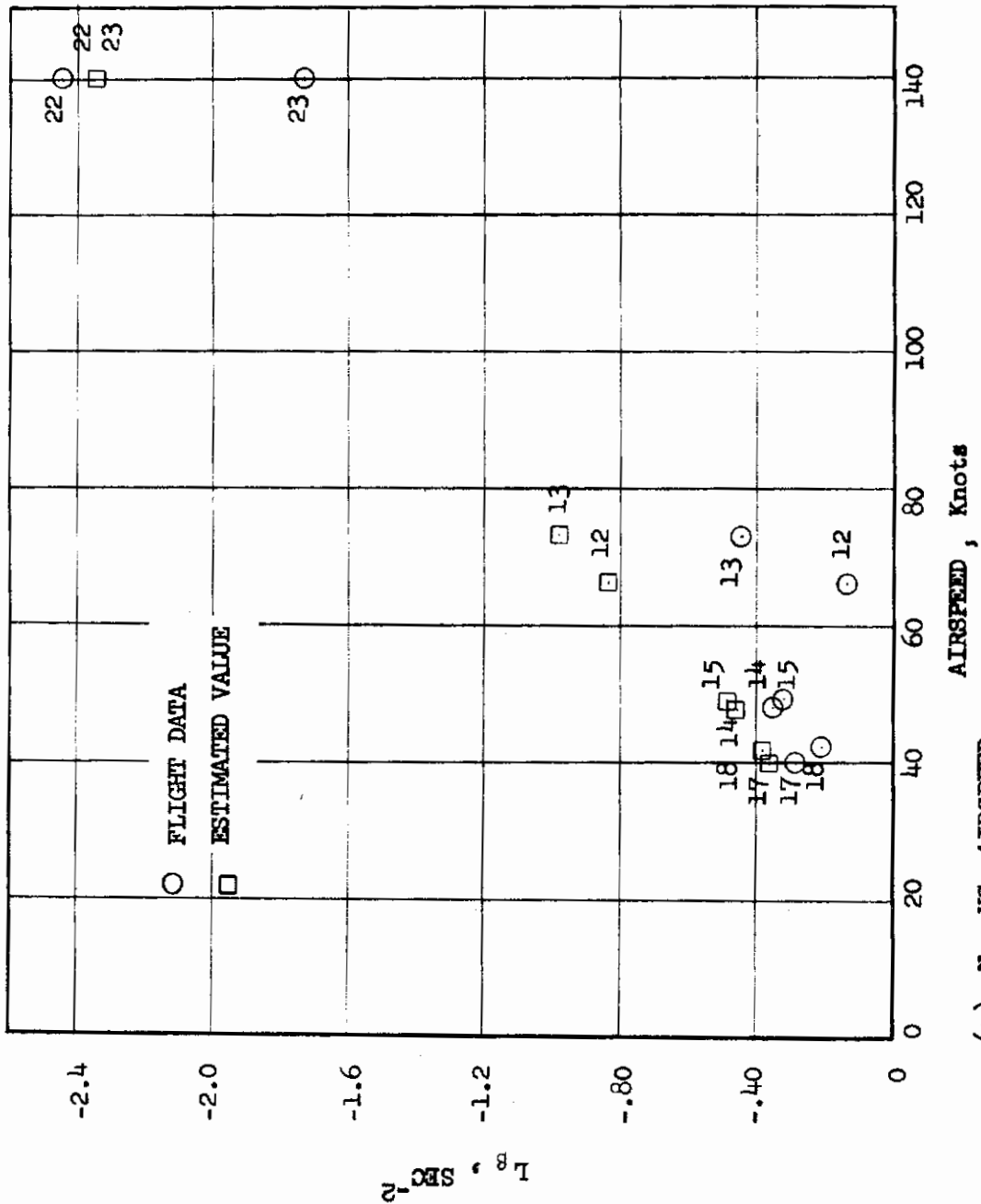
(a) N_β VS. AIRSPEED

FIGURE 50   DIHEDRAL EFFECT PARAMETER, L_β
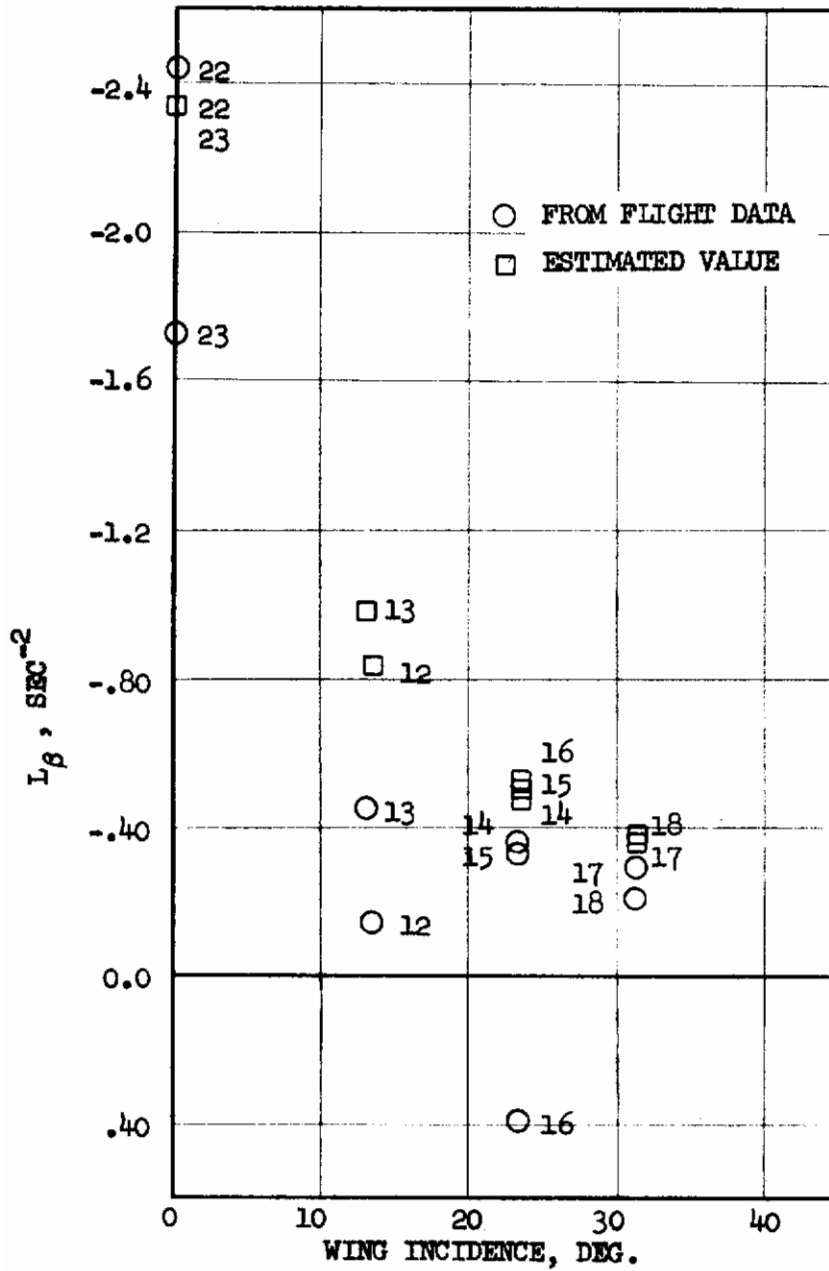
(b) L_β VS. WING INCIDENCE

FIGURE 50 (CONCLUDED)
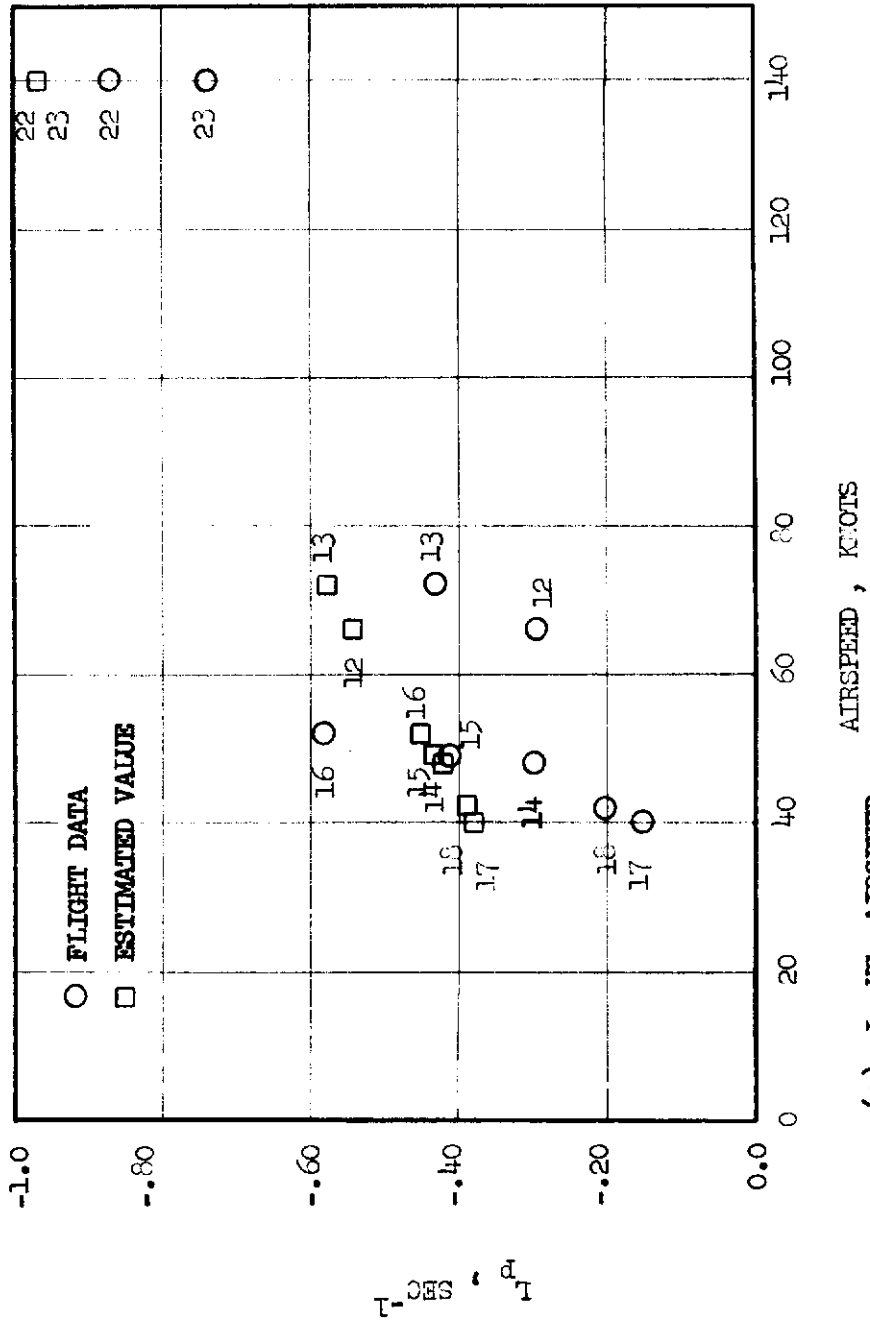
FIGURE 51 ROLL DAMPING PARAMETER, L_p
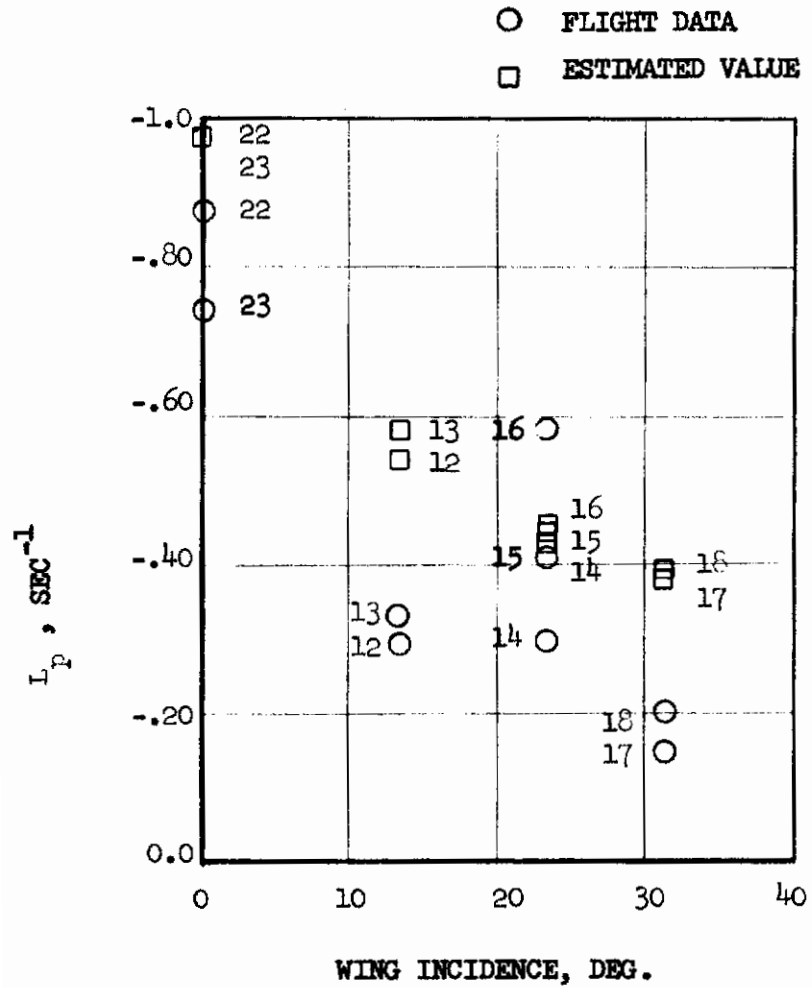
(a) L_p VS. AIRSPEED

(b) L_p VS. WING INCIDENCE

FIGURE 51 (CONCLUDED)
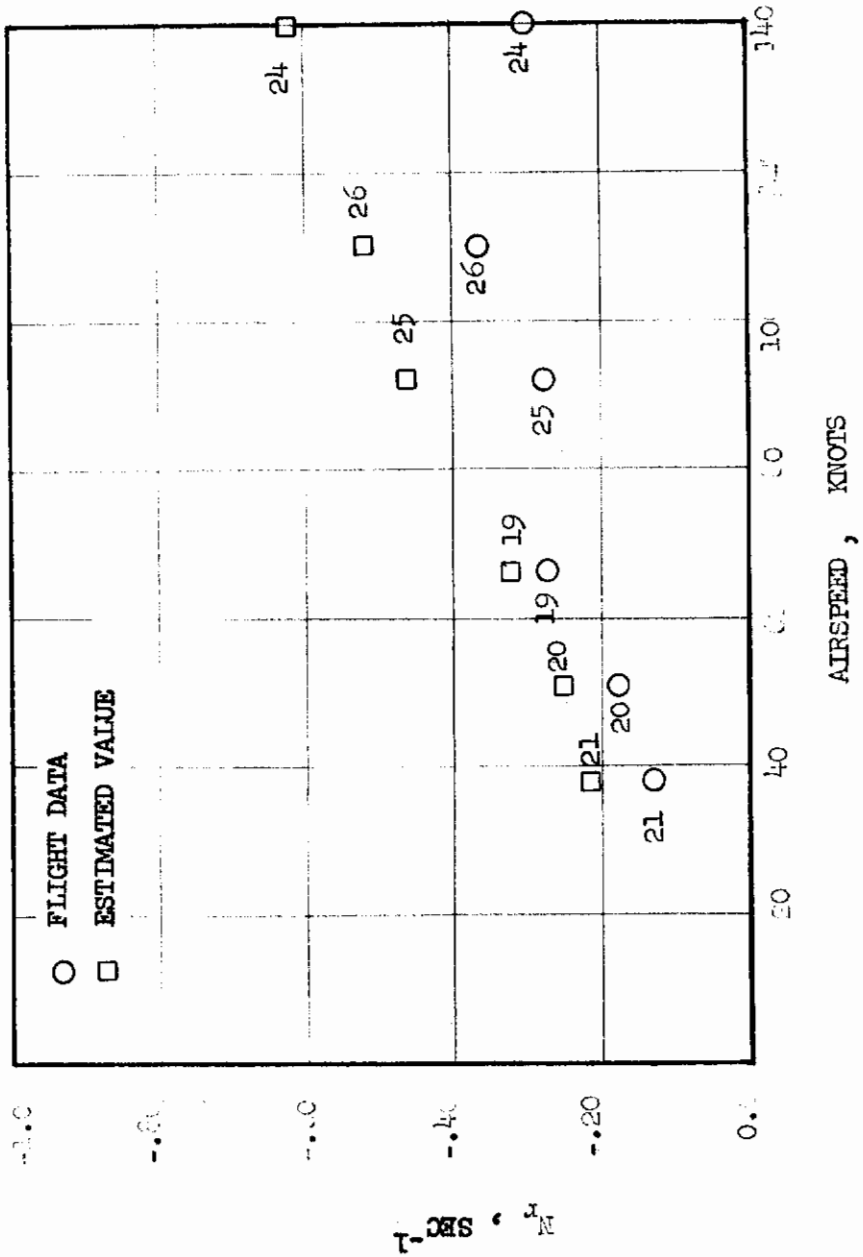
FIGURE 52 YAW DAMPING PARAMETER, N_r

(a) N_r VS. AIRSPEED

146
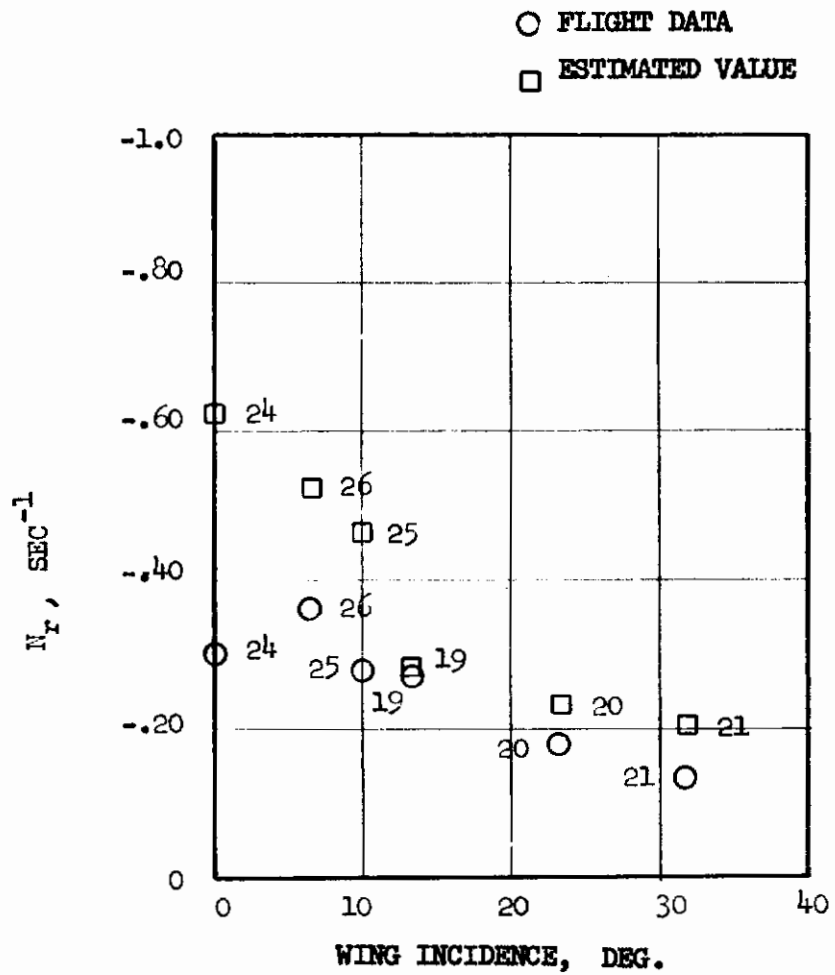
(b) N_r VS. WING INCIDENCE

FIGURE 52 (CONCLUDED)

□ $-i_W = 16°$, $\delta_F = 60°$; O $-i_W = 12°$, $\delta_F = 56°$; △ $-i_W = 0°$, $\delta_F = 0°$

BUFFET AT 56 K_{EAS}

44 K_{EAS}

54 K_{EAS}

BUFFET ONSET at 56 K_{EAS}

60 K_{EAS}

70 K_{EAS}

BUFFET ONSET at 150 K

FAIRLY SEVERE BUFFET at 133 K_{EAS}

160 K Trim

LIFT COEFFICIENT, C_L

ANGLE OF ATTACK, α, DEG.
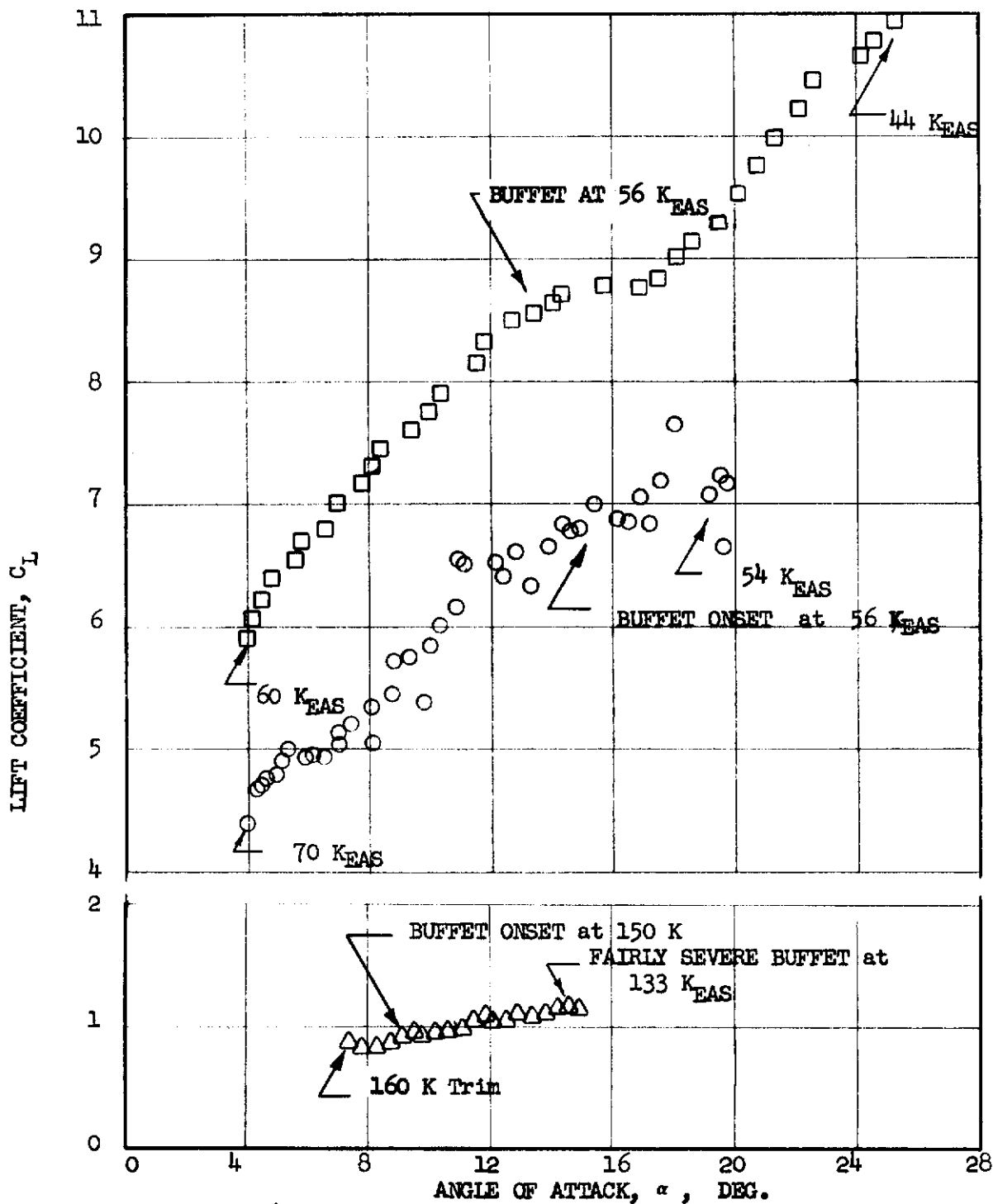
(a) C_L vs α

FIGURE 53 VARIATION OF AIRPLANE LIFT COEFFICIENT WITH ANGLE-
-OF-ATTACK

148

$i_W = 16°$, $\delta_F = 60°$

$i_W = 12°$, $\delta_F = 56°$

$i_W = 0°$, $\delta_F = 0°$
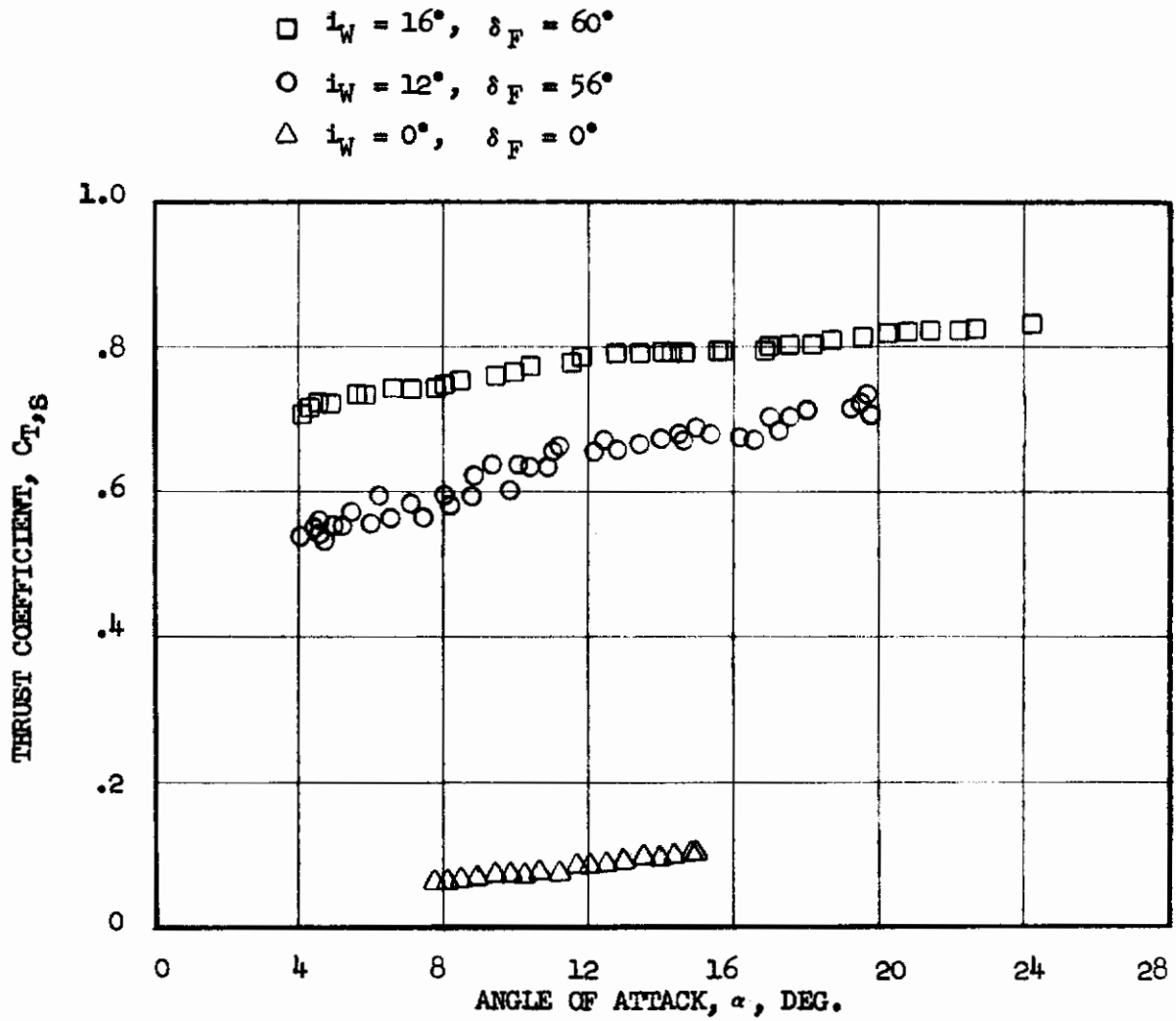
(b) $C_{T,S}$ vs α

FIGURE 53 (CONCLUDED)

149
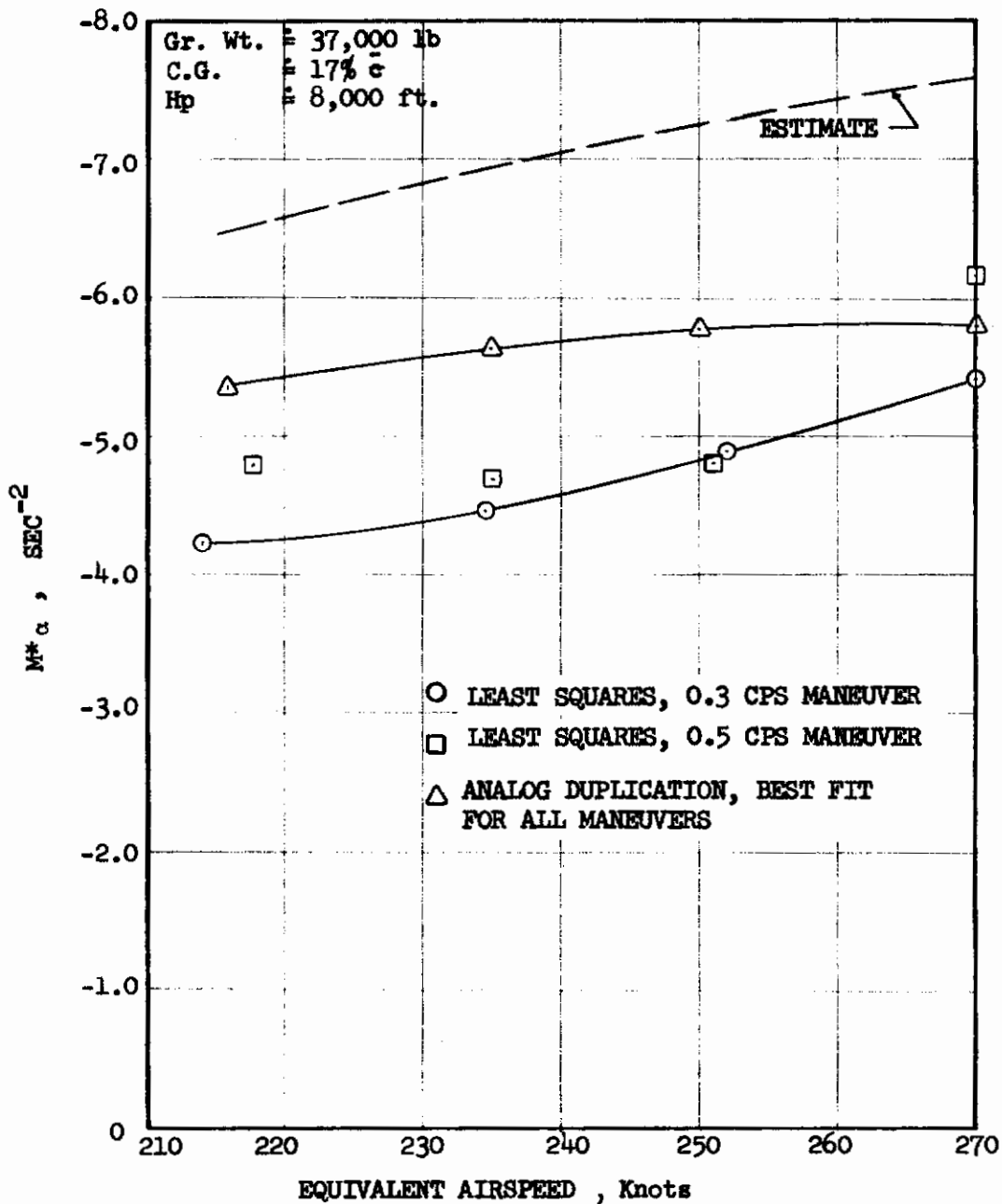
(CRUISE CONFIGURATION)

FIGURE 54 LONGITUDINAL STABILITY PARAMETER M^*_α (17% C.G.)
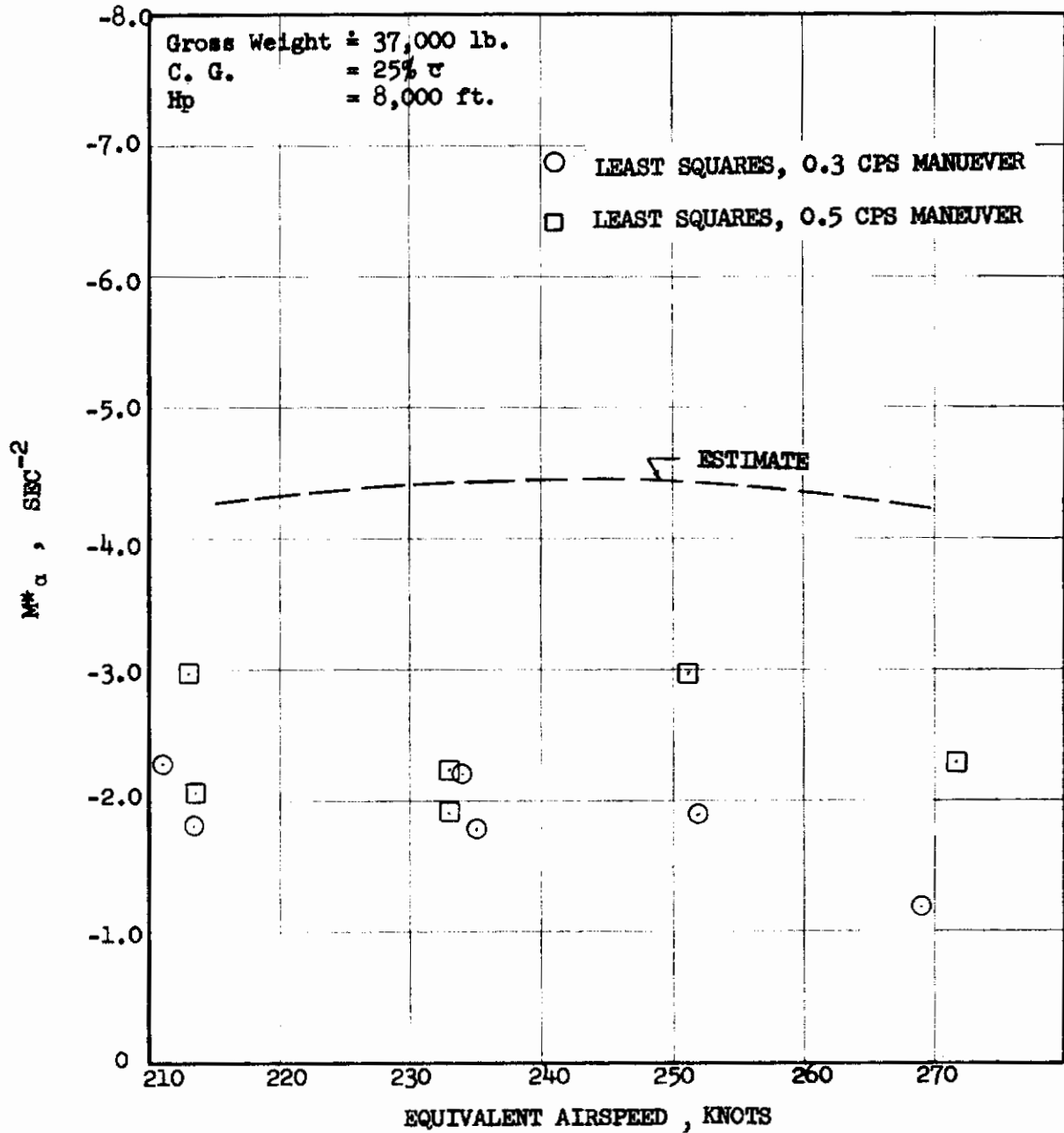
150

(CRUISE CONFIGURATION)

FIGURE 55   LONGITUDINAL STABILITY PARAMETER, M^*_α (25% C.G.)

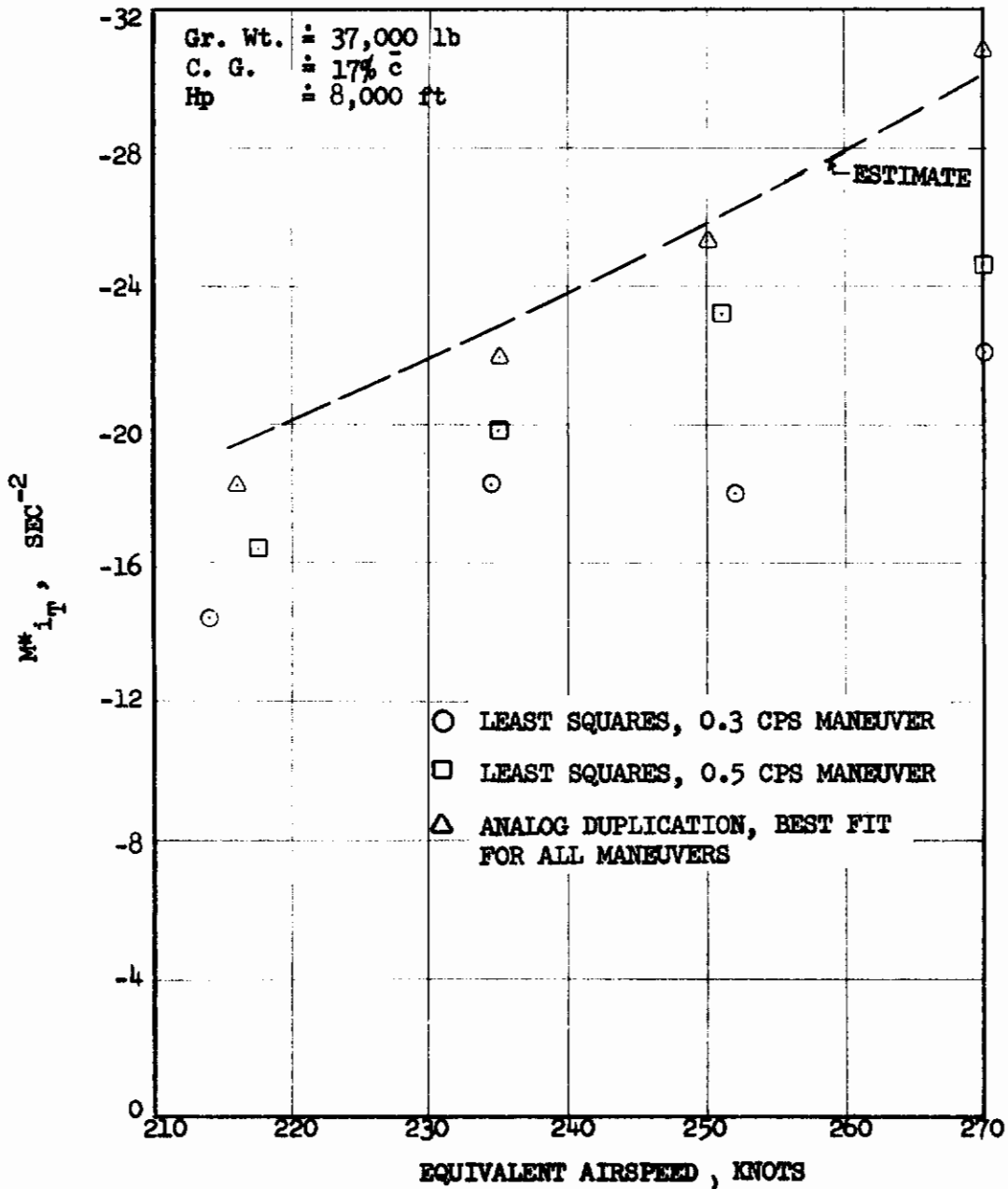(CRUISE CONFIGURATION)

FIGURE 56 LONGITUDINAL CONTROL EFFECTIVENESS, $M^*_{i_T}$ (17% C.G.)
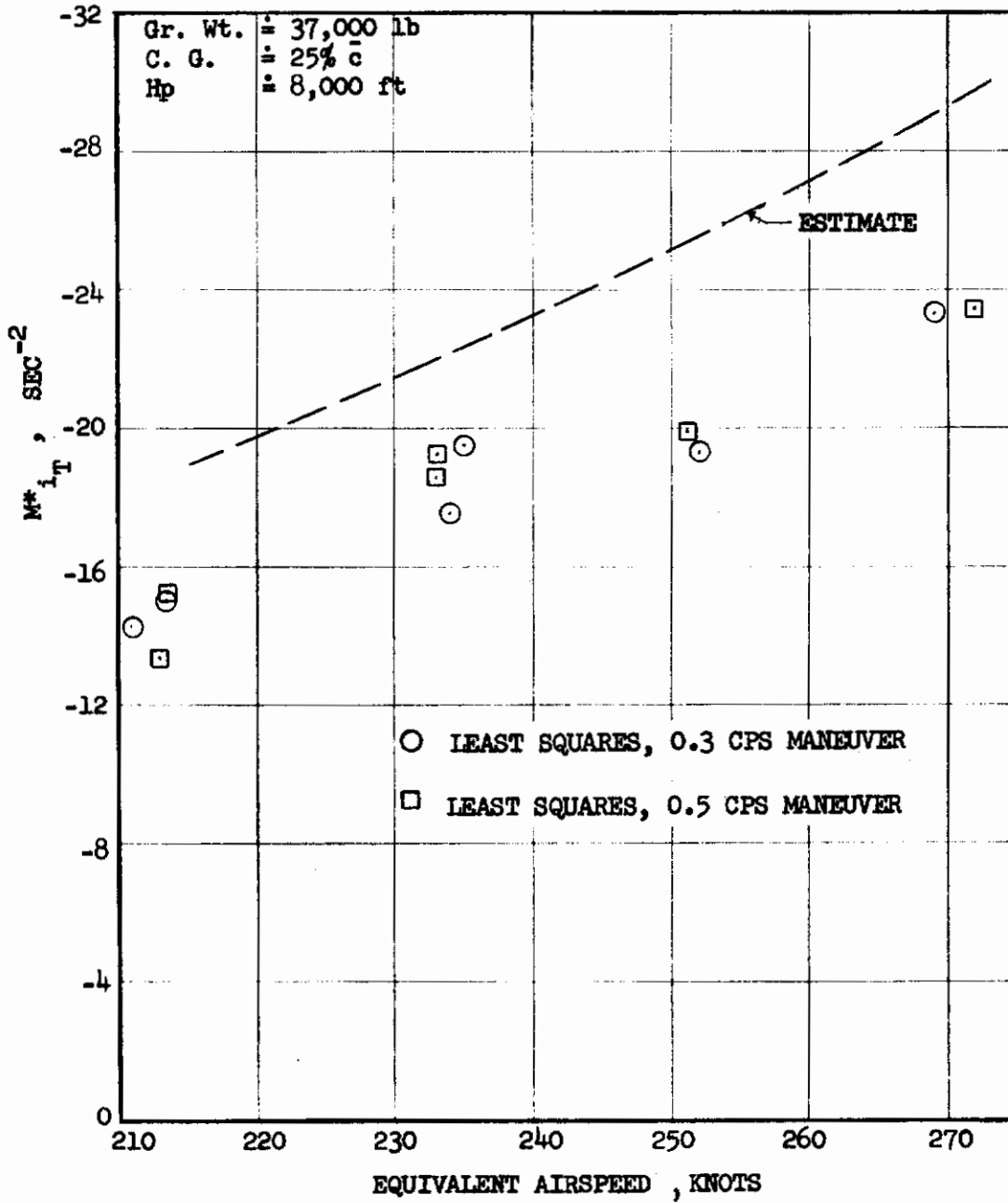
(CRUISE CONFIGURATION)

FIGURE 57   LONGITUDINAL CONTROL EFFECTIVENESS, $M^*_{i_T}$ (25% C.G.)
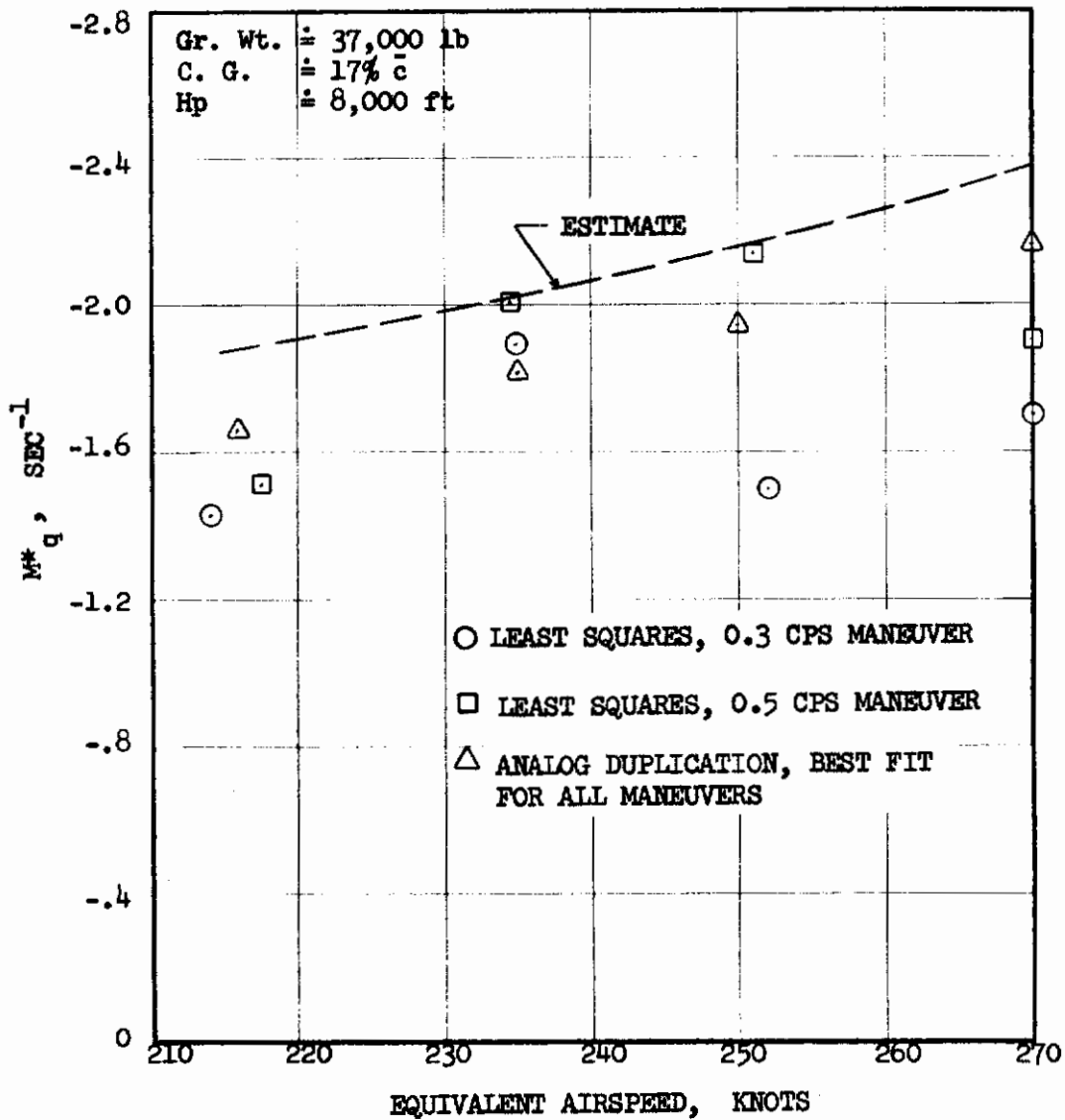
(CRUISE CONFIGURATION)

FIGURE 58   LONGITUDINAL DAMPING PARAMETER, M^*_q (17% C.G.)
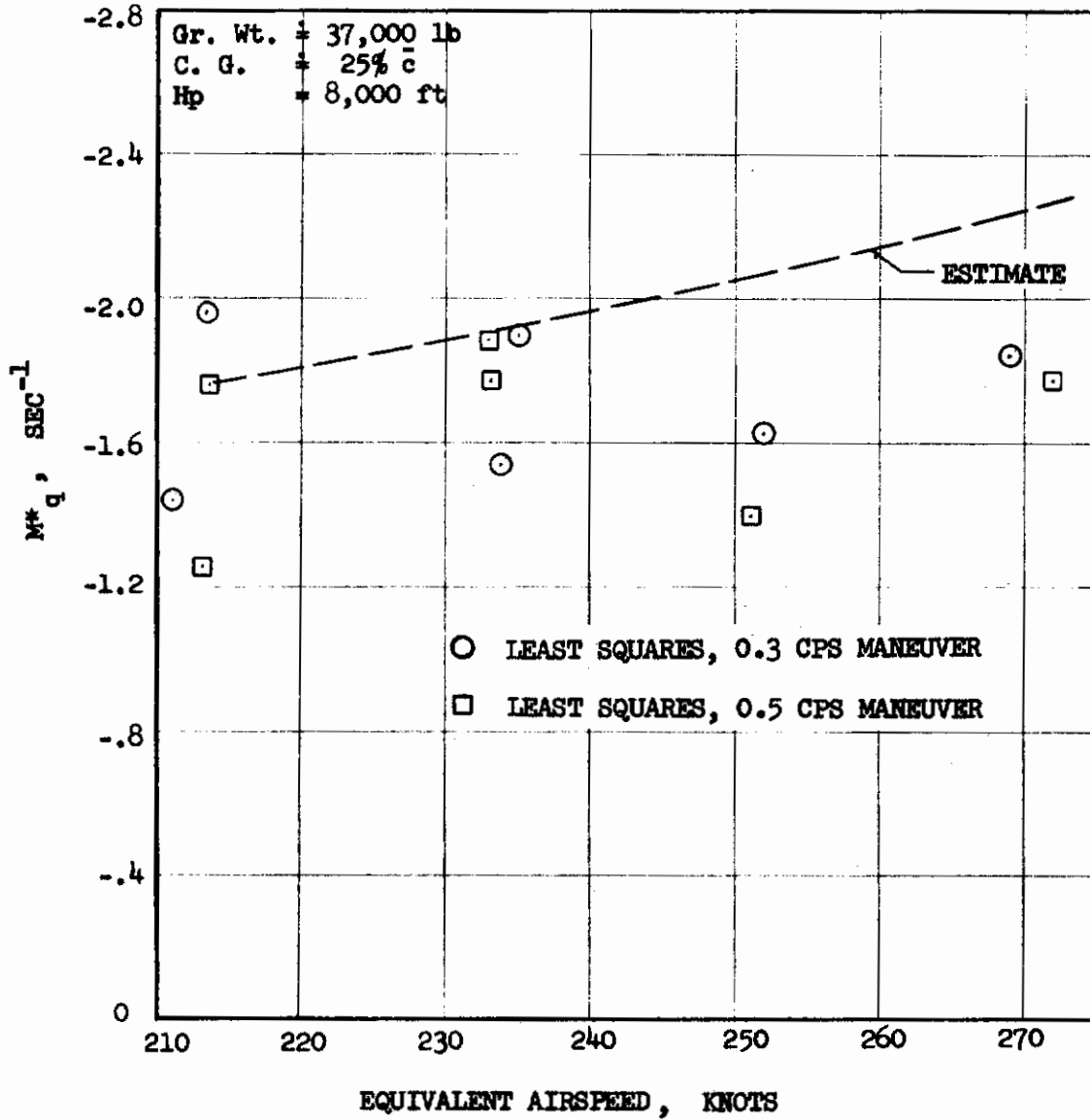
154

(CRUISE CONFIGURATION)

FIGURE 59 LONGITUDINAL DAMPING PARAMETER, M^*_q (25% C.G.)

155

(CRUISE CONFIGURATION)

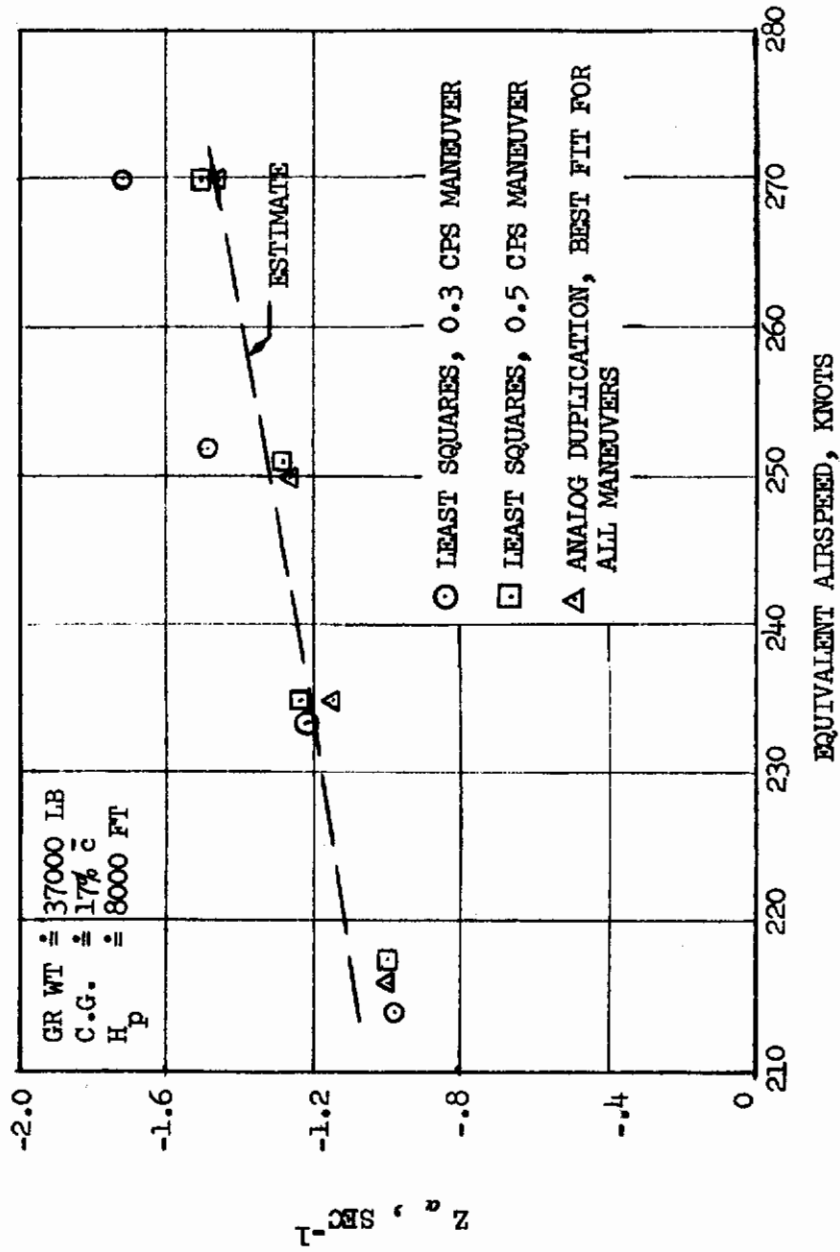FIGURE 60 LIFT CURVE SLOPE PARAMETER, Z_α (17% C.G.)

156

(CRUISE CONFIGURATION)
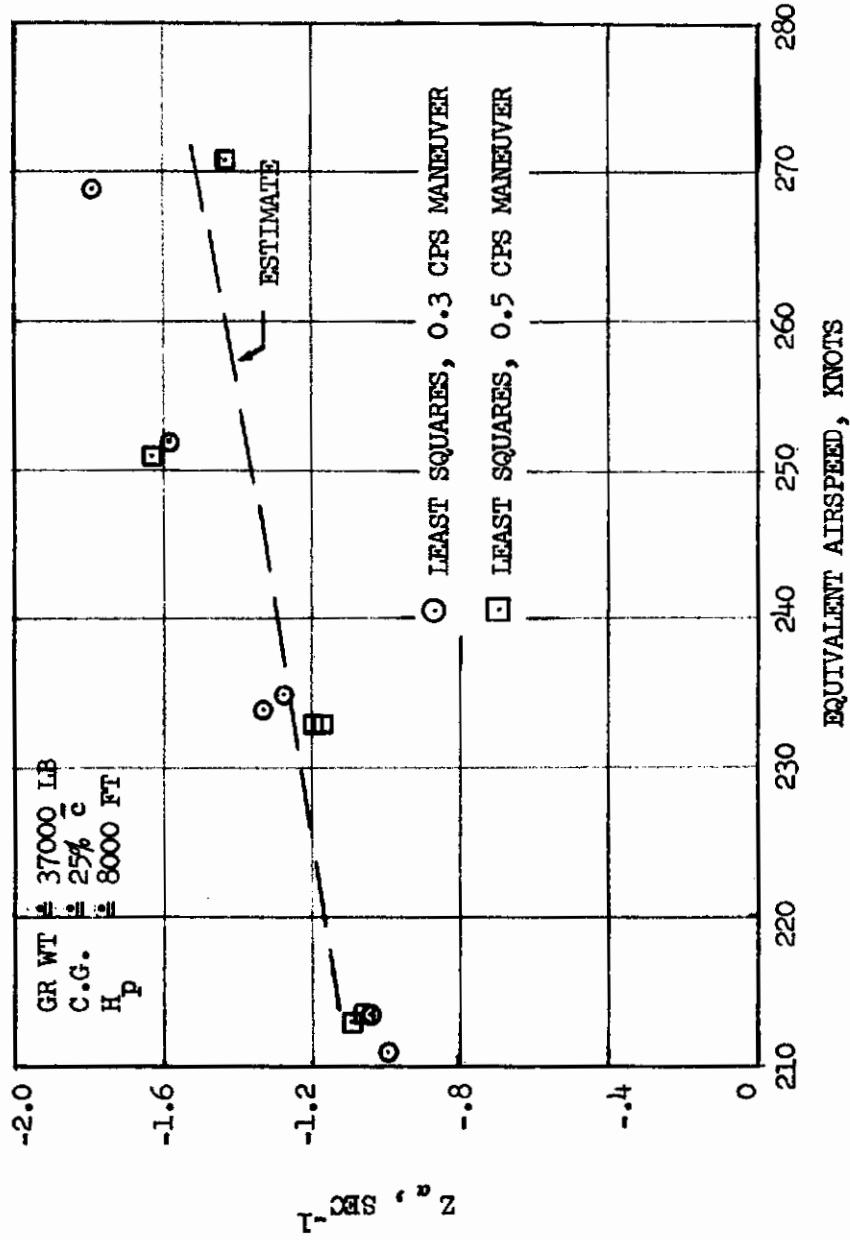
FIGURE 61   LIFT CURVE SLOPE PARAMETER, Z_α (25% C.G.)

157

O MEASURED IN FLIGHT

△ FLIGHT DATA ADJUSTED TO ST'D DAY, SEA LEVEL,
35,000 LB. GROSS WEIGHT, 95% RPM
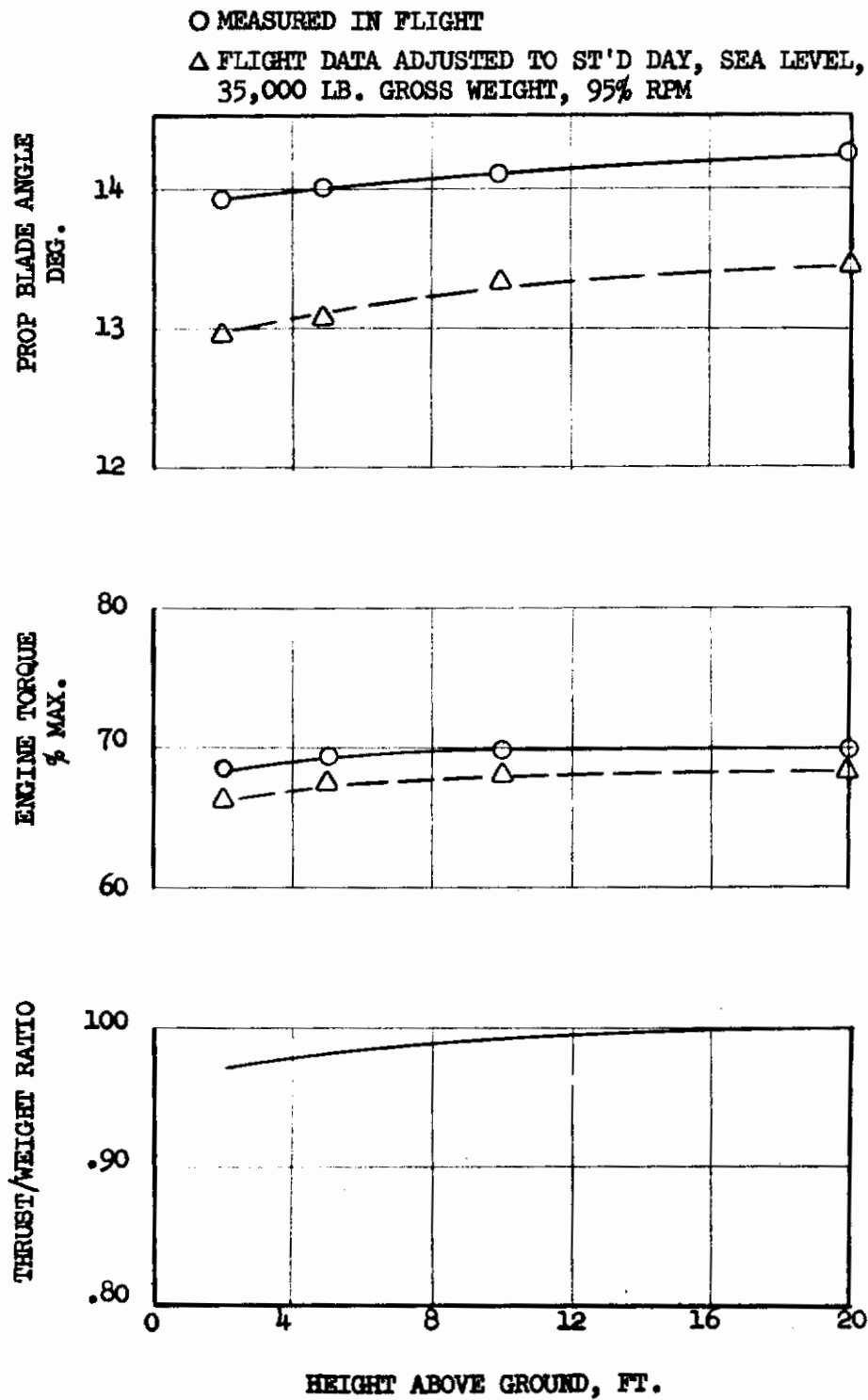
FIGURE 62   EFFECT OF GROUND PROXIMITY ON
THRUST REQUIRED IN HOVER

158
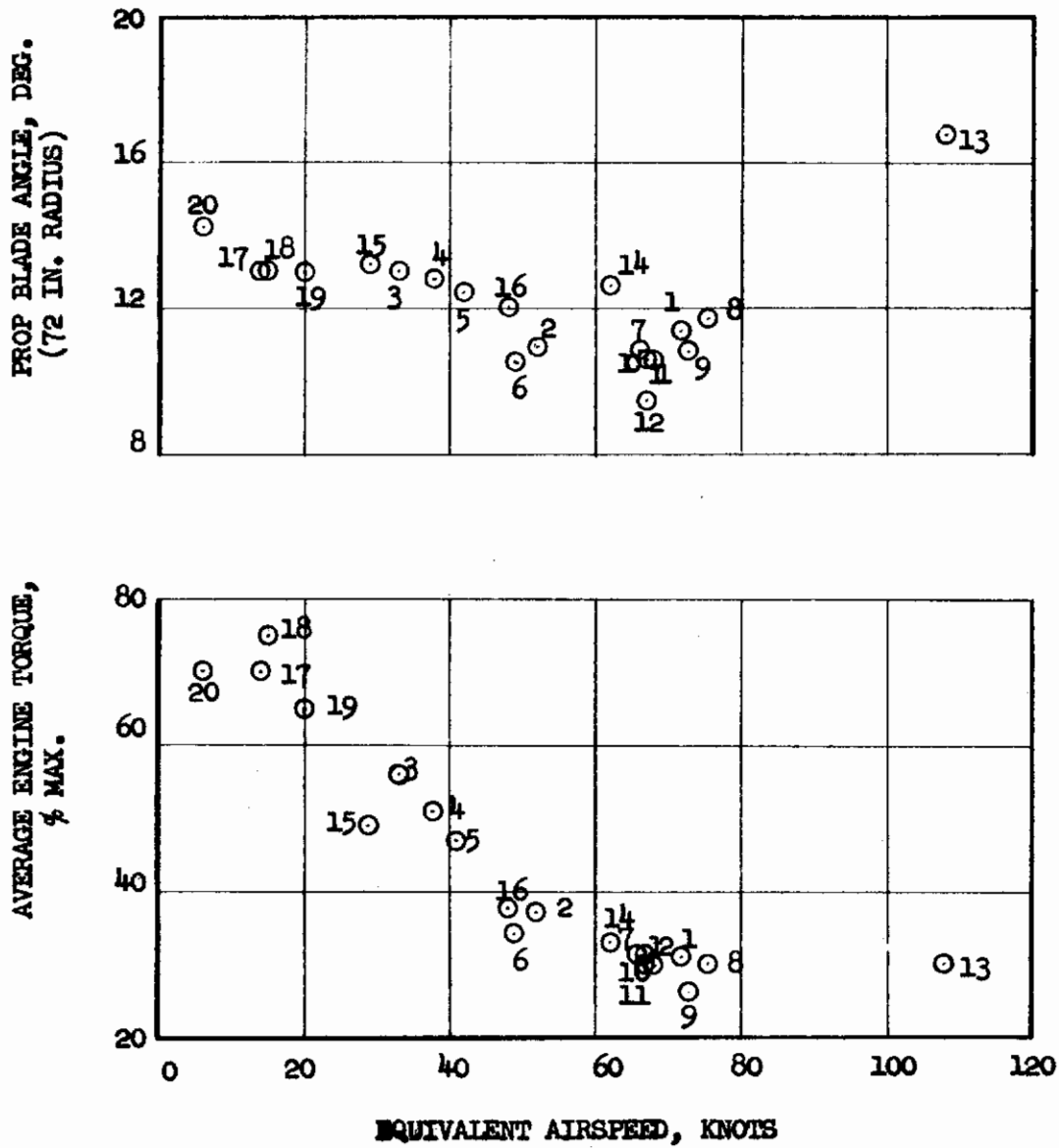
(a) BLADE ANGLE AND ENGINE TORQUE

FIGURE 63. PROPELLER BLADE ANGLE AND ENGINE TORQUE REQUIRED
FOR STEADY LEVEL FLIGHT IN TRANSITION CONFIGURATIONS

159
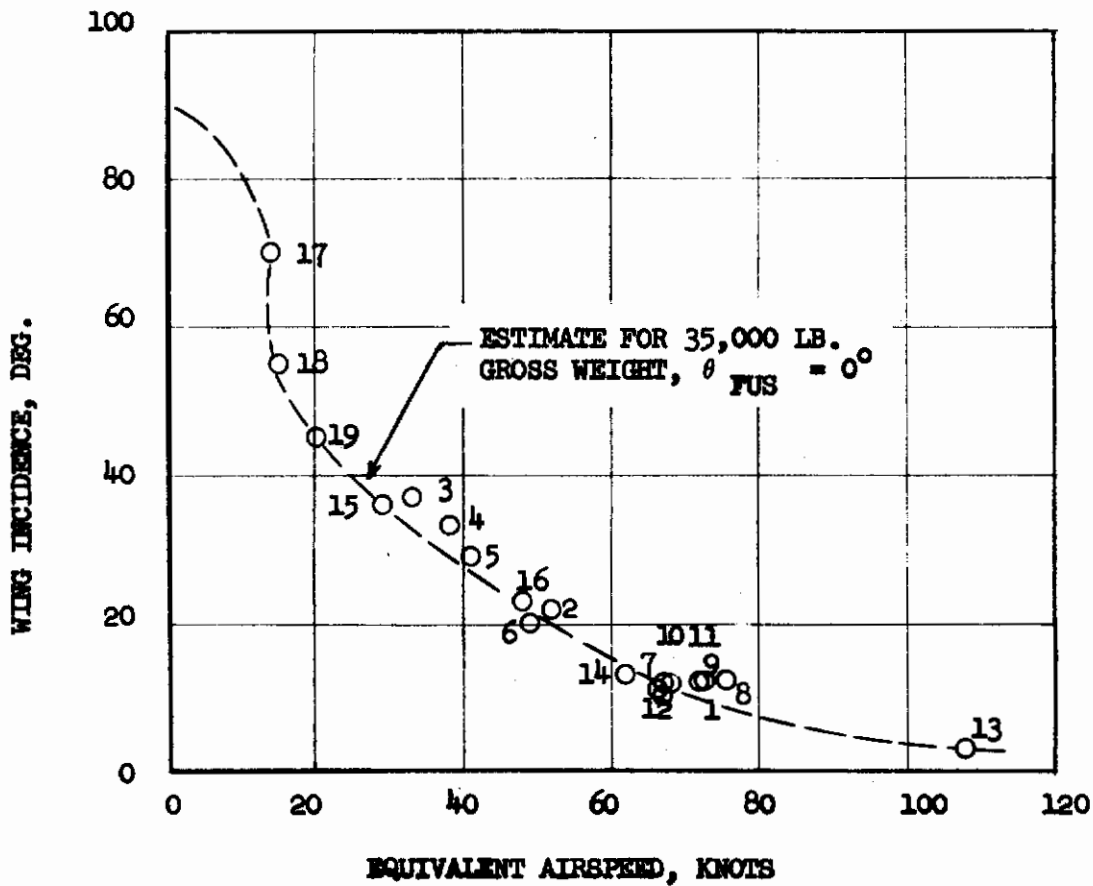
(b) WING INCIDENCE

FIGURE 63 (CONCLUDED)
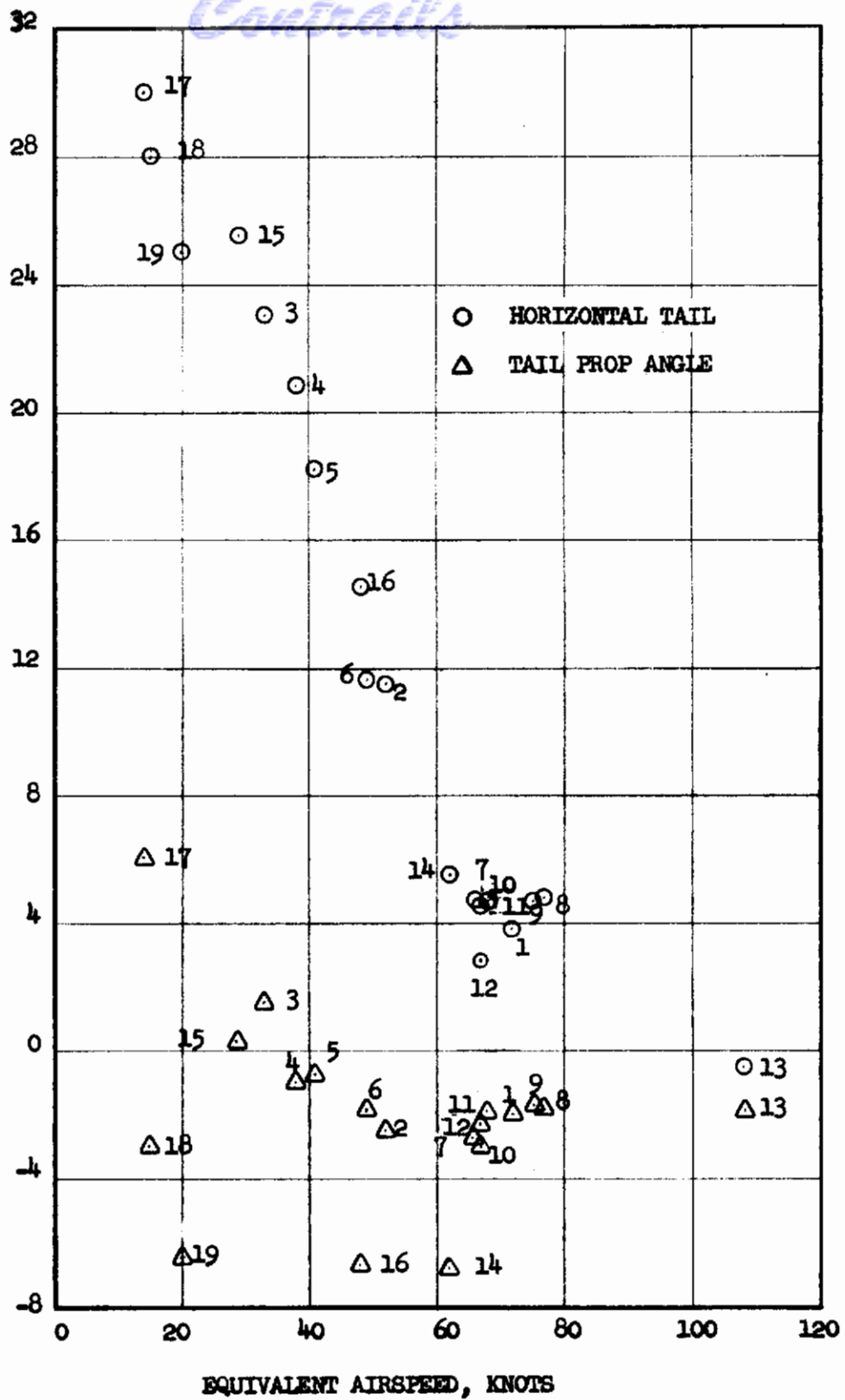
(a) i_T and β_{T_P}

FIGURE 64 PITCH TRIM CONTROL REQUIRED IN
TRANSITION CONFIGURATIONS

161
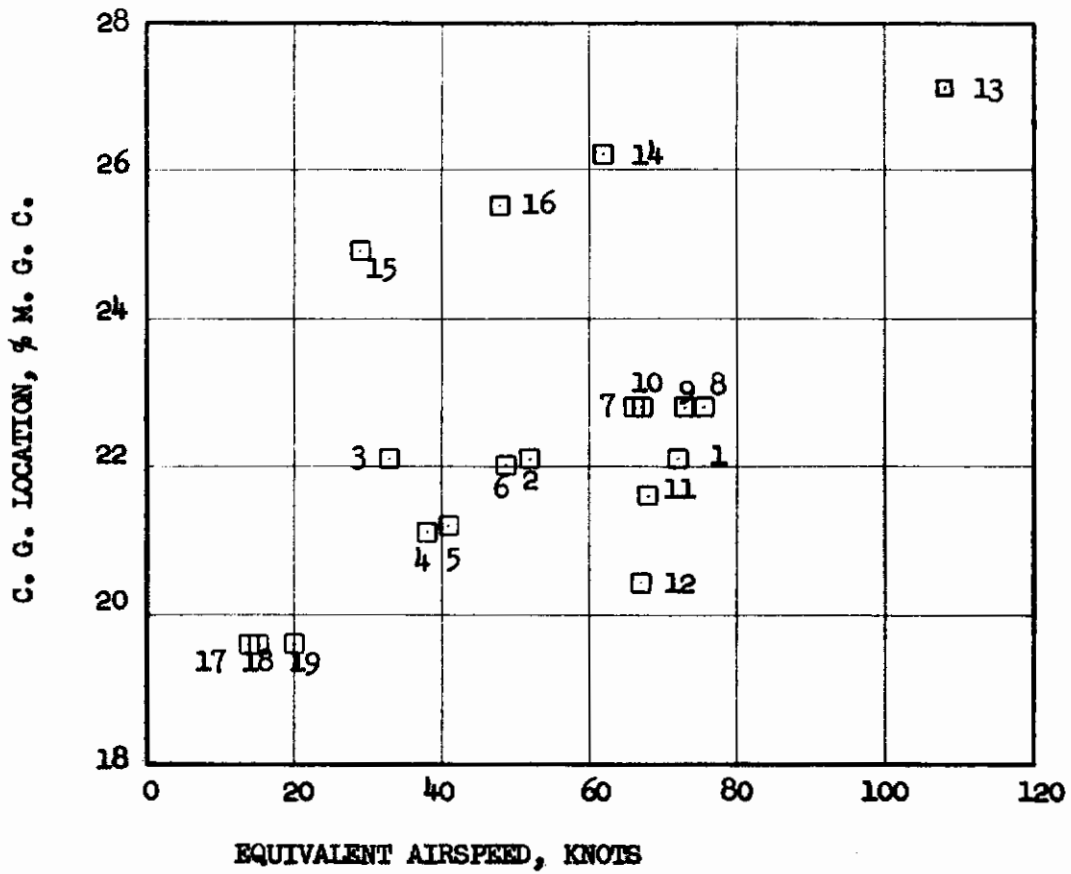
(b) C. G. Location

FIGURE 64 (CONCLUDED)

162
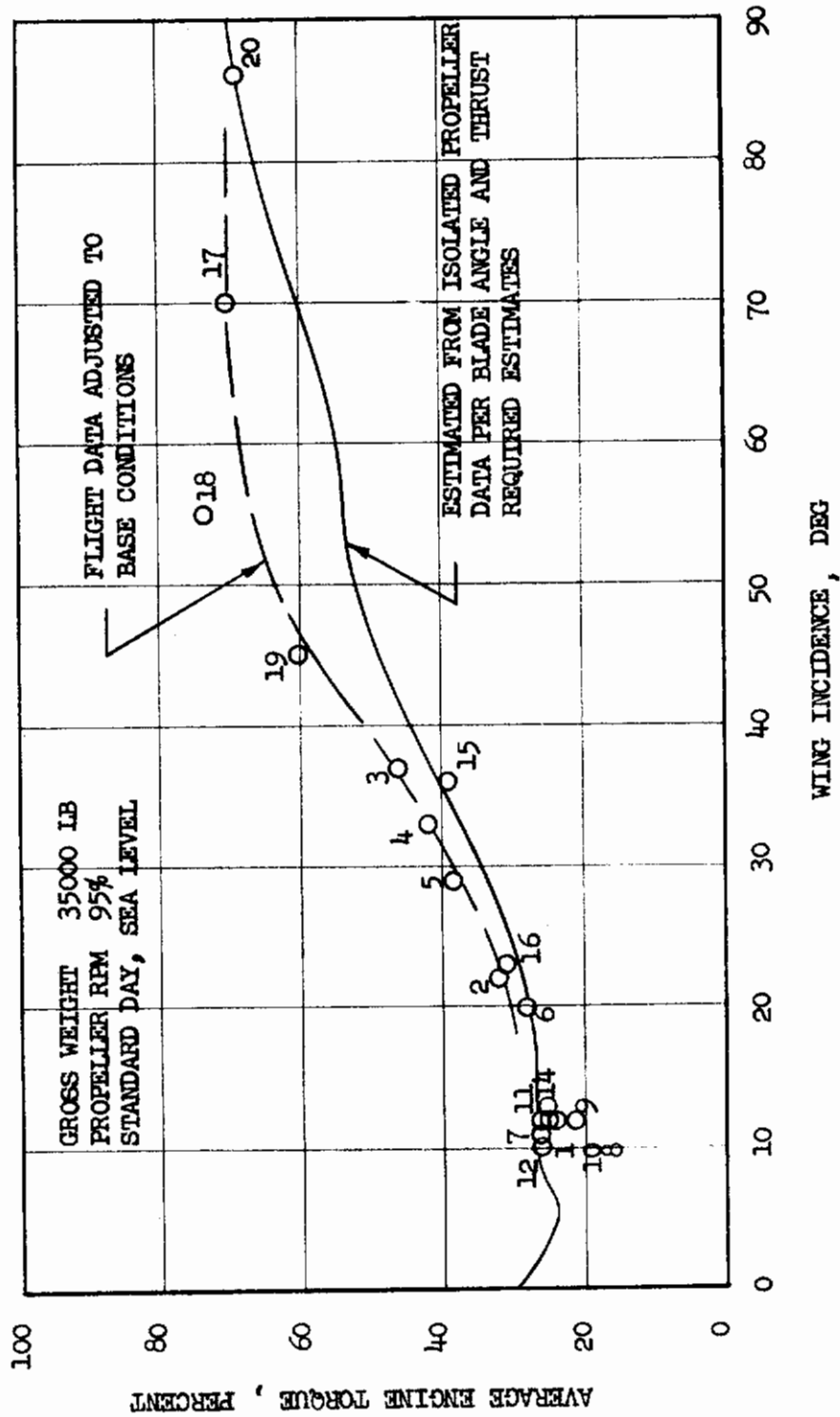
FIGURE 65 COMPARISON OF ESTIMATED AND MEASURED TORQUE REQUIRED IN TRANSITION

163
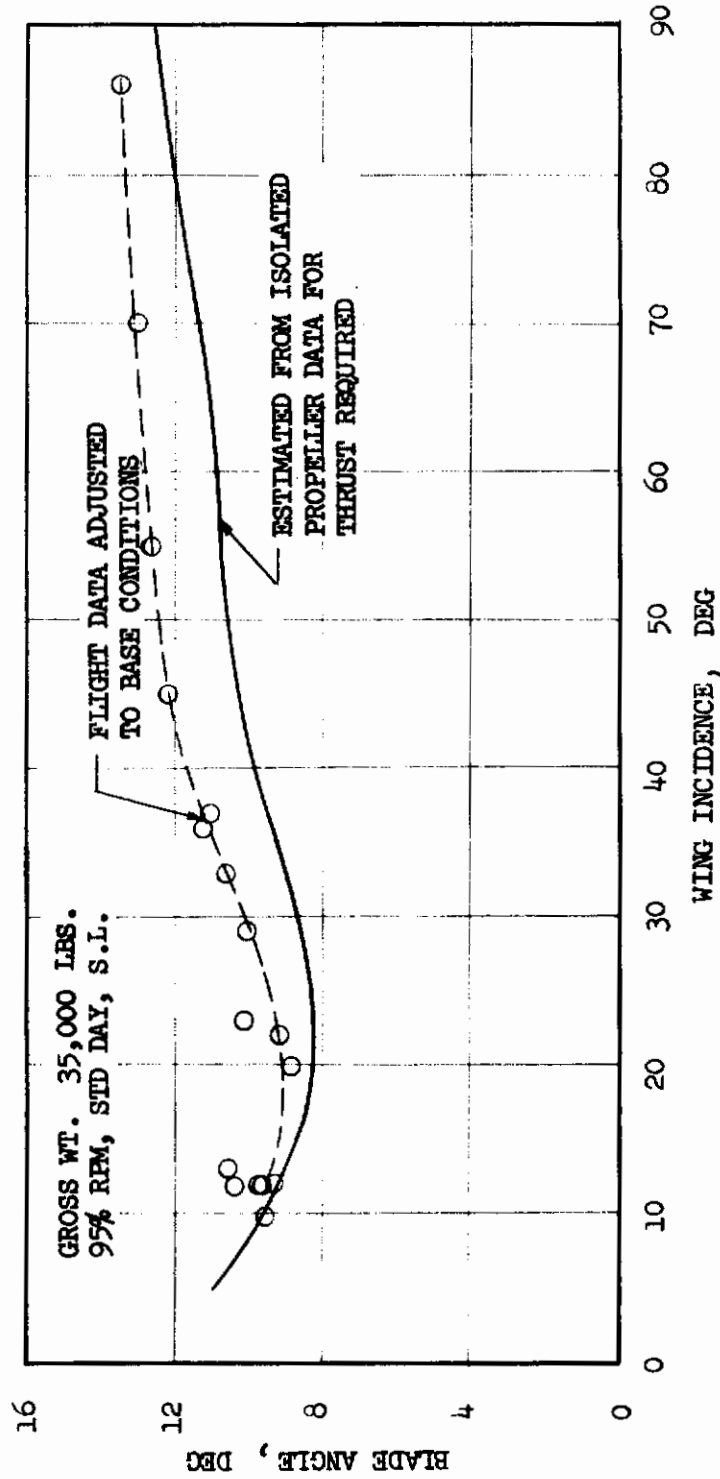
FIGURE 66   COMPARISON OF ESTIMATE AND MEASURED
BLADE ANGLE REQUIRED IN TRANSITION

(DETERMINED FROM AMES AND ASD TEST DATA)

THRUST COEFFICIENT, C_T

ADVANCE RATIO, J

β- At 72" Radius
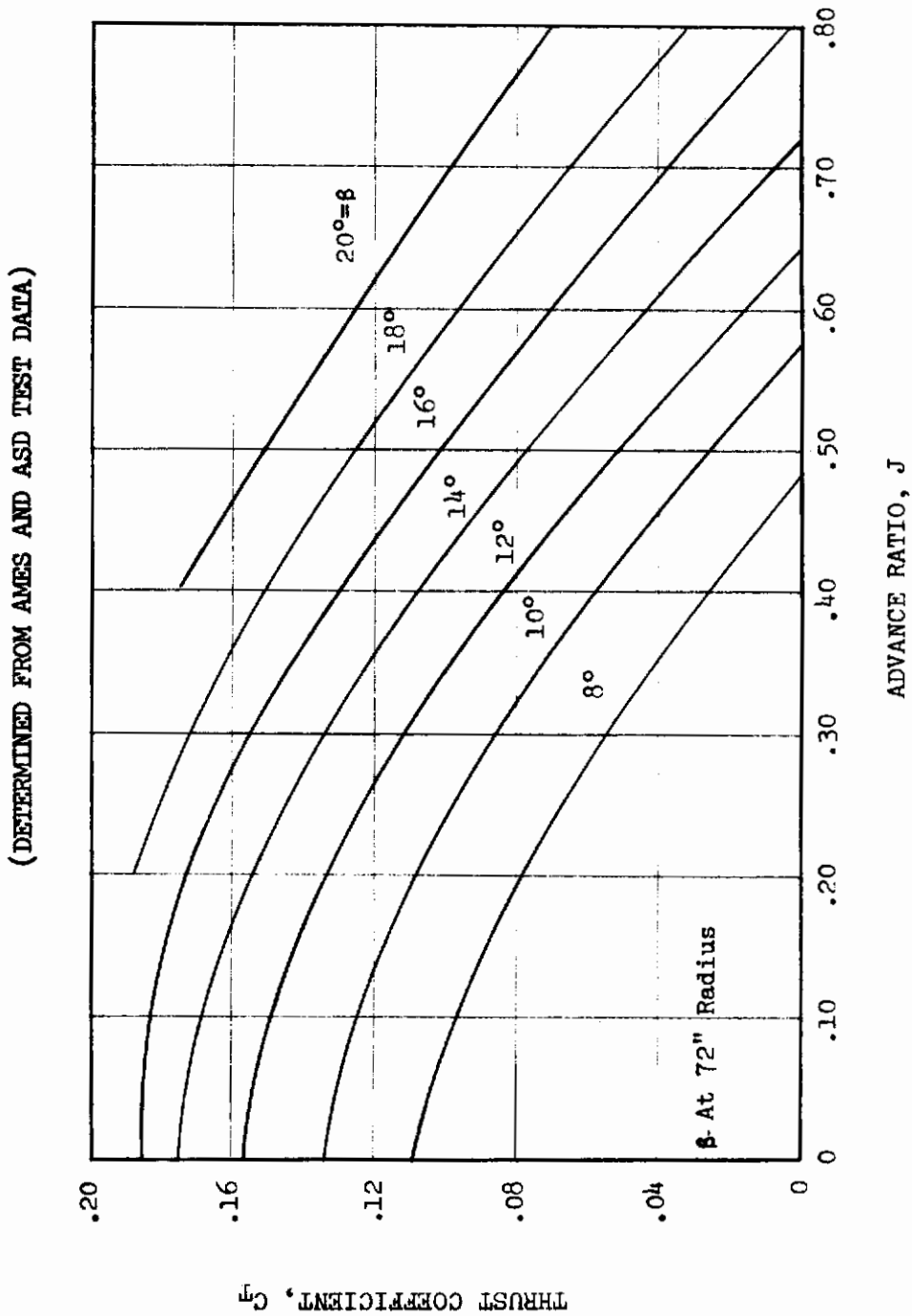
FIGURE 67   ISOLATED PROPELLER THRUST COEFFICIENT, C_T

165

(DETERMINED FROM AMES AND ASD TEST DATA)
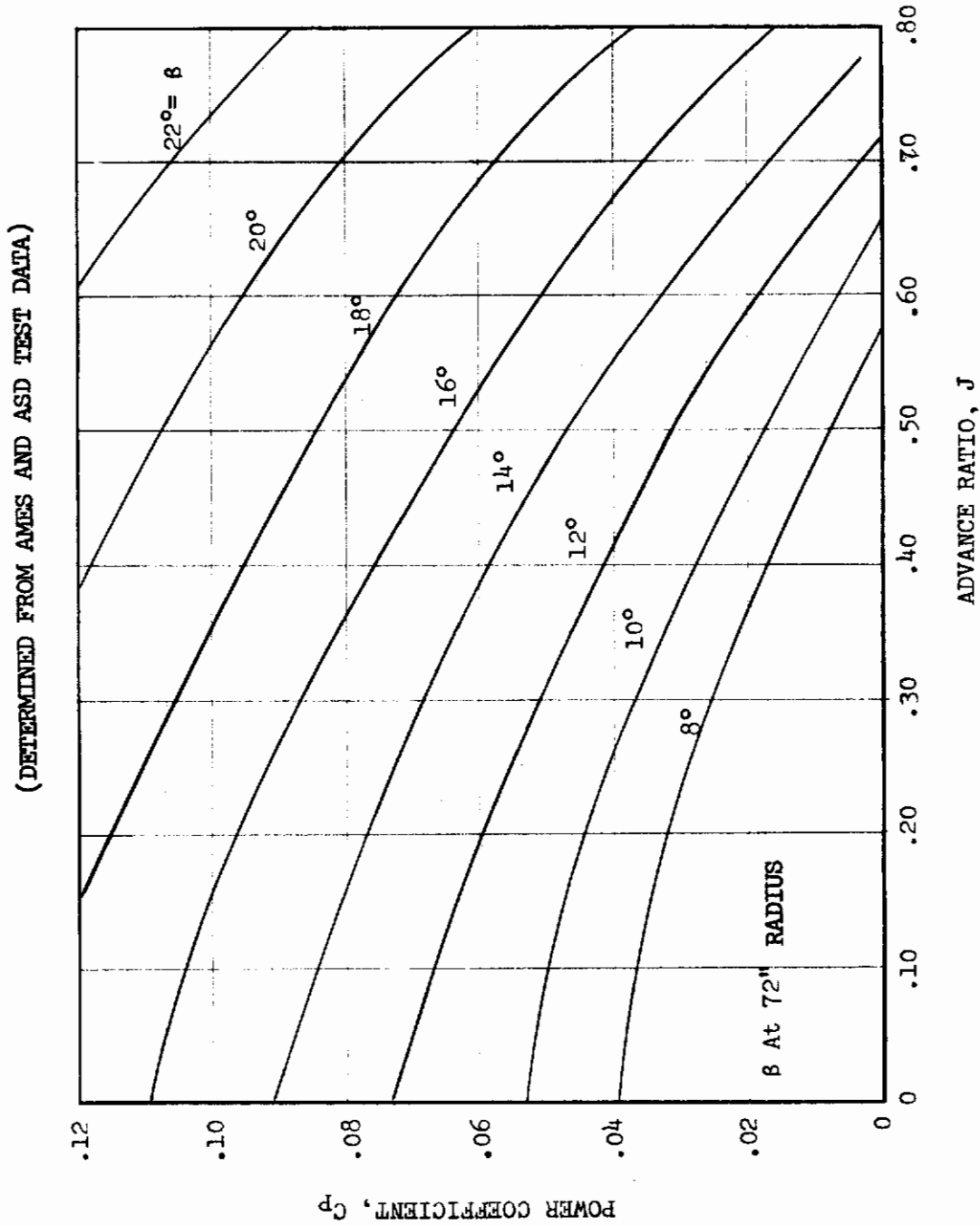
FIGURE 68   ISOLATED PROPELLER POWER COEFFICIENT, C_p

166

EQUIVALENT AIRSPEED, KNOTS

LIGHT BUFFET REGION

ESTIMATED BUFFET ONSET FROM
WIND TUNNEL MODEL WING SEPARATION

GROSS WEIGHT = 36000 LB

RATE OF SINK, FT/MIN

SYMBOL	i_w	δ_F	BUFFET
○	11.5	56.2	ONSET
◀	17.5	57.5	ONSET
□	17.8	58.3	ONSET
▷	22.8	57.6	ONSET
×	27.5	58.4	ONSET
▽	33.3	58.5	ONSET
△	35.6	58.4	ONSET
◇	17.0	61.2	LIMIT*
θ	21.4	61.2	LIMIT
0	30.5	60.9	LIMIT

* LIMIT USEFUL RATE OF DESCENT FOR
ACCEPTABLE HANDLING QUALITIES

EQUIVALENT AIRSPEED, KNOTS

FIGURE 69 BUFFET AND DESCENT BOUNDARIES

167

tion engaged about the axis being excited, but it may be desirable to allow no control inputs about other axes. This consideration must be given to the isolation of the control inputs about their respective axes when the aircraft has a blended control system, and particular flight techniques may be required in some cases. Controls fixed maneuvers, or responses; i.e., stabilization augmentation inactive as well as stick fixed, should be obtained in all flight conditions where safety permits in order to eliminate control effectiveness in the response and thus better isolate the remaining aerodynamic effects.

APPENDIX I

EQUATIONS OF MOTION FOR THE XC-142A

The following equations were assumed to represent perturbation motions of the XC-142A about any trim condition at any fixed wing and flap configuration. The equations were written for a body reference axis system with the origin at the center of gravity of the airplane.

LONGITUDINAL

(PITCH MOMENT): $\dot{q} = M_u u + M_{\dot{W}}\dot{W} + M_W W + M_q q + M_{\Delta_\beta}\Delta_\beta$

$$+ M_{\Delta_N}\Delta N + M_{i_t}\Delta_{i_t}$$

(VERTICAL FORCE): $(\dot{W} - U_o q) = Z_u u + Z_W W + Z_q q + Z_{\Delta_\beta}\Delta_\beta$

$$+ Z_{\Delta N}\Delta N + Z_{i_t}\Delta_{i_t}$$

(AXIAL FORCE): $(\dot{u} + g\theta + W_o q) = X_u u + X_W W + X_{W^2}W^2 + X_{\Delta_\beta}\Delta_\beta$

$$+ X_{\Delta N}\Delta N + X_{i_t}\Delta_{i_t}$$

LATERAL-DIRECTIONAL

(ROLL MOMENT): $(\dot{p} + J_X\dot{r}) = L_P P + L_v v + L_r r + L_{\delta_A}\delta_A + L_{\delta_\beta}\delta_\beta$

$$+ L_{\delta_R}\delta_R$$

(YAW MOMENT): $(\dot{r} + J_Z\dot{p} = N_P P + N_v v + N_r r + N_{\delta_A}\delta_A + N_{\delta_\beta}\delta_\beta$

$$+ N_{\delta_R}\delta_R$$

(SIDE FORCE): $(\dot{v} - W_o P + U_o r - g\Phi) = Y_P P + Y_v v + Y_r r + Y_{\delta_A}\delta_A$

$$+ Y_{\delta_\beta}\delta_\beta + Y_{\delta_R}\delta_R$$

Prior to developing the least squares normal equations, the preceding equations were modified to remove the linear dependence of the Z-force and pitch moment equations, and the roll and yaw moment equations. This can be done by making the following substitutions:

(1) Substitute the Z-force equation into the pitch moment equation.
(2) Substitute the roll moment equation into the yaw moment equation.
(3) Substitute the yaw moment equation into the roll moment equation.

It was also necessary to rewrite the force equations in order to use the flight accelerometer sensor measurements, substituting:

$$gn_X = (\dot{u} + W_o q + g\theta)$$

$$gn_Y = (\dot{v} - W_o P + u_o r - g\phi)$$

$$g\Delta n_Z = (\dot{w} - U_o q)$$

A final, but most significant, consideration was to include a constant in each of the force and moment expansions. This was necessary since in the inverse problem the exact trim values of the control surfaces may not be known, or the gyro and accelerometer signals may include small bias values. The body axis accelerometers should reflect the effect of the trim attitude, but this effect may be obscured or overlooked in some cases. The inclusion of a constant in each equation will prevent bias from any of these sources that can affect the least squares inverse solution significantly. The final equations used for the development of the normal equations are summarized as follows:

LONGITUDINAL

$$\dot{q} - M_u^* u - M_w^* w - M_q^* q - M_{\Delta\beta}^* \Delta\beta - M_{\Delta N}^* \Delta N - M_{i_t}^* \Delta i_t - M_o = 0$$

$$g\Delta n_Z - Z_u u - Z_w w - Z_q q - Z_{\Delta\beta}\Delta\beta - Z_{\Delta N}\Delta N - Z_{i_t}\Delta i_t - Z_o = 0$$

$$g\Delta n_X - X_u u - X_w w - X_{w^2} w^2 - X_{\Delta\beta}\Delta\beta - X_{\Delta N}\Delta N - X_{i_t}\Delta i_t - X_o = 0$$

LATERAL-DIRECTIONAL

$$\dot{P} - L_P^* P - L_v^* v - L_r^* r - L_{\delta_A}^* \delta_A - L_{\delta\beta}^* \delta_\beta - L_{\delta_R}^* \delta_R - L_o = 0$$

$$\dot{r} - N_P^* P - N_v^* v - N_r^* r - N_{\delta_A}^* \delta_A - N_{\delta\beta}^* \delta_\beta - N_{\delta_R}^* \delta_R - N_o = 0$$

$$g\Delta n_y - Y_P P - Y_v v - Y_r r - Y_{\delta_A}\delta_A - Y_{\delta\beta}\delta_\beta - Y_{\delta_R}\delta_R - Y_o = 0$$

where the asterisk coefficients represent linear combinations of the original derivatives.

$$M_u^* = M_u + M_{\dot{w}} Z_u$$

$$M_w^* = M_w + M_{\dot{w}} Z_w$$

$$M_q^* = M_q + M_{\dot{w}} (Z_q + U_o)$$

$$M_{\Delta\beta}^* = M_{\Delta\beta} + M_{\dot{w}} Z_{\Delta\beta}$$

$$M_{\Delta N}^* = M_{\Delta N} + M_{\dot{w}} Z_{\Delta N}$$

$$M_{i_t}^* = M_{i_t} + M_{\dot{w}} Z_{i_t}$$

$$L_P^* = (L_P - J_x N_P)/(1 - J_x J_z)$$

$$L_v^* = (L_v - J_x N_v)/(1 - J_x J_z)$$

$$L_r^* = (L_r - J_x N_r)/(1 - J_x J_z)$$

$$L_{\delta_A}^* = (L_{\delta_A} - J_x N_{\delta_A})/(1 - J_x J_z$$

$$L_{\delta_\beta}^* = (L_{\delta_\beta} - J_x N_{\delta_\beta})/(1 - J_x J_z)$$

$$L_{\delta_R}^* = (L_{\delta_R} - J_x N_{\delta_R})/(1 - J_x J_z)$$

$$N_P^* = (N_P - J_z L_P)/(1 - J_x J_z)$$

$$N_v^* = (N_v - J_z L_v)/(1 - J_x J_z)$$

$$N_r^* = (N_r - J_z L_r)/(1 - J_x J_z)$$

$$N_{\delta_A}^* = (N_{\delta_A} - J_z L_{\delta_A})/(1 - J_x J_z)$$

$$N_{\delta_\beta}^* = (N_{\delta_\beta} - J_z L_{\delta_\beta})/(1 - J_x J_z)$$

$$N_{\delta_R}^* = (N_{\delta_R} - J_z L_{\delta_R})/(1 - J_x J_z)$$

173

APPENDIX II

SUMMARY OF THE LEAST SQUARES NORMAL EQUATIONS

The least squares normal equations can be developed from the equations of motion summarized in Appendix I by equating each equation to a residue, R, instead of zero, and minimizing the square of this residue summed over n sets (in time) of the m variables. (In any case, the value of n must be equal or greater than (m + 1).) For example, the pitch moment equation written for the kth point in time is:

$$\dot{q}_K - M_u^* u_K - M_W^* W_K - M_q^* q_K - M_{\Delta\beta}^* \Delta\beta_K - M_N^* \Delta N_K - M_{i_t}(\Delta_{i_t})_K - M_O = (R_{\dot{q}})_K$$

Summing the n pitch moment equations gives

$$\sum_{K=1}^{n} q_K - M_u^* \sum_{K=1}^{n} u_K - M_W^* \sum_{K=1}^{n} W_K - M_q^* \sum_{K=1}^{n} q_K - M_{\Delta\beta}^* \sum_{K=1}^{n} \Delta\beta_K - M_{\Delta N} \sum_{K=1}^{n} \Delta N_K$$

$$- M_{i_t}^* \sum_{K=1}^{n} (\Delta_{i_t})_K - M_O \sum_{K=1}^{n} (1) = \sum_{K=1}^{n} (R_{\dot{q}})_K$$

The principle of least squares defines the best values of the unknown constants as those for which

$$\sum_{K=1}^{n} (R_{\dot{q}}^2)_K = minimum$$

This condition requires that the partial derivatives of this expression with respect to the unknown constants shall each be zero; i.e.,

$$\frac{\partial \left[\sum_{K=1}^{n} (R_{\dot{q}}^2)_K \right]}{\partial M_u^*} = 0, \qquad \frac{\partial \left[\sum_{K=1}^{n} (R_{\dot{q}}^2)_K \right]}{\partial M_W^*} = 0, \text{ etc.}$$

The resulting "normal equations" may be summarized in the form

$$
\begin{bmatrix}
a_{11} & a_{12} & \cdot & \cdot & \cdot & a_{1m} \\
a_{21} & a_{22} & \cdot & \cdot & \cdot & a_{2m} \\
\cdot & \cdot & \cdot & \cdot & \cdot & \cdot \\
\cdot & \cdot & \cdot & \cdot & \cdot & \cdot \\
\cdot & \cdot & \cdot & \cdot & \cdot & \cdot \\
a_{m1} & a_{m2} & \cdot & \cdot & \cdot & a_{mm}
\end{bmatrix}
\begin{bmatrix}
M_u^{*} \\
M_w^{*} \\
\cdot \\
\cdot \\
\cdot \\
M_o
\end{bmatrix}
=
\begin{bmatrix}
\sum\limits_{K=1}^{n} (u_K \dot{q}_K) \\
\sum\limits_{K=1}^{n} (W_K \dot{q}_K) \\
\cdot \\
\cdot \\
\cdot \\
\sum\limits_{K=1}^{n} (\dot{q}_K)
\end{bmatrix}
$$

where the elements of the symmetrical matrix, A, are:

$$a_{11} = \sum_{K=1}^{n} (u_K^2) \qquad\qquad a_{12} = a_{21}$$

$$a_{21} = \sum_{K=1}^{n} (u_K W_K) \qquad\qquad a_{22} = \sum_{K=1}^{n} (W_K^2)$$

$$a_{31} = \sum_{K=1}^{n} (u_K q_K) \qquad\qquad a_{32} = \sum_{K=1}^{n} (W_K q_K)$$

$$a_{41} = \sum_{K=1}^{n} (u_K \Delta\beta_K) \qquad\qquad a_{42} = \sum_{K=1}^{n} (W_K \Delta\beta_K)$$

$$a_{51} = \sum_{K=1}^{n} (u_K \Delta N_K) \qquad\qquad a_{52} = \sum_{K=1}^{n} (W_K \Delta N_K)$$

$$a_{61} = \sum_{K=1}^{n} (u_K (\Delta i_t)_K) \qquad\qquad a_{62} = \sum_{K=1}^{n} (W_K (\Delta i_t)_K)$$

$$a_{71} = \sum_{K=1}^{n} (u_K) \qquad\qquad a_{72} = \sum_{K=1}^{n} (W_K)$$

etc.

Similar equations can be derived from the other equations of motion. It is obvious that similar A matrices result from each of the longitudinal equations which differ only in that certain variables may be considered significant in one equation of motion and are considered insignificant in another. Thus, a general matrix can be written that may be applicable to any of the longitudinal equations by deletion of the row and column containing the variable which is not considered significant or is not excited during a particular maneuver. Similarly, a general matrix can be written for lateral-directional equations. These general arrays were formulated in the digital computer routine used for the least squares solutions in this program. Input instructions to the routine defined the particular variables and thus the reduced matrix to be used for the solution of each of the equations of motion.

NUMERICAL FILTERS

The following equations define the numerical filter weights for the "Martin-Graham" filters defined in the NASA Report CR-136.

Unconstrained Smoothing Weights

$$h_n = \frac{\cos[n\pi r_d]\ \sin[n\pi(2r_c + r_d)]}{n\pi(1 - 4r^2_d n^2)}$$

for $n = 1, 2, \ldots, N$ and $n = -1, -2, \ldots, -N$

$h_o = 2r_c + r_d$ for $n = 0$

where $(wN + 1)$ is the number of filter weights,

$r_c = f_c/f_s$

$r_d = (f_t - f_c)/f_s$

f_s = sampling frequency

FILTER RESPONSE

PHASE = 0°
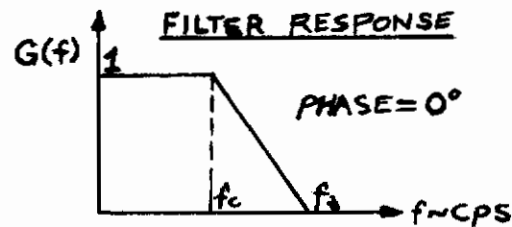
N may be arbitrarily selected for a given r_c and r_d to provide a desired response of the filter. In CR-136, it is indicated that a maximum error of 1% will result if $N \geq \dfrac{1.25}{r_d}$ is selected. For the discontinuity in the h_n equation obtained if $m = 1/2r_d$, h_m must be evaluated by

$$h_m = 2r_d^2 \sin\left[\frac{\pi(2r_c + r_d)}{2r_d}\right]$$

Constrained Smoothing Weights

$H_n = h_n + S$

$H_o = h_o + S$

where $S = \left[\dfrac{1 - h_o - 2\displaystyle\sum_{n=1}^{N} h_n}{2N + 1}\right]$

The constrained or normalized weights are the final weight values applied to the data.

177

First Derivative Smoothing Weights

$$Y_K = -f_s \left[\frac{r_t \cos 2\pi r_t k + r_c \cos 2\pi r_c k}{k(1-4r_d^2 k^2)} - \frac{h_k(1-12r_d^2 k^2)}{k(1-4r_d^2 k^2)} \right]$$

for k = 1, 2, ..., N

$Y_{-k} = -Y_k$

$Y_o = 0$

Application of Smoothing Weights

Assume that the time history of variable, β, sampled at equal increments in time, t, is represented by the array $\beta(t)$ for $t = t_1, t_2, ..., t_T$. Without applying special techniques for the first N points and the last N points, the filtered array, $\beta_F(t)$ from $t = N + 1$ to $t + (T-N)$ is given by

$$\beta_F(N+1) = \sum_{n=-N}^{N} H_n \beta(N - n+1),$$

$$\beta_F(N+2) = \sum_{n=-N}^{N} H_n \beta(N - n+2), \text{ etc.}$$

or $\quad \beta_F(i) = \sum_{n=-N}^{N} H_n \beta(i-n)$

where $i = N + 1, N + 2, ..., T - N.$

REFERENCES

1. Decker, Wallace H.; Page, V. Robert; and Dickinson, Stanley O: Large-Scale Wind Tunnel Tests of Descent Performance of an Airplane with a Tilt-Wing and Differential Propeller Thrust; NASA TN D-1857, 1964.

2. Goodson, Kenneth W: Longitudinal Aerodynamic Characteristics of a Flapped Tilt-Wing Four-Propeller V/STOL Transport Model; NASA TN D-3217, 1966.

3. Newsome, William A., Jr. and Kirby, Robert H: Flight Investigation of Stability and Control Characteristics of a 1/9-Scale Model of a Four-Propeller Tilt-Wing V/STOL Transport; NASA TN D-2443, 1964.

4. Boyden, Richmond P. and Curtiss, H. C., Jr: An Experimental Investigation of the Lateral-Directional Stability Characteristics of a Four-Propeller, Tilt-Wing VTOL Model at Low Speeds; Princeton University, Department of Aerospace and Mechanical Sciences Report No. 743, 1965.

5. White, Robert M: A Low Speed Wind Tunnel Test of a 0.11 Scale Powered XC-142 VTOL Model Investigating Flap Positions and Wing-Flap Programming in Forward Transition; Report No. 2-59730/3R/829; Vought Aeronautics Division, Dallas, Texas, 1963.

6. White, Robert M: A Low Speed Wind Tunnel Test of a 0.11 Scale Powered XC-142 VTOL Model Investigating Longitudinal and Lateral-Directional Stability and Control in Forward Transition; Report No. 2-59730/3R/831; Vought Aeronautics Division, Dallas, Texas, 1963.

7. Holbrook, J. W: A Low Speed Wind Tunnel Test of a 0.11 Scale XC-142 Powered VTOL Model Investigating Longitudinal and Lateral-Directional Stability and Control in the Cruise Configuration; Report No. 2-59730/3R/834; Vought Aeronautics Division, Dallas, Texas, 1963.

8. Oldenbuttel, R. H: A Low Speed Wind Tunnel Test of the 0.11 Scale XC-142A Powered Model Investigating Increased Descent Capability; Report No. 2-59730/3R/891; Vought Aeronautics Division, Dallas, Texas, 1963.

9. White, Robert M: A Low Speed Wind Tunnel Test of a Scale XC-142A Powered Model Conducted to Optimize the Production Slats; Report No. 2-59730/3R/900; Vought Aeronautics Division, Dallas, Texas, 1964.

10. Holbrook, J. W: A Low Speed Wind Tunnel Test of a 0.11 Scale XC-142A Model to Determine the Effect of Drag in the Cruise Configuration, the Flow Field in the Plane of the Propellers and the Power-off Component Drag of the Model; Report No. 2-59730/5R-988; Vought Aeronautics Division, Dallas, Texas, 1966.

11. Holbrook, J. W: Hover Test of the 0.11 Scale XC-142A Powered Model; Report No. 2-59730/5R/6002; Vought Aeronautics Division, Dallas, Texas, 1965.

12. Oldenbuttel, R. H: A Low Speed Wind Tunnel Test of the 0.11 Scale XC-142A for Conducting a Preliminary Investigation to Improve Directional Control Power at High Wing Incidence; Report No. 2-59730/5R/6009; Vought Aeronautics Division, Dallas, Texas, 1966.

13. White, Robert M: Isolated Propeller and Tail Propeller Calibrations of the 0.11 Scale XC-142 Model Conducted in the Chance Vought Low Speed Wind Tunnel; Report No. 2-59730/3R/830; Vought Aeronautics Division, Dallas, Texas, 1963.

14. Gillis, Clarence L.; Polhamus, Edward C.; and Gray, Joseph L., Jr: Charts for Determining Jet-Boundary Corrections for Complete Models in 7-by-10 Foot Closed Rectangular Wind Tunnels; NACA WRL-123, 1945.

15. Heyson, Harry H: Linearized Theory of Wind-Tunnel Jet-Boundary Corrections and Ground Effect for VTOL-STOL Aircraft; NASA TR R-124, 1962.

16. Kirkpatrick, D. L. I: Wind Tunnel Corrections for V/STOL Model Testing; University of Virginia, 1962.

17. Holbrook, J. W: Wind Tunnel Data Correlation Test Using the LTV 0.11 Scale XC-142A Powered Model (Phase 1 of 3) (15 x 20-Foot Test Section); Report No. 2-59730/7R-6127; Vought Aeronautics Division, Dallas, Texas, 1968.

18. Oldenbuttel, R. H: Wind Tunnel Data Correlation Test Using the LTV 0.11 Scale XC-142A Powered Model (Phase 2 of 3) (7 x 10-Foot Test Section); Report No. 2-59730/8R-6139; Vought Aeronautics Division, Dallas, Texas, 1968.

19. Oldenbuttel, R. H: Wind Tunnel Data Correlation Test Using the LTV 0.11 Scale XC-142A Powered Model (Phase 3 of 3) (21 x 23-Foot Test Section); Report No. 2-59730/8R-6138; Vought Aeronautics Division, Dallas, Texas, 1968.

20. Glauert, H: Wind Tunnel Interference on Wings, Bodies and Airscrews; R & M 1566, 1933.

21. Grunwald, Kalman J: "Wall Effects and Scale Effects in V/STOL Model Testing"; by the Staff of the Powered-Lift Aerodynamics Section, NASA Langley Research Center, Langley Station, Hampton, Virginia. Presented AIAA-Navy Aerodynamic Testing Conference, Washington, D. C., March 9-10, 1964.

22. Erlandsen, P. O.; Zarcaro, J. H.; and Olcott, J. W: Wind Tunnel Correlation Study of the North American Tilt-Wing Model Tested in the NACAL 14' x 16' Tunnel and the Airship Test Facility, the Flying Wind Tunnel; NAS Lakehurst, 1962. AD-298289

23. Davenport, Edwin E. and Kuhn, Richard E: Wind-Tunnel-Wall Effects and Scale Effects on a VTOL Configuration with a Fan Mounted in the Fuselage; NASA TN D-2560, 1965.

24. Heyson, H. H. and Grunwald, K. J: "Wind Tunnel Boundary Interference for V/STOL Testing"; Paper No. 24, Conference on V/STOL and STOL Aircraft, NASA SP-116, 1966.

25. Anders, Edward B. et al: <u>Digital Filters</u>; NASA CR-136, 1964.

26. Graham, Ronald J: <u>Determination of Analysis of Numerical Smoothing Weights</u>; NASA TR R-179, 1963.

27. Cromwell, Charles H., and Payne, Henry E: <u>A Stability Analysis of Tilt-Wing Aircraft (Analytical)</u>; Princeton University Report No. 477, 1960.

DOCUMENT CONTROL DATA - R & D

(Security classification of title, body of abstract and indexing annotation must be entered when the overall report is classified)

1. ORIGINATING ACTIVITY *(Corporate author)*	2a. REPORT SECURITY CLASSIFICATION
Vought Aeronautics Division	Unclassified
LTV Aerospace Corporation	2b. GROUP
Dallas, Texas	NA

3. REPORT TITLE

Correlation of Aerodynamic Stability and Control Derivatives Obtained from Flight Tests and Wind Tunnel Tests on the XC-142A Airplane

4. DESCRIPTIVE NOTES *(Type of report and inclusive dates)*

Final Report   June 1965   November 1968

5. AUTHOR(S) *(First name, middle initial, last name)*

Ernest L. Black
George C. Booth

6. REPORT DATE	7a. TOTAL NO. OF PAGES	7b. NO. OF REFS
April 1969	196	27

8a. CONTRACT OR GRANT NO.	9a. ORIGINATOR'S REPORT NUMBER(S)
AF 33(615)-2897	
b. PROJECT NO.	
8219	
c. TASK 821907	9b. OTHER REPORT NO(S) *(Any other numbers that may be assigned this report)*
d. BPSN 5(638219 - 62405364)	AFFDL-TR-68-167

10. DISTRIBUTION STATEMENT

This document is subject to special export controls and each transmittal to foreign governments or foreign nationals may be made only with prior approval of the Air Force Flight Dynamics Laboratory (FDCC), W-PAFB, Ohio   45433.

11. SUPPLEMENTARY NOTES	12. SPONSORING MILITARY ACTIVITY
	Air Force Flight Dynamics Laboratory
	Wright-Patterson Air Force Base, Ohio

13. ABSTRACT

A wind tunnel-flight data correlation program using the XC-142A airplane was undertaken to assess the degree of correlation attainable and to establish the areas where present wind tunnel testing and correction techniques appear to be inadequate. Wind tunnel data obtained from tests of three models of the XC-142A airplane in four different size test sections could not be satisfactorily correlated because of differences in model configuration and test conditions. Three special tests were performed using the same model but in different size test sections of the same tunnel. The results of these tests indicated that with proper equipment and techniques, valid V/STOL wind tunnel data can be acquired. The flight data were obtained from the Contractor's Category I test program. The objective of this flight test program was primarily to perform a qualitative evaluation of the airplane rather than to obtain the quantitative data desired for aerodynamic analysis purposes. The flight data were not acquired in a manner that would provide suitable quality to allow a high degree of confidence in inverse solutions for aerodynamic derivatives. It is recommended that future programs include a critical review of the instrumentation system and flight maneuvers in order to obtain the best possible data for determining the low speed flight aerodynamic characteristics. This abstract is subject to special export controls and each transmittal to foreign governments or foreign nationals may be made only with prior approval of the Air Force Flight Dynamics Laboratory (FDCC), W-PAFB, Ohio   45433.

14. KEY WORDS	LINK A		LINK B		LINK C	
	ROLE	WT	ROLE	WT	ROLE	WT
V/STOL Aerodynamics						
Aerodynamic Stability and Control						
Aerodynamic Parameters						
Aerodynamic Derivatives						
Wind Tunnel Data Correlation						
Propeller Thrust						
Wind Tunnel-Flight Data Correlation						
Flight Test Instrumentation						
Wind Tunnel Wall Corrections						

DD FORM 1 NOV 65 1473 (BACK)

(PAGE 2)